The Hong Kong Polytechnic University

Department of Applied Biology and Chemical Technology

Mechanistic studies on hydrotris(pyrazolyl)borate ruthenium complexes-catalyzed C-H bond activation and nitrile hydration reaction

By

Chung Wing LEUNG

A thesis submitted

in partial fulfillment

of the requirements

for the degree of Doctor of Philosophy

Oct 2008

Declaration

I hereby declare that this thesis is my own work and that, to the best of my knowledge and belief, it reproduces no material previously published or written, nor material that has been accepted for the award of any other degree or diploma, except where due acknowledgement has been made in the text.

Chung Wing LEUNG

Oct, 2008

Abstract of thesis entitled “Mechanistic studies on hydrotris(pyrazolyl)borate ruthenium complexes-catalyzed C-H bond activation and nitrile hydration reaction.”

Submitted by Chung Wing LEUNG

for the Degree of Doctor of Philosophy

at The Hong Kong Polytechnic University

in Oct, 2008

Abstract

Metal-catalyzed deuteration of organic compounds using the environmentally benign D_2O as deuterium source is relatively rare. The solvento-hydride complex $TpRu(PPh_3)(CH_3CN)H$ (Tp = hydrotris(pyrazolyl)borate) is found to be a catalyst for H/D exchange between D_2O and some organic solvents. This exchange can be preformed under Ar or H_2. In the former case, the hydride ligand is rapidly deuterated by D_2O forming $TpRu(PPh_3)(CH_3CN)D$. It is believed that the mechanism is similar to that of our previous work on the $TpRu(PPh_3)(CH_3CN)H$-catalyzed H/D exchange reactions between deuterated organic molecules and methane. We proposed that $TpRu(PPh_3)(CH_3CN)D$ exchanges the deuteride ligands Ru-D with R-H via the intermediacies of the η^2-R-H, η^2-H–D, and η^2-R–D σ-complexes. In the course of catalysis $TpRu(PPh_3)(CH_3CN)D$ is converted to an aquo-acetamido complex $TpRu(PPh_3)(D_2O)(NDC(O)CH_3)$, which at the later stage of the reaction generates two additional minor species, one of which is the partially deuterated carbonyl hydride complex $TpRu(PPh_3)(CO)H$ (or D). All of these complexes, however, show no catalytic activity for H/D exchange between D_2O and organic solvents.

In the catalytic reaction under H_2, dihydrogen-hydride complex $TpRu(PPh_3)(H_2)H$ and its isotopomers $TpRu(PPh_3)(H_{3-x})D_x$ formed are the active species for the H/D exchange reactions. The H-H (or D) ligand can be displaced by R-H, and the mechanism is akin to the one mentioned above. This dihydrogen-hydride

complex is less active than the solvento-hydride complex, which, due to the higher lability of the CH_3CN ligand, therefore exchanges more readily with the organic molecule (R-H) to form the η^2-R–H σ-complex.

The aquo-acetamido complex $TpRu(PPh_3)(H_2O)(NHC(O)CH_3)$ is independently synthesized by refluxing a THF solution of the solvento-hydride complex with water. The complex is formed via hydration of the CH_3CN ligand of $TpRu(PPh_3)(CH_3CN)H$; It is shown by theoretical calculations at the Becke3LYP level of DFT theory that the hydration process is promoted by a Ru-H···H-OH dihydrogen bonding interaction between the hydride ligand and the attacking water molecule. The molecular structure of the aquo-acetamido complex is determined by X-ray crystallography.

The aquo-acetamido complex is found to be active for catalytic hydration of nitriles to amides. Common mechanisms for catalytic nitrile hydration involve intramolecular nucleophilic attack of a hydroxo (or aquo) ligand or external attack of a hydroxide ion or (water) at the carbon atom of η^1-coordinated nitrile to form the metal amide intermediate and subsequent protonation of amido ligand by an adjacent aquo ligand or solvent water. Our catalysis, however, proceeds via a new mechanism involving the intermediacy of a relatively stable complex containing a chelating *N*-imidoylimidato ligand; ring-opening nucleophilic attack of this ligand by water generates the product. Formation of the *N*-imidoylimidato complex from the aquo-acetamido complex involves several steps, the initial one is displacement of the H_2O

ligand by a nitrile molecule to yield the nitrile-acetamido species $TpRu(PPh_3)(RCN)(NHC(O)CH_3)$, this is followed by an unusual linkage isomerization of the N-bonded amido ligand to an O-bonded imido, which then undergoes nucleophilic attack at the carbon atom of the nitrile ligand in the complex; facile 1,3-proton shift between the nitrogen atoms on the resulting ring completes the reaction. The catalytic cycle of the aquo-acetamido complex-catalyzed nitrile hydration reaction has been examined by theoretical calculations at the Becke3LYP level of DFT theory. It is learned that there is a substantially high barrier for the hydrolysis of the highly stable *N*-imidoylimidato complex, a step involving the ring-opening nucleophilic attack of this ligand by water, and this is probably the reason for the requirement of a relatively high reaction temperature.

More conveniently, the aquo-amido complexes $TpRu(PPh_3)(H_2O)(NHC(O)R)$ (R = Me, Ph) can be prepared by reacting $TpRu(PPh_3)(RCN)Cl$ with NaOH in THF in the presence of water. Different *N*-imidoylimidato complexes $TpRu(PPh_3)(\kappa^2$-*N*,*O*-NH=CMeN=CMeO), $TpRu(PPh_3)(\kappa^2$-*N*,*O*-NH=CPhN=CPhO), and $TpRu(PPh_3)(\kappa^2$-*N*,*O*-NH=CMeN=CPhO) were independently synthesized by heating a 1,4-dioxane solution of $TpRu(PPh_3)(H_2O)(NHC(O)R)$ (R = Me, Ph) with the corresponding nitriles. The molecular structure of $TpRu(PPh_3)(\kappa^2$-*N*,*O*-NH=CPhN=CPhO) was determined by X-ray crystallography.

The aquo-acetamido complex is found to be a catalyst for the H/D exchange between D_2O and some ketones. The result shows that activated hydrogens of

ketones such as α-hydrogens are selectively deuterated by D_2O. It is believed that tautomerization from keto to enol form is a crucial step of the catalytic cycle. In the course of catalysis, the amido hydrogen of the acetamido ligand can be deuterated readily by D_2O to form $TpRu(PPh_3)(D_2O)(NDCOCH_3)$, in which the labile ligand D_2O can be substituted by the enol; H/D exchange between the enolic hydrogen and amido deuterium then proceeds. The cycle is completed by displacement of the deuterated enol with D_2O. The reactivity of the aquo-amido complexes has also been studied. The labile aquo ligand can be readily displaced by various substrates such as alcohol, nitrile, and alkyne. An amido vinyl complex $TpRu(PPh_3)(C(NHC(O)CH_3)=CHPh)$ was synthesized by reacting a THF solution of $TpRu(PPh_3)(H_2O)(NHC(O)CH_3)$ with excess phenlyacetylene at room temperature. Formation of the amido vinyl complex involves coordination of phenylacetylene to form a vinylidene complex and subsequent intramolecular nucleophilic attack of the adjacent amido moiety to the α carbon of the vinylidene ligand. This amido vinyl complex reacted with HBF_4 very readily to give a carbene complex, $[TpRu(PPh_3)(=C(CH_2Ph)NHC(O)CH_3)][BF_4]$.

Publications

Leung, C. W.; Zheng, W.; Zhou, Z.; Lin, Z.; Lau, C. P. "Mechanism of Catalytic Hydration of Nitriles with Hydrotris(pyrazolyl)borato (Tp) Ruthenium Complexes" *Organometallics*, **2008**, 27(19), 4957-4969.

Leung, C. W.; Zheng, W.; Wang, D.; Ng, S. M.; Yeung, C. H.; Zhou, Z.; Lin, Z.; Lau, C. P. "Catalytic H/D Exchange between Organic Compounds and D_2O with $TpRu(PPh_3)(CH_3CN)H$ (Tp = hydro(trispyrazolyl)borate). Reaction of $TpRu(PPh_3)(CH_3CN)H$ with Water to Form Acetamido Complex $TpRu(PPh_3)(H_2O)(NHC(O)CH_3)$" *Organometallics*, **2007**, 26(8); 1924-1933.

Zheng, W.; Leung, C. W.; Zhou, Z.; Lau, C. P.; Lin, Z. "Structure Determination of $TpRu(PPh_3)(\kappa^2$-*N,O*-NH=CPhN=CPhO): A Story of How Computational Studies Contribute to the Structural Characterization Process" *J. Theo. & Comput. Chem.*, accepted

Leung, C. W.; Zheng, W.; Ng, S. M.; Zhou, Z.; Lin, Z.; Lau, C. P. " Mechanistic study on catalytic hydration of nitrile with hydro(trispyrazolyl)borate ruthenium complex $TpRu(PPh_3)(H_2O)(NHC(O)CH_3)$" 15^{th} Symposium on Chemistry Postgraduate Research in Hong Kong, pp I-63, 26 April 2008.

Leung, C. W.; Zheng, W.; Ng, S. M.; Lin, Z.; Lau, C. P. "Catalytic hydration of nitrile with hydro(trispyrazolyl)borate ruthenium complexes $TpRu(PPh_3)(CH_3CN)H$ and $TpRu(PPh_3)(H_2O)(NHC(O)CH_3)$" 14th International Symposium on Organometallic Chemistry Directed Towards Organic Synthesis (OMCOS), Nara, Japan, pp P-181, 2-6 August 2007.

Leung, C. W.; Zheng, W.; Ng, S. M.; Wang, D.; Yeung, C. H.; Zhou, Z.; Lin, Z.; Lau, C. P. "Ruthenium – catalyzed organic comounds/D_2O H/D exchange and nitrile hydration" 14th Symposium on Chemistry Postgraduate Research in Hong Kong, pp Oral-6, 28 April 2007

Leung, C. W.; Ho, Y. C.; Wang, D.; Ng, S. M. Lau, C. P. "Reactivity study of hydro(trispyrazolyl)borate ruthenium hydride and hydroxo complexes towards C-H bond activation" 13th Symposium on Chemistry Postgraduate Research in Hong Kong, pp I-86, 22 April 2006.

Acknowledgements

I would like to express my deepest gratitude to my supervisor Prof. C. P. Lau for his invaluable advice, supervision, and guidance throughout the course of my study. His constant encouragement and support have motivated my learning. His creative ideas, scientific intuitions, and passion in research have particularly inspired me and enriched my research. He has also contributed lots of unique, remarkable and perceptive comments and views to sharpen my research skills and optimize my thesis. It is my pleasure to learn from him. Work in his research group would be a truly rewarding and extraordinary experience in my life.

Special thanks to Prof. Z. Y. Lin and his research group in the Department of Chemistry, The Hong Kong University of Science and Technology, for their support on theoretical calculations.

It is my pleasure to pay tribute to Prof. Z. Y. Zhou for resolving the molecular structures by X-ray crystallography.

I am indebted to my postgraduate colleagues, Mr. H. W. Cheung, Mr. T. Y. Lee, Mr. C. M. So, Mr. P. H. Leung, Miss W. N. Sit, Dr. C. O. Chan, Dr. W. K. Fung, and Dr. M. L. Man, all of whom have made my study most pleasant and smooth. Special thanks are given to Mr. S. M. Ng, Mr. D. X. Wang, and Dr. K. C. Cheung who taught me technical skills from the very early stage of my study.

I am obliged to the staff and technical service crew of the Chemical Technology Section of the Department of Applied Biology and Chemical Technology, The Hong Kong Polytechnic University for their assistance throughout my postgraduate study, especially to Mr. Y. K. Au, and Mr. W. K. Kwan for their help on performing the MS and NMR spectra, respectively.

My parents deserve special mention for their warm care, patience and endless love. I am also indebted to my sister and close friends for their support and encouragement.

Finally, I would like to thank the Pao Yue-Kong Library for its Interlibrary Loans and Document Delivery Services and the Research Degree Committee of The Hong Kong Polytechnic University for awarding me a studentship and a grant to support my conference presentation in the 14th International Symposium on Organometallic Chemistry Directed Towards Organic Synthesis (OMCOS) held in Nara, Japan on 2-6 August 2007.

Table of Contents

	Abstract	iv
	Publications	viii
	Acknowledgements	x
	Table of content	xii
	List of Figures	xix
	List of Tables	xxiv
	List Schemes	xxvi
	List of Charts	xxix
	Abbreviations	xxxi

Chapter One

Introduction

1.1	C-H bond activation	1
1.2	H/D exchange reactions	3
1.3	Mechanism of C-H bond activation	4
1.4	Catalytic C-H bond activation by metal hydride complexes	9
1.5	H/D exchange by using deuterium oxide as deuterium source	14
1.6	Dihydrogen bond-mediated reaction	15

1.7	Transition metal-catalyzed nitrile hydration	19
1.8	Common mechanisms for catalytic nitrile hydration with TM	19
1.9	Hydrolytic coupling of nitrile complexes	25
1.10	Amido complexes	28
Chapter Two		
	Catalytic H/D exchange between organic compounds and D_2O with $TpRu(PPh_3)(CH_3CN)H$. Reaction of $TpRu(PPh_3)(CH_3CN)H$ with water to form acrtamido complex $TpRu(PPh_3)(H_2O)(NHC(O)CH_3)$	
2.1	Introduction	34
2.2	Experimental	37
2.2.1	Materials and instrumentation	37
2.2.2	Synthesis and reactions	38
2.2.2.1	H/D exchange between Ru─H of **1** and D_2O	38
2.2.2.2	Synthesis of $TpRu(PPh_3)(H_2O)(NHC(O)CH_3)$ (**2**)	39
2.2.2.3	Catalytic H/D exchange organic compounds and D_2O with $TpRu(PPh_3)(CH_3CN)H$ under Ar or H_2	40
2.2.2.4	The use of ^1H NMR spectroscopy to determine levels of deuteration of the organic compound	40
2.2.2.5	Reaction of **2** with H_2	41
2.2.2.6	Reaction of **2** with H_2/D_2O	42

2.2.2.7	Crystallographic structure analysis of $TpRu(PPh_3)(H_2O)(NHC(O)CH_3)$ (**2**)	42
2.3	Results and discussion	43
2.3.1	H/D exchange between organic molecules and D_2O under Ar	43
2.3.2	H/D exchange of Ru─H with D_2O at room temperature	45
2.3.3	Formation of $TpRu(PPh_3)(D_2O)(NDC(O)CH_3)$ (**2d**) and structure determination of the ruthenium-acetamido complex $TpRu(PPh_3)(H_2O)(NHC(O)CH_3)$ (**2**)	49
2.3.4	Possible mechanisms for the formation of **2**	55
2.3.5	Theoretical Study	57
2.3.6	Reaction of **2** with H_2	62
2.3.7	Reaction of **2** with H_2/D_2O	64
2.3.8	Mechanism of **1**-catalyzed H/D exchange between R─H and D_2O under Ar	65
2.3.9	Mechanism of **1**-catalyzed H/D exchange between R─H and D_2O under H_2	67
Chapter Three		
	Mechanism of catalytic hydration of nitriles with hydrotris(pyrazolyl)borato (Tp) ruthenium complexes	
3.1	Introduction	71
3.2	Experimental	74

3.2.1	Materials and instrumentation	74
3.2.2	Synthesis and reactions	75
3.2.2.1	Alternative method for synthesis of $TpRu(PPh_3)(H_2O)(NHC(O)CH_3)$ (**2**)	75
3.2.2.2	*In-situ* preparation of $TpRu(PPh_3)(NCCH_3)(NHC(O)CH_3)$ (**6**)	76
3.2.2.3	Synthesis of $TpRu(PPh_3)(\kappa^2$-*N,O*-NH=CMeN=CMeO) (**7**)	77
3.2.2.4	Synthesis of $TpRu(PPh_3)(PhCN)(Cl)$	78
3.2.2.5	Synthesis of $TpRu(PPh_3)(H_2O)(NHC(O)Ph)$ (**8**)	79
3.2.2.6	Synthesis of $TpRu(PPh_3)(NCPh)(NHC(O)Ph)$ (**9**)	80
3.2.2.7	Synthesis of $TpRu(PPh_3)(\kappa^2$-*N,O*-NH=CPhN=CPhO) (**10**)	81
3.2.2.8	Synthesis of $TpRu(PPh_3)(\kappa^2$-*N,O*-NH=CMeN=CPhO) (**11**)	82
3.2.2.9	General procedure of catalytic hydration of nitriles	82
3.2.2.10	Monitoring of **1**-catalyzed hydration of acetonitrile with NMR spectroscopy	83
3.2.2.11	Monitoring of **2**- or **8**-catalyzed hydration of acetonitrile and benzonitrile with NMR spectroscopy	83
3.2.2.12	Crystallographic structure analysis of $TpRu(PPh_3)(H_2O)(NHC(O)Ph)$ (**8**) and $TpRu(PPh_3)(\kappa^2$-*N,O*-NH=CPhN=CPhO) (**10**)	84
3.3	Results and Discussion	85
3.3.1	Catalytic hydration of nitriles to amides with $TpRu(PPh_3)(CH_3CN)H$ (**1**) and	85

	$TpRu(PPh_3)(H_2O)(NHC(O)CH_3)$ (**2**), and NMR monitoring of the **1**- and **2**-catalyzed hydration of acetonitrile	
3.3.2	Synthesis of $TpRu(PPh_3)(CH_3CN)(NHC(O)CH_3)$ (**6**)	91
3.3.3	Synthesis of $TpRu(PPh_3)(\kappa^2\text{-}N,O\text{-}NH{=}CMeN{=}CMeO)$ (**7**)	91
3.3.4	Synthesis of $TpRu(PPh_3)(H_2O)(NHC(O)Ph)$ (**8**) and $TpRu(PPh_3)(PhCN)(NHC(O)Ph)$ (**9**), and molecular structure of $TpRu(PPh_3)(H_2O)(NHC(O)Ph)$ (**8**)	93
3.3.5	NMR monitoring of $TpRu(PPh_3)(H_2O)(NHC(O)Ph)$ (**8**)-catalyzed hydration of benzonitrile	97
3.3.6	Synthesis and X-ray crystallographic study of $TpRu(PPh_3)(\kappa^2\text{-}N,O\text{-}NH{=}CPhN{=}CPhO)$ (**10**)	100
3.3.7	Synthesis of $TpRu(PPh_3)(\kappa^2\text{-}N,O\text{-}NH{=}CMeN{=}CPhO)$ (**11**)	108
3.3.8	Proposed mechanism for the catalytic hydration of nitriles to amides	108
3.3.9	Computational study	113
Chapter Four		
	Catalytic reactivity studies of $TpRu(PPh_3)(H_2O)(NHCOCH_3)$: C-H bond activation of ketones and C-N bond formation on alkyne	
4.1	Introduction	120
4.2	Experimental	121
4.2.1	Materials and instrumentation	121

4.2.2	Synthesis and reactions	123
4.2.2.1	H/D exchange between amido hydrogen of $TpRu(PPh_3)(H_2O)(NHC(O)CH_3)$ (**2**) and D_2O	123
4.2.2.2	H/D exchange between amido deuterium of $TpRu(PPh_3)(D_2O)(NDC(O)CH_3)$ (**2d**) and cyclopentanone	123
4.2.2.3	Catalytic H/D exchange between ketones and D_2O	124
4.2.2.4	Use of ^1H NMR spectroscopy to determine levels of deuteration of the ketones	124
4.2.2.5	Catalytic H/D exchange between Acetylacetone (Hacac) and D_2O with **2**	125
4.2.2.6	Reaction of **2** with acetaldehyde	126
4.2.2.7	Synthesis of $TpRu(PPh_3)(C(NHC(O)CH_3)=CHPh)$ (**13**)	126
4.2.2.8	Synthesis of $[TpRu(PPh_3)(=C(CH_2Ph)NHC(O)CH_3)][BF_4]$ (**14**)	127
4.2.2.9	Crystallographic structure analysis of $[TpRu(PPh_3)(=C(CH_2Ph)NHC(O)CH_3)][BF_4]$ (**14**)	128
4.3	Results and Discussion	129
4.3.1	H/D Exchange between Ketones and D_2O	129
4.3.2	H/D Exchange between Acetylacetone (Hacac) and D_2O under Argon	132
4.3.3	H/D Exchange of amido hydrogen of $TpRu(PPh_3)(H_2O)(NHCOCH_3)$ (**2**) with D_2O at Room Temperature	134

4.3.4	H/D Exchange between amido deuterium of $TpRu(PPh_3)(D_2O)(NDCOCH_3)$ (**2d**) and cyclopentanone	137
4.3.5	Mechanism of **2**-catalyzed H/D exchange between enolic hydrogens of ketones and D_2O	138
4.3.6	Mechanism of **2**-catalyzed H/D exchange between olefinic hydrogens of α,β-unsaturated ketones and D_2O	142
4.3.7	Reactivity studies of **2**	143
4.3.8	Synthesis of $TpRu(PPh_3)(C(NHC(O)CH_3)=CHPh)$ (**13**) and $[TpRu(PPh_3)(=C(CH_2Ph)NHC(O)CH_3)][BF_4]$ (**14**)	145
4.3.9	X-ray crystallographic study of $[TpRu(PPh_3)(=C(CH_2Ph)NHC(O)CH_3)][BF_4]$ (**14**)	146
4.3.10	Possible Mechanism of Formation of $TpRu(PPh_3)(C(NHC(O)CH_3)=CHPh)$ (**13**) and $[TpRu(PPh_3)(=C(CH_2Ph)NHC(O)CH_3)][BF_4]$ (**14**)	151
Chapter Five		
	Conclusion	155
	Appendix	158
	Reference	205

List of Figures

Figure 2.1	Molecular structure of $TpRu(PPh_3)(H_2O)(NHC(O)CH_3)$ (**2**)	52
Figure 2.2	Energy profile for the conversion process of the acetonitrile-coordinated complex **1a** to the acetamido-coordinated complex **1c**	58
Figure 2.3	B3LYP optimized structures for those species shown in Figure 2.2 and Scheme 2.5. Bond lengths are given in Å	60
Figure 2.4	400.13 MHz ^{1}H NMR spectrum of $TpRu(PPh_3)(H_2O)(NHC(O)CH_3)$ (**2**)	159
Figure 2.5	161.98 MHz $^{31}P\{^{1}H\}$ NMR spectrum of $TpRu(PPh_3)(H_2O)(NHC(O)CH_3)$ (**2**)	160
Figure 2.6	100.63 MHz $^{13}C\{^{1}H\}$ NMR spectrum of $TpRu(PPh_3)(H_2O)(NHC(O)CH_3)$ (**2**)	161
Figure 2.7	Infra-red spectrum of $TpRu(PPh_3)(H_2O)(NHC(O)CH_3)$ (**2**)	162
Figure 2.8	Mass spectrum of $TpRu(PPh_3)(H_2O)(NHC(O)CH_3)$ (**2**)	163
Figure 3.1	^{31}P NMR study of **2**-catalyzed hydration of acetonitrile	87
Figure 3.2	Molecular structure of $TpRu(PPh_3)(H_2O)(NHC(O)Ph)$ (**8**)	94
Figure 3.3	^{31}P NMR study of **8**-catalyzed hydration of benzonitrile	99
Figure 3.4	Molecular structure of $TpRu(PPh_3)(\kappa^2\text{-}N,O\text{-}NH{=}CPhN{=}CPhO)$ (**10**)	100
Figure 3.5	Energy profile for the reaction sequence shown in Scheme	116

3.4

Figure 3.6 Selected optimized structural parameters calculated for the species involved in the reaction sequence shown in Figure 3.5 and Scheme 3.5 118

Figure 3.7 400.13 MHz ^{1}H NMR spectrum of $TpRu(PPh_3)(NCCH_3)(NHC(O)CH_3)$ (**6**) 164

Figure 3.8 161.98 MHz $^{31}P\{^{1}H\}$ NMR spectrum of $TpRu(PPh_3)(NCCH_3)(NHC(O)CH_3)$ (**6**) 165

Figure 3.9 100.63 MHz $^{13}C\{^{1}H\}$ NMR spectrum of $TpRu(PPh_3)(NCCH_3)(NHC(O)CH_3)$ (**6**) 166

Figure 3.10 400.13 MHz ^{1}H NMR spectrum of $TpRu(PPh_3)(\kappa^2$-*N,O*-NH=CMeN=CMeO) (**7**) 167

Figure 3.11 161.98 MHz $^{31}P\{^{1}H\}$ NMR spectrum of $TpRu(PPh_3)(\kappa^2$-*N,O*-NH=CMeN=CMeO) (**7**) 168

Figure 3.12 100.63 MHz $^{13}C\{^{1}H\}$ NMR spectrum of $TpRu(PPh_3)(\kappa^2$-*N,O*-NH=CMeN=CMeO) (**7**) 169

Figure 3.13 Infra-red spectrum of $TpRu(PPh_3)(\kappa^2$-*N,O*-NH=CMeN=CMeO) (**7**) 170

Figure 3.14 Mass spectrum of $TpRu(PPh_3)(\kappa^2$-*N,O*-NH=CMeN=CMeO) (**7**) 171

Figure 3.15 400.13 MHz ^{1}H NMR spectrum of $TpRu(PPh_3)(PhCN)(Cl)$ 172

Figure 3.16 161.98 MHz $^{31}P\{^{1}H\}$ NMR spectrum of $TpRu(PPh_3)(PhCN)(Cl)$ 173

Figure 3.17	Mass spectrum of $TpRu(PPh_3)(PhCN)(Cl)$	174
Figure 3.18	400.13 MHz ^{1}H NMR spectrum of $TpRu(PPh_3)(H_2O)(NHC(O)Ph)$ (**8**)	175
Figure 3.19	161.98 MHz $^{31}P\{^{1}H\}$ NMR spectrum of $TpRu(PPh_3)(H_2O)(NHC(O)Ph)$ (**8**)	176
Figure 3.20	100.63 MHz $^{13}C\{^{1}H\}$ NMR spectrum of $TpRu(PPh_3)(H_2O)(NHC(O)Ph)$ (**8**)	177
Figure 3.21	Infra-red spectrum of $TpRu(PPh_3)(H_2O)(NHC(O)Ph)$ (**8**)	178
Figure 3.22	Mass spectrum of $TpRu(PPh_3)(H_2O)(NHC(O)Ph)$ (**8**)	179
Figure 3.23	400.13 MHz ^{1}H NMR spectrum of $TpRu(PPh_3)(NCPh)(NHC(O)Ph)$ (**9**)	180
Figure 3.24	161.98 MHz $^{31}P\{^{1}H\}$ NMR spectrum of $TpRu(PPh_3)(NCPh)(NHC(O)Ph)$ (**9**)	181
Figure 3.25	100.63 MHz $^{13}C\{^{1}H\}$ NMR spectrum of $TpRu(PPh_3)(NCPh)(NHC(O)Ph)$ (**9**)	182
Figure 3.26	Infra-red spectrum of $TpRu(PPh_3)(NCPh)(NHC(O)Ph)$ (**9**)	183
Figure 3.27	Mass spectrum of $TpRu(PPh_3)(NCPh)(NHC(O)Ph)$ (**9**)	184
Figure 3.28	400.13 MHz ^{1}H NMR spectrum of $TpRu(PPh_3)(\kappa^2$-*N,O*-NH=CPhN=CPhO) (**10**)	185
Figure 3.29	161.98 MHz $^{31}P\{^{1}H\}$ NMR spectrum of $TpRu(PPh_3)(\kappa^2$-*N,O*-NH=CPhN=CPhO) (**10**)	186
Figure 3.30	100.63 MHz $^{13}C\{^{1}H\}$ NMR spectrum of $TpRu(PPh_3)(\kappa^2$-*N,O*-NH=CPhN=CPhO) (**10**)	187

Figure 3.31	Infra-red spectrum of $TpRu(PPh_3)(\kappa^2$-*N,O*-NH=CPhN=CPhO) (**10**)	188
Figure 3.32	Mass spectrum of $TpRu(PPh_3)(\kappa^2$-*N,O*-NH=CPhN=CPhO) (**10**)	189
Figure 3.33	400.13 MHz ^1H NMR spectrum of $TpRu(PPh_3)(\kappa^2$-*N,O*-NH=CMeN=CPhO) (**11**)	190
Figure 3.34	161.98 MHz $^{31}P\{^1H\}$ NMR spectrum of $TpRu(PPh_3)(\kappa^2$-*N,O*-NH=CMeN=CPhO) (**11**)	191
Figure 3.35	100.63 MHz $^{13}C\{^1H\}$ NMR spectrum of $TpRu(PPh_3)(\kappa^2$-*N,O*-NH=CMeN=CPhO) (**11**)	192
Figure 3.36	Infra-red spectrum of $TpRu(PPh_3)(\kappa^2$-*N,O*-NH=CMeN=CPhO) (**11**)	193
Figure 3.37	Mass spectrum of $TpRu(PPh_3)(\kappa^2$-*N,O*-NH=CMeN=CPhO) (**11**)	194
Figure 4.1	Molecular structure of $[TpRu(PPh_3)(=C(CH_2Ph)NHC(O)CH_3)][BF_4]$ (**14**)	147
Figure 4.2	400.13 MHz ^1H NMR spectrum of $TpRu(PPh_3)(C(NHC(O)CH_3)=CHPh)$ (**13**)	195
Figure 4.3	161.98 MHz $^{31}P\{^1H\}$ NMR spectrum of $TpRu(PPh_3)(C(NHC(O)CH_3)=CHPh)$ (**13**)	196
Figure 4.4	100.63 MHz $^{13}C\{^1H\}$ NMR spectrum of $TpRu(PPh_3)(C(NHC(O)CH_3)=CHPh)$ (**13**)	197
Figure 4.5	Infra-red spectrum of $TpRu(PPh_3)(C(NHC(O)CH_3)=CHPh)$	198

(**13**)

Figure 4.6 Mass spectrum of $TpRu(PPh_3)(C(NHC(O)CH_3)=CHPh)$ (**13**) 199

Figure 4.7 400.13 MHz ^1H NMR spectrum of $[TpRu(PPh_3)(=C(CH_2Ph)NHC(O)CH_3)][BF_4]$ (**14**) 200

Figure 4.8 161.98 MHz $^{31}P\{^1H\}$ NMR spectrum of $[TpRu(PPh_3)(=C(CH_2Ph)NHC(O)CH_3)][BF_4]$ (**14**) 201

Figure 4.9 100.63 MHz $^{13}C\{^1H\}$ NMR spectrum of $[TpRu(PPh_3)(=C(CH_2Ph)NHC(O)CH_3)][BF_4]$ (**14**) 202

Figure 4.10 Infra-red spectrum of $[TpRu(PPh_3)(=C(CH_2Ph)NHC(O)CH_3)][BF_4]$ (**14**) 203

Figure 4.11 Mass spectrum of $[TpRu(PPh_3)(=C(CH_2Ph)NHC(O)CH_3)][BF_4]$ (**14**) 204

List of Tables

Table 2.1	H/D exchange of organic solvents and D_2O by **1** under argon	45
Table 2.2	Crystal data and structure refinement for $TpRu(PPh_3)(H_2O)(NHC(O)CH_3)$ (**2**)	53
Table 2.3	Selected bond distances (Å) and bond angles (^{o}) for $TpRu(PPh_3)(H_2O)(NHC(O)CH_3)$ (**2**)	54
Table 2.4	H/D exchange of organic solvents and D_2O by **1** under hydrogen	70
Table 3.1	Comparison on **1**- and **2**-catalyzed nitrile hydration	85
Table 3.2	Catalytic hydration of nitriles with $TpRu(PPh_3)(H_2O)(NHC(O)CH_3)$ (**2**)	90
Table 3.3	Crystal data and structure refinement for $TpRu(PPh_3)(H_2O)(NHC(O)Ph)$ (**8**)	95
Table 3.4	Selected bond distances (Å) and bond angles (^{o}) for $TpRu(PPh_3)(H_2O)(NHC(O)Ph)$ (**8**)	96
Table 3.5	Crystal data and structure refinement for $TpRu(PPh_3)(\kappa^2$-*N,O*-NH=CPhN=CPhO) (**10**)	101
Table 3.6	Selected bond distances (Å) and bond angles (^{o}) for $TpRu(PPh_3)(\kappa^2$-*N,O*-NH=CPhN=CPhO) (**10**)	102
Table 4.1	Deuteration of H/D exchange between D_2O and ketones by	130

2

Table 4.2 Crystal data and structure refinement for [TpRu(PPh$_3$)(=C(CH$_2$Ph)NHC(O)CH$_3$)][BF$_4$] (**14**) 148

Table 4.3 Selected bond distances (Å) and bond angles (^{o}) for [TpRu(PPh$_3$)(=C(CH$_2$Ph)NHC(O)CH$_3$)][BF$_4$] (**14**) 149

List of Schemes

Scheme 1.1	Two reaction pathways: oxidative addition (Top) and σ-bond metathesis (Bottom) of a H-X moiety	4
Scheme 1.2	Oxidative addition of R-H to $K[(\eta^2\text{-Tp'})PtMe_2]$ in the presence of $B(C_6F_5)_3$	5
Scheme 1.3	Catalytic cycle of $[(PPh_3)_3(CO)RhH]$ catalyzed alkene hydrogenation	10
Scheme 1.4	Interconversion of 2,6-diarylpyridine Ir (III) complexes	11
Scheme 1.5	Interconversion between a dihydrogen agostic Ru complex and a dihydrogen aryl Ru complex via a bis(dihydrogen) species	12
Scheme 1.6	Imination of coordinated aldehyde with 2-aminophenol or 4-aminophenol	17
Scheme 1.7	Catalytic hydration of nitriles by $(C_9H_7)Ru(dppm)H$	18
Scheme 1.8	Proposed mechanism of nitrile hydration via $[Cp'_2Mo(OH)(OH_2)]^+$	21
Scheme 1.9	Two possible pathways for regeneration of [Mo]-OH complex	22
Scheme 1.10	Proposed mechanism of nitrile hydration via $[Co(cyclen)(OH_2)_2]^{3+}$	23
Scheme 1.11	Two proposed mechanisms of catalytic nitrile hydration by	24

	aquo Pd complexes	
Scheme 1.12	Hydration of benzonitrile catalyzed by cis-$Ru(acac)(PPh_2py)_2$	25
Scheme 1.13	Reactions of trans- and cis- $[PtCl_4(NCNR_2)_2]$ complexes with water	27
Scheme 1.14	Proposed mechanism of Al(III)-catalyzed transamination	33
Scheme 2.1	Proposed mechanism of $TpRu(PPh_3)(CH_3CN)H$ catalyzed H/D exchange between methane and deuterated organic solvent	36
Scheme 2.2	Proposed mechanism of H/D exchange between hydride in **1** and D_2O via protonation	47
Scheme 2.3	Proposed mechanism of H/D exchange between hydride in **1** and D_2O via hydrogen-bonded ion pair	48
Scheme 2.4	Interaction between metal hydride and proton donor HX	48
Scheme 2.5	Proposed mechanism of formation of **2**	57
Scheme 2.6	Hydration of coordinated CH_3CN in **1a'**	61
Scheme 2.7	Reaction of **2** with H_2	63
Scheme 2.8	Proposed catalytic cycle of H/D exchange between D_2O and organic solvents	66
Scheme 2.9	H/D exchange between D_2 and H_2O by diiron (II) complex	69
Scheme 2.10	H/D exchange between D_2 and ROH by Ir complex without assistance of hydride ligand	69
Scheme 2.11	H/D exchange between D_2 and ROH by Ir complex with	70

	assistance of hydride ligand	
Scheme 3.1	Proposed mechanism for the hydration of nitriles by phosphinito complexes	72
Scheme 3.2	Proposed mechanism of intramolecular nitrile hydration catalyzed by a ferrous complex	73
Scheme 3.3	Proposed mechanism of formation of **D**	103
Scheme 3.4	Proposed mechanism of formation of $TpRu(PPh_3)(\kappa^2\text{-}N,O\text{-}NH{=}CPhN{=}CPhO)$ (**10**)	105
Scheme 3.5	Proposed mechanism of hydration of nitrile catalyzed by $TpRu(PPh_3)(H_2O)(NHC(O)R)$ R = Me or Ph	111
Scheme 3.6	Proposed mechanism of formation of **11** and **7** from **10**	113
Scheme 3.7	Equilibrium of **2A** and **3A** in presence of acetonitrile	114
Scheme 4.1	Proposed mechanism 1 of H/D exchange between the amido hydrogen and D_2O	135
Scheme 4.2	Proposed mechanism 2 of H/D exchange between the amido hydrogen and D_2O	136
Scheme 4.3	Proposed mechanism of catalytic H/D exchange between enolic hydrogen and D_2O	139
Scheme 4.4	Reaction sequence between **2** and acetaldehyde	144
Scheme 4.5	Proposed mechanism of formation of **13**	152
Scheme 4.6	Proposed mechanism of formation of **14**	154

List of Charts

Chart 1.1	Molecular structure of $(CH_3)TiCl_3$(dmpe)	2
Chart 1.2	Molecular structure of aryl hydride Rh (III) complex	15
Chart 1.3	Structure of $[(PMe_3)_4IrH(OH)]PF_6$	16
Chart 1.4	Structure of *N*-imidoylimidate Ru complex	26
Chart 1.5		27
Chart 1.6	Three different binding modes of amido ligands	28
Chart 2.1	Formation of the anion-stabilized dihydride	49
Chart 2.2	Isomerization of amido ligand	50
Chart 3.1	Molecular structure of TpRu(PPh$_3$)(κ^2-*N,O*-NH=CMeN=CMeO) (**7**)	93
Chart 3.2	Molecular structure of κ^2-*N,N* chelating complexes **D** and **D'**	103
Chart 3.3	Molecular structure of acetylacetonate, 3-azapentane-2,4-diiminate and *N*-imidoylimidate	106
Chart 3.4	Molecular structure of $(PPh_3)(CO)Ir(\kappa^2$-*N,N*-NH=C(CF$_3$)C(C(CH$_3$)=CH$_2$)=C(CF$_3$)NH)	106
Chart 3.5	Resonance structure of *N*-imidoylimidate	107
Chart 4.1	Tautomerization of ketone	132
Chart 4.2	Resonance structures of acetylacetone	133
Chart 4.3	Two tautomers of methyl ketone	140

Chart 4.4	Sigmatroptic rearrangement of 3-penten-2-one	141
Chart 4.5	Conjugation of α,β-unsaturated ketone	142
Chart 4.6	Molecular structure of TpRu(Haapy)Cl	146
Chart 4.7	Molecular structure of $RuHCl(P^iPr_3)_2(C_6H_9NO)$	150
Chart 4.8	Molecular structure of $TpRu(=C(CH_2Ph)aapy)Cl$	151
Chart 4.9	Molecular structures of 2-oxacycloheptylidene complexes	153

Abbreviations

δ	Chemical shift (NMR)
η	Descriptor for hapticity
μ	Descriptor for bridging
L	Generalized ligand, in particular a $2e^-$ ligand
[M]	Generalized metal fragment with n ligands
ESI-MS	Electro-spray ionization mass spectroscopy
FAB-MS	Fast atom bombardment mass spectroscopy
IR	Infra-red
NMR	Nuclear magnetic resonance spectroscopy
THF	Tetrahydrofuran
TMS	Tetramethylsilane
MeOH	Methanol
EtOH	Ethanol
Et_2O	Diethyl ether
DMSO	Dimethylsulphoxide
DMF	N,N-dimethylformamide
Hacac	Acetylacetone
py	Pyridine
COD	1,5-cyclooctidiene
Tp	Hydrotris(1-pyrazolyl) borate

Tp’	Hydrotris(3,5-dimethylpyrazolyl) borate
Cp	Cyclopentadienyl
Cp*	Pentamethylcyclopentadienyl
Ind	Indenyl
P^iPr_3	Triisopropylphosphine
PPh_3	Triphenylphosphine
PMe_3	Trimethylphosphine
dppm	Bis(diphenylphosphino)methane
R	Generalized alkyl group
Me	Methyl
Et	Ethyl
^iPr	Isopropyl
^tBu	t-butyl
^nBu	n-butyl
Ph	Phenyl
e^-	Electron
br	Broad
s	Singlet
d	Doublet
t	Triplet
q	Quartet
m	Multiplet
HSAB	Hard Soft Acid Base

(**1**) TpRu(PPh$_3$)(NCCH$_3$)H

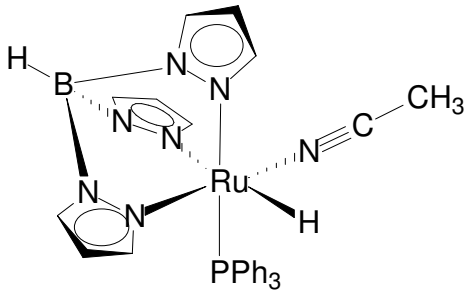

(**2**) TpRu(PPh$_3$)(H$_2$O)(NHC(O)CH$_3$)

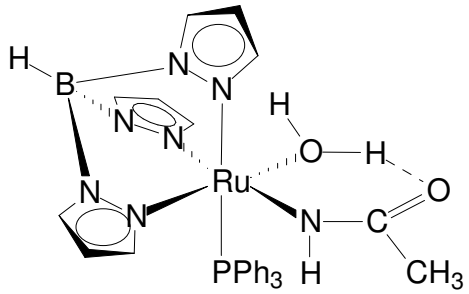

(**3**) TpRu(PPh$_3$)(CO)H

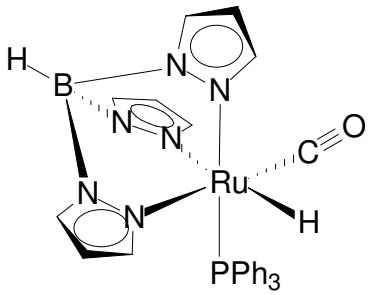

(**5**) TpRu(PPh$_3$)(H$_2$)H

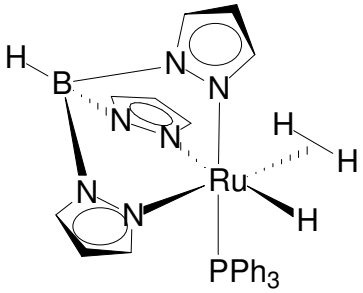

(**6**) TpRu(PPh$_3$)(NCCH$_3$)(NHC(O)CH$_3$)

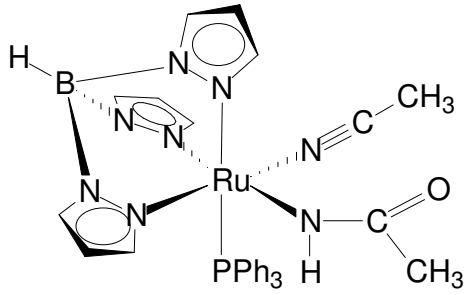

(**7**) TpRu(PPh$_3$)(κ^2-*N*,*O*-NH=CMeN=CMeO)

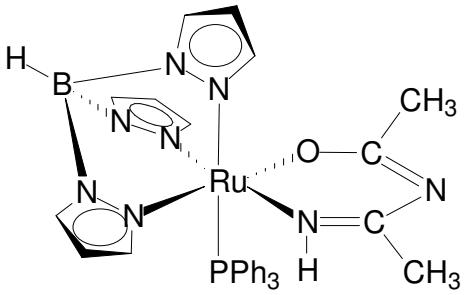

(**8**) TpRu(PPh$_3$)(H$_2$O)(NHC(O)Ph)

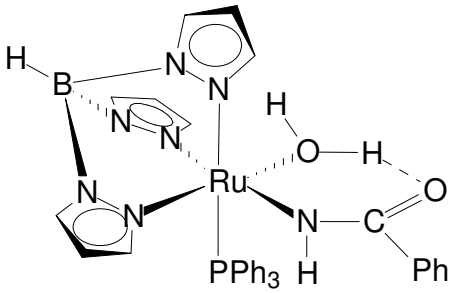

(**9**) TpRu(PPh$_3$)(NCPh)(NHC(O)Ph)

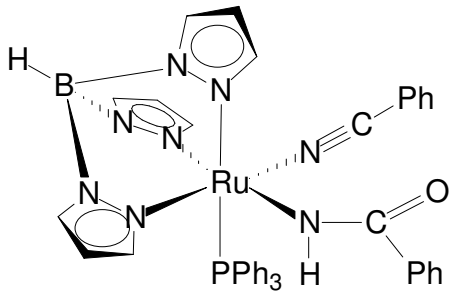

(**10**) TpRu(PPh$_3$)(κ^2-*N*,*O*-NH=CPhN=CPhO)

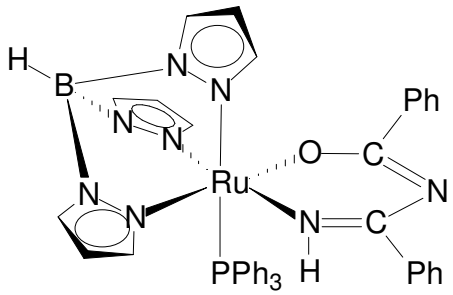

(**11**) TpRu(PPh$_3$)(κ^2-*N*,*O*-NH=CMeN=CPhO)

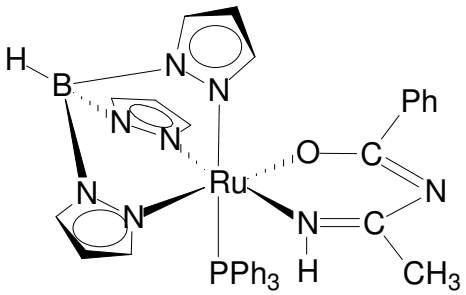

(**13**) $TpRu(PPh_3)(C(NHC(O)CH_3)=CHPh)$

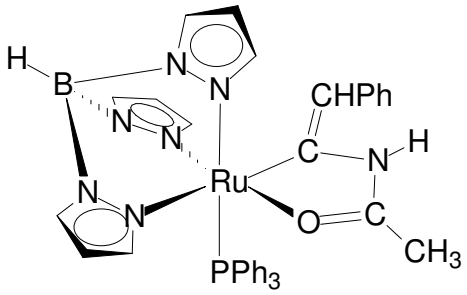

(**14**)

$[TpRu(PPh_3)(=C(CH_2Ph)NHC(O)CH_3)][BF_4]$

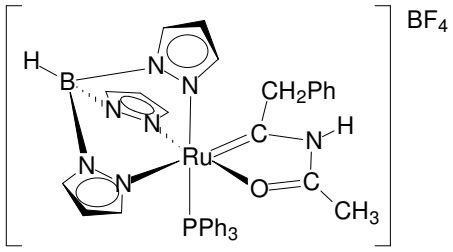

Chapter 1 Introduction

1.1 C-H bond activation

Hydrocarbons such as alkanes and arenes are the major constituents of oil and natural gas, and they are used as the main feedstock in the chemical industry. How to directly and catalytically transform hydrocarbons into more valuable products such as alcohols, ketones, and acids is a fundamental question for synthetic chemists. Creation of an atom economic and clean transformation process is more challenging, due to the high strength and the low polarity of C-H bonds, which cannot be readily activated (e.g. methane 105 kcal/mol; benzene, 110 kcal/mol). On the contrary, halide compounds (C-X, X = Cl, Br, or I) in place of hydrocarbons (C-H) are utilized in organic synthesis in most cases especially for arene compounds.[1, 2] While a reaction that uses aryl halides as reagents is catalytically efficient, the manufacture of these aryl halides is not an environmentally benign process. Moreover, halide salts as byproducts are typically produced. Thus, C-H bond functionalization has become a matter of increasing importance among both industrial and academic research units over the last few decades.[3-5]

Transition metal (TM)-catalyzed C-H bond activation implies that inert C-H bonds can be converted into other functional groups, and it provides indirect evidence for the existence of the rarely isolable agostic complexes.

Sigma(σ)-complexes involve C-H···M interactions, which were coined 'agostic' by Brookhart and Green.[6, 7] They recognized the importance of such interactions to fundamental organometallic transformations such as C-H activation and α- and β-hydride elimination. Agostic interactions involve a three-centre, two-electron system, with donation of C-H bonding electrons into a vacant orbital on the transition metal. The strength of agostic interactions is estimated to be 10 kcal mol^{-1}. These interactions are difficult to characterize by standard spectroscopic techniques. NMR and IR spectroscopies are often unable to show unequivocally evidence of the existence of such weak and fluxional C-H···M interactions. X-ray crystallography fails to clarify the C-H···M moiety. $(CH_3)TiCl_3(dmpe)$ (**Chart 1.1**) is one of the rare examples that has been studied by neutron diffraction. The Ti-C-H angle is 93.5° and Ti···H distance is 2.54 Å.[8] Agostic complexes are recognized as important intermediacies of the C-H bond cleavage reaction.(See Section 1.3)

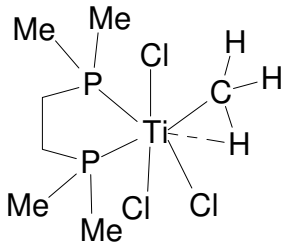

Chart 1.1 Molecular structure of $(CH_3)TiCl_3(dmpe)$

1.2 H/D exchange reactions

Isotope (H/D) exchange reaction is a common method to demonstrate C-H bond activation. Incorporation of deuterium into C-H bonds can be catalyzed by acid [9, 10], base [11], or transition metal. Transition metal-catalyzed H/D exchange reactions offer many advantages over other conventional methods. Comparably mild reaction conditions and high tolerance towards a great variety of functional groups are beneficial to suppress some undesirable side reactions such as hydrolysis, dehalogenation, and deuterium addition to unsaturated organic functions. Moreover, efficient deuterium incorporation with high regioselectivity can be achieved by TM-catalyst systems.[12]

H/D exchange reactions are also important for synthesizing isotopically labeled compounds. Exchange of hydrogen for deuterium in a target molecule is a more efficient and cost effective method than direct synthesis of the deuterium-labeled molecule. These isotopically labeled compounds can be used as internal standards in mass spectrometry for pharmaceutical and biochemical studies, as they display the same retention and ionization behavior in LC/MS with their original compounds, but with different mass. Moreover, these deuterated compounds are used as reagents in mechanistic investigations and as solvents for NMR spectroscopy.[12]

1.3 Mechanism of C-H bond activation

It is commonly known that TM-catalyzed C-H σ bond activation is achieved by an oxidative addition reaction to form an alkyl hydride complex, which, in some cases, is isolable at very low temperature.[13-24] Full oxidative addition of a C-H σ bond is prompted by the higher degree of *d*-electron back-donation from the metal center to the σ* anti-bonding orbital of the C-H bond. On the other hand, the cleavage of a C-H bond can be achieved via 4-centre σ-bond metathesis in which the η^2- coordinated ligand (H-X), added across the metal-ligand bond (M-Y), undergoes ligand exchange mediated by the metal center without formal oxidative addition.(**Scheme 1.1**) The difference between these two pathways is that in an oxidative addition mechanism, the hydrogen atom transfers to the metal center to form a metal hydride, but in the σ-bond metathesis, it transfers to the cis-ligand only.

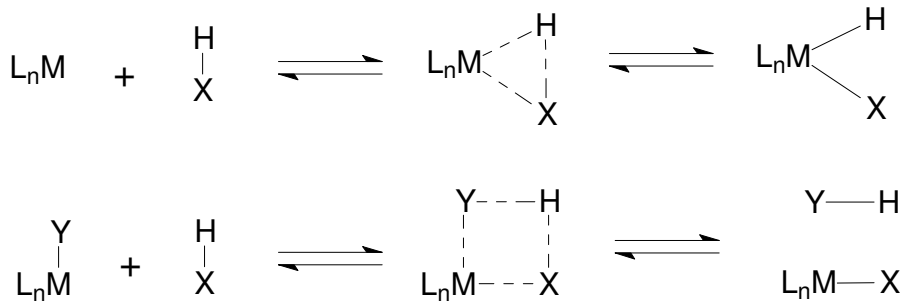

Scheme 1.1 Two reaction pathways: oxidative addition (Top) and σ-bond metathesis (Bottom) of a H-X moiety

In 1969, Shilov *et al.* demonstrated the first example of activation reactions of C-H bonds in alkanes by using Pt(II) salts as catalysts.[25] They then discovered an

alkane oxidation system and proposed the mechanism that consists of the activation of alkane by a Pt(II) complex to generate an alkyl Pt(II) complex, subsequent oxidation of the metal center to form a Pt(IV) alkyl intermediate and reductive elimination to yield the oxidized alkane and to regenerate the Pt(II) complex.[5, 26]

Wick and Goldberg have reported reactions of a Pt(II) complex K[(η^2-Tp')$PtMe_2$] (Tp' = hydridotris(3,5-dimethylpyrazolyl)) with $B(C_6F_5)_3$ in arene and alkane solvents such as benzene, pentane, and cyclohexane (R-H), to yield a Pt(IV) complex, (η^3-Tp')PtMeRH. (**Scheme 1.2**) It is the first example of intermolecular oxidative addition of C-H bonds to a Pt(II) metal center to form a stable Pt(IV) alkyl hydride complex.[17]

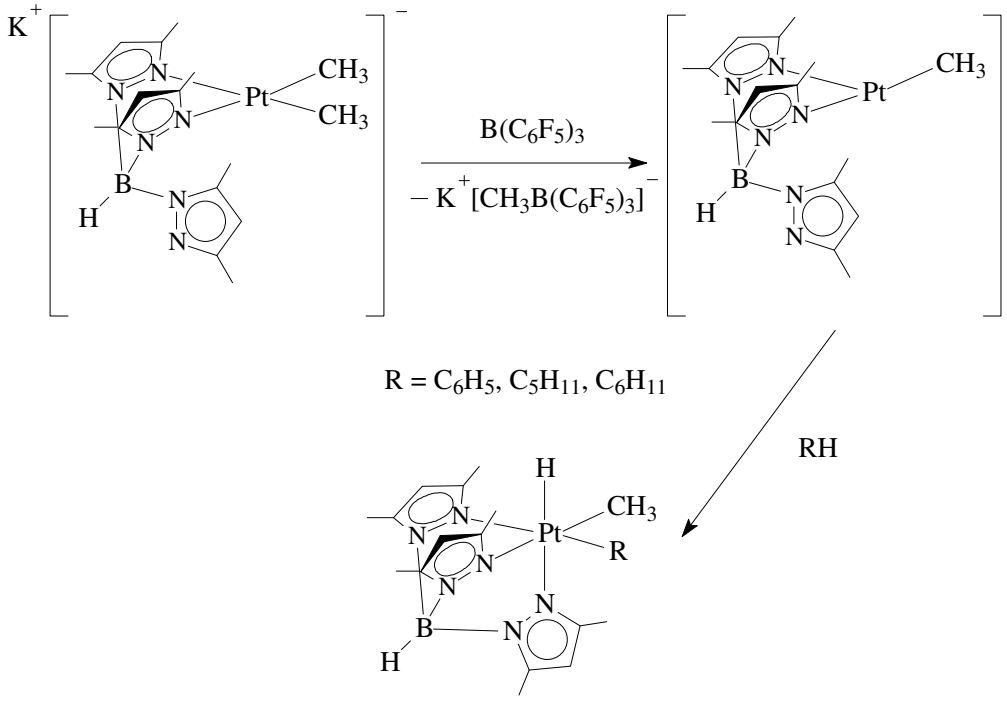

Scheme 1.2 Oxidative addition of R-H to K[(η^2-Tp')$PtMe_2$] in the presence of $B(C_6F_5)_3$

Tilset *et al.* have also observed that an oxidative addition product [(N-N)Pt$(CH_3)_2$(H)(L)][BF_4] (L = H_2O or trifluoroethanol; N-N = ArN=CMe-CMe=NAr where Ar = 3,5-$(CF_3)_2C_6H_3$) is formed in situ by reacting a dichloromethane solution of (N-N)Pt$(CH_3)_2$ with HBF_4 at – 78 ^oC. At temperatures above – 40 ^oC, this Pt(IV) hydride complex [(N-N)Pt$(CH_3)_2$(H)(L)][BF_4] decomposes to release methane and gives an unidentified product. It raises the possibility that the observed C-H bond activation of benzene by [(N-N)Pt$(CH_3)(H_2O)$][BF_4] proceeds by an oxidative addition pathway. The catalytic C-H bond activation was investigated with DFT calculations. The result showed that the oxidative addition pathway is favored by 12 kJ/mol relative to the σ-bond metathesis.[18]

A similar conclusion was drawn by Hush *et al.* in a theoretical study of the activation of methane by trans- and cis- platin systems (Shilov type reaction). In the case of cis-platin the C-H activation is expected to emerge from both σ-bond metathesis and oxidative addition because of the comparable energy barriers of these two pathways. On the other hand, it is predicted that the C-H bond cleavage occurs predominantly via an oxidative addition pathway in a trans-Pt(II) system ($PtCl_2(NH_3)_2$), as the σ-bond metathesis is associated with a much higher energy barrier. They also found that, in line with accepted ideas on trans influence, the methyl and hydride ligands in the Pt(IV) complexes formed by oxidative addition reactions are always cis to each other. In light of this finding, the energies of several methyl hydrido Pt(IV) bisulfate complexes (cis-isomers) were also recalculated; the new results provide evidence for the thermodynamic feasibility of the oxidative

addition of methane to catalysts such as $[Pt(NH_3)_2(OSO_3H)_2]$ and $[Pt(NH_3)_2(OSO_3H)(H_2SO_4)]^+$.[19]

Iridium(III) system $[Cp^*Ir(PMe_3)(Me)]^+$ has been found to be an effective catalyst for C-H bond functionalization.[20, 23, 24] Much effort has been contributed to figuring out the reaction pathway, but among these studies, neither the oxidative addition pathway nor σ-bond metathesis can be eliminated from each other. Although theoretical studies support an oxidative addition pathway via Ir(V) intermediates[21], only a few examples of stable Ir(V) complexes have been prepared and isolated.[22] Very recently, Bergman and co-workers [16] have demonstrated an intramolecular transformation between two different Ir(V) complexes via an Ir(III) intermediate. It supports an Ir(III) → Ir(V) → Ir(III) mechanistic pathway (oxidative addition/reductive elimination) in C-H bond activation. They also synthesized an isolable and fully-characterized aryl hydride Ir(V) complex with a silylene supporting unit from an Ir(III) precursor. It is an additional support for the viability of the Ir(III) to Ir(V) C-H oxidative addition reaction. This experimental evidence provides more clues for assigning the mechanistic pathway.

On the other hand, four–center σ-bond metathesis involving the addition of a C-H bond across a metal-ligand bond in high-valent electrophilic complexes is exemplified by C-H bond activation by early TM, lanthanide or actinide complexes.[27-32] Some early TM hydrides, especially those without d-electron (d^0),

that are unable to support oxidative addition, are capable of catalyzing transformation reactions through the σ-bond metathesis pathway. Meanwhile, theoretical studies and Hückel MO analysis suggest that the d^0 metal centers favor the σ-bond metathesis mechanism. [33-35]

Siegbahn and Carbtree re-examined the Shilov reaction by quantum chemical studies. They found that in the Pt(II) model trans-$PtCl_2(H_2O)_2$, the activation of C-H bonds of methane proceeding via the transfer of a hydrogen atom from a methane σ complex to a neighboring Cl ligand is best described as σ-bond metathesis. An oxidative addition/reductive elimination sequence, however, cannot be safely excluded in this case. For the models of Pd(II)- and Hg(II)-catalyzed C-H bond activation, a σ-bond metathesis pathway must be involved due to the instability of Pd(IV) and the nonexistence of Hg(IV).[36] It is a rare example to suggest a late TM preferentially undergoing the σ-bond metathesis in C-H bond activation.

Whether a C-H bond activation process involves the oxidative addition or σ-bond metathesis is a fundamental question. However, it is very difficult to distinguish experimentally a σ-bond metathesis pathway from an oxidative addition/reductive elimination sequence. Tentatively, we can conclude that the oxidative addition pathway preferentially emerges in late TM complexes.

1.4 Catalytic C-H bond activation by metal hydride complexes

Since Wilkinson published the first transition metal (TM) hydride complex Cp_2ReH in 1955 [37], hydride complexes have drawn much attention. A lot of research has been contributed to the characterization and reactivity studies of hydride complexes. To date, transition metal hydrides are an important class of organometallic complexes in academic studies and industrial processes.[38-41]

Hydride is a versatile ligand due to its nucleophilicity. It can insert into unsaturated organic functions. Classical transition metal hydrides are well known as an important intermediate of catalytic hydrogenation of unsaturated organic functions.[42] The metal hydride is commonly formed via oxidative addition of dihydrogen to the metal center.

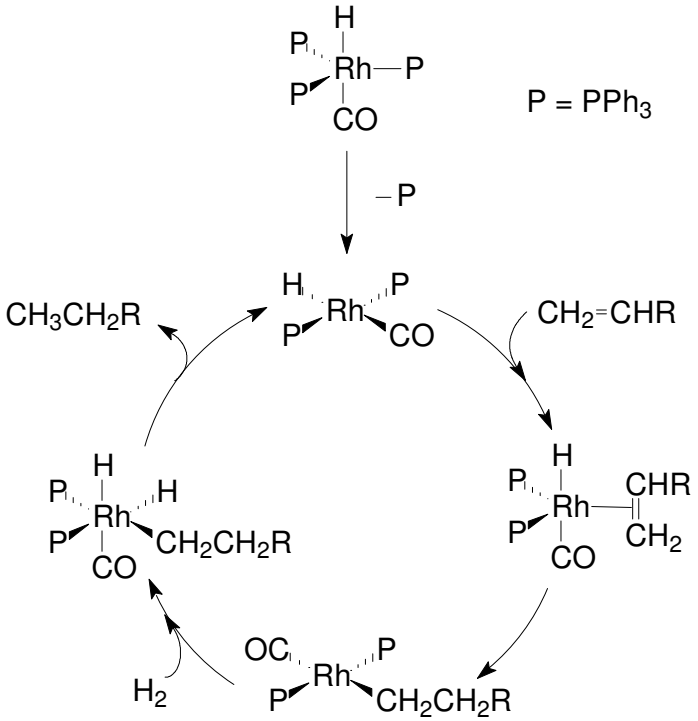

Scheme 1.3 Catalytic cycle of $[(PPh_3)_3(CO)RhH]$ catalyzed alkene hydrogenation

As shown in Scheme 1.3, the catalytic hydrogenation of olefins with $[(PPh_3)_3(CO)RhH]$ is initiated by the insertion of olefins to the Rh-H bond to form an Rh-alkyl complex. Subsequent oxidative addition of hydrogen forms a dihydride intermediate. The hydrogenation is completed by reductive elimination of the alkane product.

Hydride ligand also facilitates the external nucleophilic attack (see Section 1.6, dihydrogen bond-mediated reactions), and activates the adjacent ligand (nucleophilic abstraction). We can notice in this section that hydride activates the adjacent agostic C-H bond to form a dihydrogen species.

Alb é niz and Crabtree have reported that the 2,6-diarylpyridine Ir (III) complexes contain an agostic C-H bond trans to an Ir-aryl (Ir-C) moiety. (**Scheme 1.4**) Rapid interconversion between C-H···Ir-C and C-Ir···H-C was observed at room temperature. This reversible metalation of an agostic C-H bond of the aryl moiety proceeds via a η^2-H_2 complex. Oxidative addition of the second *o*-C-H bond in the second phenyl ring is unlikely because of inadequate basicity of the Ir(III) center. It is an example of C-H bond cleavage via abstraction of a proton by a hydride to give a dihydrogen complex.[43, 44]

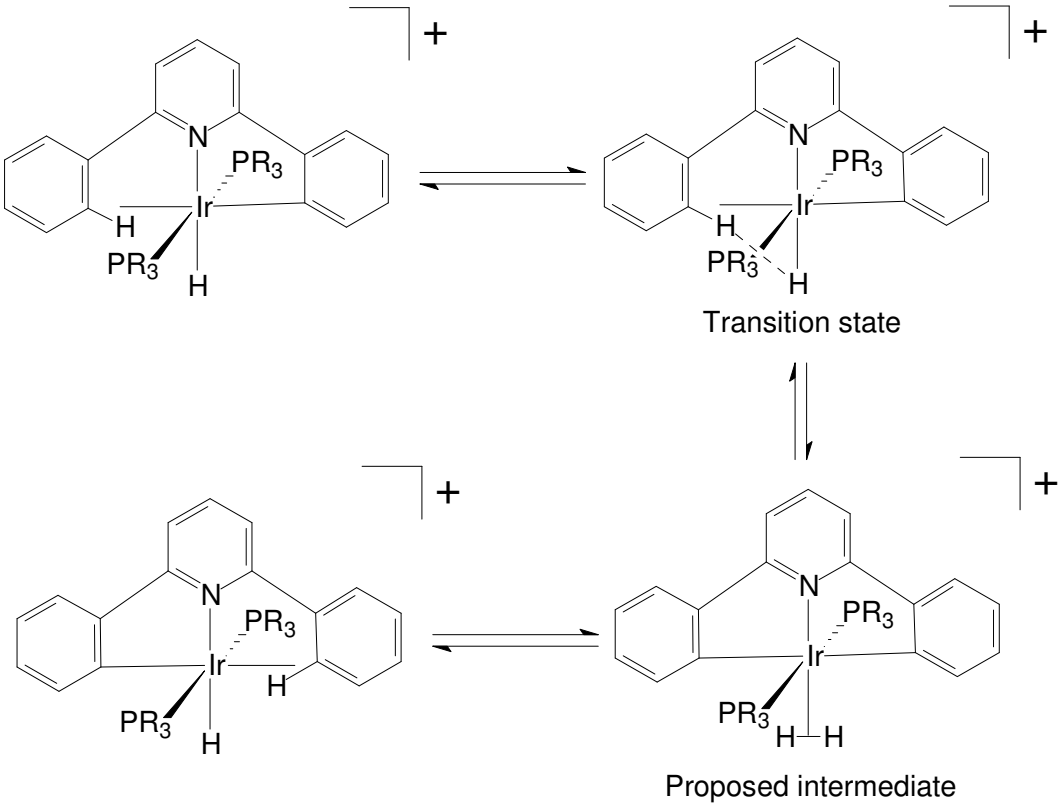

Scheme 1.4 Interconversion of 2,6-diarylpyridine Ir (III) complexes

Chaudret *et al.* have shown a rare Ru complex $[RuH(H_2)(o\text{-}C_6H_5py)(P^iPr_3)_2][BArf]$ [BArf = $B[C_6H_3(CF_3)_2]_4$] that contains both a dihydrogen ligand and a weak agostic bond. It is in equilibrium with a metalated η^2-H_2 aryl complex by releasing a hydrogen molecule. (**Scheme 1.5**) Density functional theory calculations showed that the activation energy of this process is low, because the simultaneous presence of cis hydride and dihydrogen ligands enables the proton transfer.[45]

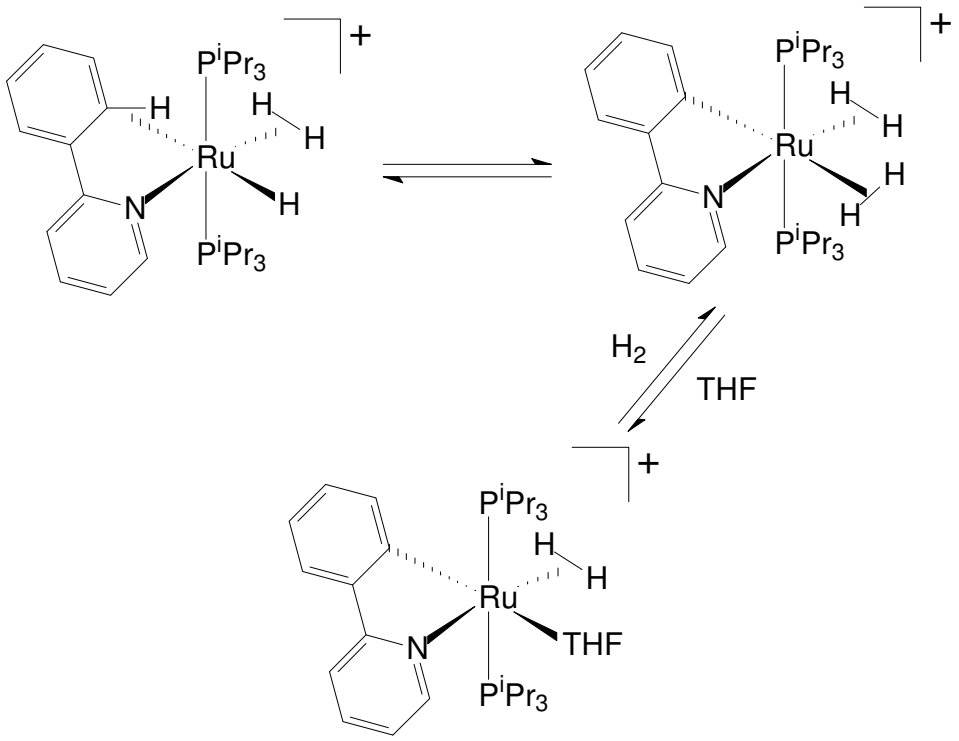

Scheme 1.5 Interconversion between a dihydrogen agostic Ru complex and a dihydrogen aryl Ru complex via a bis(dihydrogen) species

Lau *et al.*demonstrated that a Ru(II) complex $TpRu(PPh_3)(CH_3CN)H$ catalyzes H/D exchange between CH_4 and some deuterated organic solvents such as benzene-

d_6, tetrahydrofuran-d_8 and dioxane-d_6. A detailed mechanistic study of the C-H bond activation by density functional theory calculations was carried out. Theoretical studies showed that σ-complexes $TpRu(PPh_3)(\eta^2\text{-H-R})H$ are active species in the exchange process. In the course of the H/D exchange processes, the reversible transformations of $TpRu(PPh_3)(\eta^2\text{-H-R})H$ to $TpRu(PPh_3)(\eta^2\text{-H-H})R$ are the crucial step. Interestingly, the transition states for the transformations correspond to seven-coordinated $TpRu(PPh_3)(R)(H)(H)$ species, which result from the oxidative addition of H-R to the metal center. This seven-coordinated Ru(IV) complex is transient, in compliance to the fact that the Tp ligand generally enforces an octahedral geometry about the metal center.[46]

Bergman and co-workers [47] synthesized an Ir(III) complex $[Cp^*(PMe_3)IrH(ClCH_2Cl)][MeB(C_6F_5)_3]$, which is capable of C-H bond activation at an unexpectedly high rate and surprisingly low temperature. They proposed that the most likely mechanism for the C-H bond activation with this Ir(III) complex involves the intermediacy of the dihydrido alkyl Ir(V) species $[Cp^*(PMe_3)IrH_2R]^+$ resulting from the oxidative addition of a C-H bond to the metal center. An interesting feature of this Ir(V) complex is that elimination of R-H is preferential to release of an H_2 molecule.[48] Although the function of the hydride ligand is not specified in this case, we believe that hydride can facilitate the C-H bond activation.

1.5 H/D exchange by using deuterium oxide as deuterium source

Deuterated compounds are widely used as reagents in mechanistic investigation and as solvents for NMR spectroscopy. Preparation of deuterated compounds by using environmentally benign D_2O as deuterium source is rare. Bergman *et al.* [49] have recently reported that the Ir(III) complex $Cp^*(PMe_3)IrCl_2$ effectively catalyzes the H/D exchange between D_2O and organic molecules unlike the pioneering K_2PtCl_4 system which requires addition of stabilizers and acid for preventing disproportionation of the catalyst and maintaining homogeneity.[25, 50-52]

The O-donor iridium–methoxo complexes [Ir(acac-*O,O*)$_2$(OMe)(L)] (L = pyridine or methanol) are capable of catalyzing H/D exchange between D_2O and benzene at 160^{o}C, albeit with very low turnover frequency. It is anticipated that the Ir-OCH_3 group is converted to an Ir-OH moiety which can reversibly activate the C-H bonds of benzene, generating Ir-Ph and water. Theoretical calculations showed that this system favors a σ-bond metathesis mechanism over one that involves an oxidative addition pathway. Possible reasons for this are that the lone pair on the methoxo oxygen facilitates the hydrogen transfer, and the lower electron density of the Ir center disfavors the oxidative addition process.[53]

A rhodium (I) precursor reacts with a PC type ligand, benzyl (di-*tert*-butyl)phosphane (aryl-PC) to form an aryl hydride Rh(III) complex (**Chart 1.2**), which undergoes reversible *o*-aryl C-H bond activation of the PC ligand and

promotes catalytic H/D exchange between vinylic hydrogens of olefins with deuterated methanol or water. DFT calculations were preformed to describe the oxidative addition of the *o*-aryl C-H bond to the Rh(I) precursor via η^2-C-H agostic intermediates. From the detailed studies of the structure of these agostic intermediates, it is found that the agostic hydrogen is acidic in nature; increase in acidity implies that the donation of the η^2-C-H σ-bond to the metal center is strong. When the donation is high enough, the agostic hydrogen can be expelled as a proton or abstracted by a base. The acidic agostic hydrogen thus is capable of exchanging with deuterated water or methanol.[54]

S = Solvent such as THF, methanol, and acetone

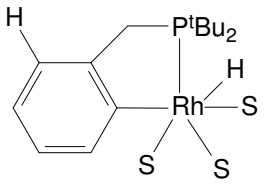

Chart 1.2 Molecular structure of aryl hydride Rh (III) complex

1.6 Dihydrogen bond-mediated reaction

Milstein and co-workers have reported a neutron-diffraction structure of a Ir(III) complex $[(PMe_3)_4IrH(OH)]PF_6$ (**Chart 1.3**) in which the distance between the hydride and hydroxyl proton is 2.4 Å, within the range of the van der waals contact distance.[55] Carbtree *et al.* [56] have prepared an iminol iridium complex $[((C_9H_6N)N=C(OH)Me)IrH_2(PPh_3)_2]SbF_6$ in which the intramolecular dihydrogen bonding between Ir-H and H-O bonds stabilizes the rare iminol tautomer. The

dihydrogen bond distance is estimated at 1.8 Å by NMR T_1 measurements. Morris *et al.* [57] have reported another iridium complex $[(C_5H_5NS)_2IrH_2(PCy_3)_2]BF_4$, which shows two close dihydrogen-bond distances between Ir-H and H-N bonds, estimated at 1.75 Å by NMR T_1 measurements.

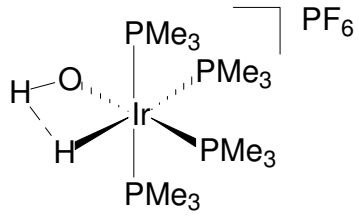

Chart 1.3 Structure of $[(PMe_3)_4IrH(OH)]PF_6$

Dihydrogen bonding can be utilized to control the reactivity and regioselectivity of chemical reactions. Yao and Crabtree [58] demonstrated the promotion of the reaction rate of imination of a coordinated aldehyde by a dihydrogen bonding interaction. They found that the *ortho* isomer of the aminophenols which can intramolecularly dihydrogen-bond to the hydride ligand of $[IrH_2(\eta^2\text{-}2\text{-}C_5H_4NCHO\text{-}N,O)(PPh_3)_2]^+$ in the imination reaction, gives a reaction rate higher than that of the *para* isomer. It is believed that the intramolecular dihydrogen bonding between O-H and Ir-H can stabilize the transition state of the reaction. (**Scheme 1.6**)

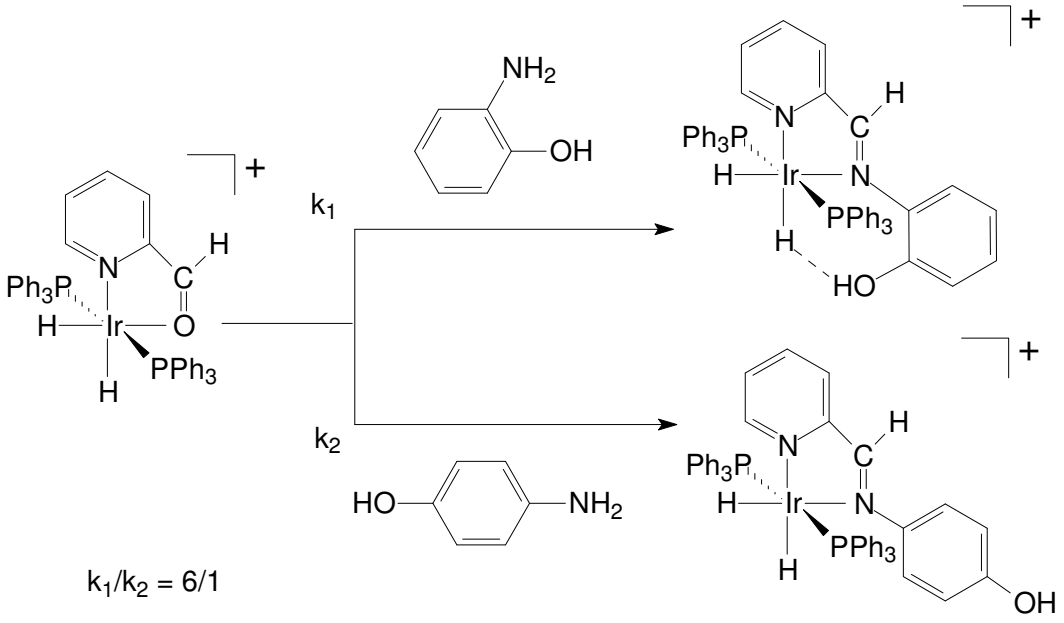

Scheme 1.6 Imination of coordinated aldehyde with 2-aminophenol or 4-aminophenol

Our research group has also demonstrated a dihydrogen-bond-promoted catalytic hydration reaction of nitriles. An indenyl ruthenium hydride complex (η^5-C_9H_7)Ru(dppm)H was found to be active in catalyzing the hydration of nitriles to amides. The chloro analogue (η^5-C_9H_7)Ru(dppm)Cl, however, was found to be inactive. If the common nucleophilic attack of H_2O at the carbon of the bound nitrile is the crucial step of this hydration reaction, the chloro analogue containing an electron withdrawing ligand (Cl) should render the nitrile carbon more susceptible to water attack. The proposed mechanism is that the process is initiated by the dissociation of an arm of the bidentate ligand (dppm) or the η^5 - η^3 ring slippage of indenyl ligand,[59, 60] and followed by nitrile coordination. Subsequently, the incoming water, with the assistance of the dihydrogen-bonding interaction with the

hydride ligand, attacks the bound nitrile carbon to form an iminol moiety. The cycle is completed by the dissociation of an iminol product to regenerate the indenyl complex. (**Scheme 1.7**) Density functional theory calculations at the B3LYP level provide explanations for the difference between the hydride- and chloro- complex-catalyzed nitrile hydration. The dihydrogen-bonding interaction between the metal hydride and the incoming water molecule can lower the activation energy of the C-O bond formation step of the hydration reaction. A similar dihydrogen bond-promoting effect is believed to be responsible for the catalytic activity of the Tp ruthenium complex $TpRu(PPh_3)(CH_3CN)H$ in CH_3CN hydration.[61]

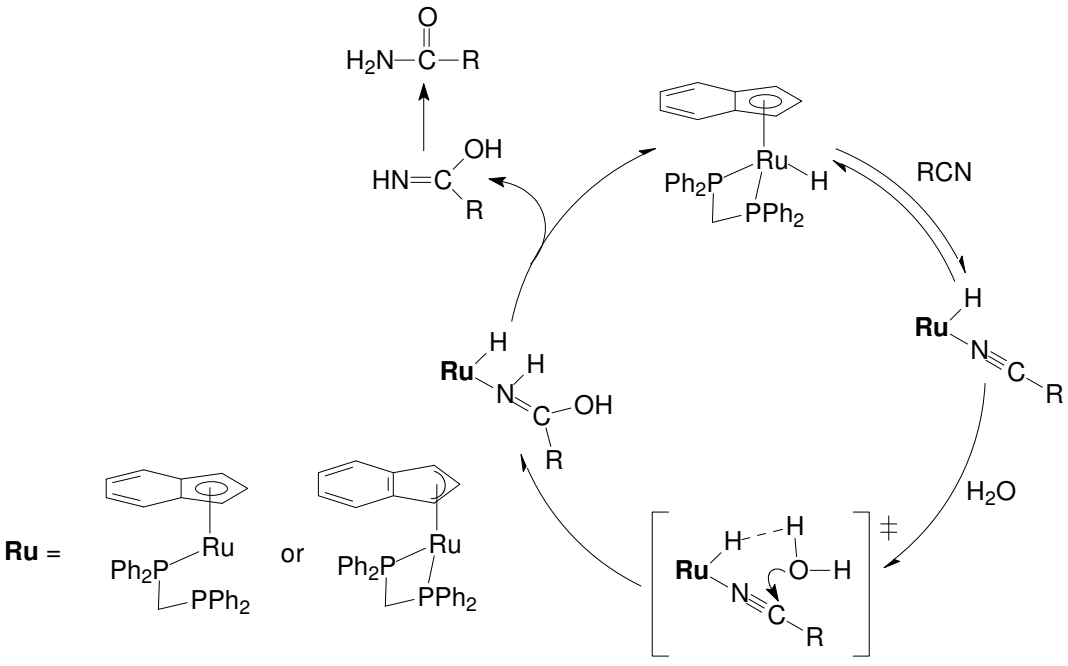

Scheme 1.7 Catalytic hydration of nitriles by $(C_9H_7)Ru(dppm)H$

1.7 Transition metal-catalyzed nitrile hydration

Preparation of amides from hydration of nitriles is important in view of industrial applications and pharmacological interest. Traditional preparative methods involve addition of acid or base into the catalytic systems. In the vast majority of cases, a base-catalyzed reaction leads to further hydrolysis of amides to carboxylate salt due to the fact that the hydrolysis (conversion of amides to carboxylic acids) is often faster than the hydration (conversion of nitriles to amides), the reaction thus proceeds to the final product rather than stopping at the amide stage. On the other hand, addition of acids requires a careful control of the temperature and the ratio of reagents to prevent the formation of polymer promoted by the exothermic hydrolysis reaction.[62] Moreover, further product purification is required to remove salts formed by neutralization of acid or base.[63] These difficulties can be overcome with the use of TM as an activator. Advantages of TM-catalyzed nitrile hydration over conventional acid- or base- catalyzed reactions include milder reaction conditions, higher tolerance to other functional groups and a higher reaction rate.[64-66]

1.8 Common mechanisms of catalytic nitrile hydration with transition metal

Common mechanisms of TM-catalyzed nitrile hydration involve intramolecular nucleophilic attack of a hydroxo (or aquo) ligand or external attack of a hydroxide ion (or water) at the carbon atom of the η^2-coordinated nitrile to form the metal

amide intermediate and subsequent protonation of amido ligand by an adjacent aquo ligand or solvent water.[67-76] Tyler *et al.* [77] have demonstrated that a monomer $[Cp'_2Mo(OH)(H_2O)]^+$ (Cp' = η^5-$CH_3C_5H_4$) formed by dissolving $[Cp'_2Mo(\mu\text{-}OH)_2MoCp'_2]^{2+}$ in aqueous solution catalyzes nitrile hydration under mild conditions. They proposed a mechanism (**Scheme 1.8**) that involves several steps: the initial step is dissociation of the water ligand to create a vacant site for the association of the nitrile. Intramolecular nucleophilic attack of hydroxo ligand on the coordinated nitrile to form a η^2-amido complex is the subsequent step. The final step can occur in two pathways; one is the coordination of water, followed by proton transfer and subsequent dissociation of the amide, another involves the oxidative addition of water and reductive elimination of amide to regenerate the active catalyst.[78-80] (**Scheme 1.9**)

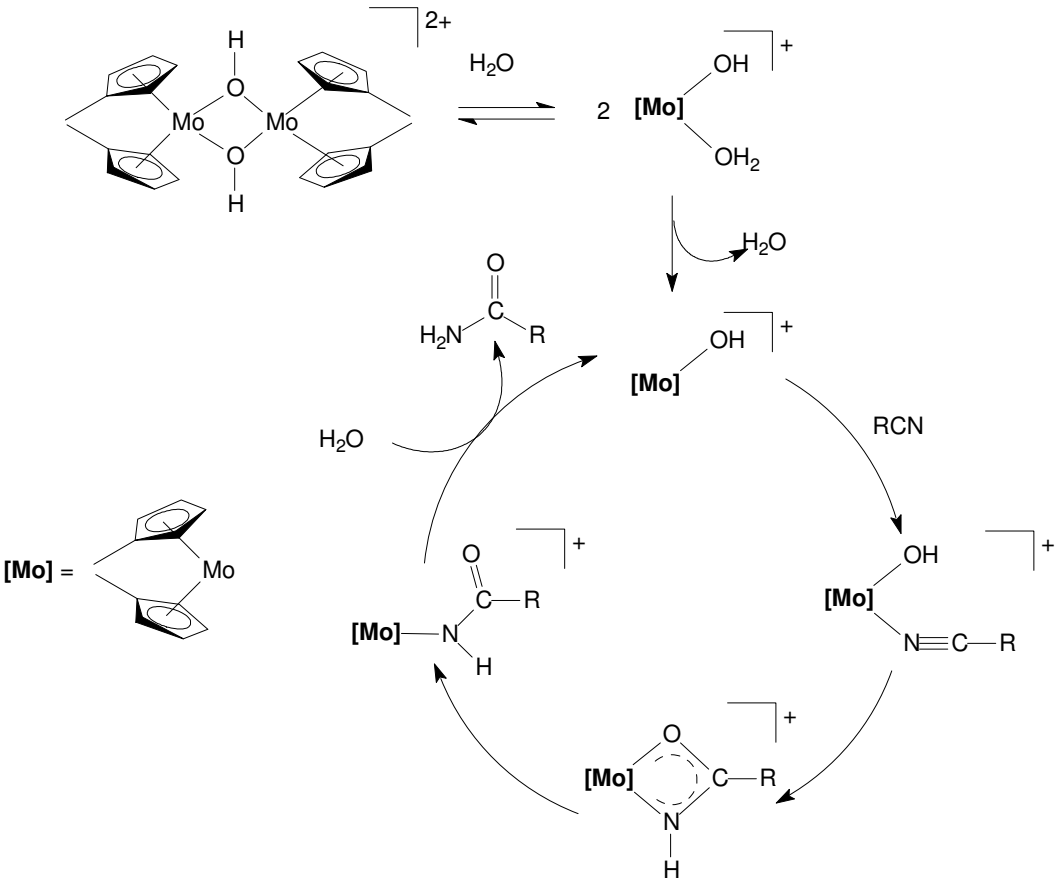

Scheme 1.8 Proposed mechanism of nitrile hydration via $[Cp'_2Mo(OH)(OH_2)]^+$

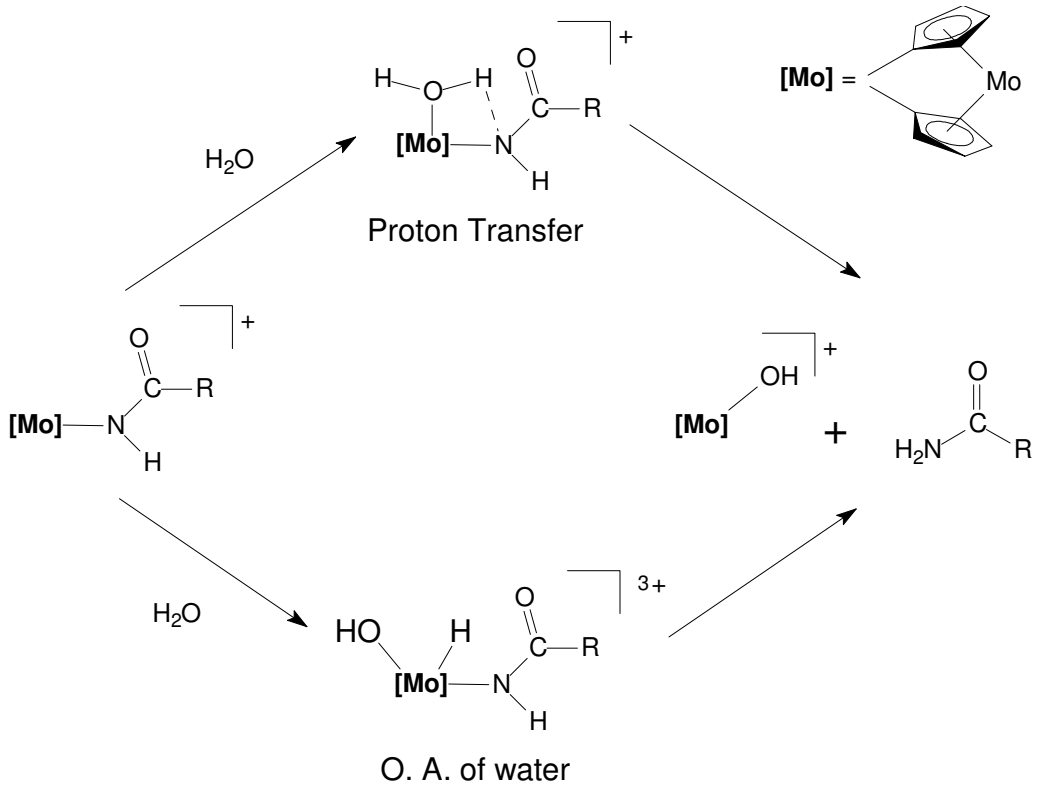

Scheme 1.9 Two possible pathways for regeneration of [Mo]-OH complex

Chin and coworkers reported that $[Co(cyclen)(OH_2)_2]^{3+}$ (cyclen = 1,4,7,11-tetraazacyclododecane) is an effective catalyst for hydration of nitriles at 40 ^oC, albeit with a low catalytic turnover number. Supported by detailed kinetic study, they proposed mechanism that involves coordination of nitrile to the cobalt complex followed by intramolecular nucleophilic attack of hydroxo ligand on the coordinated nitrile to form a stable chelated amido complex and eventual protonation of the chelated amido ligand and dissociation of the amide to regenerate the aquo hydoxo cobalt complex. (**Scheme 1.10**) The structure of $[Co(cyclen)(\eta^2\text{-}N,O\text{-benzamide})](ClO_4)_2$, one of the key intermediates in the catalytic cycle, was determined by X-ray crystallography.[81]

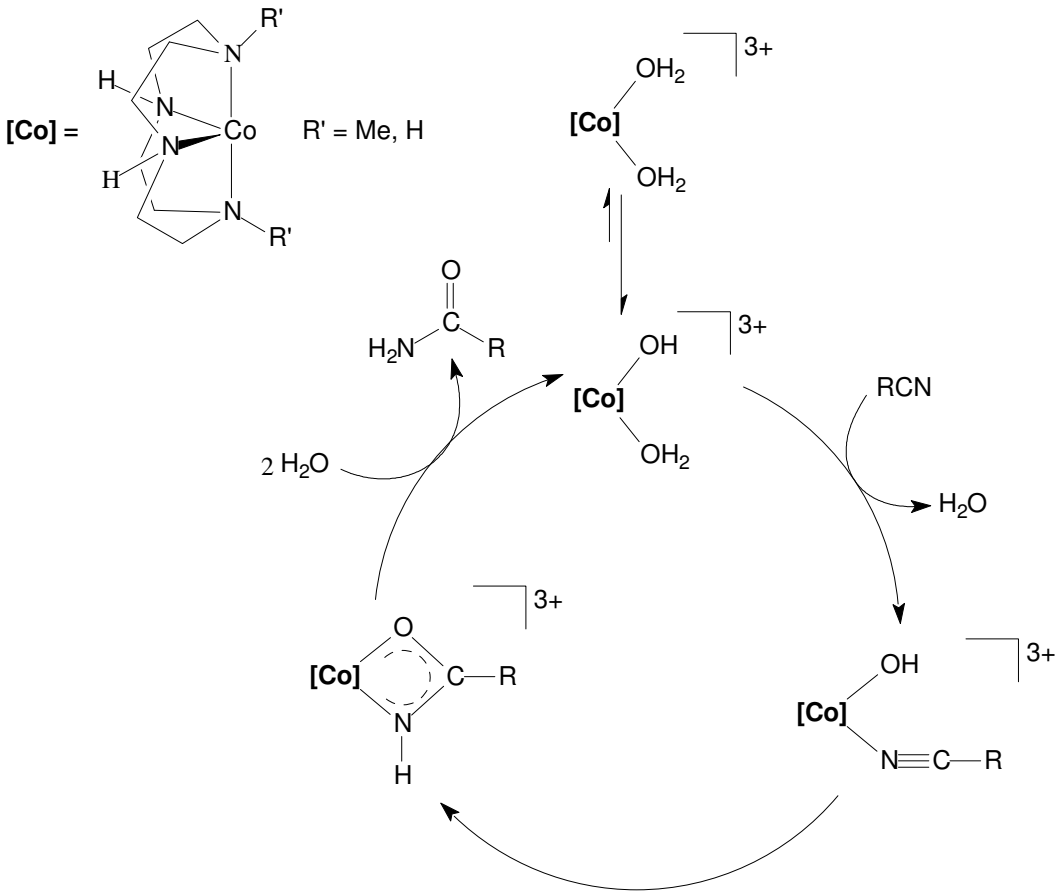

Scheme 1.10 Proposed mechanism of nitrile hydration via $[Co(cyclen)(OH_2)_2]^{3+}$

Kaminskaia and Kostic [82] have also carried out detailed kinetic investigation of aquo palladium complexes that are capable of catalyzing hydration of nitriles to amides. They proposed a general mechanism that is composed of two connected cycles: each cycle consists of four steps: coordination of the nitrile to the catalyst; attack of water and formation of coordinated iminol (bidentate iminol for internal attack and monodentate iminol for external attack); tautomerization of the iminol into amide; and dissoication of the amide product. Release of amide can occur by displacement of water or nitrile, depending on their concentration in the system.

They mentioned that formation of iminol results from both internal and external attacks, which occur at a similar rate on the nitrile ligand by the neighboring aqua ligand and the solvent water, respectively.(**Scheme 1.11**)

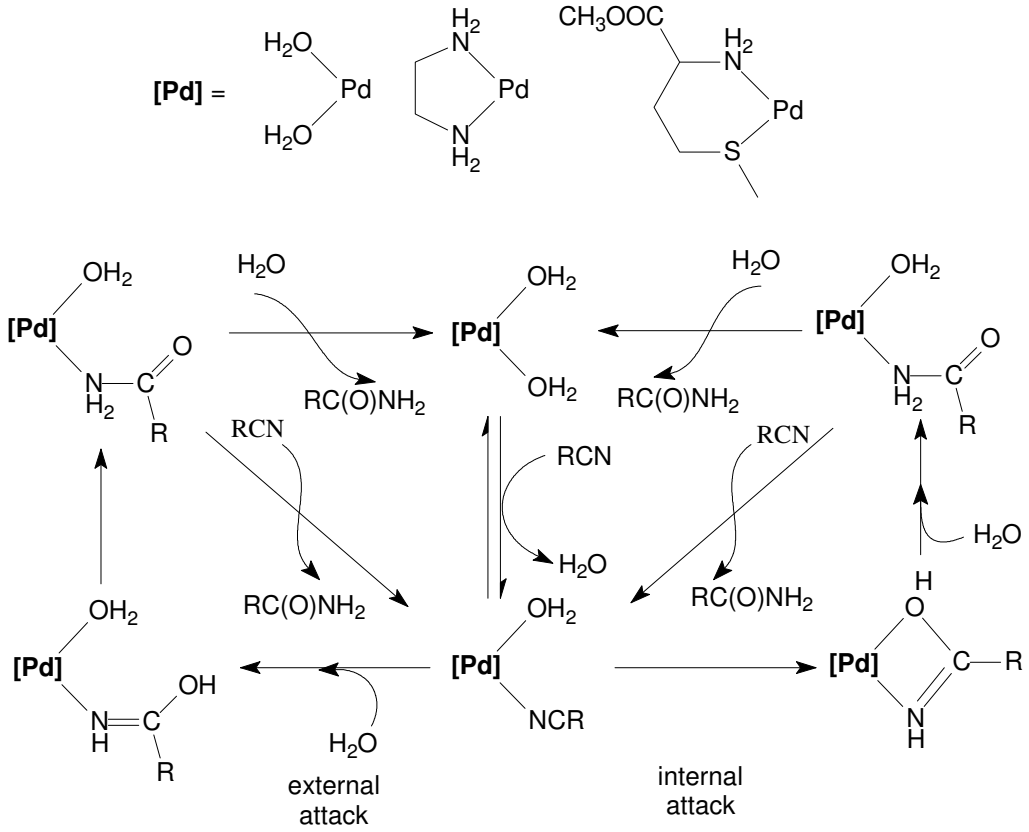

Scheme 1.11 Two proposed mechanisms of catalytic nitrile hydration by aquo Pd complexes

It has recently been reported that the ruthenium complex *cis*-Ru(acac)(PPh_2py)$_2$ (acac = acetylacetonate; PPh_2py = 2-diphenylphosphinopyridine) is an excellent catalyst for the hydration of nitriles to amides under neutral condition. The feature of the proposed mechanism is that the nucleophilic addition of water to the nitrile

ligand is promoted by the hydrogen-bonding interaction of the former with the pendant pyridinyl moiety of the PPh_2py ligand.[83] (**Scheme 1.12**)

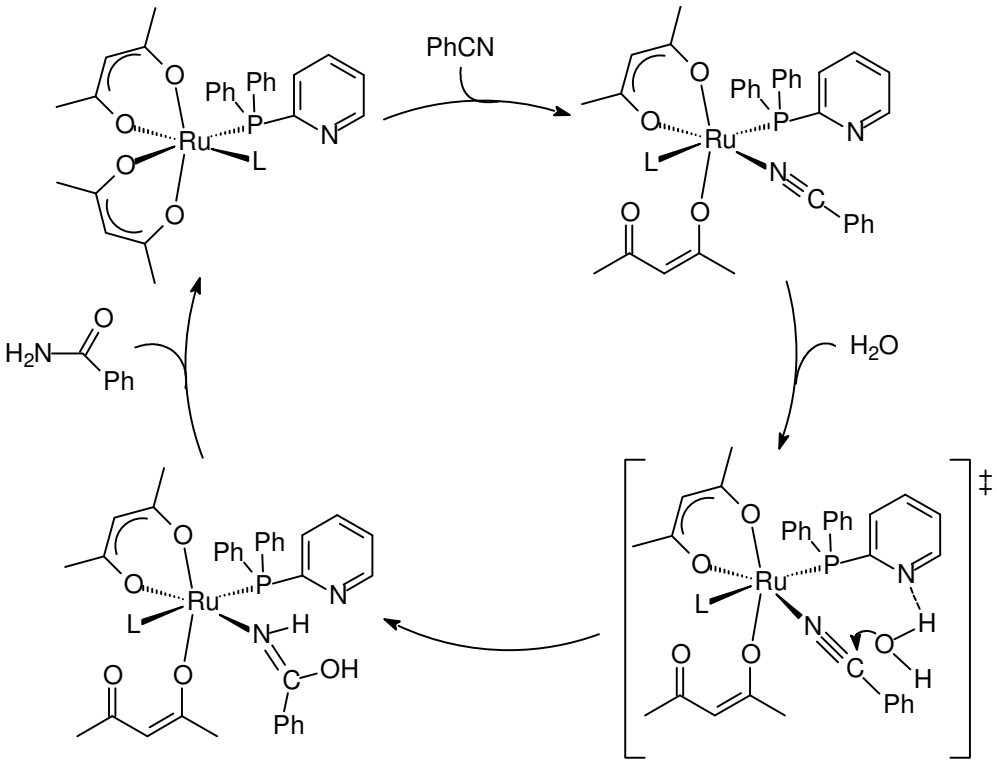

Scheme 1.12 Hydration of benzonitrile catalyzed by cis-Ru(acac)(PPh_2py)$_2$

1.9 Hydrolytic coupling of nitrile complexes

Many TM-mediated nitrile hydration systems are not catalytic. A plausible reason is that the active form of the catalysts cannot be regenerated after the formation of some highly stable metal-bound amido complexes. Complexes such as $[(NH_3)_5M(MeCN)]^{x+}$ (M = Ru(II), Ru(III), Rh(III), and Ir(III)), and $[(NH_3)_4Co(\mu\text{-}OH)(\mu\text{-}NH_2)(Co)(NH_3)_4]^{4+}$ are examples of these systems.[84-86] It is believed that

the amido ligands, which are capable of binding to a great variety of metal ions via N and/or O atoms based on the HSAB principle, are bound strongly and not readily removable from the TM center. Some unusual hydrolytic transformations such as hydrolytic coupling of nitriles have thus been observed.

Hiraki *et al.* have reported that the complex [RuCl(H)(CO)(PPh_3)$_3$] is converted to the *N*-imidoylimidate complex (**Chart 1.4**) by reacting with *p*-MeC_6H_4CN and water at 120°C. The addition of water is essential for this transformation. It was indicated that the formation of this metallacycle proceeds via an initial hydration of ArCN to give the amido species followed by the *N*(amido)-to-*C*(nitrile) coupling with another nitrile molecule.[87]

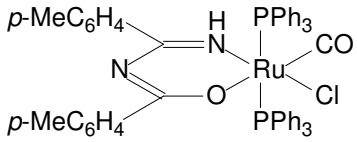

Chart 1.4 Sturcture of *N*-imidoylimidate Ru complex

An unusual metallacycle platinum(II) complex has been reported by Melanson and coworkers.[88] This hydrolytic coupling of nitriles is observed when K[$PtCl_3(Me_2SO)$] is treated with Cl_3CCN in aqueous media. A possible mechanism involves the hydration of Cl_3CCN to the corresponding amide, followed by *N*(amido)-to-*C*(nitrile) coupling with the adjacent nitrile and subsequent hydrolysis of the imino group thus formed. This metallacycle is stabilized by deprotonation to generate an aromatic system.(**Chart 1.5**)

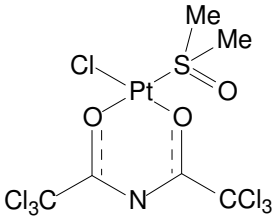

Chart 1.5

Platinum (IV) complex trans-$[PtCl_4(NCNMe_2)_2]$ undergo hydrolysis in a solution of undried Et_2O and CH_2Cl_2 to produce a dialkylcyanamide complex trans-$[PtCl_4(N(H)=C(NMe_2)OH)_2]$, but the cis-isomer does not. Hydrolytic coupling of the adjacent (cis-orientation) dialkylcyanamide ligands gives the metallacycle $[PtCl_4(NH=C(NMe_2)OC(NMe_2)=NH)]$, the formation of which probably proceeds via an initial hydration of the coordinated Me_2NCN to the corresponding iminol, followed by the *OH*(iminol)-to-*C*(nitrile) coupling. (**Scheme 1.13**) It is clearly demonstrated that the coupling occurs only when the two ligands are oriented in a cis fashion to one another. [89]

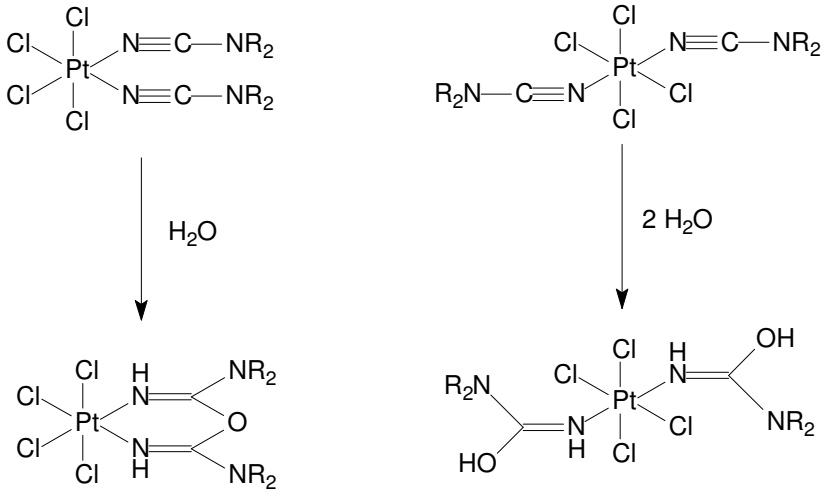

Scheme 1.13 Reactions of trans- and cis-$[PtCl_4(NCNR_2)_2]$ complexes with water

1.10 Amido complexes

Amides are readily synthesized and widely available organic compounds. Synthesis of amides with a large variety of steric and electronic properties is accessible due to the availability of inexpensive and commercially available starting materials such as acid chlorides and amines. Amides thus can be utilized as easily tunable proligands.

Besides hydration of coordinated nitriles, deprotonation of amide proligands is a common synthetic method of monoanionic amido ligands in which the negative charge is delocalized throughout the N, C, and O atoms.[90-93] The amido ligands are capable of binding a large variety of metal ions via the N and/or O atoms. These different coordination modes result in numerous potential coordination isomers in the synthesis of amido metal complexes. This thus keeps the amido ligands from being fully exploited as auxiliary ligands.

There are four fully characterized coordination modes: i) monodentate via O atom, ii) monodentate via N atom, iii) bridging, and iv) chelating. (**Chart 1.6**) For a

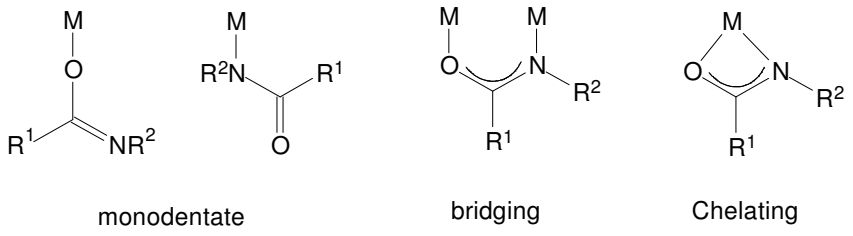

Chart 1.6 Three different binding modes of amido ligands

monomeric fashion via either the oxygen or nitrogen atoms, coordination occurs through the more basic oxygen with "hard" metals,[94] but through the nitrogen to "soft" metal centers.[95] Isomerization between *O* and *N*-bound amido ligand has seldom been reported except when changing the pH and oxidation state of the TM.[96] Neutral amides typically coordinate through oxygen to the metal center,[94] unless the amide ligand tautomerizes to its iminol form, which can be stabilized by polar solvents, or "soft" metal centers.[97-99]

Another common bonding motif is "bridging" in which the amido ligand bridges two TM centers. These complexes have been investigated for their interesting structural features. Structurally interesting heterotrimetallic complexes containing two platinum atoms and a Cu, Co, Mn, Cd, In, or Ni atom have been formed with various amido ligands bridging two metal centers.[70, 75, 76, 88, 100-103] In the last bonding type, an amido ligand chelates through nitrogen and oxygen atoms to a single metal center.[81, 90-92, 104-108] Many chelating amido complexes have been synthesized by reacting TM-alkyls with isocyanates. Newly formed chelating amido complexes were obtained by inserting phenyl or methyl isocyanates into $Nb(Me)_3Cl_2$ and $Ta(Me)_3Cl_2$ complexes (**eq 1.1**).[109] Analogous reactions occur with $[Cp_2ZrMe_2]$ [110] and Cp_2TiR [109] complexes and different isocyanates to generate chelating amido complexes.

$$M(Me)_3Cl_2 \xrightarrow{RNCO} M(Me)Cl_2(NRC(O)Me)_2 \qquad \textbf{1.1}$$

M = Nb, Ta ; R = Ph, Me

Apart from the studies of structural and coordination chemistry on the amido complexes, most importantly, the catalytic potential of these complexes with tunable amido auxiliary ligands has been largely unexplored. Some reports on amido complex-catalyzed-alkene [106, 107, 111-114]and alkyne [92, 108, 115] hydroaminations have been published recently. Hydroamination is the addition of nitrogen and hydrogen across a carbon-carbon multiple bond. This leads to the formation of enamines, imines, and amines, which are important building blocks in the pharmaceutical and dye industries.

A series of bis(amido)bis(amino)-titanium and zirconium complexes were synthesized with amide proligands possessing different steric hindrances and electronic properties such as *N*-tert-butylbenzamide, *N*-tert-butylperfluorophenylamide, and *N*-tert-butyl-2-methylpropanamide. Schafer *et al.* have demonstrated that these titanium and zirconium complexes are capable of catalyzing intramolecular alkyne hydroamination of (5-phenyl-4-pentyn-1-yl)amine to cyclic imine and the titanium complexes are more active catalysts than the corresponding zirconium complexes. They have also demonstrated regioselective alkyne hydroamination with tert-butyl amine by using similar titanium complexes with sterically bulky amido ligands. The complex with the bulkiest substituent on the amido nitrogen is the most effective, giving the highest yield, in the lowest reaction time, and with excellent regioselectivity.[93, 108, 115]

A more challenging enantioselective alkene hydroamination reaction has also been catalyzed with chiral bis(amido) coordinated-zirconium complexes. Schafer and co-workers have reported that these chiral zirconium complexes are capable of catalyzing enantioselective intramolecular alkene hydroamination of aminoalkene.[62]

Amido complexes are suggested as one of the intermediates or transition states of catalytic reactions involving amides as a reagent such as hydroamidation [116-118] and transamidation.[119, 120]

Catalytic addition of amides to alkynes is an ideal synthetic method for enamides due to the availability of starting materials and atom-economy. Deng *et al.* have reported that [Ru(methallyl)$_2$(cod)] is capable of catalyzing anti-Markovnikov addition of secondary amides to terminal alkynes. They have also proposed that a conceivable mechanism for the formation of trans enamides might involve the oxidative addition of the N-H bond of amide to the ruthenium, followed by insertion of the alkynes into the amido moiety, and subsequent reductive elimination of the enamide product.[116]

Chang and co-workers have revealed that excellent stereoselectivity of cis-enamides formed by conjugated olefins and primary amides is obtained by a Pd/Cu co-calatyzed oxidative amidation system. They have suggested a plausible catalytic cycle which is initiated by the displacement of the benzonitrile ligand from

$[PdCl_2(PhCN)_2]$ by the C=C bond of conjugated alkene, followed by the coordination of amide to the palladium complex and the subsequent intramolecular nucleophilic attack of the amido ligand at the coordinated olefin, and upon the loss of HCl, to generate a σ-alkylpalladium species. The enamide product is formed by β-hydride elimination of the σ-alkylpalladium species.[117]

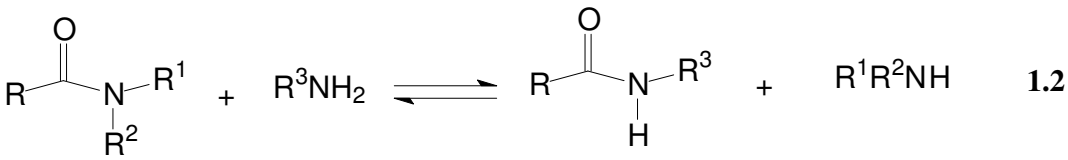

1.2

Transamidation (**eq 1.2**) is a rare reaction, because the C-N bond of secondary amides is generally thermodynamically and kinetically unreactive. Stahl *et al.* have discovered that the trisaminoaluminum (III) dimer $Al_2(NMe_2)_6$ catalyzes facile tansamidation between simple secondary amides and primary amines under moderate conditions.[119] Very recently, they have reported a mechanism of this Al (III) – catalyzed transamidation as shown in Scheme 1.14.[120]

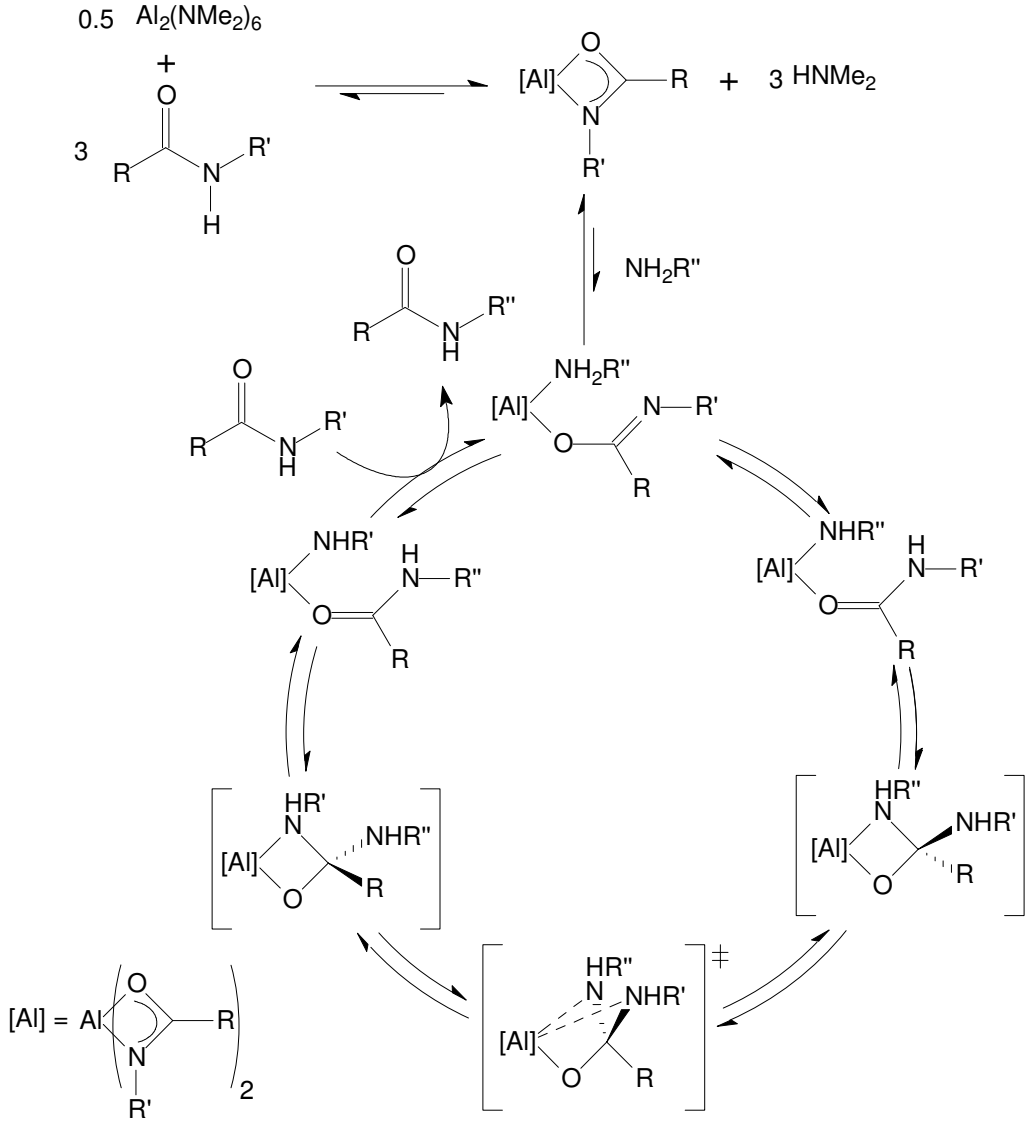

Scheme 1.14 Proposed mechanism of Al(III)-catalyzed transamination

The aluminum (III) dimer reacts rapidly with secondary amides to yield a tris-amido aluminum complex that has been identified as the catalyst resting state. It is proposed that the reaction of this tris-amido aluminum complex with primary amine and the subsequent proton transfer from amine to a coordinated amido ligand initiate the stepwise transamidation mechanism.

Chapter 2 Catalytic H/D exchange between organic compounds and D_2O with $TpRu(PPh_3)(CH_3CN)H$. Reaction of $TpRu(PPh_3)(CH_3CN)H$ with water to form acrtamido complex $TpRu(PPh_3)(H_2O)(NHC(O)CH_3)$

2.1 Introdution

Incorporation of deuterium into C–H bonds of organic molecules is important in preparative chemistry of deuterium-labeled materials, which have a number of important uses from solvents for NMR spectroscopy to reagents for mechanistic investigation. Deuterium oxide, due to its low cost and low toxicity, is an attractive isotopic source. However, metal-catalyzed H/D exchange between C–H bonds and D_2O are relatively rare.[50, 52, 121, 122] Very recently, Sajiki and coworkers have developed an efficient Rh/C system on catalytic H/D exchange between alkanes and D_2O with high deuterium incorporation. It is anticipated that the mechanism involves oxidative addition of alkane to the Rh to generate an alkyl hydride Rh complex.[123]

Another example from Leitner et al. [124] demonstrated that a ruthenium hydride complex is an effective catalyst for H/D exchange between aromatic substrates and D_2O. DFT calculations support a catalytic cycle comprising σ-bond metathesis as the key step for the H/D exchange processes including reversible exchanges between Ru-H and D_2O, and Ru-D and C-H (benzene in calculation). It is also a rare example of late TM catalyzed C-H bond activation via σ-bond metathesis.

We have recently reported that the ruthenium complex $TpRu(PPh_3)(CH_3CN)H$ (**1**) catalyzes H/D exchange between CH_4 and some deuterated organic molecules such as benzene-d_6, tetrahydrofuran-d_8, diethyl ether-d_{10}, and 1,4-dioxane-d_8. Theoretical study on the reaction mechanism suggests that the six-coordinate σ-complexes $TpRu(PPh_3)(\eta^2\text{-H–R})H$ and $TpRu(PPh_3)(\eta^2\text{-H─CH}_3)H$ are important intermediates in the exchange processes, during which reversible transformations between these σ-complexes and the dihydrogen species $TpRu(PPh_3)(\eta^2\text{-H–H})R$ and $TpRu(PPh_3)(\eta^2\text{-H–H})(CH_3)$, respectively, are the crucial steps. All these transformations, however, go through transition states corresponding to the seven-coordinate species $TpRu(PPh_3)(R)(H)(D)$ and $TpRu(PPh_3)(CH_3)(H)(D)$ (**Scheme 2.1**).[46]

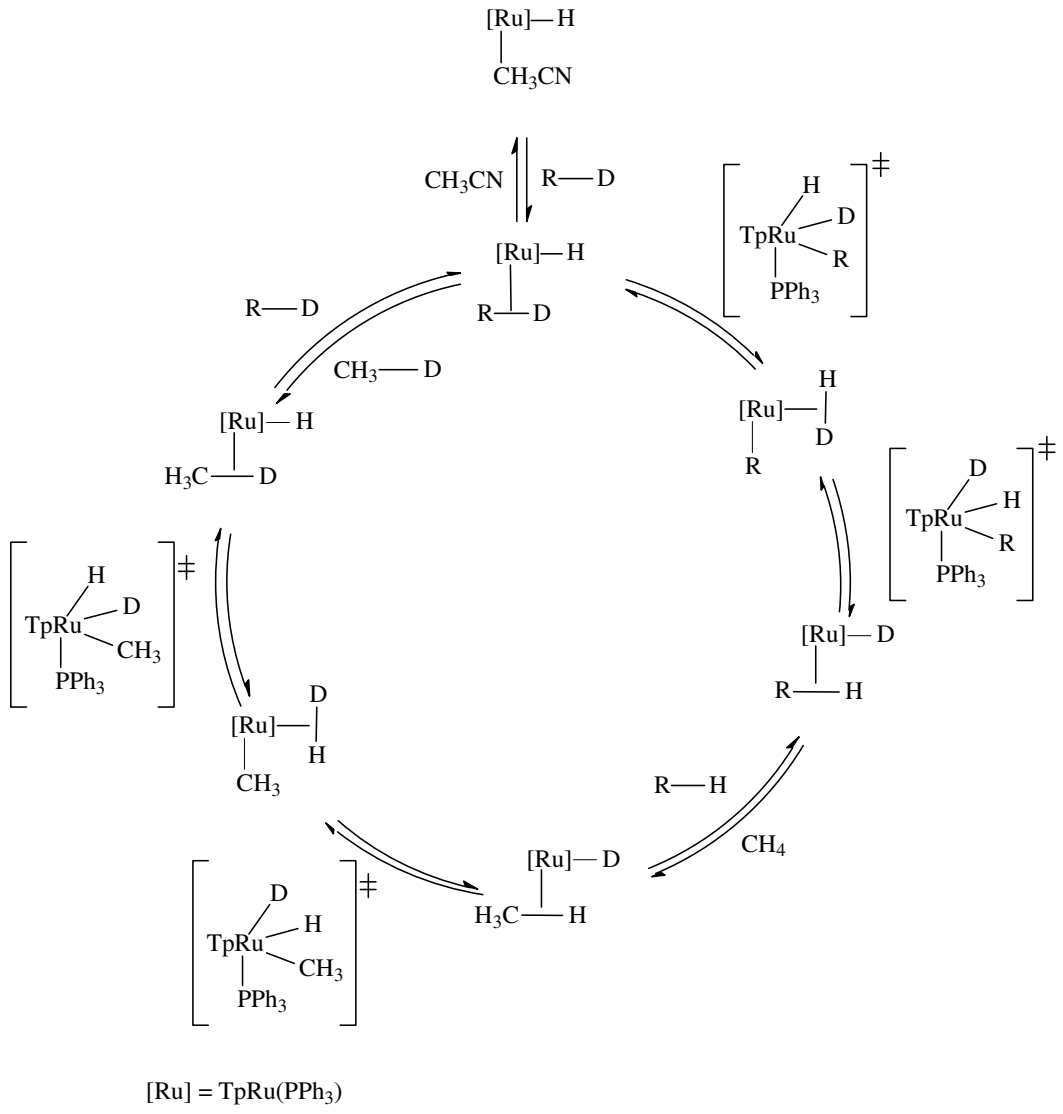

Scheme 2.1 Proposed mechanism of $TpRu(PPh_3)(CH_3CN)H$ catalyzed H/D exchange between methane and deuterated organic solvent

Continuing our research in C–H bond activation, we study the **1**-catalyzed deuteration of C–H bonds of organic molecules, using D_2O as the deuterium source. It has been briefly mentioned in recent reports that a similar Tp-ruthenium complex $TpRu(PMe_3)_2OH$ is able to promote H/D exchange between H_2O and deuterated

arenes (C_6D_6 and $C_6H_5CD_3$), the turnovers for the exchange are, however, very low. [125, 126]

2.2 Experimental

2.2.1 Materials and Instrumentation

Ruthenium trichloride, $RuCl_3 \cdot 3H_2O$, pyrazole, sodium borohydride, triphenylphosphine, and organic solvents were obtained from Aldrich. Triphenylphosphine was recrystallized from ethanol before use. Solvents were distilled under a dry nitrogen atmosphere with appropriate drying agents: hexane, diethyl ether, tetrahydrofuran, benzene, 1,4-dioxane, and toluene with sodium-benzophenone; dichloromethane, acetonitrile, and chloroform with calcium hydride. The complexes $TpRu(PPh_3)(CH_3CN)H$ [127] and $TpRu(PPh_3)(CH_3CN)Cl$ [127] were prepared according to literature methods. Deuterated NMR solvents, purchased from Armar, were dried with P_2O_5. High purity hydrogen and argon gases were supplied by Hong Kong Oxygen.

Proton NMR spectra were obtained from a Bruker DPX 400 spectrometer. Chemical shifts were reported relative to residual protons of the deuterated solvents. ^{31}P NMR spectra were recorded on a Bruker DPX 400 spectrometer at 161.70 MHz, chemical shifts were externally referenced to 85% H_3PO_4 in D_2O. $^{13}C\{^1H\}$ NMR spectra were taken on a Bruker DPX 400 spectrometer at 100.61 MHz; chemical

shifts were internally referenced to C_6D_6 (δ = 128.1 ppm). ^{2}H NMR spectra were taken on a Bruker DPX 400 spectrometer at 61.42 MHz; chemical shifts were internally referenced to TMS (δ = 0.00 ppm). High-pressure NMR studies were carried out in commercial 5 mm Wilmad pressure-valved NMR tubes. Infrared spectra were obtained from a Bruker Vector 22 FT-IR spectrophotometer. Electrospray ionization mass spectrometry was carried out with a Finnigan MAT 95S mass spectrometer with the samples dissolved in dichloromethane. Elemental analyses were performed by M-H-W Laboratories, Phoenix, AZ, USA.

2.2.2 Synthesis and Reactions

2.2.2.1 H/D exchange between Ru—H of 1 and D_2O.

A sample of $TpRu(PPh_3)(CH_3CN)(H)$ (**1**) (～5 mg) was loaded into a 5 mm NMR tube, which was then sealed with a septum. The tube was evacuated using a needle and filled with nitrogen for three cycles. THF (0.3 mL) and D_2O (8 μL) were added to the tube using syringes and needles. The solution was allowed to stand at room temperature for 10 minutes, after which the $^{31}P\{^1H\}$, ^{1}H, and ^{2}H NMR spectra of the solution were immediately recorded. The $^{31}P\{^1H\}$ NMR spectrum showed a slightly broadened singlet at δ 79.5 ppm, the chemical shift of which was identical to that of the signal of **1**. The ^{1}H NMR spectrum showed all the signals of **1** except the upfield hydride signal. ^{2}H NMR spectrum showed a singlet at δ -13.94 ppm (br, Ru-*D*).

2.2.2.2 Synthesis of $TpRu(PPh_3)(H_2O)(NHC(O)CH_3)$ (2)

A sample of $TpRu(PPh_3)(CH_3CN)H$ (0.12 g, 0.20 mmole) was loaded into a two-necked round-bottom flask which was then evacuated and flushed with nitrogen for four cycles. Freshly distilled THF (6 mL) and water (0.2 mL) were added to the flask and the resulting solution was refluxed with stirring for 24 h. After cooling the solution to room temperature, the solvent was removed under vacuum and 10 mL of dichloromethane was added to the residue. The mixture was filtered to remove some insoluble solids; the filtrate was brought to dryness by vacuo to afford a green solid. The solid was washed with hexane (2 x 6 mL) and 5/1 hexane/diethyl ether (2 x 6 mL); it was collected and dried under vacuum for several hours at room temperature. Yield: 0.073 g (56 %).

Elemental analysis calcd (%) for $C_{29}H_{31}BN_7O_2PRu$: C 53.39, H 4.79, N 15.03; found: C 53.31, H 4.81, N 15.09.

IR (KBr, cm^{-1}): υ(C=O) = 1540 (med), υ(N-H) = 3337 (med), υ(B-H) = 2461 (med).

^1H NMR (400.13 MHz, C_6D_6, 25 ˚C): δ = 2.05 (s, 3H; $CH_3C(O)NH$), 4.67 (s, 1H; $CH_3C(O)NH$), 5.93 (t, 1H of Tp), 5.97 (t, 1H of Tp), 6.28 (t, 1H of Tp), 6.87 (d, 1H of Tp), 7.29 (d, 1H of Tp), 7.78 (d, 1H of Tp), 7.85 (d, 2H of Tp), 8.24 (d, 1H of Tp) (all coupling constants for Tp proton resonances are about 2 Hz), 7.24 – 7.68 ppm (2 multiplets, 15H of PPh_3).

$^{31}P\{^1H\}$ NMR (161.7 MHz, C_6D_6, 25 ˚C): δ = 63.3 (s).

$^{13}C\{^1H\}$ NMR (100.61 MHz, C_6D_6, 25 ˚C):$_3$ δ = 181.2 (s, $CH_3C(O)NH$), 25.7 (s, $CH_3C(O)NH$), other signals which are due to the Tp and PPh_3 ligands: δ 144.1,

143.8, 140.9, 135.5, 135.2, 134.8, 134.6, 133.6, 133.5, 128.1, 105.5, 105.4, 105.2, 105.0.

ESI-MS (CH_2Cl_2): *m/z*: 635 $[M-H_2O]^+$.

2.2.2.3 Catalytic H/D exchange organic compounds and D_2O with $TpRu(PPh_3)(CH_3CN)H$ under Ar or H_2

A 5mm pressure-valved NMR tube was loaded with $TpRu(PPh_3)(CH_3CN)H$ (～6 mg) and then flushed with Ar for a few minutes. Freshly distilled organic solvent (0.2 mL) and degassed D_2O (0.1 mL) were added to the tube under Ar, and the tube was then pressured with Ar or H_2 (10 atm). It was heated at 110 ˚C for 24 h. ^1H NMR spectroscopy was used to analyze the percentage of deuterium incorporation into the organic compound

2.2.2.4 The use of ^1H NMR spectroscopy to determine levels of deuteration of the organic compound

For THF and 1,4-dioxane, which are miscible with water, no internal standard was used for the calculation of the level of deuteration. In the catalytic H/D exchange reaction, for example, between 1,4-dioxane and D_2O, the total number of hydrogen atoms (the exchanging hydrogen atoms of 1,4-dioxane and the residual hydrogen atoms of D_2O) is constant throughout the catalytic reaction. Based on the integrals of the residual D_2O peak and that of the exchanging hydrogen of 1,4-

dioxane, before and after the exchange reaction, the percent deuterium incorporation into the organic compound can be calculated. For benzene, toluene, and diethyl ether, which are not miscible with D_2O, an internal standard, CH_2Cl_2 was used for the determination of the levels of deuteration. In a typical experiment, a standard solution containing 10 μL of the organic compound and 10 μL of CH_2Cl_2 in $CDCl_3$ in an NMR tube was prepared. After the H/D exchange reaction of the organic compound with D_2O was quenched, the catalytic system was allowed to stand for several hours at room temperature to ensure good separation of the organic and aqueous phases. A $CDCl_3$ solution (the sample solution) containing 10 μL of the organic phase and 10 μL of the internal standard was prepared in an NMR tube. The ^1H NMR spectra of the sample solution and the standard solution were recorded. Based on the ratios of the integration of the signal of the exchanging hydrogen of the organic compound and that of the CH_2Cl_2 in the spectra of both solutions, the level of deuteration can be calculated.

2.2.2.5 Reaction of 2 with H_2

A sample of $TpRu(PPh_3)(H_2O)(NHC(O)CH_3)$ (**2**) (6 mg) loaded in a 5 mm pressure-valved NMR tube was dissolved in 1,4-dioxane-d_8 (0.3 mL); the tube was then pressurized with 10 bars of H_2. The tube was heated at 110 ˚C for 16 h. ^1H and $^{31}P\{^1H\}$ NMR spectra were recorded, and it was evidenced from these spectra that **2** was completely converted to the known complex $TpRu(PPh_3)(H_{3-x})D_x$ (**5d$_x$**).

2.2.2.6 Reaction of 2 with H_2/D_2O

A sample of $TpRu(PPh_3)(H_2O)(NHC(O)CH_3)$ (**2**) (6 mg) was loaded into a 5mm pressure-valved NMR tube, to which THF (0.2 mL) and D_2O (0.05 mL) were added. The tube was then pressured with 10 bars of H_2 and heated at 110 ˚C for 6 h. The tube was cooled to room temperature and the $^{31}P\{^1H\}$ NMR spectrum was recorded. $^{31}P\{^1H\}$ NMR (161.7 MHz, 25 ˚C): δ 68.8 ppm (s). The solution in the NMR tube was then transferred to a 50 mL 2-necked flask. The flask was flushed with nitrogen and the solvent of the solution was removed by vacuo. The residue was washed with hexanes (2 mL x 2). ^1H and $^{31}P\{^1H\}$ NMR spectra of a $CDCl_3$ solution of the residue were taken; these spectra confirmed that the residue is the known carbonyl hydride complex $TpRu(PPh_3)(CO)H$ (**3**).

2.2.2.7 Crystallographic structure analysis of $TpRu(PPh_3)(H_2O)(NHC(O)CH_3)$ (2)

Yellowish green crystals of **2** suitable for X-ray diffraction study were obtained by layering of diethyl ether on a CH_2Cl_2 solution of the complex. A suitable crystal with dimensions of 0.50 x 0.40 x 0.40 mm was mounted on a Bruker CCD area detector diffractomer and subject to MoK_α radiation (λ = 0.71073 Å) from a generator operating at 50 kV and 30 mA. The intensity data of **2** were collected in the range of 2θ = 3─55˚ with oscillation frames of ϕ and ω in the range 0─180˚. 1321 Frames were taken in four shells. An empirical absorption correction of the

SADABS (Sheldrick, 1996) program based on Fourier coefficient fitting was applied. The crystal structure was solved by Patterson function methods, and expanded by difference Fourier syntheses, refined by full-matrix least squares on F^2 using the Bruker Smart and Bruker SHELXTL program packages. All non-hydrogen atoms were refined anisothropically. Hydrogen atoms were placed in ideal positions and refined as riding atoms, except the two on the aqua ligand and the one on the boron atom of the Tp ligand, which were located by difference electron density map. The final cycle of the full-matrix least-squares refinement based on 7609 observed reflections (I>2 sigma(I)) and 425 parameters converged to the R and R_w values of 0.0372 and 0.1042 for $TpRu(PPh_3)(H_2O)(NHC(O)CH_3)$.

2.3 Results and Discussion

2.3.1 H/D exchange between organic molecules and D_2O under Ar

For convenience of measuring by ^1H spectroscopy the degree of deuterium incorporation into the organic compounds, the H/D exchange reactions were carried out in 5-mm Wilmad pressure-valved NMR tubes under 10 atm of argon. The argon pressure was applied to increase the boiling points of the organic compounds and D_2O so that they did not boil at the reaction temperature of 110 ˚C. Results of the **1**-catalyzed H/D exchange between organic molecules and D_2O under Ar are shown in Table 2.1. Reproducibility of the H/D exchange reactions was assured by duplicating each reaction using a different batch of catalyst. Each of the results in Table 2.1 is

the average of two runs. In comparison with the iridium complex $Cp^*(PMe_3)IrCl_2$, [49] for example, ~0.4 mol % of **1** is able to affect in 24 h total incorporation levels of 24 and 13 % in the deuteration of Et_2O and THF, respectively with D_2O, whereas incorporation levels with the iridium system in 40 h are 36 and 61 %, respectively, but with 5 mol % catalyst. Although THF and 1,4-dioxane have much better miscibility with D_2O than the other substrates, these cyclic ethers do not seem to give higher percent deuteration of their C─H bonds. In our previous work on the **1**-catalyzed H/D exchange between CH_4 and deuterated organic compounds, it was found that the exchange reaction between C_6D_6 and CH_4 exhibits higher degree of H/D exchange than the THF-d_8/CH_4 and 1,4-dioxane-d_8/CH_4 exchange reactions. In the present study, the exchange of the α-hydrogens of THF is preferred over that of the β-hydrogens; on the other hand, the methyl hydrogens of diethyl ether undergo H/D exchange to a larger extent than the methylene hydrogens. These results are similar to the outcome of the CH_4/THF-d_8 and CH_4/diethyl ether-d_{10} exchange reactions which we have previously described in detail. [46] Unfortunately, it is difficult to study the H/D exchange of aliphatic R─H with D_2O due to solubility problems of **1** in both substrates.

Table 2.1 H/D exchange of organic solvents and D_2O by 1 under Argon[a]

Entry	Substrate	% deuteration		total TON[b]	Mol % of **1**[c]
1	Benzene	27		390	0.41
		aliphatic:	16		
2	Toluene	o and p:	16	256	0.48
		m:	12		
		α hydrogen:	20		
3	Tetrahydrofuran			288	0.37
		β hydrogen:	6		
4	1,4-dioxane	12		240	0.40
		α hydrogen:	19		
5	diethyl ether			490	0.48
		β hydrogen:	27		

[a]Reaction condition: catalyst, 0.0091 mmol; substrate, 0.2 mL; D_2O, 0.1mL; pressure: Ar = 10 atm; temperature, 110°C; reaction time, 24 h. [b]Total TON = mole of C-H bond activated/mol of catalyst. [c]Relative to the organic substrate

2.3.2 H/D exchange of Ru—H with D_2O at room temperature

It is noted that the hydride ligand of **1** is readily deuterated in the presence of D_2O. In a THF-d_8 solution, the hydride signal of **1** (δ -13.50 ppm) was easily discernable by ^{1}H NMR spectroscopy, and its intensity remained unaltered over an extended period of time at room temperature, indicating that the hydride ligand did

not undergo H/D exchange with THF-d_8 at this temperature. However, the ^{1}H NMR spectrum of **1** taken 10 minutes after the addition of excess D_2O to the solution showed that the hydride signal had disappeared while all the other proton signals of the complex remained unchanged, thus indicative of fast deuteration of only the hydride ligand of **1** by D_2O at room temperature; the hydride ligand deuteration was confirmed by ^{2}H NMR spectroscopy which showed the Ru─D signal at δ -13.94 ppm. H/D exchange between metal hydride and D_2O has been reported. [128-132]

Mebi and Frost have reported that a water soluable ruthenium hydride complex $CpRu(PTA)_2H$ (PTA = 1,3,5-triaza-7-phosphaadamantane) undergoes H/D exchange with D_2O. The proposed mechanism involves reversible protonation of the hydride ligand by water, generating a dihydrogen intermediate, and subsequent deprotonation of the intermediate by the resultant hydroxide ion. [132]

In view of the propensity of the $TpRuL_2^+$ fragments to form η^2-H_2 complexes, [127, 133-135] we initially thought that H/D exchange between the hydride ligand of **1** and D_2O might proceed via the reaction sequence depicted in Scheme 2.2. A major concern, however, over this mechanism is that D_2O might not be acidic enough to protonate the metal hydride. In fact, we have shown in our previous work that **1** can only be protonated with strong acid such as HBF_4 to form the dihydrogen complex $[TpRu(PPh_3)(CH_3CN)(H_2)]BF_4$; [127] we have also measured the pseudo aquo pKa value, which is equal to 8.9, of the complex. [136] Since water is a very weak acid, it

is probably true that D_2O is not acidic enough to protonate **1** to form the dihydrogen complex.

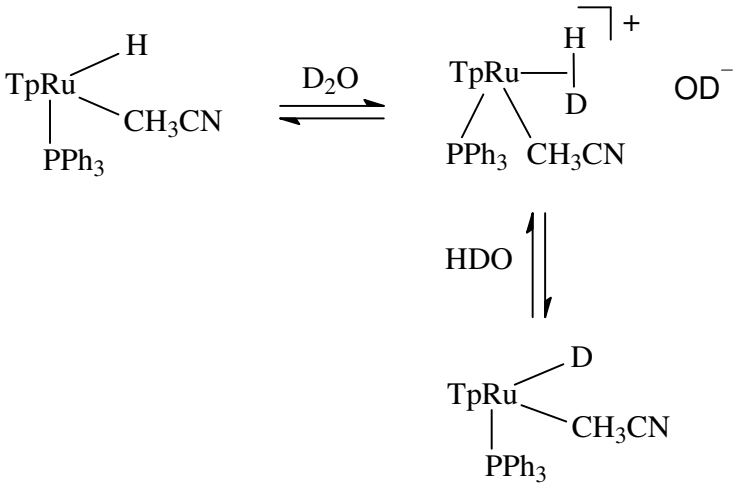

Scheme 2.2 Proposed mechanism of H/D exchange between hydride in 1 and D_2O via protonation

Scheme 2.3 shows a probable mechanism for the H/D exchange between Ru─H of **1** and D_2O. The reaction may be initiated by an interaction between the Ru─H and D─OD forming a Ru─H···D─OD dihydrogen-bonded species; [40, 137-140] the H/D exchange reaction then proceeds via the intermediacies of the hydrogen-bonded ion pairs (**Scheme 2.3**). Similar mechanisms have been proposed for M─H/D_2O exchange reactions. [129] The interaction of transition metal hydride with a proton donor H-X can be visualized as shown in Scheme 2.4. The far right is the free ion pair; while **B** is the hydrogen-bonded ion pair and **A** is the dihydrogen-bonded species; whether **A**, **B**, or **C** would predominate is very dependent on the proton donor strength of H-X.[140, 141]

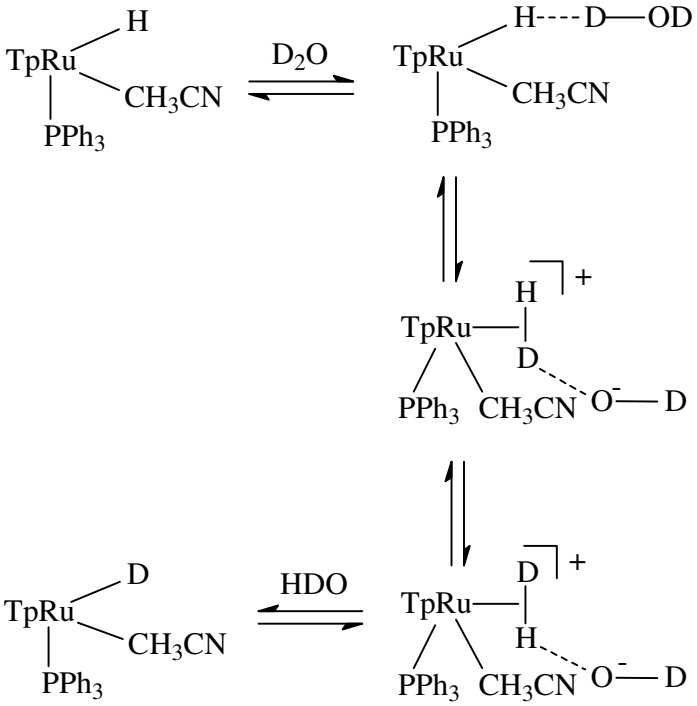

Scheme 2.3 Proposed mechanism of H/D exchange between hydride in 1 and D_2O via hydrogen-bonded ion pair

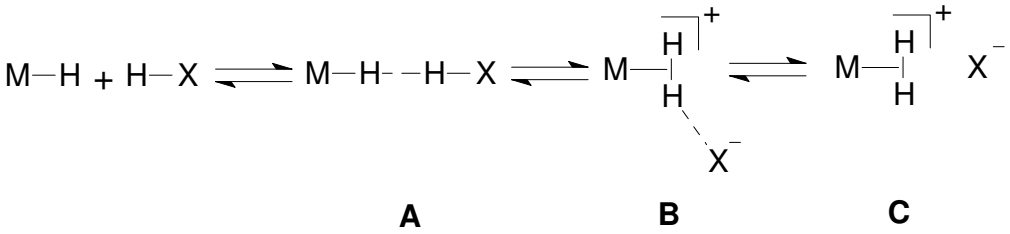

Scheme 2.4 Interaction between metal hydride and proton donor HX

Arndt *et al.* [128] reported a facile H/D exchange reaction of hydride of carbonyl hydride complexes $HM(CO)_4L^-$ (M = Cr, W; L = CO, $P(OMe)_3$) with CH_3OD, D_2O, and CH_3COOD. The exchange reaction was proposed to proceed via

an anion-stabilized dihydrides intermediate (**Chart 2.1**), which is similar to the hydrogen-bonded ion pair in our case.

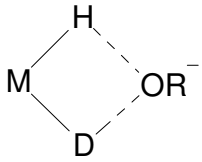

$OR^- = CH_3O^-, OD^-$, or CH_3OO^-

Chart 2.1 Formation of the anion-stabilized dihydride

2.3.3 Formation of $TpRu(PPh_3)(D_2O)(NDC(O)CH_3)$ (2d) and structure determination of the ruthenium-acetamido complex $TpRu(PPh_3)(H_2O)(NHC(O)CH_3)$ (2)

A **1**-catalyzed THF/D_2O exchange reaction was monitored by ^1H and $^{31}P\{^1H\}$ NMR spectroscopy. It was observed that 20 minutes into the catalytic reaction, approximately two thirds of **1** was converted to a new complex **2d**, and **1** was basically not observable on the $^{31}P\{^1H\}$ NMR spectrum after about 80 minutes. $^{31}P\{^1H\}$ NMR spectroscopy showed that **2d** corresponds to a singlet at δ 62.3 ppm. ^1H NMR spectroscopy showed that the singlet corresponding to the methyl protons of the acetonitrile ligand of **1** at δ 1.93 ppm disappeared, and any new methyl signal might have been masked by the large peaks of THF. Complex **2d** remained the only detectable species by $^{31}P\{^1H\}$ NMR spectroscopy for about 6h, after which two additional species **3** and **4** became detectable as shown by the appearance of 2 minor signals at δ 68.8 ppm and 71.5 ppm, respectively; the abundance of **3** and **4**

increased at the expense of **2d**. After 15h, **2d**, **3**, and **4** were present in approximately 2:1:1 ratio. The increase of % deuteration of the α- and β-hydrogens of THF with time was also monitored; it was observed that the % deuteration of both types of hydrogens increased steadily with time and began to level off after about 24 h.

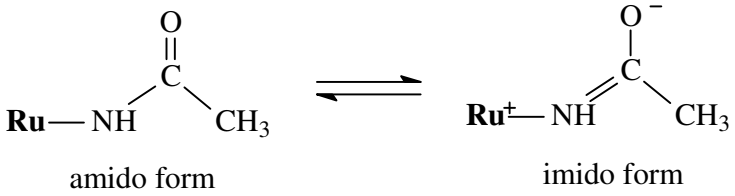

amido form imido form

Chart 2.2 Isomerization of amido ligand

Complex **2** was independently prepared by refluxing a THF solution of **1** containing 150 equiv of H_2O for 24 h. Yellowish green crystals of **2** suitable for X-ray diffraction study were obtained by slow diffusion of diethyl ether into a solution of the complex in dichloromethane. Figure 2.1 shows the molecular structure of **2** (the solvent molecule CH_2Cl_2 is not shown). The crystal data and refinement details are given in Table 2.2. Selected bond distances and angles are given in Table 2.3. Complex **2** contains an acetamido ligand and a coordinated water molecule; the hydrogen atoms of the aquo ligand were located and refined. The acetamido ligand can have two resonance structures, the amido form and the imido form (**Chart 2.2**). The bond distances of C(10)−O(1), 1.268(3) Å and C(10)−N(7), 1.303(3) Å of **2** are, respectively, longer and shorter than those of the corresponding amido-type ligands such as glycinamidotetraammine ruthenium(III) [142], $[(NH_3)_5Ru(NHC(O)4\text{-py-}N\text{-}$

Me)]$(ClO_4)_3$ [143], and $[Ru(tpy)(bpy)(BNAH)]^{2+}$ (BNAH = 1-benzyl-1,4-dihydronicotinamide) [144]. The ranges of C=O and C-N bond length in these amido ligands are around 1.232 Å to 1.255 Å and 1.313 Å to 1.375 Å respectively. On the other hand, the bond distances of C(10)–O(1) and C(10)–N(7) are shorter and longer, respectively than the corresponding C─O (1.288(4) Å) and C─N (1.290(5) Å) bond distances of the imido ligand in *cis*-$[Ru(NO)(NHC(OH_{0.5})CH_3)(bpy)_2]^{2.5+}$ [145]. Thus, the C─O and C─N bond distances of the acetamido ligand of **2** indicate that both amido and imido forms have contributions to the structure. Yi *et al.* [146] have also reported that C-N and C-O bond distances of the acetamido ruthenium complex syn-$[(PCy_3)_2(CO)(CH_3CONH)(^iPrOH)RuH]BF_4$, containing an intramolecular hydrogen bonding between the amido oxygen and adjacent alcoholic hydrogen, are 1.308(5) Å and 1.258(5) Å respectively. These bond lengths are comparable to that of the corresponding amido moiety of **2**. A feature of molecular structure of **2** is that one of the hydrogen atoms of the aquo ligand is intramolecularly hydrogen-bonded to the carbonyl oxygen of the acetamido ligand, while the other hydrogen exhibit intermolecular hydrogen-bonding interaction with the carbonyl function of the acetamido ligand of another molecule. The intra- and inter-molecular O····O distances are 2.593(2) Å (O(1W)····O(1)) and 2.7411(19) Å (O(1W)····O(1A)), respectively; these O····O distances fall in the range of hydrogen-bonding interactions. [147, 148]

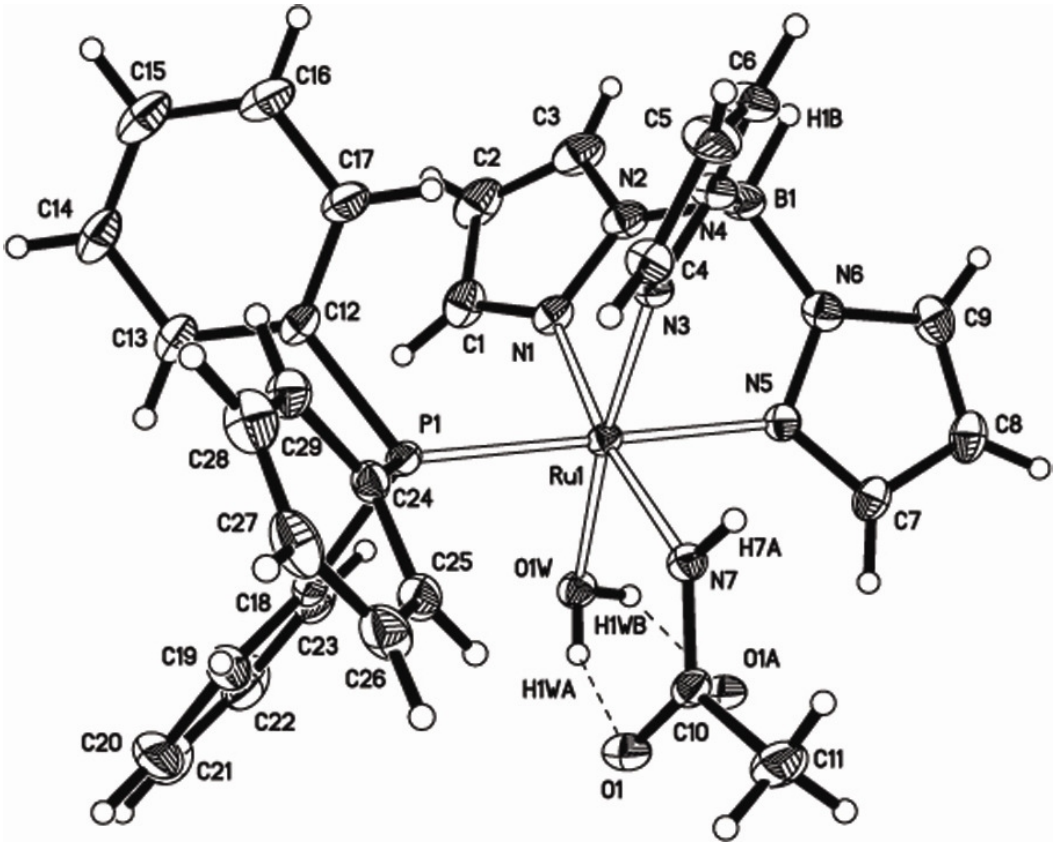

Figure 2.1 Molecular structure of $TpRu(PPh_3)(H_2O)(NHC(O)CH_3)$ (2)

Table 2.2 Crystal data and structure refinement for $TpRu(PPh_3)(H_2O)(NHC(O)CH_3)$ (2)

	2
Empirical formula	$Ru(H_2O)(NHCOCH_3)(P(C_6H_5)_3)(C_9H_9N_6BH)\cdot(CH_2Cl_2)$
Formula weight	736.38
Temperature	294(2) K
Wavelength	0.71073 Å
Crystal system	Monoclinic
Space group	P2(1)/c
Unit cell dimensions	a = 11.3769(17) Å $\alpha = 90^o$ b= 19.318(3) Å $\beta = 108.474(2)^o$ c = 15.830(2) Å $\gamma = 90^o$
Volume	3299.6(9) $Å^3$
Z	4
Density (calculated)	1.482 Mg/m^3
Absorption coefficient	0.725 mm^{-1}
F(000)	1500
Crystal size	0.50 x 0.40 x 0.40 mm^3
θ range for data collection	1.75 to 27.55°
Index ranges	$-14 \le h \le 14$, $-25 \le h \le 25$, $-20 \le l \le 20$
No. of Reflections collected	30427
No. of Independent reflections	7608 [R(int) = 0.0342]
Completeness to θ = 27.55°	99.8%
Absorption correction	Semi-empirical from equivalents
Max. and Min. transmission	0.9333 and 0.8923
Refinement method	Full-matrix least-squares on F^2
No. of data / restraints / params	7608 / 4 / 425
Goodness-of-fit on F^2	1.001
Final R indices [$I > 2\sigma(I)$]	R1 = 0.0371, wR2 = 0.1030
R indices (all data)	R1 = 0.0463, wR2 = 0.1107
Largest diff peak and hole	0.830 and -0.476 e. $Å^{-3}$

Table 2.3 Selected Bond distances (Å) and Bond angles (^{o}) for $TpRu(PPh_3)(H_2O)(NHC(O)CH_3)$ (2)

Bond Distances (Å)			
Ru – N(1)	2.1116(17)	Ru – N(3)	2.0419(16)
Ru – N(5)	2.1210(15)	Ru – N(7)	2.0769(17)
Ru – O(1W)	2.1393(14)	C(10) – O(1)	1.268(3)
O(1W) – O(1)	2.593(2)	C(10) – N(7)	1.303(3)
O(1W) – O(1A)	2.7411(19)	O(1W) – H(1WA)	0.9098
O(1W) – H(1WB)	0.9150		

Bond Angles (^{o})			
N(3)-Ru(1)-N(1)	88.10(7)	N(3)-Ru(1)-N(5)	85.69(6)
N(3)-Ru(1)-N(7)	88.68(7)	N(3)-Ru(1)-P(1)	94.42(4)
N(1)-Ru(1)-N(5)	85.95(6)	N(1)-Ru(1)-O(1W)	93.70(6)
N(1)-Ru(1)-P(1)	93.84(4)	N(7)-Ru(1)-N(5)	85.90(6)
N(7)-Ru(1)-O(1W)	88.71(6)	N(7)-Ru(1)-P(1)	94.31(4)
N(5)-Ru(1)-O(1W)	88.53(6)	O(1W)-Ru(1)-P(1)	91.36(4)
C(10)-N(7)-Ru	130.75(14)	O(1)-C(10)-N(7)	122.86(19)
O(1)-C(10)-C(11)	117.5(2)	N(7)-C(10)-C(11)	119.6(2)

The ^{1}H NMR spectrum of **2** shows the N-H as a slightly broadened singlet at δ 4.67 ppm; a singlet which corresponds to the methyl proton of the acetamido ligand is seen at δ 2.05 ppm. The carbonyl carbon of the acetamido ligand appears as

a singlet at δ 181.2 ppm in the $^{13}C\{^{1}H\}$ NMR spectrum. The low carbonyl stretching frequency ($\nu_{(C=O)}$ = 1540 cm^{-1}) shown by IR spectroscopy corroborates the fact that the imido form makes significant contribution to the structure. The ruthenium-acetamido complex syn-$[(PCy_3)_2(CO)(CH_3CONH)(^{i}PrOH)RuH]BF_4$, which is effective in catalyzing the stepwise transfer hydrogenation of carbonyl compounds and imines, also exhibits a low carbonyl amide stretching frequency ($\upsilon_{(C=O)}$ = 1545 cm^{-1}). [146], suggesting extensive π-delocalization of the amido ligand. The N-H stretching frequency of **2** can be observed at 3334 cm^{-1}, it is shifted to 2402 cm^{-1} (theoretical value is 2363 cm^{-1}) for **2d**, which can be prepared by reacting **1** with D_2O instead of H_2O.

2.3.4 Possible mechanisms for the formation of 2

Formation of the acetamido ligand in **2** requires nucleophilic attack by water (or hydroxide) at the carbon center of the coordinated acetonitrile ligand of **1**. Mechanistic study of diaquo cobalt complex-catalyzed hydration of nitriles indicated that intramolecular metal hydroxide attack on the coordinated nitrile resulting in the formation of chelated amido is the crucial step in the catalysis (See **Scheme 1.10**). [81] The aquo-hydroxy cobalt complex, which is the active form of the catalyst for hydration of nitrile, is preferentially formed in equilibrium with the diaquo complex at the pH that the catalysis takes place. It has also been postulated that the hydration of nitriles catalyzed by the water-soluble molybdocene $[(MeCp)_2Mo(OH)(H_2O)]^{+}$ occurs by an intramolecular attack of a hydroxide ligand on a coordinated nitrile. [77]

This aquo-hydoxy molybdenum complex is formed by the cleavage of two Mo-OH bonds in the $[(MeCp)_2Mo(\mu\text{-}OH)_2Mo(CpMe)_2]^{2+}$ complex in water (See **Scheme 1.8**). On the basis of the kinetic experiments, a mechanism for the palladium-catalyzed nitrile hydration reactions was proposed; in the catalysis, internal attack on the nitrile ligand by the aqua ligand and external attack on the nitrile ligand by solvent water occur at similar rates (See **Scheme 1.11**). [82] Since in the present hydration reaction, there is no additional base to generate the hydroxide ion, the conversion of the acetonitrile to the acetamido ligand might involve external nucleophilic attack of the former by water. It was, however, learned that the chloro analogue of **1**, $TpRu(PPh_3)(CH_3CN)Cl$, in which the nitrile carbon should be more activated toward nucleophilic attack, remained unchanged after heating a THF solution of this complex in the presence of excess water overnight. In view of this fact, we are prompted to suggest a reaction sequence shown in Scheme 2.5 for the hydration of **1** to form **2**. The feature of the proposed sequence is that the attack of water at the acetonitrile is promoted by the dihydrogen-bonding interaction of the hydride ligand of **1** with the attacking water molecule. We have recently reported a similar dihydrogen-bond-promoted catalytic hydration of nitriles with an indenylruthenium hydride complex; it was shown by density functional theory calculations that the presence of a strong Ru–H···H–OH interaction in the transition state lowers the barrier of the nucleophilic attack of H_2O at the carbon atom of the bound nitrile. [61] Complex **1** has been found to be active in catalyzing hydration of acetonitrile to give acetamide in our preliminary study, the catalytic hydration of nitriles with **1** and **2** are reported in Chapter 2.

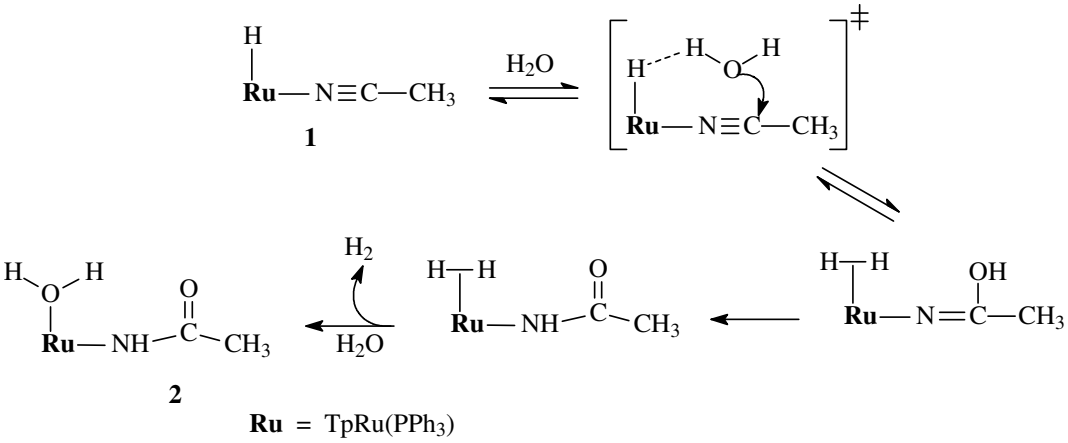

Scheme 2.5 Proposed mechanism of formation of 2

2.3.5 Theoretical Study

To study the feasibility of the proposed reaction mechanism shown in Scheme 2.5 for the reaction of hydride complex **1** with H_2O leading to the formation of complex **2**, theoretical calculations were performed at the Becke3LYP level of DFT theory to examine the most important step corresponding to the conversion of the acetonitrile ligand to the acetamido ligand. To reduce the computer cost, PH_3 was used to model PPh_3 in our calculations.

Figure 2.2 illustrates the relative electronic energies ΔE and the relative Gibbs free energies ΔG° at 298 K relevant to the conversion of the acetonitrile-coordinated complex **1**, which has a dihydrogen-bonding interaction between the hydride ligand and one of the two protons of H_2O, to the acetamido-coordinated complex **1c** having a Ru-(η^2-H_2) bond. As shown in Figure 2.2, the conversion can be summarized in two main elementary steps. The first one is the nucleophilic attack

of the oxygen atom in water at the carbon center of the acetonitrile ligand to form an imino-coordinated complex **1b** with an energy barrier of 31.95 kcal/mol; then a proton transfer occurs from the hydroxy group to the imino nitrogen to form the acetamido-coordinated complex **1c**. The second step corresponds to an enol-to-keto tautomerization, which commonly exists in organic chemistry and is expected to have a very small energy barrier in solution. [149-152]

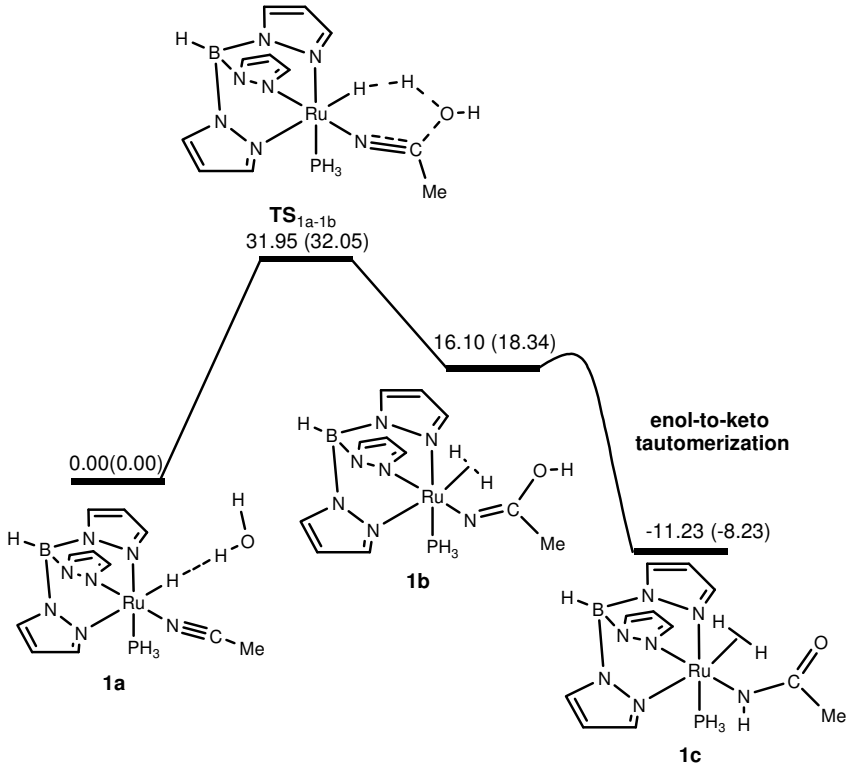

Figure 2.2 Energy profile for the conversion process of the acetonitrile-coordinated complex 1a to the acetamido-coordinated complex 1c. The calculated relative electronic energies and free energies (in parentheses) are given in kcal/mol

Figure 2.3 gives the optimized structures of species involved in the conversion process shown in Figure 2.2. The acetonitrile-coordinated complex **1a** is

a hydride that contains dihydrogen bonding to a water molecule, with an H---H distance of 1.772 Å. The dihydrogen-bonding interaction is strengthened in the transition state $\mathbf{TS_{1a\text{-}1b}}$, leading to shrinking of the H---H distance to 1.003 Å. Simultaneously, the distance between oxygen and the nitrile carbon decreases from 3.039 Å in **1a** to 1.744 Å in $\mathbf{TS_{1a\text{-}1b}}$. These structural changes directly lead to the formation of the complex **1b**, in which a dihydrogen and an imino ligands are formed. The H–H distance in **1b** is 0.838 Å. The C≡N triple bond of nitrile in **1a** (1.161 Å) changes to a double bond in **1b** (1.251 Å). **1b** lies 16.10 kcal/mol higher in electronic energy than **1a**, but as expected, its keto form **1c** is 11.23 kcal/mol lower than **1a**. The most relevant changes upon the enol-to-keto tautomerization concern the C–O bond, which decreases by 0.165 Å, and the C–N bond, which increases by 0.082 Å. From the conversion of **1a** to **1b**, we clearly see the structural change from a dihydrogen bond to a dihydrogen ligand, supporting the notion that the dihydrogen-bonding interaction assists the hydration process.

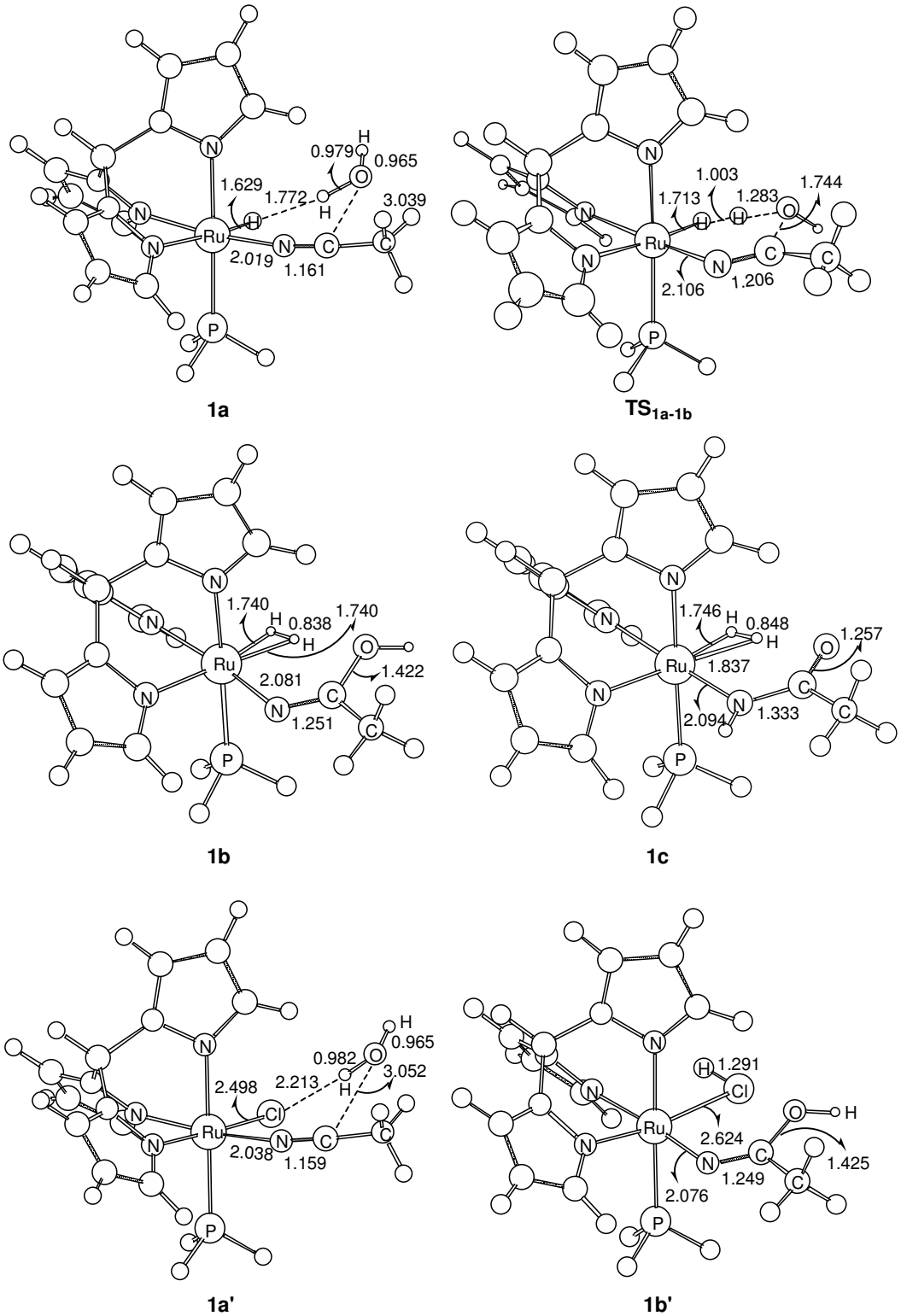

Figure 2.3 B3LYP optimized structures for those species shown in Figure 2.2 and Scheme 2.5. Bond lengths are given in Å

It is worth noting that, experimentally, such conversion of the acetonitrile ligand to the acetamido ligand is not observed for the chloro analogue of **1**. To gain insight into the reason, we calculated the reaction energy of **1a′** → **1b′** shown in Scheme 2.6. Examination of the scheme is seen that the imino-coordinated complex **1b′** is energetically located at 52.84 kcal/mol above the acetonitrile-coordinated complex **1a′**, indicating that **1b′** is thermodynamically very unstable in comparison with **1a′**. As a result, the chloro complex **1a′** does not undergo the conversion of the acetonitrile ligand to the acetamido ligand. To understand why the complex **1b′** is so unstable in comparison with the complex **1a′**, we have checked the geometric and electronic properties of these complexes. It is noted that the formation of H–Cl bond decreases the net negative charge of Cl dramatically from –0.56 to –0.12, weakening the coordination capability of the ligand remarkably. Of course, this dramatic charge reduction results in the corresponding structural modifications (**Figure 2.3**), i.e., the increase of Ru–Cl distance from 2.498 Å in **1a′** to 2.624 Å in **1b′**, which decreases the stability of the complex. In the case of complex **1b**, the dihydrogen ligand contributes to its stability in view of the fact that there are a large number of dihydrogen complexes reported in the literature. [127, 133-135, 153, 154]

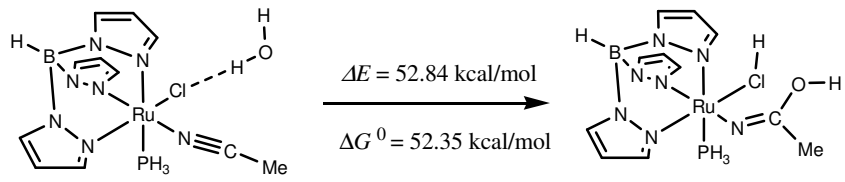

Scheme 2.6 Hydration of coordinated CH_3CN in 1a'

2.3.6 Reaction of 2 with H_2

The reaction of **2** in THF with H_2 (10 atm) was carried out in 1,4-dioxane-d_8 in a 5mm pressure-valved NMR tube. After heating the tube at 110 ˚C overnight, $^{31}P\{^1H\}$ and ^1H NMR spectroscopy showed that **2** was completely converted to $TpRu(PPh_3)(H_{3-x})D_x$ (**5d$_x$**), the isotopomers of the dihydrogen-hydride complex $TpRu(PPh_3)(H_2)H$ (**5**) (**eq 2.1**); we have previously reported the synthesis and reactivity of **5** and **5d$_x$**. [135] The presence of free acetamide was evidenced by detection of a singlet at δ 1.97 ppm in the ^1H NMR spectrum. Apparently, H_2 underwent H/D exchange with 1,4-dioxane-d_8 to give HD and D_2, which were the sources of deuterium in the isotopomers (eq 2.1). We have, in fact, demonstrated that **5** catalyzes H/D exchange between H_2 and R─D (R─D = THF-d_8, C_6D_6, and diethyl ether-d_{10}). [46]

$$\underset{\mathbf{2}}{TpRu(PPh_3)(H_2O)(NHCCH_3)} + H_2 \xrightarrow{\text{1,4-dioxane-}d_8} \underset{\mathbf{5d_x}}{TpRu(PPh_3)H_{3-x}D_x} + CH_3{-}C(=O){-}NH_2 \qquad \mathbf{2.1}$$

The formation of **5** from **2** and H_2 can be rationalized in terms of the reaction sequence shown in Scheme 2.7. Substitution of H_2O in **2** by H_2 forms the η^2-dihydrogen intermediate (See **1c** in **Fig. 2.2**), protonation of the acetamido ligand by η^2-H_2 gives free acetamide, and subsequent coordination of another H_2 molecule yields the dihydrogen-hydride complex. 1,2-addition of coordinated H─H across Ru─N bond of amido-type ligand is well-documented. [155-158] Gunnoe *et al.*

showed that an amido complex (PCP)Ru(CO)(NH_2) (PCP = 2,6-($CH_2P^tBu_2$)$_2C_6H_3$) can readily activate dihydrogen at room temperature to yield ammonia NH_3 and a hydride complex (PCP)Ru(CO)H. The ability of this amido complex to cleave the H-H bond is attributed to the combination of a vacant coordination site for binding and activation of dihydrogen, and a basic amido ligand. [156]

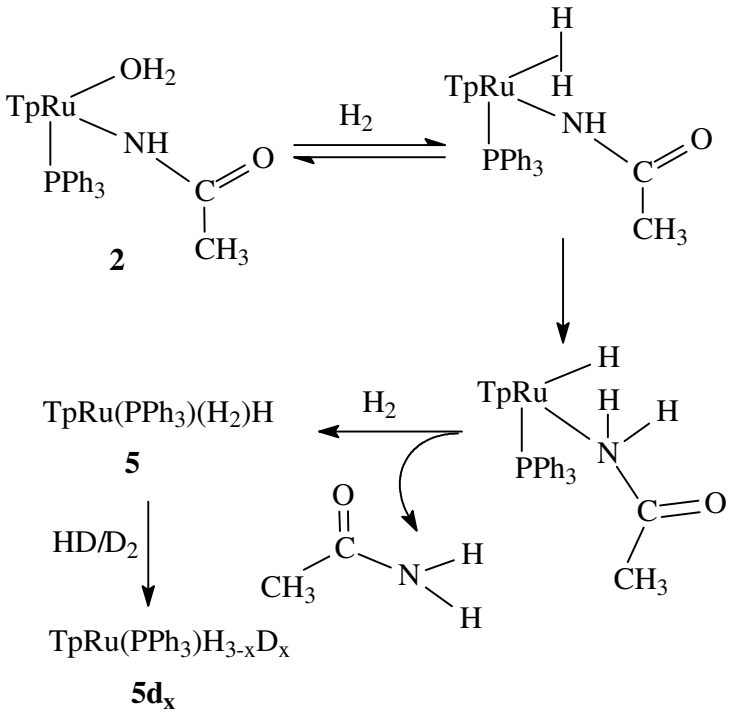

Scheme 2.7 Reaction of 2 with H_2

Morris and co-workers reported that the chiral catalyst $Ru(H)_2$(R-binap)($NH_2CMe_2CMe_2NH_2$), which is capable of catalyzing hydride and proton transfer (hydrogenation) to ketones to form chiral alcohols, can lose a H_2 molecule to produce Ru(H)(R-binap)($NHCMe_2CMe_2NH_2$) under argon, nitrogen and vacuum, but not H_2 pressure. This reversible intramolecular heterolytic splitting of

dihydrogen is rare and may proceed by an η^2-dihydrogen intermediate. [157] Rettig *et al*. have reported heterolytic cleavage of H_2 with $RuCl(PPh_3)[N(SiMe_2CH_2PPh_2)_2]$; it reacts with H_2 to form two isomeric amine-hydride derivates of the formula $RuCl(PPh_3)H[NH(SiMe_2CH_2PPh_2)_2]$. [158]

2.3.7 Reaction of 2 with H_2/D_2O

The reaction of **2** (in THF-d_8) with H_2 (10 atm) in the presence of excess D_2O was studied in a 5 mm pressure-valved NMR tube. It was found by $^{31}P\{^1H\}$ NMR spectroscopy that after heating the tube at 110 ˚C for 6 h, **2** was completely converted to a new species which showed a slightly broadened singlet at δ 68.8 ppm. The chemical shift of this signal is identical to that of the signal corresponding to one of the two minor species (**3**) which we detected at the later stage of the **1**-catalyzed THF/D_2O exchange reaction (vide supra). The solution was removed from the NMR tube and the volatile materials were removed by vacuo. The residue was washed several times with hexanes and then subjected to ^1H and $^{31}P\{^1H\}$ NMR studies which revealed that **3** is in fact the carbonyl hydride complex $TpRu(PPh_3)(CO)H$ that was previously reported by our group. [135] The hydride ligand of **3** was partially deuterated, as indicated by the diminished integration of the upfield hydride signal. We are not sure, at this stage, of the reaction sequence that leads to the formation of **3** (**eq 2.2**). Complex **3** detected in the course of the $TpRu(PPh_3)(CH_3CN)H$ (**1**)-catalyzed THF/D_2O exchange reaction probably resulted from the reaction of D_2O and the H_2 generated with **2**.

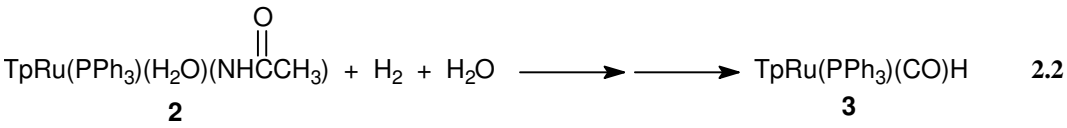

2.2

The catalytic activity of **2** in the H/D exchange reaction of THF with D_2O was studied; it was found that the complex was inactive for the exchange reaction. The **2**-catalyzed H/D reaction was again attempted in the presence of small amount of H_2; $^{31}P\{^1H\}$ NMR monitoring indicated that after an extended period of time, minute amounts of **3** and the other unidentified species **4** were formed, the H/D exchange reaction, however, remained undetected. Thus, like **2**, **3** and **4** are also inactive for the H/D exchange reaction.

2.3.8 Mechanism of 1-catalyzed H/D exchange between R─H and D_2O under Ar

In the light of our previous work on the **1**-catalyzed H/D exchange between CH_4 and R─D and the fact that the hydride ligand of **1** is rapidly deuterated by D_2O, we suggest that the H/D exchange between R─H and D_2O catalyzed by **1** proceeds via the sequence depicted in Scheme 2.8 (outer cycle). The hydride of **1** is acting as a go-between enabling the exchange the deuterium of D_2O with the hydrogen of R─H. Ru─H is rapidly deuterated by D_2O to form Ru─D, which then undergoes H/D exchange with R─H; we have previously investigated the exchange process between Ru─D and R─H by density funcitional theory calculations (See also **Scheme 2.1**). [46]

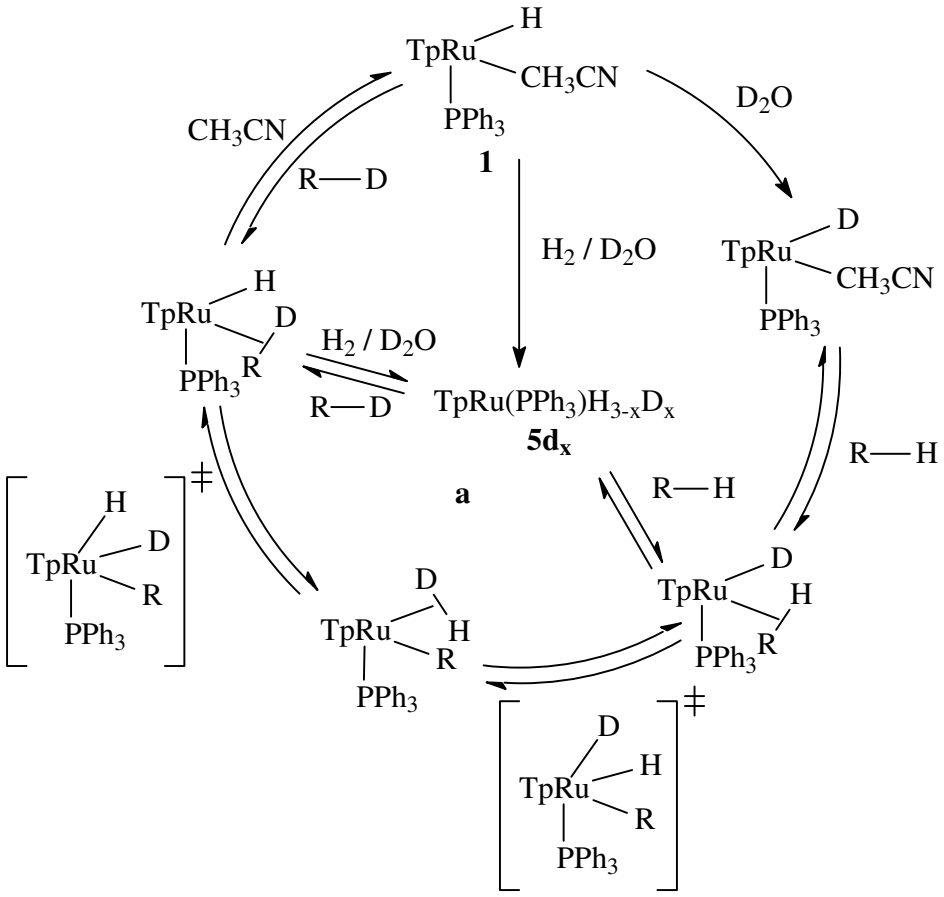

Scheme 2.8 Proposed catalytic cycle of H/D exchange between D_2O and organic solvents

In the course of the catalytic reaction, most of the complex **1** is converted to **2d**, **3**, and **4**; these complexes are found to be inactive (vide supra). Probably, **1**, which is the active species, was present in such a small amount that it is not detectable by $^{31}P\{^{1}H\}$and ^{1}H NMR spectroscopy.

2.3.9 Mechanism of 1-catalyzed H/D exchange between R−H and D_2O under H_2

We have also studied the H/D exchange reactions of the substrates with D_2O under H_2 (10 atm) instead of Ar; the results of which are shown in Table 2.4. It can be seen that the overall results of the exchange reactions are similar to those of the reactions under Ar. We monitored the behavior of the complex during a THF/D_2O exchange reaction under H_2 with ^1H and $^{31}P\{^1H\}$ NMR spectroscopy, it was observed that **1** was readily converted to a mixture of the HD isotopomers $TpRu(PPh_3)(H_{3-x})D_x$ (**5d$_x$**) of the dihydrogen-hydride complex $TpRu(PPh_3)(H_2)H$ (**5**), and it remained the only NMR detectable metal-containing species throughout the reaction. Unlike the exchange reaction performed under Ar, the acetamido complex **2d** and the other two species **3** and **4** were not formed in the present case. Thus, in the exchange reaction under H_2, **5d$_x$** is the active species of the catalytic system. The dihydrogen-hydride complex **5** is fluxional, [135, 159-162] the three hydrogen atoms interchange readily and are readily deuterated by D_2O. In fact, **5** is capable of catalyzing H/D exchange between H_2 and D_2O, and itself being deuterated to form **5d$_x$**. Similar to **1**, **5d$_x$** exchanges its Ru−D with R−H via the intermediacies of the σ-complexes (**Scheme 2.8**, cycle **a**). It is, however, suggested that **1** is more active than **5d$_x$** in the exchange reactions. The abundance of **5d$_x$** is much higher than that of **1** during the catalysis, and the former does not seem to degrade to other inactive species; however, due to its thermodynamic stability, it is expected to be more difficult for **5d$_x$**, in comparison with **1**, to generate the R−H σ-complex via the exchange of a H_2 or HD ligand for the R−H molecule.

Transition metal-catalyzed H/D exchange between H_2 and D_2O is well-documented. [163-168]Darensbourg *et al.* [167] have recently reported that diiron(II) complexes are capable of catalyzing H/D exchange between D_2 and water. The only requirement is the availability of a vacant site on Fe(II) center for binding of D_2 (or H_2); the coordinated D_2 (or H_2) is deprotonated by the external H_2O (or D_2O). (**Scheme 2.9**) Another example of isotopic exchange of η^2-D_2 ligand with H_2O is shown by Hoff and co-worker with the transition complex $W(CO)_3(P^iPr_3)_2(\eta^2\text{-}D_2)$. [165] Pápai *et al.* have investigated the interaction between a dihydride complex system $[RhH_2Cl(PR_3)_3]$ with D_3O^+ by means of theoretical studies. Their calculation suggested that the mechanism involves protonation of one of the hydrides by D_3O^+ via a dihydrogen-bonded complex resulting in the formation of the $RhH\text{-}(H\text{-}D)^+$ intermediate. The η^2-HD ligand can undergo fast internal rearrangement and a proton is transferred back to the D_2O molecule. The rotation energy for η^2-H_2 is calculated as ~3 kcal/mol. Crabtree *et al.* have indicated that $[Ir(bq)(PPh_3)_2H(H_2O)]SbF_6$ (bq = 7,8-benzoquinolinato) is an efficient catalyst for the H/D exchange between ROH and D_2. They mentioned two possible mechanisms; one of which, based on deprotonation of the η^2-D_2 ligand by ROH, is similar to the Pápai's one mentioned above. (**Scheme 2.10**) Another mechanism, involving H/D exchange between Ru-H and the η^2-D_2 ligand, is shown in Scheme 2.11. [164]

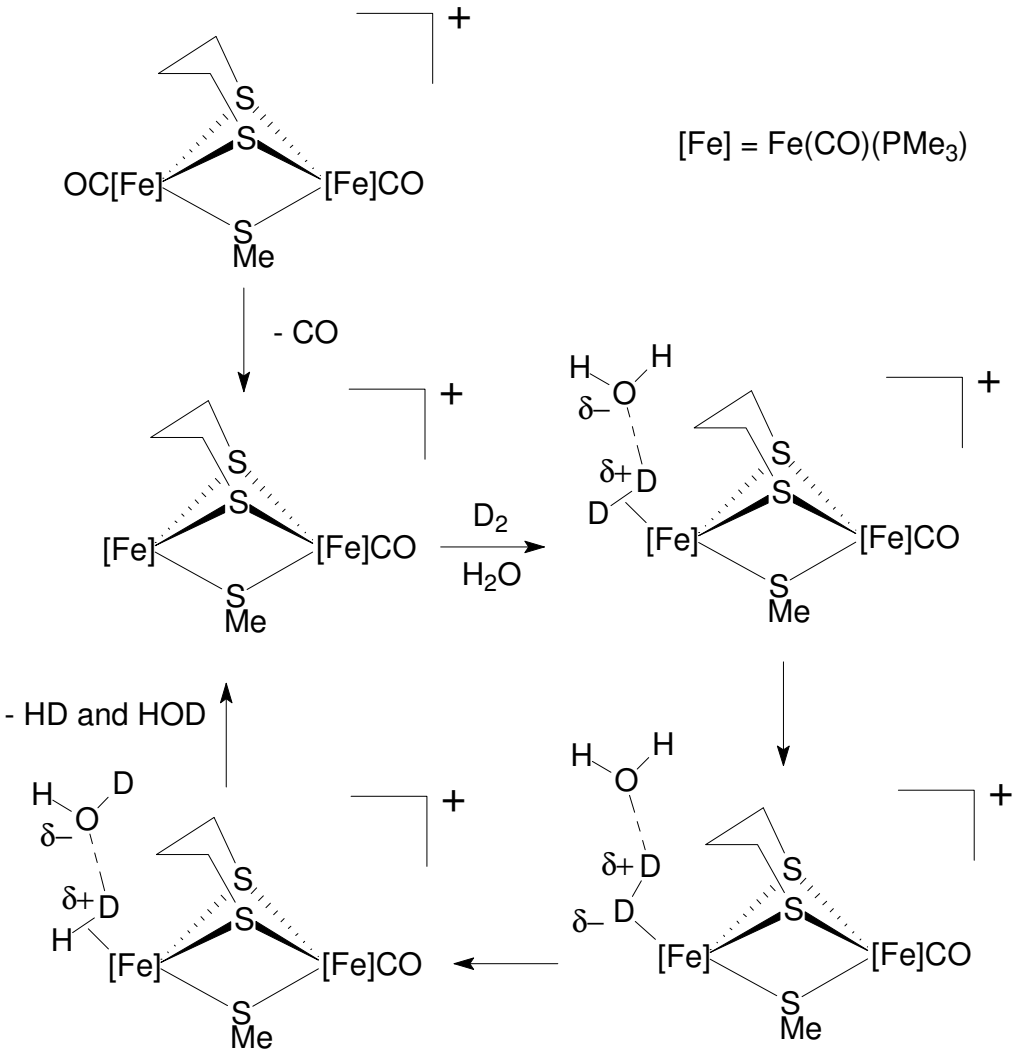

Scheme 2.9 H/D exchange between D_2 and H_2O by diiron(II) complex

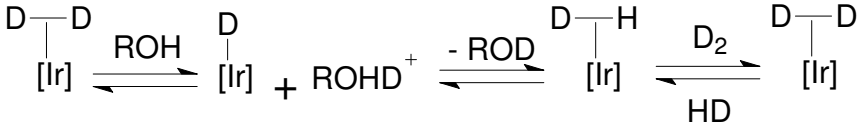

[Ir] = $Ir(PPh_3)_2(bq)H$

Scheme 2.10 H/D exchange between D_2 and ROH by Ir complex without assistance of hydride ligand

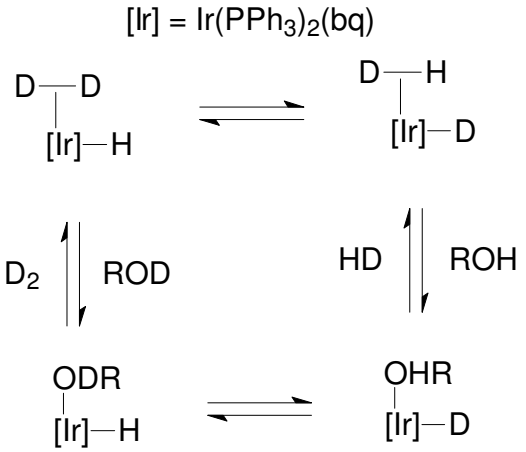

Scheme 2.11 H/D exchange between D_2 and ROH by Ir complex with assistance of hydride ligand

Table 2.4: H/D exchange of organic solvents and D_2O by 1 under Hydrogen[a]

Entry	Substrate	% deuteration		total TON[b]	mol % of **1**[c]
1	Benzene	22		318	0.41
2	Toluene	aliphatic:	13	289	0.48
		o and p:	17		
		m:	26		
3	Tetrahydrofuran	α hydrogen:	17	264	0.37
		β hydrogen:	7		
4	1,4-dioxane	20		408	0.40
5	diethyl ether	α hydrogen:	13	400	0.48
		β hydrogen:	23		

[a]Reaction condition: catalyst, 0.0091 mmol; substrate, 0.2 mL; D_2O, 0.1mL; pressure: H_2 = 10 atm; temperature, 110°C; reaction time, 24 h. [b]Total TON = mole of C-H bond activated/mol of catalyst. [c]Relative to the organic substrate.

Chapter 3 Mechanism of Catalytic Hydration of Nitriles with Hydrotris(pyrazolyl)borato (Tp) Ruthenium Complexes

3.1 Introduction

Catalytic hydration of nitriles to amides is an important transformation both in laboratory scale and in industry. In addition to higher chemoselectivity, i.e., the amides are not further hydrolyzed to the undesirable carboxylic acids, other advantages of the transition-metal-complex-catalyzed nitrile hydration reactions over the conventional acid- and base-catalyzed reactions include milder reaction conditions and higher tolerance to other functional groups.[64] A well-known mechanism for the transition-metal-catalyzed nitrile to amide conversion involves intramolecular nucleophilic attack of a hydroxo ligand or external attack of a hydroxide ion at the carbon atom of the η^1-coordinated nitrile molecule and subsequent protonation of the nitrogen atom.[81, 169, 170]

Parkins's homogeneous platinum phosphinito complex $[PtH(PMe_2OH)(PMe_2O)_2H]$ represents one of the most efficient catalysts for hydration of nitriles to amides (**Scheme 3.1**). The cationic nitrile complex $[Pt(RCN)(PMe_2OH)(PMe_2O)_2H]^+$ is the active species responsible for the catalysis, which begins by intramolecular nucleophilic attack of the PMe_2OH hydroxyl at the carbon center of the nitrile ligand, forming an intermediate that contains a five-membered-ring iminol-type ligand; addition of a H_2O molecule across the C=N bond

of the iminol-type ligand and subsequent proton transfer yields the amide. Coordination of a nitrile to the metal center regenerates the active species.[68, 171] Intramolecular attack by the hydroxo ion, bound to one metal center, at the nitrile molecule bonded to the other metal center in dinuclear iron, [70, 172] cobalt, [71, 84] copper, [72] palladium, [73] rhenium, [74] and nickel [75, 76] systems has also been reported.

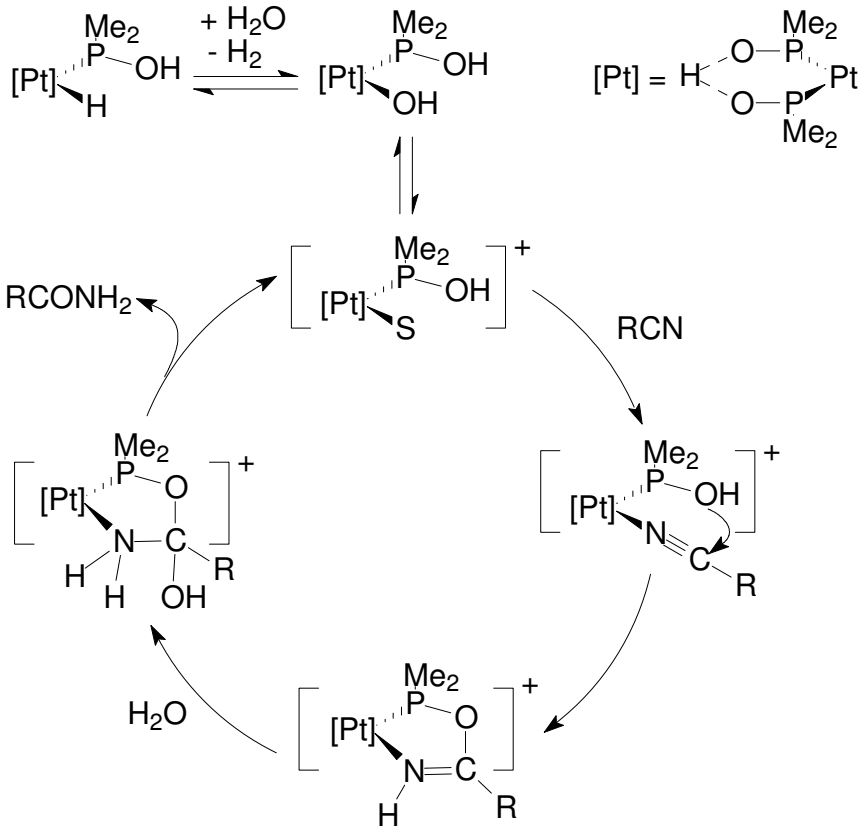

Scheme 3.1 Proposed mechanism for the hydration of nitriles by phosphinito complexes

Very recently, it was reported that the cyano moiety of the ligand (6-cyano-2-pyridylmethyl)bis(2-pyridylmethyl)amine in a dichloroferrous complex was hydrated to the corresponding carboxamide; this is the first example of hydration of

nitrile on a ferrous complex. It is proposed that the hydration proceeds via an "outer-sphere mechanism", which does not require the coordination of the nitrile moiety; it is activated in the vicinity of a metal-coordinated water molecule (Scheme 3.2). [173]

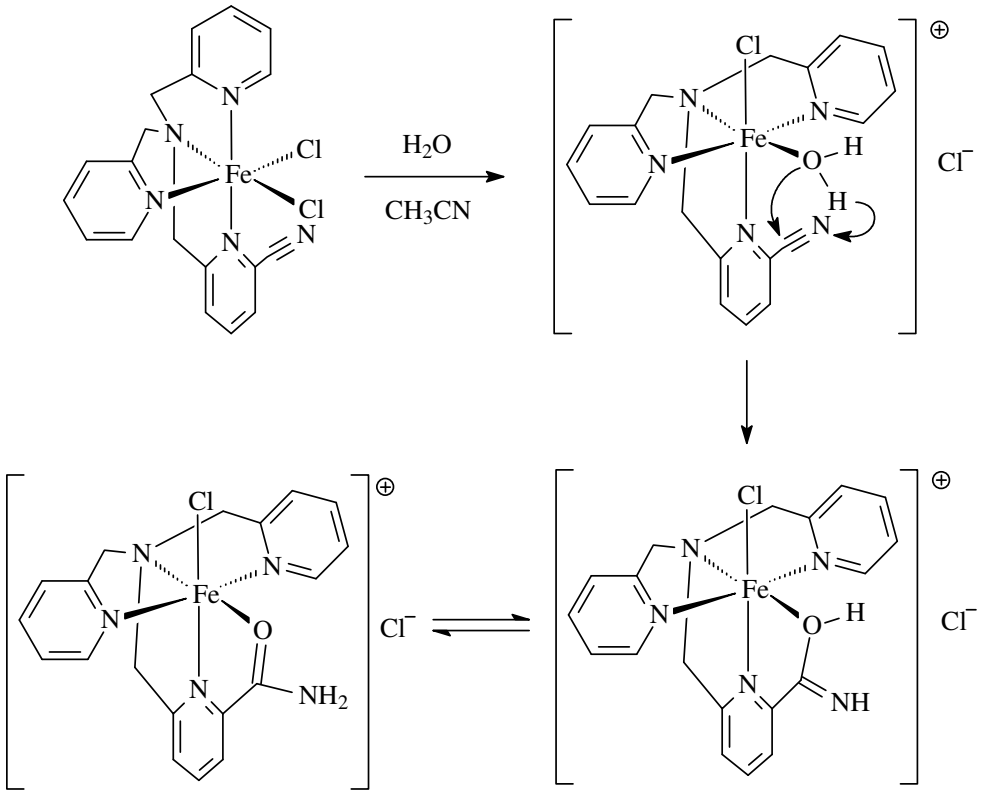

Scheme 3.2 Proposed mechanism of intramolecular nitrile hydration catalyzed by a ferrous complex

As mentioned in Chapter 2, the acetonitrile ligand of $TpRu(PPh_3)(CH_3CN)H$ (**1**) is readily attacked by water to yield the aquo-acetamido complex $TpRu(PPh_3)(H_2O)(NHC(O)CH_3)$ (**2**), but that of the chloro analogue $TpRu(PPh_3)(CH_3CN)Cl$ does not. The proposed reaction sequence featuring dihydrogen bond-mediated nucleophilic attack of water at the bound nitrile was shown in Scheme 2.5. [174] Examples of hydrogen-bond- and dihydrogen-bond-

mediated nitrile hydration were presented in Chapter 1 (**Schemes 1.7** and **1.12**). We report in this chapter the catalytic hydration of nitriles to amides with **2** and its benzamido analogue $TpRu(PPh_3)(H_2O)(NHC(O)Ph)$ (**8**) and discuss the detailed mechanism of the catalytic reaction. The uniqueness of this mechanism, in comparison to those of the transition metal-catalyzed-nitrile hydration reactions reported in the literature, will be demonstrated.

3.2 Experimental

3.2.1 Materials and Instrumentation

Ruthenium trichloride, $RuCl_3 \cdot 3H_2O$, pyrazole, sodium borohydride, triphenylphosphine, and organic substrates were obtained from Aldrich, International Laboratory and Acros. Triphenylphosphine was recrystallized from ethanol before use. Solvents were distilled under a dry nitrogen atmosphere with appropriate drying agents: hexane, diethyl ether, tetrahydrofuran, and 1,4-dioxane with sodium benzophenone; dichloromethane, acetonitrile, and chloroform with calcium hydride. All manipulations were carried out under a nitrogen atmosphere using standard Schlenk techniques. The complexes $TpRu(PPh_3)(CH_3CN)H$, [127] $TpRu(PPh_3)(CH_3CN)Cl$ [127] and $TpRu(PPh_3)_2Cl$ [175] were prepared according to literature methods. Deuterated NMR solvents, purchased from Armar and Cambrigde Isotope Laboratories, were dried with P_2O_5. High-purity argon gas was supplied by Hong Kong Oxygen.

Proton NMR spectra were obtained from a Bruker DPX 400 spectrometer. Chemical shifts were reported relative to residual protons of the deuterated solvents. ^{31}P NMR spectra were recorded on a Bruker DPX 400 spectrometer at 161.70 MHz, chemical shifts were externally referenced to 85% H_3PO_4 in D_2O. $^{13}C\{^1H\}$ NMR spectra were taken on a Bruker DPX 400 spectrometer at 100.61 MHz; chemical shifts were internally referenced to C_6D_6 (δ = 128.1 ppm), and 1,4-dioxane-d_8 (δ = 67.16 ppm). High-pressure NMR studies were carried out in commercial 5 mm Wilmad pressure-valved NMR tubes. Infrared spectra were obtained from a Bruker Vector 22 FT-IR spectrophotometer. Electrospray ionization mass spectrometry was carried out with a Finnigan MAT 95S mass spectrometer with the samples dissolved in dichloromethane. Elemental analyses were performed by M-H-W Laboratories, Phoenix, AZ, USA.

3.2.2 Synthesis and Reactions

3.2.2.1 Alternative method for synthesis of $TpRu(PPh_3)(H_2O)(NHC(O)CH_3)$ (2)

The complex $TpRu(PPh_3)(CH_3CN)Cl$ (0.20g, 0.31 mmol) and KOH (0.018 g, 1.5 equiv) were loaded into a two-necked round-bottom flask, which was then evacuated and flushed with nitrogen for four cycles. Freshly distilled THF (20 mL) and water (0.1 mL) were added to the flask and the resulting solution was refluxed with stirring for 24 h. The solution was cooled to room temperature, the volume of which was reduced to 6 mL in vacuo and 5 mL of hexane was added. The mixture

was filtered to remove some insoluble solids; the filtrate was brought to dryness in vacuo to afford a yellow solid. The solid was recrystallized with dichloromethane and diethyl ether; it was collected and dried under vacuum for several hours at room temperature.

Yield: 0.13 g (66 %).

Anal. Calcd (%) for $C_{29}H_{31}BN_7O_2PRu$: C 53.39, H 4.79, N 15.03; found: C 53.31, H 4.81, N 15.09.

IR (KBr, cm^{-1}): υ(C=O) = 1540 (med), υ(N-H) = 3337 (med), υ(B-H) = 2461 (med).

^1H NMR (400.13 MHz, C_6D_6, 25 ˚C): δ 2.05 (s, 3H; C*H*$_3$C(O)NH), 4.67 (s, 1H; $CH_3C(O)N$*H*), 5.93 (t, 1H of Tp), 5.97 (t, 1H of Tp), 6.28 (t, 1H of Tp), 6.87 (d, 1H of Tp), 7.29 (d, 1H of Tp), 7.78 (d, 1H of Tp), 7.85 (d, 2H of Tp), 8.24 (d, 1H of Tp) (all coupling constants for Tp proton resonances are about 2 Hz), 7.24 – 7.68 ppm (2 multiplets, 15H of PPh_3).

$^{31}P\{^1H\}$ NMR (161.7 MHz, 1,4-dioxane-d_8 25 ˚C): δ 59.3 (s).

$^{13}C\{^1H\}$ NMR (100.61 MHz, C_6D_6, 25 ˚C): δ 181.2 (s, CH_3*C*(O)NH), 25.7 (s, *C*H_3C(O)NH).

ESI-MS (CH_2Cl_2): *m/z*: 635 $[M-H_2O]^+$.

3.2.2.2 *In-situ* preparation of $TpRu(PPh_3)(NCCH_3)(NHC(O)CH_3)$ (6)

Acetronitrile (45 μL, 86 mmol) was added to a solution of $TpRu(PPh_3)(H_2O)(NHC(O)CH_3)$ (**2**) (5.0 mg, 7.7 μmol) in 0.4 mL of 1,4-dioxane-d_8 in a 5 mm NMR tube. The NMR tube was allowed to stand at room temperature

for 3 h. A ^{1}H NMR spectrum of the solution was taken. Two sets of Tp signals (signal intensity ratio is over 9:1) in the low field region are visible in the spectrum; the set with higher signal intensity is due to **6** and the set with smaller signal intensity is due to **2**. Complex **6** was characterized in situ by NMR spectroscopy.

^{1}H NMR (400.13 MHz, 1,4-dioxane-d_8, 25 ˚C): δ 1.73 (s, 3H; CH_3C(O)NH), 2.05 (s, 1H; CH_3CN), 3.22 (s, 1H; CH_3C(O)N*H*), 5.92 (t, 1H of Tp), 5.93 (t, 1H of Tp), 6.22 (t, 1H of Tp), 6.71 (d, 1H of Tp), 6.83 (d, 1H of Tp), 7.68 (d, 1H of Tp), 7.78 (d, 1H of Tp), 7.82 (d, 1H of Tp), 7.95 (d, 1H of Tp) (all coupling constants for Tp proton resonances are about 2 Hz), 7.19-7.31 (m, 15H of PPh_3).

^{31}P{^{1}H} NMR (161.7 MHz, 1,4-dioxane-d_8, 25 ˚C): δ 58.8 (s).

^{13}C{^{1}H} NMR (100.61 MHz, 1,4-dioxane-d_8, 25 ˚C):$_3$ δ 178.85 (s, CH_3*C*(O)NH).

3.2.2.3 Synthesis of TpRu(PPh_3)(κ^2-*N,O*-NH=CMeN=CMeO) (7)

A sample of TpRu(PPh_3)(H_2O)(NHC(O)CH_3) (**2**) (70 mg, 0.11 mmol) was loaded into a 11 mm tube with a Telfon screw cap, which was then evacuated and flushed with nitrogen for four cycles. Acetonitrile (0.56 mL, 100 equiv) and 1,4-dioxane (3 mL) were then added to the tube via syringes. The tube was heated in a 150^{o}C oil bath overnight. The solution was cooled and transferred to a 25 mL 2-neck flask; the solvent of the solution was removed by vacuum. Hexane (3 mL) was added to the residual paste with vigorous stirring to produce a pale yellow complex. It was collected and dried under vacuum for several hours at room temperature.

Yield: 25 mg (34%).

Anal. Calcd (%) for $C_{31}H_{32}BN_8OPRu$: C 55.12, H 4.77, N 16.59. Found: C 55.08, H 4.71, N 16.51.

IR (KBr, cm^{-1}): υ(C=N) = 1578, 1654 (med), υ(N-H) = 3382 (med), υ(B-H) = 2478 (med).

^1H NMR (400.13 MHz, C_6D_6, 25 ˚C): δ 2.06 (s, 3H; NH=CC*H*$_3$N=CCH$_3$O), 2.47 (s, 1H; NH=CCH$_3$N=CC*H*$_3$O), 5.98 (t, 1H of Tp), 6.03 (t, 1H of Tp), 6.23 (t, 1H of Tp), 6.92 (d, 1H of Tp), 7.00 (s, 1H, N*H*), 7.75 (d, 1H of Tp), 7.81 (d, 1H of Tp), 7.86 (d, 1H of Tp), 7.88 (d, 1H of Tp), 7.89 (d, 1H of Tp) (all coupling constants for Tp proton resonances are about 2 Hz), 7.22(m, 10H of PPh_3), 7.58 (m, 5H of PPh_3).

$^{31}P\{^1H\}$ NMR (161.7 MHz, C_6D_6, 25 ˚C): δ 60.0 (s).

$^{13}C\{^1H\}$ NMR (100.61 MHz, C_6D_6, 25 ˚C): δ 176.1, 168.1 (s, NH=*C*MeN=*C*MeO).

ESI-MS $[M^+]$ = 676.35.

3.2.2.4 Synthesis of TpRu(PPh$_3$)(PhCN)(Cl)

A sample of TpRu(PPh$_3$)$_2$Cl (0.55 g, 0.63 mmol) was loaded into a two-necked round-bottom flask, which was then evacuated and flushed with nitrogen for four cycles. Freshly distilled THF (15 mL) and benzonitrile (0.15 mL) were added into the flask. The mixture was refluxed for 3 h. The solvent was then removed in vacuo to afford an orange paste. Hexane (5 mL) was added to the residue, with stirring, to produce a yellow solid. The solid was collected and washed with hexane (3 X 5 mL); it was dried under vacuum for several hours at room temperature.

Yield: 0.29 g (65 %).

Anal. Calcd (%) for $C_{34}H_{30}BClN_7PRu$: C 57.12, H 4.23, N 13.71. Found: C 57.05, H 4.21, N 13.09.

^{1}H NMR (400.13 MHz, $CDCl_3$, 25 ˚C): δ 5.75 (t, 1H of Tp), 5.85 (t, 1H of Tp), 6.23 (t, 1H of Tp), 6.61 (d, 1H of Tp), 7.20 (d, 1H of Tp), 7.64 (d, 2H of Tp), 7.68 (d, 1H of Tp), 8.11 (d, 1H of Tp) (all coupling constants for Tp proton resonances are about 2 Hz), 6.96-7.37 (m, 15H of PPh_3 and m, 5H of PhCN).

^{31}P{^{1}H} NMR (161.7 MHz, $CDCl_3$, 25 ˚C): δ 49.3 (s).

ESI-MS [M^+] = 715.24.

3.2.2.5 Synthesis of $TpRu(PPh_3)(H_2O)(NHC(O)Ph)$ (8)

Complex **8** was prepared by using the same procedure as for the preparation of **2** except that $TpRu(PPh_3)(PhCN)Cl$ was used in place of $TpRu(PPh_3)(CH_3CN)Cl$. Yield: 86 mg (43 %).

Anal. Calcd (%) for $C_{34}H_{33}BN_7O_2PRu$: C 57.15, H 4.66, N 13.72. Found: C 56.98, H 4.72, N 13.73.

IR (KBr, cm^{-1}): υ(C=O) = 1525 (med), υ(N-H) = 3354 (med), υ(B-H) = 2463 (med).

^{1}H NMR (400.13 MHz, C_6D_6, 25 ˚C): δ 5.92 (s, 1H of N*H*), 5.96 (t, 1H of Tp), 5.99 (t, 1H of Tp), 6.16 (t, 1H of Tp), 6.91 (d, 1H of Tp), 7.31 (d, 1H of Tp), 7.75 (d, 1H of Tp), 8.01 (d, 2H of Tp), 8.21 (d, 1H of Tp), 7.32(d, 1H of phenyl ring of benzamido), 7.87 (m, 2H of phenyl ring of benzamido), 7.18, (m, 10H of PPh_3), 7.65 (m, 5H of PPh_3 and 2H of phenyl ring of benzamido).

^{31}P{^{1}H} NMR (161.7 MHz, C_6D_6, 25 ˚C): δ 58.8 (s).

$^{13}C\{^{1}H\}$ NMR (100.61 MHz, C_6D_6, 25 ˚C): δ 181.5 (s, Ph*C*(O)NH).

ESI-MS [M^+-H_2O] = 697.04.

3.2.2.6 Synthesis of TpRu(PPh_3)(NCPh)(NHC(O)Ph) (9)

A sample of TpRu(PPh_3)(H_2O)(NHC(O)Ph) (**8**) (0.30 g, 0.42 mmol) was loaded into a 50 mL round-bottom flask, which was then evacuated and flushed with nitrogen for four cycles. Benzonitrile (81 μL; 2 equiv) and THF (3 mL) were added to the flask. The mixture was stirred overnight at room temperature. The solvent was then removed under vacuum to afford a yellow paste. Hexane (5 mL) was added to the residue, with stirring, to produce a yellow solid. The solid was collected and dried in vacuo.

Yield: 0.22 g (65%).

Anal. Calcd (%) for $C_{41}H_{36}BN_8OPRu$: C 61.58, H 4.54, N 14.01. Found: C 61.50, H 4.58, N 14.16.

IR (KBr, cm^{-1}): υ(C=O) = 1602 (s), υ(C≡N) = 2238 (med), υ(N-H) = 3359 (b), υ(B-H) = 2482 (med).

^{1}H NMR (400.13 MHz, C_6D_6, 25 ˚C): δ 5.03 (s, 1H of N*H*), 5.99 (t, 1H of Tp), 6.13 (t, 1H of Tp), 6.16 (t, 1H of Tp), 7.45 (d, 1H of Tp), 7.53 (d, 1H of Tp), 7.87(d, 1H of Tp), 8.19 (d, 1H of Tp), 8.21 (d, 1H of Tp), 8.33 (d, 1H of Tp), 7.03 (m, 3H of phenyl ring of benznitrile), 7.75 (m, 2H of phenyl ring of benzamido), 7.21, (m, 10H of PPh_3), 7.91 (m, 5H of PPh_3 and 2H of phenyl ring of benzamido).

$^{31}P\{^{1}H\}$ NMR (161.7 MHz, C_6D_6, 25 ˚C): δ 57.1 (s).

$^{13}C\{^{1}H\}$ NMR (100.61 MHz, C_6D_6, 25 ˚C): δ 178.4 (s, Ph*C*(O)NH).

ESI-MS $[M^+]$ = 800.14.

3.2.2.7 Synthesis of TpRu(PPh_3)(κ^2-*N,O*-NH=CPhN=CPhO) (10)

Complex **10** was prepared by using the same procedure as for the preparation of **7** except that TpRu(PPh_3)(H_2O)(NHC(O)Ph) **8** and benzonitrile (3 equiv) were used instead of TpRu(PPh_3)(H_2O)(NHC(O)CH_3) **2** and acetonitrile (100 equiv).

Yield: 44 mg (56%).

Anal. Calcd (%) for $C_{41}H_{36}BN_8OPRu$: C 61.58, H 4.54, N 14.01. Found: C 61.42, H 4.51, N 13.92.

IR (KBr, cm^{-1}): υ(C=N) = 1586, 1975 (med), υ(N-H) = 3320 (med), υ(B-H) = 2481 (med).

^{1}H NMR (400.13 MHz, C_6D_6, 25 ˚C): δ 5.96 (t, 1H of Tp), 6.06 (t, 1H of Tp), 6.09 (t, 1H of Tp), 7.03 (d, 1H of Tp), 7.07 (m, 10H of PPh_3), 7.49 (m, 5H of PPh_3 and 6H of phenyl rings of NH=CPhN=CPhO), 7.66 (d, 1H of Tp), 7.81 (dd, 2H of phenyl ring of NH=CPhN=CPhO), 7.92 (dd, 2H of phenyl ring of NH=CPhN=CPhO), 8.19 (d, 1H of Tp), 8.21 (d, 1H of Tp), 8.46 (s, 1H of N*H*), 8.89 (d, 1H of Tp), 8.91 (d, 1H of Tp).

$^{31}P\{^{1}H\}$ NMR (161.7 MHz, C_6D_6, 25 ˚C): δ 57.6 (s).

$^{13}C\{^{1}H\}$ NMR (100.61 MHz, C_6D_6, 25 ˚C): δ 165.7, 170.9 (s, NH=*C*PhN=*C*PhO).

ESI-MS $[M^+]$ = 800.09.

3.2.2.8 Synthesis of $TpRu(PPh_3)(\kappa^2\text{-}N,O\text{-}NH{=}CMeN{=}CPhO)$ (11)

Complex **11** was prepared by using the same procedure as for the preparation of **10** except that acetonitrile (50 equiv) was used instead of benzonitrile (3 equiv).

Yield: 29 mg (40%).

Anal. Calcd (%) for $C_{36}H_{34}BN_8OPRu$: C 58.62, H 4.65, N 15.19. Found: C 58.14, H 4.80, N 15.12.

IR (KBr, cm^{-1}): υ(C=N) = 1671, 1973 (med), υ(N-H) = 3305 (med), υ(B-H) = 2468 (med).

^1H NMR (400.13 MHz, C_6D_6, 25 ˚C): δ 2.13 (s, 3H of NH=CCH_3N=CPhO), 6.03 (t, 1H of Tp), 6.07 (t, 2H of Tp), 7.01 (d, 1H of Tp), 7.13 (m, 10H of PPh_3), 7.44 (m, 3H of phenyl ring of NH=CMeN=CPhO), 7.53 (m, 5H of PPh_3), 7.68 (d, 1H of Tp), 7.74 (d, 1H of Tp), 7.81 (d, 2H of Tp), 7.92 (m, 2H of phenyl ring of NH=CMeN=CPhO), 8.84 (d, 1H of Tp), 8.86 (d, 1H of Tp).

$^{31}P\{^1H\}$ NMR (161.7 MHz, C_6D_6, 25 ˚C): δ 59.1 (s).

$^{13}C\{^1H\}$ NMR (100.61 MHz, C_6D_6, 25 ˚C): δ 168.7, 170.4 (s, NH=*C*MeN=*C*PhO).

ESI-MS $[M^+]$ = 738.09.

3.2.2.9 General procedure of catalytic hydration of nitriles

The reactions were carried out in 5 mm pressure-valved NMR tubes. In a typical run, the catalyst (2.5 mg) was dissolved in a mixture of H_2O (0.14 mL, 2000 equiv), nitrile (0.04mL, 200 equiv) and 1,4-dioxane (~0.2 mL). The tube was

pressurized with 10 bar of argon and heated in a 150 ^{o}C silicon oil bath for 24 h. At the end of the reaction time, the tube was cooled to room temperature; a 0.1 mL aliquot of the solution was removed and analyzed by ^{1}H NMR spectroscopy (in $CDCl_3$). Comparison of the integrations of the characteristic peaks of the amide and the remaining nitrile gave the percent conversion of the reaction.

3.2.2.10 Monitoring of 1-catalyzed hydration of acetonitrile with NMR spectroscopy

A sample of **1** (2.7 mg) was loaded into a 5mm pressure-valved NMR tube. The tube was evacuated and filled with nitrogen for three cycles. Acetonitrile (6 μL, 25 equiv), water (3 μL, 30 equiv) and 1,4-dioxane-d_8 (0.2 mL) were added via syringes. The resulting solution was heated at 90 ^{o}C under 10 bar Ar. At different time intervals, the tube was cooled down to room temperature and ^{1}H and ^{31}P NMR spectra of the solution were taken.

3.2.2.11 Monitoring of 2- or 8-catalyzed hydration of acetonitrile and benzonitrile with NMR spectroscopy

Acetonitrile or benzonitrile (6 μL, 25 equiv) was added to a 5 mm pressure-valved NMR tube loaded with **2** (2.5 mg) or **8** (2.5 mg), respectively. Water (12 μL, 180 equiv) and 1,4-dioxane-d_8 (0.2 mL) were then added into the tube via syringes.

The tube was heated inside the probe of the NMR spectrometer; ^{1}H and ^{31}P NMR spectra were collected at different temperatures. (See **Figures 3.1** and **3.2**).

3.2.2.12 Crystallographic Structure Analysis of TpRu(PPh$_3$)(H$_2$O)(NHC(O)Ph) 8 and TpRu(PPh$_3$)(κ^2-*N,O*-NH=CPhN=CPhO) 10

Yellow crystals of **8** and **10** suitable for X-ray diffraction study were obtained by layering of *n*-hexane on a dichloromethane solution of the complex. A suitable crystal **8** with dimensions 0.28 × 0.14 × 0.10 mm or **10** with dimensions 0.40 x 0.32 x 0.18mm was mounted on a Bruker CCD area detector diffractomer and subject to Mo Kα radiation (λ = 0.71073 Å) from a generator operating at 50 kV and 30 mA. The intensity data of **8** and **10** were collected in the range θ = 1.92 – 27.57^{o} and 2.05 – 27.66^{o}, respectively, with oscillation frames of ψ and ω in the range 0 – 180^{o}. A total of 1464 frames in **8** and 1840 frames in **10** were taken in four shells. An empirical absorption correction of the SADABS (Sheldrick, 1996) program based on Fourier coefficient fitting was applied. The crystal structures were solved by Patterson function methods and expanded by difference Fourier synthesis, and refined by full-matrix least-squares on F^2 using the Bruker Smart and Bruker SHELXTL program packages. All non-hydrogen atoms were refined anisotropically. Hydrogen atoms were placed in ideal positions and refined as riding atoms, except for the two on the aqua ligand in **8** and the proton on *N*-imidoylimidato moiety in **10**; they were located by difference electron density map. The R and R_w values of **8** are 0.086 and 0.2099, respectively, and those of **10** are 0.0453 and 0.1044, respectively.

3.3 Results and Discussion

3.3.1 Catalytic hydration of nitriles to amides with $TpRu(PPh_3)(CH_3CN)H$ (1) and $TpRu(PPh_3)(H_2O)(NHC(O)CH_3)$ (2), and NMR monitoring of the 1- and 2-catalyzed hydration of acetonitrile

In view of the fact that **1** reacts readily with water to form the aquo-acetamido complex **2**, we anticipated that **1** might be a catalyst for the hydration of nitriles to amides. In fact **1** was found to be active for the catalysis. The results of a few cases of **1**-catalyzed hydration of nitriles to amides are shown in Table 3.1.

Table 3.1. Comparison on 1- and 2-catalyzed nitrile hydration[a]

Substrate	Conversion (%)[b]	
	$TpRu(PPh_3)(CH_3CN)(H)$ (**1**)	$TpRu(PPh_3)(NHCOCH_3)(H_2O)$ (**2**)
Acetonitrile[c]	8.3	8.7
Benzonitrile	7.3	8.8
Benzyl cyanide	Nil	Nil
Propionitrile	11.8	14.5
Crotononitrile	37.5	39.8

[a] Reaction conditions: catalyst, 4.6 μmol; nitrile: water: catalyst = 500:600:1; solvent, 1,4-dioxane (0.5 mL); reaction condition: 72 h; 120 ^oC; temperature (oil bath) 120 ºC. [b] Determined by ^1H NMR spectroscopy; based on nitrile used. [c] nitrile: water: catalyst = 1000:1000:1; neat substrate.

In the **1**-catalyzed hydration of acetonitrile (in 1,4-dioxane-d_8) carried out in a sealed NMR tube, after heating at 90 ºC for 230 min, the $^{31}P\{^1H\}$ spectrum of the solution taken at room temperature showed signals at δ 61.6, 66.6, and 69.4 ppm. Another signal at δ 60.8 ppm started to emerge after heating for 470 min. This signal gained intensity at the expense of the other signals and finally became the only signal after 1700 min; we later verified that it corresponds to **7**, which is the most stable species in the catalytic cycles of the **1**- and **2**-catalyzed acetonitrile hydration reactions (vide infra). As can be seen from Table 3.1, the catalytic activity of the aquo-acetamido complex **2** is very similar to that of **1**. A **2**-catalyzed hydration reaction of acetonitrile was monitored by NMR spectroscopy (Figure 3.1).

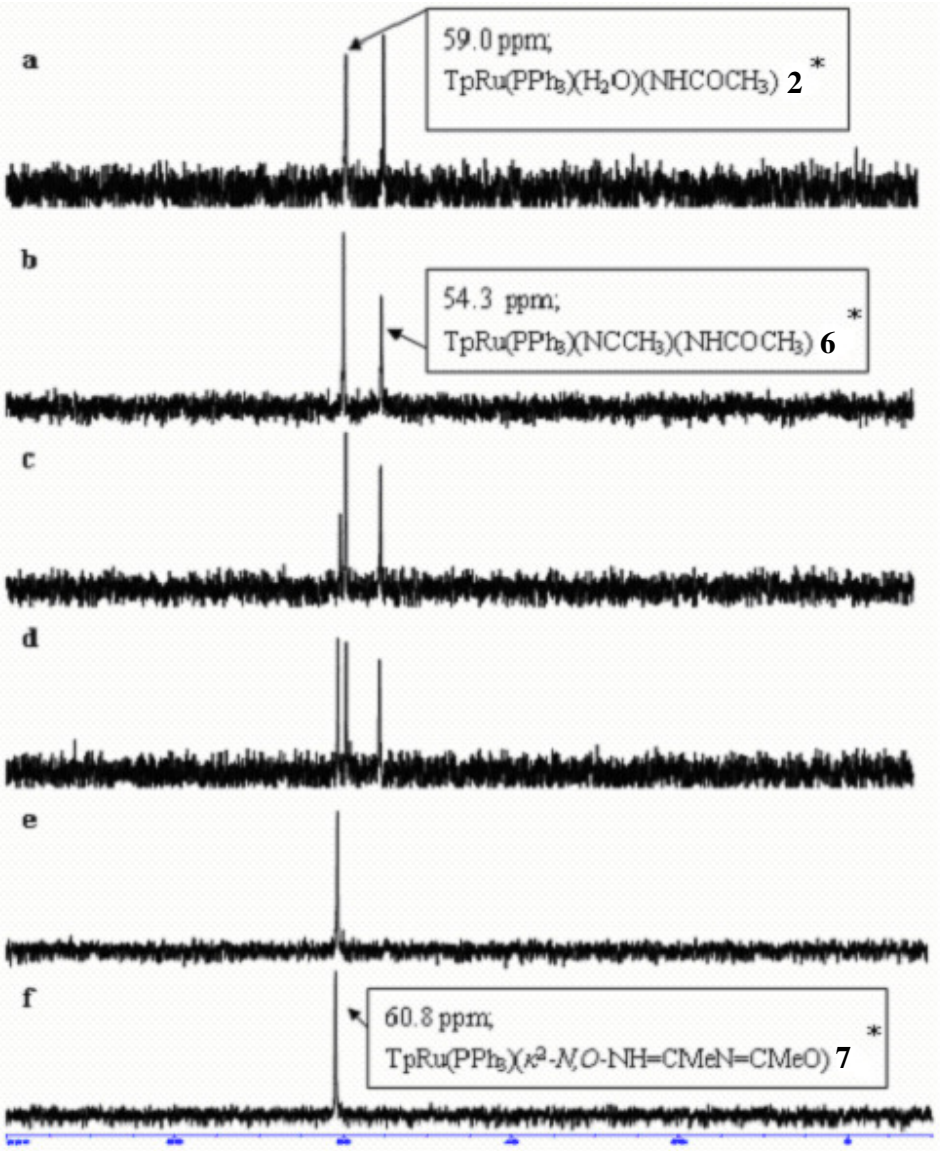

Figure 3.1. ^{31}P NMR study of 2-catalyzed hydration of acetonitrile: (a) immediately after addition of nitrile and water at room temperature; (b) 12 h at room temperature; (c) 50 ^{o}C for 30 min; (d) 75 ^{o}C for 30 min; (e) 90 ^{o}C for 30 min; (f) 105 ^{o}C for 30 min. ^{31}P{^{1}H} NMR spectra were taken at temperatures indicated.*The chemical shifts of 2, 6, and 7 in the presence of water and nitrile are slightly different from those of the authentic samples taken in 1,4-dioxane-d_8.

The room-temperature ^{31}P{^{1}H} NMR spectrum of a 1,4-dioxane-d_8 solution of **2** in a needle-valved NMR tube immediately taken after the addition of 25 equiv

of acetonitrile and 180 equiv of water and application of 10 atm of Ar gas (to prevent boiling of the solution at high temperatures) showed a singlet at δ 59.0 ppm corresponding to **2** and another singlet of approximately equal intensity at δ 54.3 ppm; this signal is due to the nitrile-amido complex $TpRu(PPh_3)(CH_3CN)(NHC(O)CH_3)$ (**6**) which we later synthesized and characterized in situ. After heating the solution in the NMR tube in the probe at 50 ºC for 30 min, the $^{31}P\{^1H\}$ NMR spectrum taken at this temperature showed, in addition to the signals of **2** and **6**, a new singlet at δ 60.8 ppm; this signal is due to complex **7**, which contains a chelating *N*-imidoylimidato ligand, κ^2-*N,O*-$NH{=}CMeN{=}CMeO^-$. The ratio **2**: **6**: **7** was ~ 2: 2: 1. After heating the tube for another 30 min at 75 ºC, the $^{31}P\{^1H\}$ spectrum (at 75 ºC) of the solution showed that the ratio **2**: **6**: **7** was approximately 1: 1: 1. Heating the solution at a higher temperature (90 ºC) for another 30 min led to total conversion of **2** and **6** to **7**, as indicated by the presence of only one signal, which is due to **7**, in the $^{31}P\{^1H\}$ NMR spectrum. The solution was further heated for 200 min at 120 ºC; at the end of this period, complex **7** remained the only detectable species by $^{31}P\{^1H\}$ NMR spectroscopy. It should be pointed out that the ^1H NMR spectra taken concurrently with the ^{31}P spectra showed that the hydration of acetonitrile began to occur and proceed to a very small extent at 90 ºC; the catalysis occurred more readily at 120 ºC and approximately 30% of the acetonitrile was converted to acetamide after heating at this temperature for 200 min. The above-mentioned NMR monitoring experiments seem to indicate that the **2**-catalyzed nitrile hydration is more amenable to a detailed mechanistic study, and in view of the fact that its catalytic activity might be similar

to that of **1**, we therefore decided to carried out a detailed investigation of nitrile hydration with **2** and its analogues with different amido ligands. Moreover, we have learned later that **2** can be more conveniently synthesized by reacting $TpRu(PPh_3)(CH_3CN)Cl$ with KOH in THF in the presence of a small amount of water (eq 3.1).

$$TpRu(PPh_3)(CH_3CN)Cl + KOH \xrightarrow{THF/H_2O} \underset{\mathbf{2}}{TpRu(PPh_3)(H_2O)(NH{-}\overset{\overset{O}{\|}}{C}{-}CH_3)} \quad \mathbf{3.1}$$

The results of the **2**-catalyzed hydration of nitriles are shown in Table 3.2; the reactions were carried out at 150 ºC (oil bath temperature) instead of 120 ºC since conversions at this temperature are much higher than those at the lower temperature. The Ar pressure was applied to prevent the solution from boiling too vigorously in the tube. In general, aryl nitriles are hydrated more readily than the aliphatic analogues. The order of reactivity of the aryl nitriles, 4-chlorobenzonitrile > benzonitrile > 4-methoxybenzonitrile, seems to indicate that nucleophilic attack of H_2O at the nitrile is an important step of the catalytic reaction. Using the hydration of acetonitrile as an example, it can be seen that catalytic activity of **2** (TOF = 5.3) is low compared to that of Parkins's highly efficient platinum complex $[PtH(PMe_2OH)(PMe_2O)H]$ (TOF = 380) [171] and other platinum complexes $[PtH(H_2O)(PMe_3)_2]OH$ (TOF = 178) [169] and $[PtH(H_2O)(PEt_3)_2]OH$ (TOF = 70) [169], but is comparable with those of the less effective catalysts such as [Cp*Ir(η^3-

$CH_2CHCHPh)(NCCH_3)]^+$ (TOF = 8.3) [99], $[(MeCp)_2Mo(OH)(H_2O)]^+$ (TOF = 4.2) [77], and (η^3-C_9H_7)Ru(dppm)H (TOF = 12) [61]. Complex **2** is not a very active catalyst for nitrile hydration; however, as will be shown in later sections, catalysis with this complex proceeds by a mechanism very different from the conventional ones.

Table 3.2. Catalytic hydration of nitriles with $TpRu(PPh_3)(H_2O)(NHC(O)CH_3)$ (2)[a]

Entry	Substrate	Turnover number (TON)[b,c]	Turnover frequency (TOF)[d]
1	Anisonitrile	174	7.3
2	Benzonitrile	182	7.6
3	4-Chlorobenzonitrile	200	8.3
4	Acetonitrile	128	5.3
5	Benzyl cyanide	80	3.3
6	Butyronitrile	112	4.7
7	Crotononitrile	74	3.1
8	Hexanenitrile	62	2.6
9	Isobutyronitrile	100	4.2
10	Propionitrile	96	4.0
11[e]	Acetonitrile	118	4.9
12[e]	Benzonitrile	178	7.4

[a] Reaction conditions: catalyst, 4.6 μmol; catalyst: nitrile: water = 1:200:2000; solvent, 1,4-dioxane (to fill up to a total volume of ~0.4mL); pressure: Ar = 10 atm; temperature (oil bath) 150 ºC; time : 24 h. [b] Determined by ^{1}H NMR spectroscopy; based on nitrile used. [c] Mole of product per mole of catalyst. [d] Mole of product per mole of catalyst per hour. [e] Catalyst: $TpRu(PPh_3)(\kappa^2$-*N,O*-NH=CMeN=CMeO) (**7**).

3.3.2 Synthesis of TpRu(PPh$_3$)(CH$_3$CN)(NHC(O)CH$_3$) (6)

Complex **2** reacted with excess acetonitrile at room temperature in THF to form **6**; however, during the workup when the acetonitrile was removed under reduced pressure, a small portion of **6** was reconverted to **2**, probably due to the fact that the small amount of water present in the solution was not as readily removed as the acetonitrile and therefore its concentration in the solution increased. Complex **6** prepared by this method is therefore always contaminated by a small amount of **2**. Complex **6** prepared in 1,4-dioxane-d_8 in an NMR tube can, however, be characterized in situ by ^{1}H , ^{13}C{^{1}H}, and ^{31}P{^{1}H} NMR spectroscopy. The ^{1}H NMR spectrum of **6** shows the typical nine-peak pattern of the Tp ligand in the downfield region (δ 7.19 -7.31 ppm), indicative of the presence of three inequivalent ligands trans to the pyrazolyl moieties of the Tp ligand. The N–H is shown as a slightly broadened singlet at δ 3.22 ppm. The methyl protons of the acetamido ligand and the coordinated acetonitrile appear as two singlets at δ 1.73 and 2.05 ppm, respectively. A singlet that corresponds to the carbonyl carbon of the acetamido ligands is seen at δ 178.9 ppm in the ^{13}C{^{1}H} NMR spectrum. The ^{31}P{^{1}H} NMR spectrum shows a singlet at δ 58.8 ppm.

3.3.3 Synthesis of TpRu(PPh$_3$)(κ^2-*N*,*O*-NH=CMeN=CMeO) (7)

Complex **7**, the most stable species observed in the course of the **2**-catalyzed hydration of acetonitrile, was independently prepared by reacting **2** with excess

CH_3CN in 1,4-dioxane in a sealed tube at an oil bath temperature of 130 ºC. We initially took **7** as the acetamide-acetamido complex $TpRu(PPh_3)(NH_2C(O)CH_3)(NHC(O)CH_3)$ since the NMR and IR spectroscopic data of the complex seem to be consistent with this structure; we thought that $TpRu(PPh_3)(NH_2C(O)CH_3)(NHC(O)CH_3)$ could have been readily formed by exchange of the water ligand of **2** for a nitrile molecule and subsequent hydration of the latter. Several attempts to grow single crystals of **7** for X-ray crystallographic study failed. However, a successful X-ray crystallographic study of $TpRu(PPh_3)(\kappa^2$-*N*,*O*-NH=CPhN=CPhO) **10**, the phenyl analogue of **7**, and density functional theory study (*vide infra*) later help to deduce that **7** is not the acetamido-acetamide complex, it is instead a complex containing a chelating *N*-imidoylimidato ligand, $TpRu(PPh_3)(\kappa^2$-*N*,*O*-NH=CMeN=CMeO) (see Chart 3.1). The NMR and IR data can be accounted for with this structure. Thus, in the ^1H NMR spectrum, the two singlets at δ 2.06 and 2.47 are due to the two methyl groups of the ring; the three legs trans to the Tp ligand are inequivalent, therefore giving rise to the nine-peak pattern in the low field region. The two peaks observed at δ 168.1 and 176.1 ppm in the $^{13}C\{^1H\}$ NMR spectrum are accountable by the two imino carbons (C=N) of the chelate ligand, and the presence of the imino groups in the ring is corroborated by the stretching frequencies of 1577 and 1654 cm^{-1} in the IR spectrum, which also shows the N–H stretch at 3382 cm^{-1}. The $^{31}P\{^1H\}$ NMR spectrum shows a singlet at δ 60.0 ppm. Therefore, the reaction of **2** with acetonitrile at room temperature is a simple ligand substitution reaction in which the water ligand exchanges for a CH_3CN molecule, forming **6**; at elevated temperature, **6** evolves into **7**.

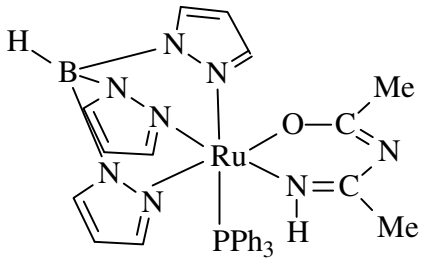

Chart 3.1 Molecular Structure of TpRu(PPh$_3$)(κ^2-*N*,*O*-NH=CMeN=CMeO) (7)

3.3.4 Synthesis of TpRu(PPh$_3$)(H$_2$O)(NHC(O)Ph) (8) and TpRu(PPh$_3$)(PhCN)(NHC(O)Ph) (9), and molecular structure of TpRu(PPh$_3$)(H$_2$O)(NHC(O)Ph) (8)

The aquo-benzamido complex **8** was readily prepared by reacting TpRu(PPh$_3$)(PhCN)Cl with KOH in THF/H$_2$O. The molecular structure of **8** was determined by X-ray diffraction study and is shown in Figure 3.2. The crystal data and refinement details are given in Table 3.3. Selected bond distances and angles are given in Table 3.4. Similar to complex **2**, the molecular structure of which has been reported in Chapter 2 Section 2.3.3, [174] both the amido (Ru–NH–C(=O)Ph) and imido (Ru^+–NH=C(–O^-)Ph) form of the benzamido ligand of **8** have contributions to the structure. The C(10)–N(7) bond distance, 1.307(5) Å, in **8** is shorter than the corresponding C–N bond distance of the amido-type ligand but longer than that of the imido-type ligand. Moreover, the C(10)–O(1) bond distance, 1.281(4) Å in **8** is in between the C–O bond distances in the amido- and imido-type [146] ligands. The C-N and C-O bond lengths of amido- and imido-type ligands in some ruthenium complexes are reported in Chapter 2 Section 2.3.3. [142-144] Like **2**, one of the

hydrogen atoms of the aquo ligand in **8** is intramolecularly hydrogen-bonded to the carbonyl oxygen of the benzamido ligand, while the other hydrogen atom exhibits an intermolecular hydrogen-bonding interaction with the carbonyl oxygen of the benzamido ligand of another molecule. The intra- and intermolecular O···O distances of 2.621(4) Å and 2.708(3) Å, respectively, fall in the range of hydrogen-bonding interactions. Yi *et al.* showed that a strong hydrogen-bonding interaction between the amido oxygen and alcoholic oxygen in the acetamido ruthenium complex $[(PCy_3)_2(CO)(CH_3CONH)(^iPrOH)RuH]BF_4$, facilitating the syn configuration, is evidenced by a relatively short bond distance between two oxygen atoms 2.580(4) Å. [146]

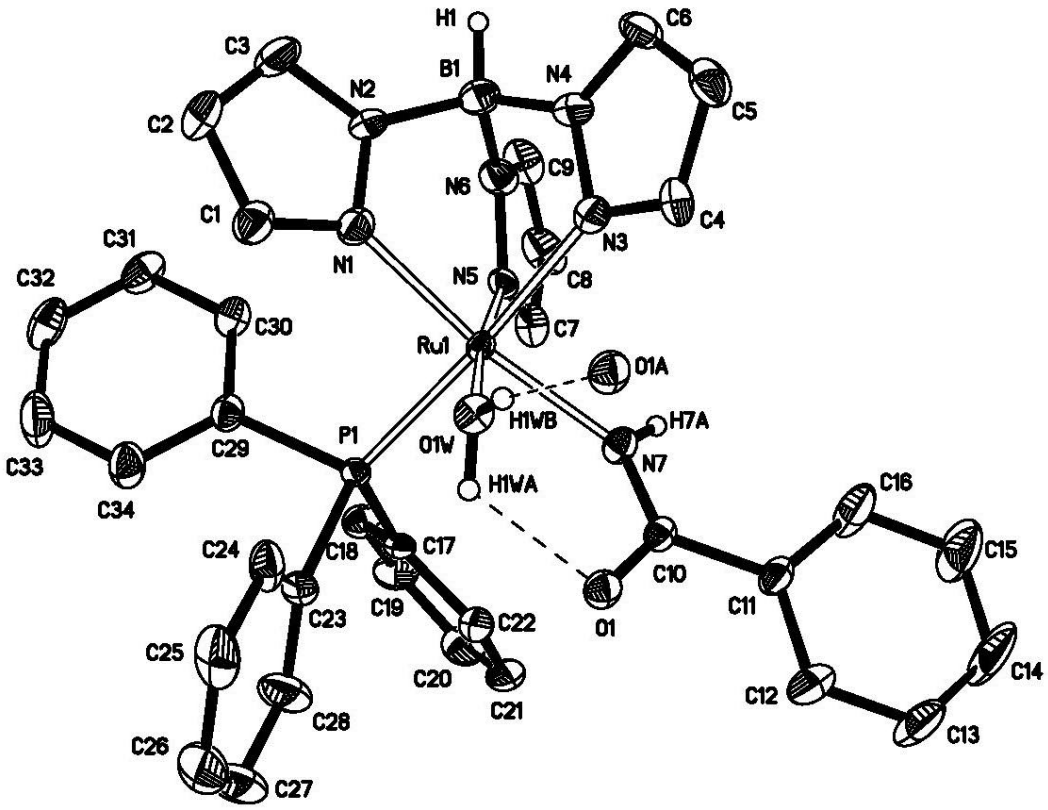

Figure 3.2. Molecular structure of $TpRu(PPh_3)(H_2O)(NHC(O)Ph)$ (8)

Table 3.3. Crystal data and structure refinement for $TpRu(PPh_3)(H_2O)(NHC(O)Ph)$ (8)

	8	
Empirical formula	$Ru(H_2O)(NHCOC_6H_5)(P(C_6H_5)_3)(C_9H_9N_6BH)$	
Formula weight	714.52	
Temperature	294(2) K	
Wavelength	0.71073 Å	
Crystal system	Monoclinic	
Space group	P2(1)/n	
Unit cell dimensions	a = 14.216(3) Å	$\alpha = 90^o$
	b = 13.421(3) Å	$\beta = 102.204(4)^o$
	c = 17.806(4) Å	$\gamma = 90^o$
Volume	3320.6(13) $Å^3$	
Z	4	
Density (calculated)	1.429 Mg/m^3	
Absorption coefficient	0.563 mm^{-1}	
F(000)	1464	
Crystal size	0.28 x 0.14 x 0.10 mm^3	
θ range for data collection	1.92 to 27.57°	
Index ranges	$-18 \leq h \leq 18, -17 \leq h \leq 17, -22 \leq l \leq 23$	
No. of Reflections collected	30469	
No. of Independent reflections	7674 [R(int) = 0.0640]	
Completeness to $\theta = 27.55^o$	99.8%	
Absorption correction	Semi-empirical from equivalents	
Max. and Min. transmission	1.000 and 0.783	
Refinement method	Full-matrix least-squares on F^2	
No. of data / restraints / params	7674 / 0 / 415	
Goodness-of-fit on F2	1.002	
Final R indices [$I > 2\sigma(I)$]	R1 = 0.0860, wR2 = 0.2099	
R indices (all data)	R1 = 0.1041, wR2 = 0.2213	
Largest diff peak and hole	0.958 and -1.015 e. $Å^{-3}$	

Table 3.4. Selected bond distances (Å) and bond angles (°) for $TpRu(PPh_3)(H_2O)(NHC(O)Ph)$ (8)

Bond Distances (Å)			
Ru – N(1)	2.083(3)	Ru – N(3)	2.126(3)
Ru – N(5)	2.054(3)	Ru – N(7)	2.084(3)
Ru – O(1W)	2.127(2)	C(10) – O(1)	1.281(4)
O(1W) – O(1)	2.624(4)	C(10) – N(7)	1.307(5)
O(1W) – O(1A)	2.708(3)	O(1W) – H(1WA)	0.8561
O(1W) – H(1WB)	0.8559		

Bond Angles (°)			
N(3)-Ru(1)-N(1)	83.08(12)	N(3)-Ru(1)-N(5)	85.86(11)
N(3)-Ru(1)-N(7)	88.27(12)	N(3)-Ru(1)- O(1W)	89.13(10)
N(1)-Ru(1)-N(5)	90.82(12)	N(1)-Ru(1)- P(1)	92.53(9)
N(1)-Ru(1)- O(1W)	92.06(11)	N(7)-Ru(1)-N(5)	88.71(12)
N(7)-Ru(1)-O(1W)	87.63(10)	N(7)-Ru(1)-P(1)	96.11(9)
N(5)-Ru(1)- P(1)	93.84(8)	O(1W)-Ru(1)-P(1)	91.43(7)
C(10)-N(7)-Ru(1)	130.5(2)	O(1)-C(10)-N(7)	121.5(3)
O(1)-C(10)-C(11)	117.0(3)	N(7)-C(10)-C(11)	121.3(3)

The ^{1}H NMR spectrum of **8** shows the N–H as a slightly broadened singlet at δ 5.92 ppm. The carbonyl carbon of the benzamido ligand appears as a singlet at δ 181.5 ppm in the $^{13}C\{^{1}H\}$ NMR spectrum. The $^{31}P\{^{1}H\}$ spectrum shows a singlet at δ 58.8 ppm, corresponding to the phosphine ligand of **8**. The low carbonyl stretching frequency ($\nu_{(C=O)}$ = 1525 cm^{-1}) is consistent with the fact that the imido form makes

significant contribution to the structure. It was reported that a ruthenium-acetamido complex exhibits a low carbonyl amide stretching frequency ($\nu_{(C=O)}$ = 1545 cm^{-1}). [146] Complex **2** which reported in the previous chapter also displays a low carbonyl stretching frequency ($\nu_{(C=O)}$ = 1540 cm^{-1}). [174], suggesting that the amido complexes contain extensive π-delocalization in the amido ligand. The N–H stretching frequency of **8** can be observed at 3354 cm^{-1}; it is shifted to 2360 cm^{-1} (theoretical value is 2377 cm^{-1}) for $TpRu(PPh_3)(D_2O)(NDC(O)Ph)$.

Unlike the acetonitrile-acetamido complex **6**, which cannot be prepared in pure form due to contamination by a small amount of **2**, the benzonitrile-benzamido complex $TpRu(PPh_3)(PhCN)(NHC(O)Ph)$ (**9**) can be readily synthesized in pure form by reacting **8** with excess benzonitrile at room temperature in THF. The ^1H NMR spectrum of **9** shows the N–H as a slightly broadened singlet at δ 5.03 ppm. The carbonyl carbon appears at a singlet at δ 178.4 ppm in the $^{13}C\{^1H\}$ NMR spectrum, while the triphenylphosphine shows up as a singlet at δ 57.1 ppm in the $^{31}P\{^1H\}$ NMR spectrum. The IR spectrum (KBr) of this complex shows the C=O, C≡N and N-H stretchings, respectively, at 1602, 2238, and 3359 cm^{-1}.

3.3.5 NMR monitoring of $TpRu(PPh_3)(H_2O)(NHC(O)Ph)$ (8)-catalyzed hydration of benzonitrile

A **8**-catalyzed hydration reaction of benzonitrile (in 1,4-dioxane-d_8) was monitored by NMR spectroscopy. Benzonitrile (25 equiv) and water (180 equiv)

were added to a 1,4-dioxane-d_8 solution of **8** in a pressure-valved NMR tube, which was then pressurized with Ar (10 atm); the $^{31}P\{^1H\}$ NMR spectrum of the solution immediately taken showed that **8** was completely converted to a new species corresponding to a singlet at δ 54.3 ppm (Figure 3.3). The new species is the benzonitrile-benzamido complex $TpRu(PPh_3)(PhCN)(NHC(O)Ph)$ (**9**). After heating the solution at 75 ºC in the probe for 15 min, the $^{31}P\{^1H\}$ NMR spectrum taken at this temperature showed a new and small singlet at δ 59.5 ppm, and ^1H NMR spectroscopy indicated that a trace amount of hydration product benzamide was generated. The probe temperature was then raised to 105 ºC and after 35 min, 40 % of product (based on the benzonitrile added) was formed. $^{31}P\{^1H\}$ NMR spectroscopy indicated that **9** completely changed to a species corresponding to a singlet at δ 59.5 ppm. This signal was due to the *N*-imidoylimidato complex $TpRu(PPh_3)(\kappa^2\text{-}N,O\text{-}NH{=}CPhN{=}CPhO)$ (**10**) which was later synthesized independently and characterized by X-ray crystallography. The solution was then heated for a further 240 min at 120 ºC, at the end of this period, the conversion of benzonitrile to benzamide was 44 % and **10** remained the only detectable species by $^{31}P\{^1H\}$ NMR spectroscopy.

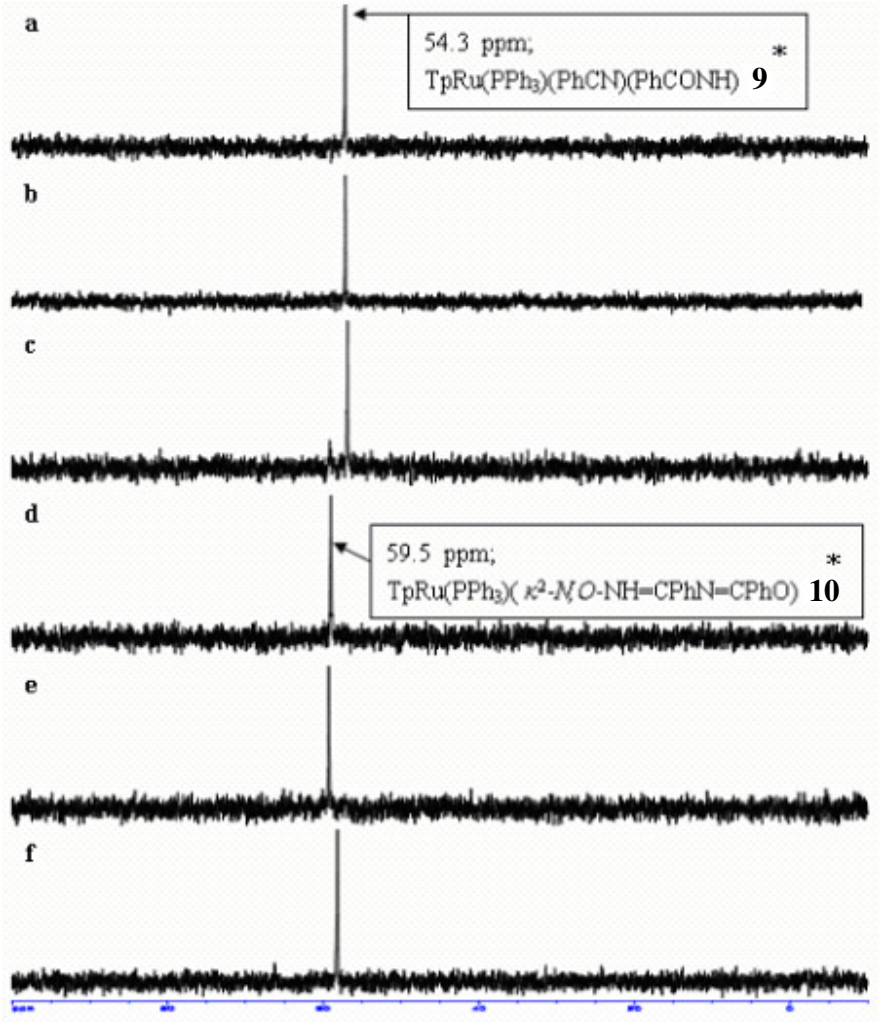

Figure 3.3. ^{31}P NMR study of 8-catalyzed hydration of benzonitrile: (a) immediately after addition of substrate and water at room temperature; (b) 50 ^{o}C for 15 min; (c) 75 ^{o}C for 15 min; (d) 105 ^{o}C for 35 min; (e) 120 ^{o}C for 30 min; (f) 120 ^{o}C for 210 min. ^{31}P{^{1}H} NMR spectra were taken at temperature indicated. *The chemical shifts of 9 and 10 in the presence of water and nitrile are slightly different from those of the authentic samples taken in 1,4-dioxane-d_8.

3.3.6 Synthesis and X-ray crystallographic study of $TpRu(PPh_3)(\kappa^2\text{-}N,O\text{-}NH{=}CPhN{=}CPhO)$ (10)

Analogous to **7**, complex **10** was synthesized by reacting $TpRu(PPh_3)(H_2O)(NHC(O)Ph)$ (**8**) with benzonitrile in 1,4-dioxane at elevated temperature. Crystals of **10** suitable for the X-ray diffraction study were obtained by layering hexane on a CH_2Cl_2 solution of the complex. Figure 3.4 shows the molecular structure of **10**. The crystal data and refinement details are given in Table 3.5. Selected bond distances and angles are listed in Table 3.6.

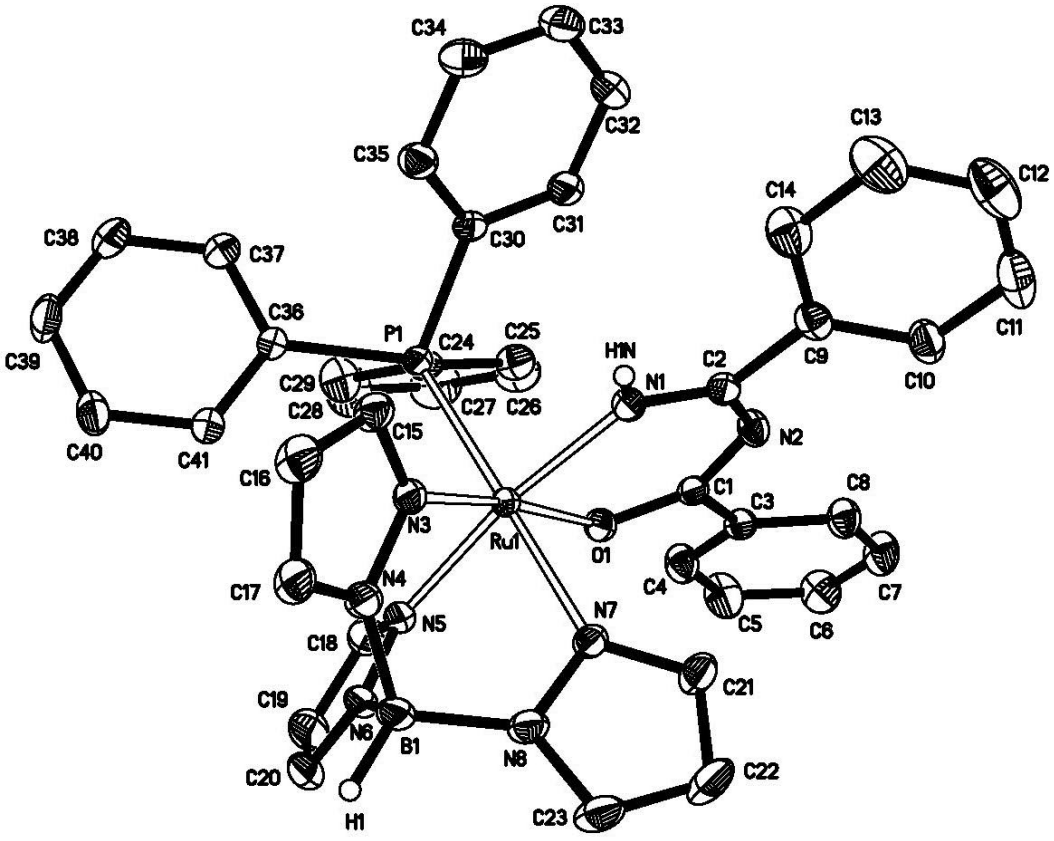

Figure 3.4. Molecular structure of $TpRu(PPh_3)(\kappa^2\text{-}N,O\text{-}NH{=}CPhN{=}CPhO)$ (10)

Table 3.5. Crystal data and structure refinement for $TpRu(PPh_3)(\kappa^2$-*N,O*-NH=CPhN=CPhO) (10)

	10	
Empirical formula	$Ru(C_2ON_2Ph_2)(P(C_6H_5)_3)(C_9H_9N_6BH).C_6H_{14}$	
Formula weight	885.8	
Temperature	296(2) K	
Wavelength	0.71073 Å	
Crystal system	Monoclinic	
Space group	P2(1)/c	
Unit cell dimensions	a = 9.7128(3) Å	α = 90°
	b = 22.7762(8) Å	β = 94.3970(10)°
	c = 19.9220(7) Å	γ = 90°
Volume	4394.2(3) $Å^3$	
Z	4	
Density (calculated)	1.339 Mg/m^3	
Absorption coefficient	0.439 mm^{-1}	
F(000)	1840	
Crystal size	0.40 x 0.32 x 0.18 mm^3	
θ range for data collection	2.05 to 27.66°	
Index ranges	$-12 \le h \le 12$, $-29 \le h \le 29$, $-26 \le l \le 25$	
No. of Reflections collected	101213	
No. of Independent reflections	10224 [R(int) = 0.0596]	
Completeness to θ = 27.55°	99.8%	
Absorption correction	None	
Max. and Min. transmission	1.000 and 0.770	
Refinement method	Full-matrix least-squares on F^2	
No. of data / restraints / params	10224 / 0 / 536	
Goodness-of-fit on F2	1.002	
Final R indices [$I > 2\sigma(I)$]	R1 = 0.0453, wR2 = 0.1044	
R indices (all data)	R1 = 0.0625, wR2 = 0.1183	
Largest diff peak and hole	0.484 and -0.555 e. $Å^{-3}$	

Table 3.6. Selected bond distances (Å) and bond angles (°) for TpRu(PPh$_3$)(κ^2-*N,O*-NH=CPhN=CPhO) (10)

Bond Distances (Å)			
Ru(1) – N(1)	2.0178(19)	Ru(1) – N(3)	2.0654(19)
Ru(1) – N(5)	2.081(2)	Ru(1) – N(7)	2.127(2)
Ru(1) – O(1)	2.0461(16)	C(1) – O(1)	1.276(3)
C(1) – N(2)	1.330(3)	C(2) – N(2)	1.359(3)
N(1) – C(2)	1.291(3)	N(1) – H(1N)	0.6226

Bond Angles (°)			
N(1)-Ru(1)-O(1)	87.59(7)	N(1)-Ru(1)-N(3)	92.92(8)
O(1)-Ru(1)-N(5)	89.35(7)	N(3)-Ru(1)- N(5)	89.10(8)
N(1)-Ru(1)-N(7)	86.71(8)	O(1)-Ru(1)- N(7)	87.26(7)
N(3)-Ru(1)- N(7)	85.20(8)	N(5)-Ru(1)-N(7)	85.43(8)
N(1)-Ru(1)-P(1)	93.58(6)	O(1)-Ru(1)-P(1)	93.36(5)
N(3)-Ru(1)- P(1)	94.18(6)	N(5)-Ru(1)-P(1)	94.31(6)
C(2)-N(1)-Ru(1)	127.16(17)	C(1)-O(1)-Ru(1)	125.22(16)
C(2)-N(1)- H(1N)	110.9	Ru(1)-N(1)- H(1N)	121.9
O(1)-C(1)- N(2)	129.4(2)	N(1)-C(2)-N(2)	126.6(2)
C(1)-N(2)-C(2)	123.7(2)		

The determination of the structure of **10** deserves some comments. Similar to **7**, **10** was first thought to be the benzamide-benzamido complex TpRu(PPh$_3$)(NH$_2$C(O)Ph)(NHC(O)Ph); but initial X-ray structural refinement gave a reasonably good structure **D** (Chart 3.2) containing a κ^2-*N,N* chelate ligand instead of the benzamide-benzamido structure. It seems that the κ^2-*N,N* chelate ligand might

have been formed in a straightforward manner via nucleophilic attack of the benzamido ligand at the carbon center of the bound benzonitrile (Scheme 3.3).

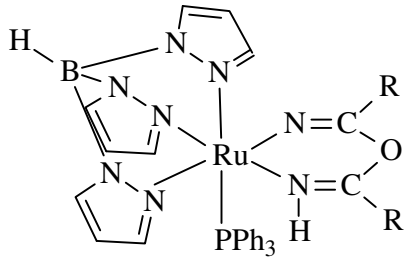

D (R = Ph) **D'** (R = Me)

Chart 3.2 Molecular structure of κ^2-N,N chelating complexes D and D'

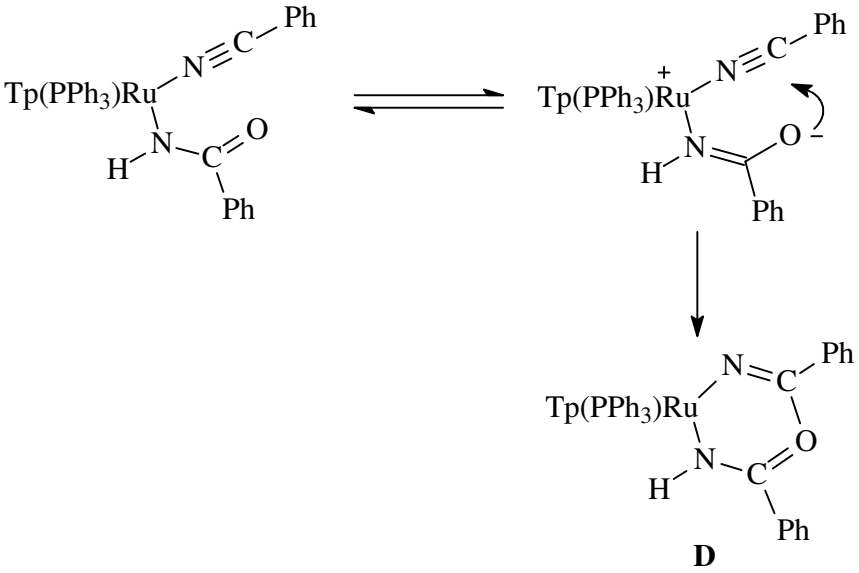

D

Scheme 3.3 Proposed mechanism of formation of D

However, when we later carried out density functional theory calculations to elucidate the mechanism of the **2**-catalyzed hydration of nitriles, it was learned that **D'**, the methyl analogue of **D** (Chart 3.2), is a highly unstable species; it lies 21.6

kcal/mol higher in electronic energy than **2** + MeCN. This finding is in sharp contrast to the NMR study described above, which clearly indicated that **7** or **10** is the most stable species observed in the course of the **2**- or **8**-catalyzed hydration of nitrile. Such a serious disagreement between the DFT calculations and the experimental NMR results is quite unexpected. We therefore suspected that we might have taken a nitrogen atom for an oxygen atom and vice versa in the initial X-ray crystallography analysis and therefore interchanged the iminato nitrogen with the oxygen atom. With this N/O exchange, X-ray structure refinement gave a good structure for **10**, shown in Figure 3.4. DFT calculations also show that **7**, the methyl analogue of **10**, is a very stable structure, being 5.6 kcal/mol (electronic energy) more stable than **2** + MeCN. Taking a nitrogen atom for an oxygen atom and vice versa is not uncommon in X-ray crystallography analysis. This part of our work represents a very good example demonstrating that computational chemists might be of great help to their experimental counterparts in structure elucidation. Apparently, at elevated temperature, the N-bound benzamido ligand changes its bonding mode to become an O-bonded imido ligand; nucleophilic attack at the carbon atom of the benzonitrile ligand followed by 1,3-proton shift results in the formation of **10** (Scheme 3.4). The reaction of the O-bonded imido ligand with the coordinated benzonitrile to form the *N*-imidolylimidato chelate ligand in **10** is similar to the addition of the N−H bond of a pyrazole across the coordinated nitrile C≡N bond to form a metal-ligated pyrazolylamidino group (eq 3.2). [176]

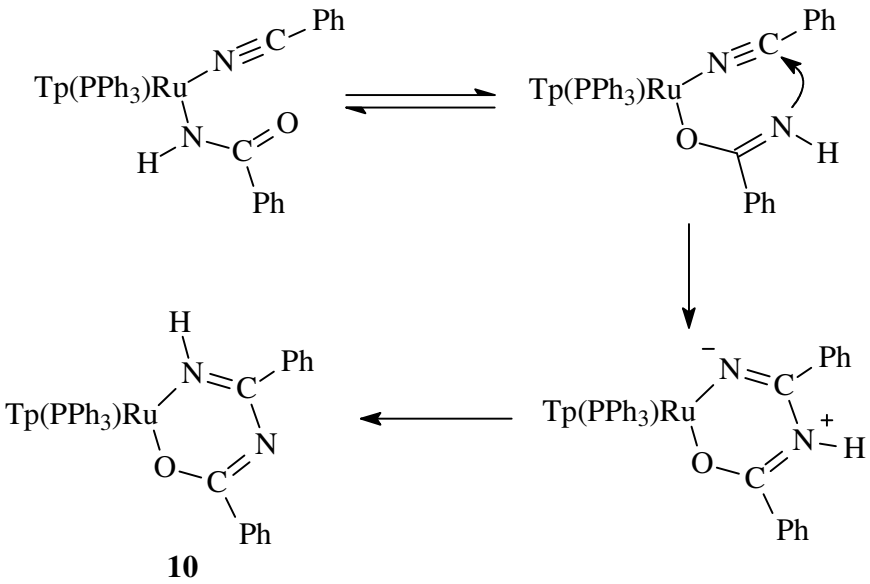

10

Scheme 3.4 Proposed mechanism of formation of TpRu(PPh$_3$)(κ^2-*N*,*O*-NH=CPhN=CPhO) (10)

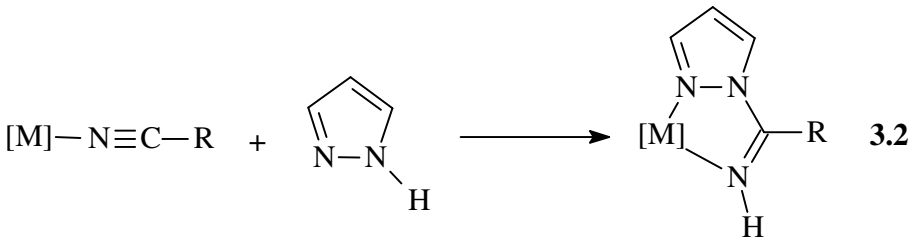

3.2

The *N*-imidolylimidato ligands in **7** and **10** are isoelectronic with acetylacetonate and 3-azapentane-2,4-diiminate anions [177-179] (Chart 3.3). Aromaticity of the chelate rings in **7** and **10** imparts high stability to the complexes. The coordinated nitrile is essential for the synthesis of these chelate rings. Woodward and co-worker indicated that CpRu(PPh$_3$)(κ^2-*N*,*N*-NH=C(CF$_3$)N=C(CF$_3$)NH) is synthesized by reacting a methanol solution of CpRu(PPh$_3$)(NCCF$_3$)Cl with NH$_4$[PF$_6$] and NCCF$_3$. [178] Another six-membered

chelate ring (Chart 3.4) with the similar structure of 3-azapentane-2,4-diiminate is generated by two coordinated nitrile molecules. Green *et al.* reported that [Ir(π-2-Me-C_3H_4)(CO)(PPh_3)$_2$] reacts with $NCCF_3$ to afford (PPh_3)(CO)Ir(κ^2-*N*,*N*-NH=C(CF_3)C(C(CH_3)=CH_2)=C(CF_3)NH). [179]

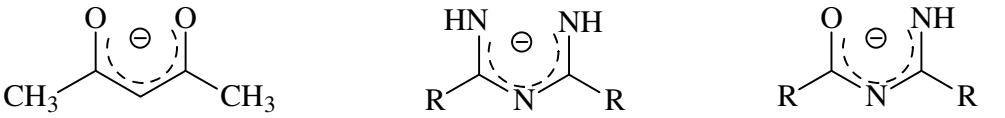

Acetylacetonate 3-azapentane-2,4-diiminate *N*-imidolylimidate

Chart 3.3 Molecular structures of acetylacetonate, 3-azapentane-2,4-diiminate and *N*-imidoylimidate

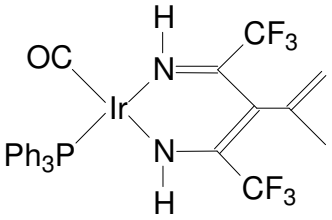

Chart 3.4 Molecular structure of (PPh_3)(CO)Ir(κ^2-*N*,*N*-NH=C(CF_3)C(C(CH_3)=CH_2)=C(CF_3)NH)

The *N*-imidolylimidato chelate ring in **10** (Figure 3.4) is basically planar. The six atoms of the ring deviate within 0.012 Å from the best plane. The three C-N bonds in the chelate ring are longer than the normal C=N double bond and shorter than the normal C−N single bond, while the C-O bond distance falls between normal C−O single and C=O double bonds. [180] Hence π-bond delocalization is present in the ring. In other words, the two limiting structures, *N*-imidoylimidate and *N*-acylamidinate (Chart 3.5), contribute to the bond lengths in the chelate ring. The

N(1)–C(2) bond distance (1.291(3) Å) is shorter than that of N(2)–C(1) (1.330(3) Å) and significantly shorter than the N(2)–C(2) bond length (1.359(3)Å).

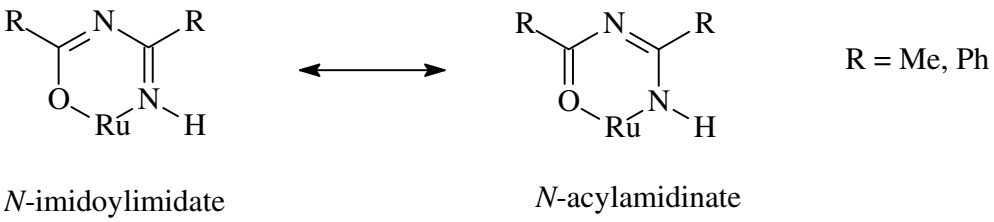

N-imidoylimidate *N*-acylamidinate

Chart 3.5 Resonance Structures of *N*-imidoylimidate

Reports on molecular structures of *N*-imidoylimidato complexes are rare; in fact, there is only one report in the literature describing the X-ray structures of two *N*-imidoylimidato complexes, RuCl(κ^2-*N*,*O*-NH=C(C_6H_4Me-*p*)N=C(C_6H_4Me-*p*)O)(CO)(PPh_3)$_2$ and RuCl(κ^2-*N*,*O*-NH=C(C_6H_4Me-*p*)N=CPhO)(CO)(PPh_3)$_2$. [87] The C-N bond distances in the chelate ring of **10** are comparable to the corresponding C-N bond distances in the chelate rings of the two reported *N*-imidoylimidatoruthenium complexes. The O(1)–C(1) bond distance (1.276(3) Å) in the ring of **10** is slightly shorter than that (1.284(8) Å) in the chelate ligand of RuCl(κ^2-*N*,*O*-NH=C(C_6H_4Me-*p*)N=C(C_6H_4Me-*p*)O)(CO)(PPh_3)$_2$, but slightly longer than the corresponding bond length (1.267(4) Å) in RuCl(κ^2-*N*,*O*-NH=C(C_6H_4Me-*p*)N=CPhO)(CO)(PPh_3)$_2$.

3.3.7 Synthesis of TpRu(PPh_3)(κ^2-*N,O*-NH=CMeN=CPhO) (11)

The unsymmetrical *N*-imidoylimidato complex **11** was prepared by reacting TpRu(PPh_3)(H_2O)(NHC(O)Ph) (**8**) with acetonitrile in 1,4-dioxane at elevated temperature and was characterized by NMR and IR spectroscopies. The proton NMR signal of N−H is difficult to identify, it is probably masked by the peaks of the Tp ligand and the aromatic signals of the phosphine ligand; the methyl signal appears as a singlet at 2.13 ppm in the ^{1}H NMR spectrum. The ^{31}P{^{1}H} spectrum shows a singlet at δ 59.1 ppm, corresponding to the phosphine ligand of **11**. The two imino carbons (C=N) of the *N*-imidoylimidato ligand appear as two singlets at δ 168.72 and 170.37 ppm in the ^{13}C{^{1}H} NMR spectrum. The IR spectrum (KBr) of this complex shows the stretching frequencies of the two C=N bonds at 1671 and 1973 cm^{-1}. The N-H stretching can be observed at 3305 cm^{-1}. Mass spectroscopy shows the parent peak with m/z 738.09. Unfortunately, we have not been able to grow single crystals of **11** for X-ray crystallographic study.

3.3.8 Proposed mechanism for the catalytic hydration of nitriles to amides

Taking into account the results of the NMR-monitored catalytic reactions shown in Figures 3.1 and 3.3, we propose a mechanism for the catalytic hydration of nitriles to amides with the aquo-amido complex (Scheme 3.5). It is interesting to note that unlike many known catalytic systems for hydration of nitriles to amides in which the product-generating step is internal protonation of the amido ligand by an

adjacent aquo ligand [81, 169, 170], the aquo-amido complexes **2** and **8** are very stable species; the coordinated water in **2** or **8** does not protonate the amido ligand but involves in intra- and intermolecular hydrogen-bonding interactions with it. The reaction begins with displacement of the aquo ligand in the aquo-amido complex by the nitrile to form the nitrile-amido complex such as **6** and **9**. At elevated temperatures, the N-bonded amido ligand of the nitrile-amido complex isomerizes to the O-bonded imido ligand, forming **6′** and **9'**. It is quite surprising that this linkage-isomerization would occur since the N-bonded imido ligand should be a better match with the metal center than the O-bonded imido from the HSAB point of view. Nucleophilic attack of the imido nitrogen at the carbon center of the coordinated nitrile and subsequent proton shift leads to the formation of the *N*-imidoylimido complex such as **7** and **10**, which is the most stable species in the catalytic cycle. Attack of water at the carbon center between the two nitrogen atoms in the *N*-imidoylimido ligand breaks the C–N bond and opens the ring, and subsequent protonation of the nitrogen atom results in the generation of the amido-iminol intermediate **12**. The cycle is completed by ligand exchange of the iminol molecule with a substrate nitrile molecule and subsequent tautormerization of the iminol to the product amide or tautormerization of the iminol ligand (in **12**) to an amide ligand and subsequent ligand exchange of the latter with a substrate nitrile molecule. Independently prepared *N*-imidoylimido complex **7** has been found to exhibit catalytic activity in nitrile hydration basically identical to that of $TpRu(PPh_3)(H_2O)(NHC(O)CH_3)$ (**2**) (Table 3.2, entries 14, 15). It is worth pointing out $RuCl(\kappa^2\text{-}N,O\text{-}NH{=}CRN{=}CR'O)(CO)(PPh_3)_2$ (R, R' = aromatic groups), the only

N-imidoylimido complexes reported to date, do not catalyze the hydration of nitriles. [87]

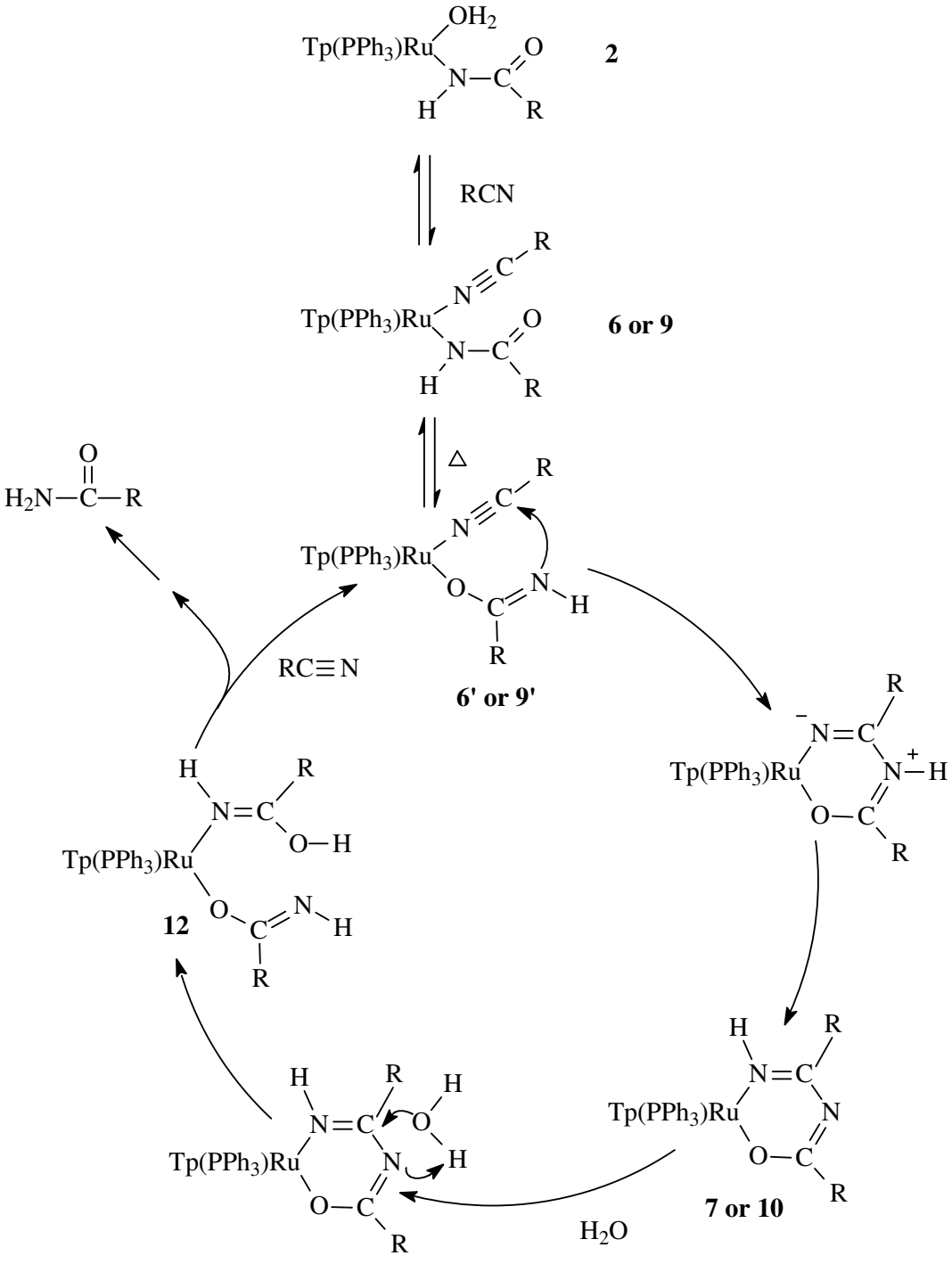

Scheme 3.5 Proposed mechanism of hydration of nitrile catalyzed by $TpRu(PPh_3)(H_2O)(NHC(O)R)$ R = Me or Ph

Side reactions might also occur outside the catalytic cycle, as demonstrated by an experiment using TpRu(PPh_3)(κ^2-*N,O*-NH=CPhN=CPhO) (**10**) as a catalyst for the hydration of acetonitrile. The reaction was carried out in a NMR tube in 1,4-dioxane at 100 ºC with 25 equiv and 100 equiv of acetonitrile and water, respectively to give product conversion of 44 % after 24 h; at the end of the reaction, it was found by $^{31}P\{^1H\}$ NMR spectroscopy that **10** was partially converted to TpRu(PPh_3)(κ^2-*N,O*-NH=CMeN=CPhO) (**11**) and TpRu(PPh_3)(κ^2-*N,O*-NH=CMeN=CMeO) (**7**). The three *N*-imidoylimido complexes **10**, **11**, and **7** were present in a 1:2:1 ratio. The conversion of **10** to **11** and **7** can probably be accounted for by the reaction sequence depicted in Scheme 3.6. The hydration product acetamide can attach to the metal center, transfer of one of its NH_2 protons to the O-bonded imido ligand and subsequent ligand displacement would generate the acetonitrile-acetamide species **E**, which would form **7** via N-bond amido/O-bonded imido isomerization and subsequent cyclization.

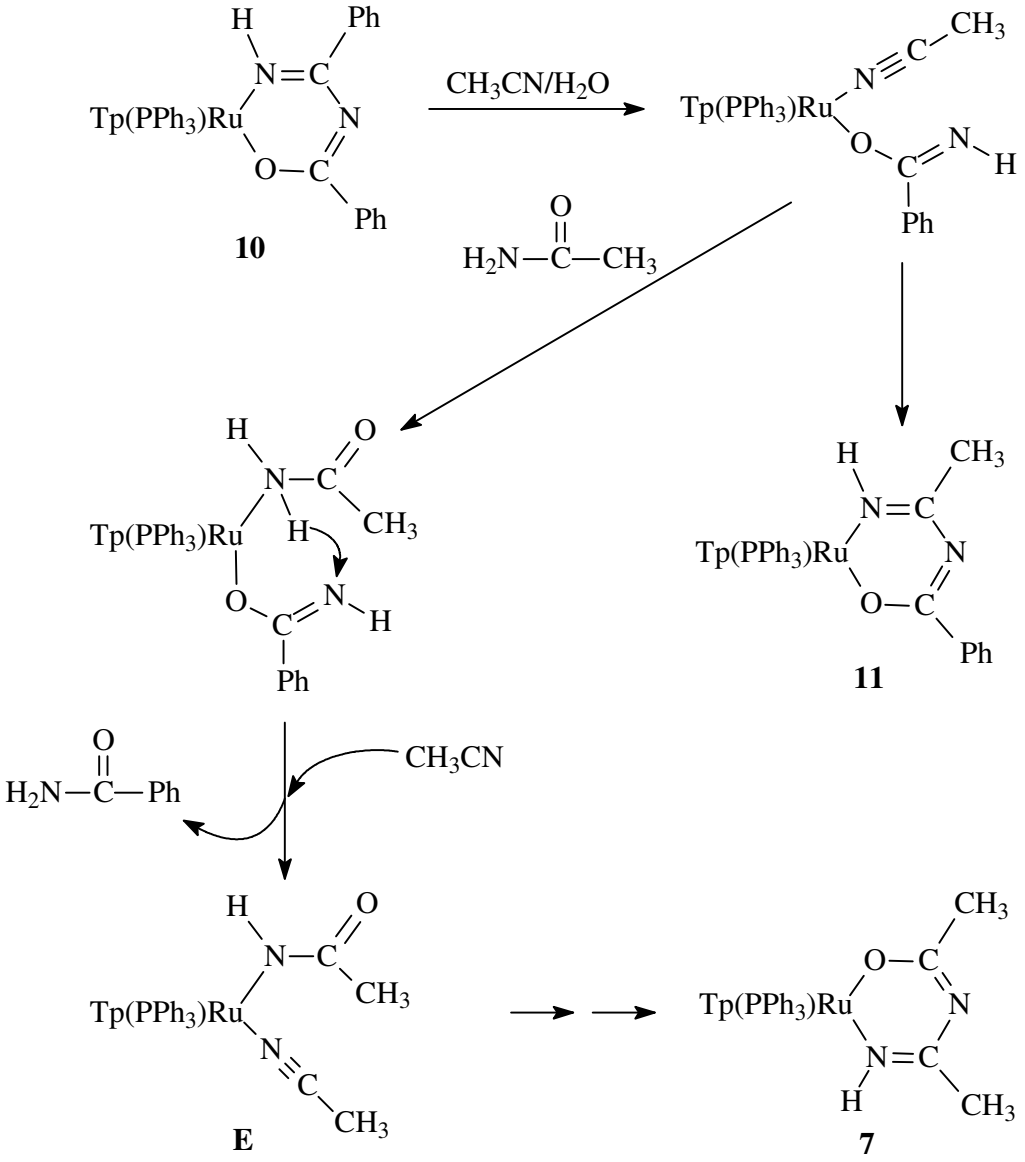

Scheme 3.6 Proposed mechanism of fromation of 11 and 7 from 10

3.3.9 Computational Study

To study the feasibility of the proposed reaction mechanism shown in Scheme 3.5 for the catalytic hydration of nitriles to amides, theoretical calculations were performed at the Becke3LYP level of DFT theory to examine the whole

catalytic cycle for R = CH_3. To reduce the computer cost, PH_3 was used to model PPh_3 in our calculations. The errors incurred from the simplification in the phosphine ligand can be cancelled out because the phosphine ligand is present in every species calculated and only the relative energies among the different species calculated are important in our discussion.

Experiments described above show that the addition of acetonitrile and water to the 1,4-dioxane solution of **2** led to an equilibrium between **2** and **6** at room temperature in the experiments. We first investigated the relative stability of complexes **2** and **6**. Considering the coexistence of acetonitrile, water, and complexes in the solution, it is necessary to add acetonitrile to **2** and water to **6** for addressing the important hydrogen bonding in the calculations. The calculation results reveal that the electronic energy difference between **2A**, a model complex of **2**, with acetonitrile and **6A**, a model complex of **6**, with water is only 0.1 kcal/mol (Scheme 3.7), consistent with the experimental observation that the ratio **2** : **6** is ~ 1 : 1.

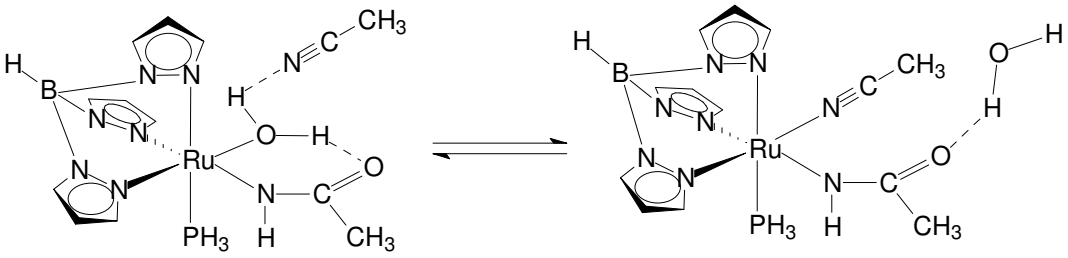

2A + MeCN

6A + H_2O

Scheme 3.7 Equilibrium of 2A and 3A in presence of acetonitrile

The energetics related to the proposed reaction sequence shown in Scheme 3.5 is illustrated in Figure 3.5. Selected optimized structural parameters of the species involved in the reaction sequence are shown in Figure 3.6. As expected, the energy barrier of 28.9 kcal/mol for isomerization of N-bonded amido-coordinated **6A** to O-bonded imido-coordinated **6A'** is relatively high, consistent with an elevated temperature being needed in the experiments. **6A'**, which corresponds to the active species in the catalytic cycle (Scheme 3.5), is energetically located at 8.0 kcal/mol above **6A**. Nucleophilic attack of the imido nitrogen at the carbon center of the coordinated nitrile in **6A'** to form a cyclic complex **7A'** needs to overcome an energy barrier of only 6.4 kcal/mol. Although **7A'** is energetically more stable than **6A'**, it is a zwitterionic species. A subsequent 1,3-proton shift could occur easily with the aid of water molecules, [181] leading to the formation of the complex **7A** (a model complex for **7**). Along with the isomerization of **7A'** to **7A**, a good π–conjugated system is formed in the *N*-imidoylimido ligand, making **7A** the most stable species in the catalytic cycle. Comparison of the structural parameters obtained from calculations for **7A** and experiments for **10** (the X-ray structure of **7** is not available) (Figure 3.6) reveals that the calculated structure reproduces well the experimental one.

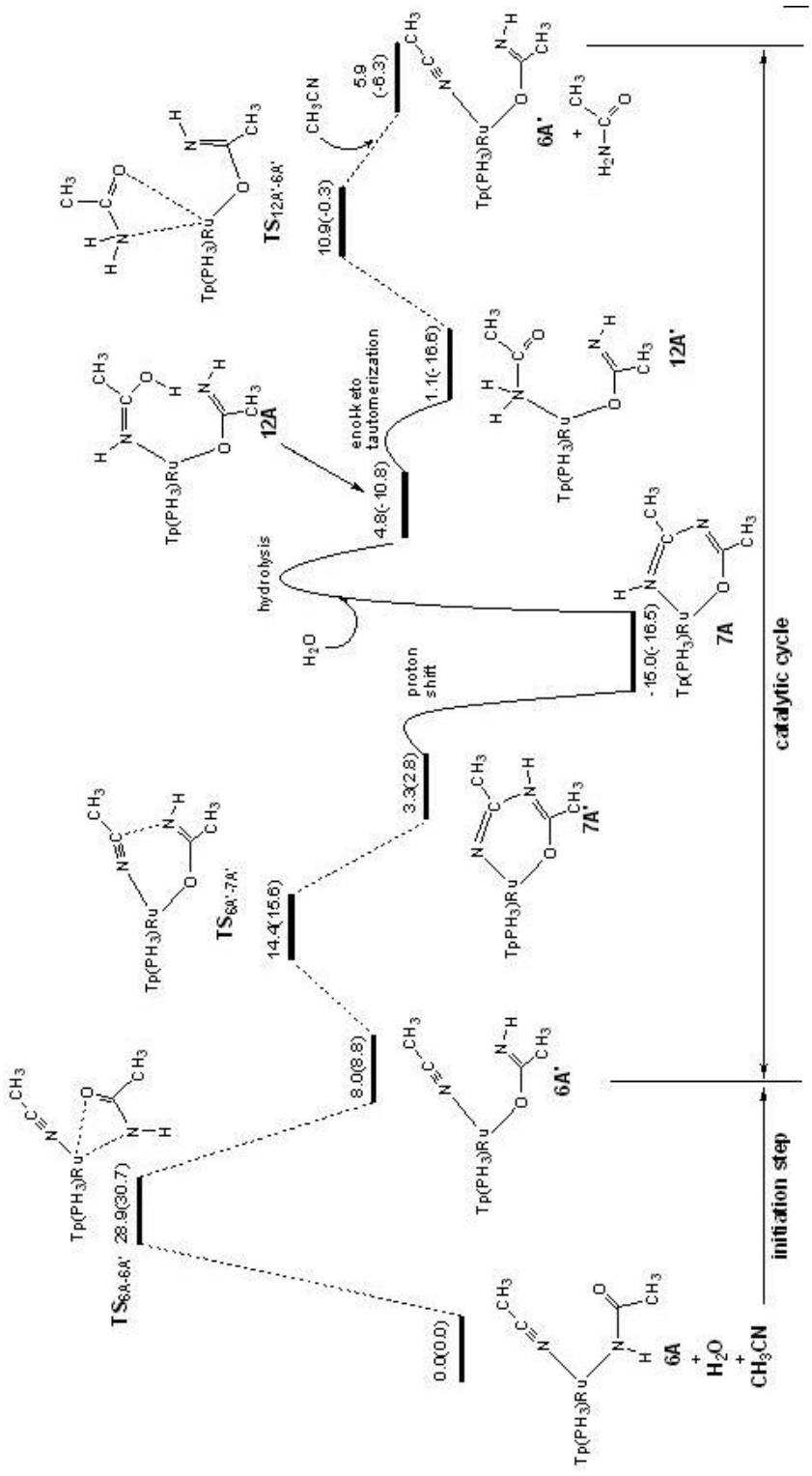

Figure 3.5. Energy profile for the reaction sequence shown in Scheme 3.4. The calculated relative free energies and electronic energies (in parentheses) are given in kcal/mol

The hydrolysis of **7A** starts from attack of water at the carbon center between the two nitrogen atoms in the *N*-imidoylimido ligand and finishes with the breaking of C-N bond, resulting in the generation of the imido-iminol intermediate **12A**, which is slightly more unstable than **7A'**. **12A** can then undergo an enol-to-keto tautomerization to give energetically more stable imido-amide intermediate **12A'**. We did not calculate the barriers for the hydrolysis and enol-to-keto tautomerization processes involved. Enol-to-keto tautomerization processes are commonly found in organic chemistry and are believed to have very small barriers in solution. [149-152] Calculations of the hydrolysis and tautomerization processes are difficult computationally because solvation, which influences significantly the proton transfer processes, needs to be considered.

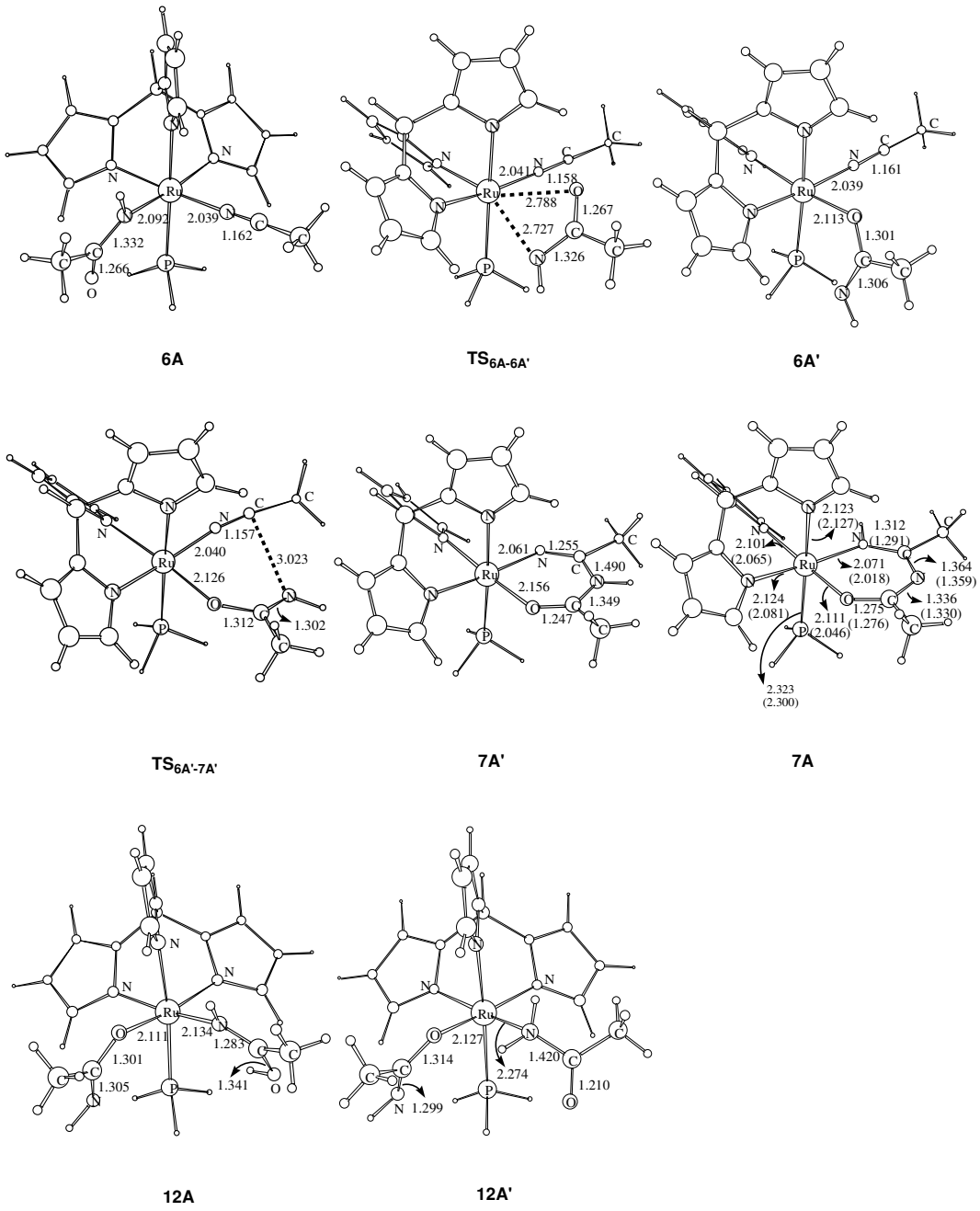

Figure 3.6. Selected optimized structural parameters calculated for the species involved in the reaction sequence shown in Figure 3.5 and Scheme 3.5. Bond lengths are given in Å. Experimental data of 10 are shown in parentheses

In **12A'**, the hydration product molecule, acetamide ($NH_2C(O)CH_3$), acts as a ligand. It can easily dissociate from **12A'** to form a 16e metal fragment that takes an

acetonitrile (CH_3CN) to regenerate **6A'**, completing the catalytic circle. We calculated the dissociation barrier roughly by fixing the distances between the Ru atom and the O and N atoms of acetamide both to 5.0 Å in the calculations. The barrier is evaluated to be 10.9 kcal/mol. Moreover, the free energy increases by only 4.8 kcal/mol for the ligand exchange process, indicating that the ligand exchange can occur.

The computational results indicate that the formation of the highly stable intermediate **7A** and a substantially high barrier for the hydrolysis step to regenerate the active species **6A'** hinder the catalytic reactions.

Chapter 4 Catalytic reactivity studies of $TpRu(PPh_3)(H_2O)(NHCOCH_3)$: C-H bond activation of ketones and C-N bond formation on alkyne

4.1 Introduction

It has been learned from the pervious chapter that $TpRu(PPh_3)(H_2O)(NHCOCH_3)$ (**2**) is capable of catalyzing hydration of nitrile to amide. In this chapter other **2**-catalyzed reactions such as H/D exchange between ketones and D_2O and formation of C-N bond between the amido ligand and phenylacetylene are reported. The amido moiety of **2** acts as an auxiliary ligand in the former case, but is involved in the C-N bond formation reaction as one of the reagents in the latter case. The reactions demonstrate the versatility of the amido complex.

The potential usage of catalytic isotopic labeling reactions varies from standards for NMR spectroscopy and mass spectrometry to highly specific labeling of drugs with tritium for physiological studies. [182-186] Highly specific isotope-labeled compounds are utilized in mechanistic studies of catalytic processes, enabling the improvement of chemical processes. [187] Furthermore, recent advances in pharmacokinetics and metabolism studies for new drugs prompt a need for isotopic labeling methods more efficient than the incorporation of isotopes into drug precursors in the early stages of drug synthesis. [188] Fels et al. [189] have shown that cyclooctadieneiridium (I) acetylacetonate complex is capable of

catalyzing stereoselective H/D exchange between ketones and D_2O. They reported that only the *ortho* hydrogens of benzophenone and acetophenone oxime and the methyl hydrogens of 2-hydroxy-4-methoxyacetophenone are deuterated by D_2O.

Both primary and secondary amide units are fundamental components of biological and synthetic polymers such as proteins and nylons. Formation of these amides using the widely available starting materials amides and unsaturated hydrocarbons, is an efficient and effective method. Enamide, one of the versatile primary amides, is widely present as a key structural moiety in numerous natural products. [190] Thus, several protocols have been devised for the preparation of enamides. [191-203] Some metal-mediated C-N bond formation reactions have been developed, such as Ru- or Cu-catalyzed addition of amides to alkynes. [118, 204, 205] However, such catalytic reactions often suffer from low conversion. Rare examples by Deng et al. [116] and Chang et al. [117] showed both high yields and stereoselectivity in hydroamidation.

4.2 Experimental

4.2.1 Materials and Instrumentation

Ruthenium trichloride, $RuCl_3 \cdot 3H_2O$, pyrazole, sodium borohydride, triphenylphosphine, and organic substrates were obtained from Aldrich,

International Laboratory, and Acros. Triphenylphosphine was recrystallized from ethanol before use. Solvents were distilled under a dry nitrogen atmosphere with appropriate drying agents: hexane, diethyl ether, tetrahydrofuran, and 1,4-dioxane with sodium-benzophenone; dichloromethane, acetonitrile, and chloroform with calcium hydride. All manipulations were carried out under a nitrogen atmosphere using standard Schlenk techniques. The complexes $TpRu(PPh_3)(CH_3CN)H$, [117] $TpRu(PPh_3)(CH_3CN)Cl$, [127] and $TpRu(PPh_3)_2Cl$ [175] were prepared according to literature methods. Deuterated NMR solvents, purchased from Armar and Cambrigde Isotope Laboratories, were dried with P_2O_5. High purity argon and carbon monoxide gases were supplied by Hong Kong Oxygen.

Proton NMR spectra were obtained from a Bruker DPX 400 spectrometer. Chemical shifts were reported relative to residual protons of the deuterated solvents. ^{31}P NMR spectra were recorded on a Bruker DPX 400 spectrometer at 161.70 MHz, chemical shifts were externally referenced to 85% H_3PO_4 in D_2O. $^{13}C\{^1H\}$ NMR spectra were taken on a Bruker DPX 400 spectrometer at 100.61 MHz; chemical shifts were internally referenced to C_6D_6 (δ = 128.1 ppm), $CDCl_3$ (δ = 77.7 ppm) and 1,4-dioxane-d_8 (δ = 67.16 ppm). High-pressure NMR studies were carried out in commercial 5 mm Wilmad pressure-valved NMR tubes. Infrared spectra were obtained from a Bruker Vector 22 FT-IR spectrophotometer. Electrospray ionization mass spectrometry was carried out with a Finnigan MAT 95S mass spectrometer with the samples dissolved in dichloromethane. Elemental analyses were performed by M-H-W Laboratories, Phoenix, AZ, USA.

4.2.2 Synthesis and Reactions

4.2.2.1 H/D exchange between amido hydrogen of $TpRu(PPh_3)(H_2O)(NHC(O)CH_3)$ (2) and D_2O

A sample of $TpRu(PPh_3)(H_2O)(NHC(O)CH_3)$ (**2**) (～5 mg) was loaded into a 5 mm NMR tube, which was then sealed with a septum. The tube was evacuated using a needle and filled with nitrogen for three cycles. Benzene-d_6 (0.3 mL) and D_2O (10 μL) were added to the tube using syringes and needles. The solution was allowed to stand at room temperature overnight after which the $^{31}P\{^1H\}$ and ^1H NMR spectra of the solution were recorded. The ^1H NMR spectrum showed all the signals of **2** except the amido hydrogen at δ 4.67ppm.

4.2.2.2 H/D exchange between amido deuterium of $TpRu(PPh_3)(D_2O)(NDC(O)CH_3)$ (2d) and cyclopentanone

A sample of $TpRu(PPh_3)(D_2O)(NDC(O)CH_3)$ (**2d**) (～5 mg) was loaded into a 5 mm NMR tube, which was then sealed with a septum. The tube was evacuated using a needle and filled with nitrogen for three cycles. Benzene-d_6 (0.3 mL) and cyclopentanone (0.4 μL) were added to the tube using syringes and needles. The solution was allowed to stand at room temperature overnight after which the $^{31}P\{^1H\}$ and ^1H NMR spectra of the solution were recorded. The tube was then heated at 90°C overnight. The ^1H spectrum of the resulting solution showed significant

increase and decrease in the amido hydrogen signal and α hydrogen signal of the cyclopentanone, respectively. The Tp signals were used as internal standard.

4.2.2.3 Catalytic H/D exchange between ketones and D_2O

A 11 mm tube with a Teflon screw cap was loaded with $TpRu(PPh_3)(H_2O)(NHC(O)CH_3)$ (**2**) (2 mg) and then evacuated and flushed with N_2 for four cycles. Freshly distilled ketone (0.13 mL) and degassed D_2O (0.12 mL) were added to the tube via syringes. The tube was heated at 110 ˚C for 44 h. ^1H NMR spectroscopy was used to analyze the percentage of deuterium incorporation into the ketone.

4.2.2.4 Use of ^1H NMR spectroscopy to determine levels of deuteration of the ketones

For the ketones containing hydrogen atoms other than the α hydrogens and α,β-unsaturated ketones containing α, β, and γ hydrogens, no internal standard was needed for the calculation of the level of deuteration. In the catalytic H/D exchange reaction, for example, between cyclopentanone and D_2O, the β hydrogen can be the internal standard for calculation of the percentage of deuterium incorporation into the α position of cyclopentanone. For the ketones which contain only the α hydrogen and for α,β-unsaturated ketones which contain only α, β, and γ hydrogens, CH_2Cl_2 was used as an internal standard for the determination of the levels of deuteration. In

a typical experiment, a standard solution, containing 10 μL of CH_2Cl_2 and a 10 μL aliquot from a 0.13 mL of ketone/0.12 mL of H_2O mixture (for miscible ketones) or from the organic layer of the ketone/H_2O solution (for immiscible ketones) in $CDCl_3$, was prepared in an NMR tube. After the H/D exchange reaction of the ketone with D_2O was quenched, the catalytic system was allowed to stand at room temperature for several hours to ensure good separation of the organic and aqueous phases (for immiscible ketones). A $CDCl_3$ solution (the sample solution) containing a 10 μL aliquot of the sample mixture or the organic layer of the sample solution and 10 μL of the internal standard was prepared in an NMR tube. The ^1H NMR spectra of the sample solution and the standard solution were recorded. The level of deuteration can be calculated based on the ratios of the integration of the signal of the exchanging hydrogen of the organic compound and that of the CH_2Cl_2 in the spectra of both solutions.

4.2.2.5 Catalytic H/D exchange between Acetylacetone (Hacac) and D_2O with 2

A sample of $TpRu(PPh_3)(H_2O)(NHC(O)CH_3)$ (**2**) (2 mg) loaded into a 5 mm NMR tube was dissolved in 1,4-dioxane-d_8 (0.3 mL); acetylacetone (30 μL, 100 equiv), and D_2O (30 μL, 480 equiv) were added to the tube using syringes. ^1H NMR spectrum was recorded. The tube was heated at 110 ˚C for 12 h. After cooling the tube to room temperature, ^1H NMR spectrum was recorded. The percentage of deuteration was calculated by comparing the integrations of the characteristic peaks of acac in these two ^1H NMR spectra.

4.2.2.6 Reaction of 2 with acetaldehyde

A sample of $TpRu(PPh_3)(H_2O)(NHC(O)CH_3)$ (**2**) (10 mg) was loaded into a 5mm pressure-valved NMR tube, to which THF (0.2 mL) and acetaldenyde (13 μL) were added. The tube was then pressurized with 10 bars of Ar and heated at 110 ˚C overnight. The tube was then cooled to room temperature and the $^{31}P\{^1H\}$ NMR spectrum was recorded. $^{31}P\{^1H\}$ NMR (161.7 MHz, 25 ˚C): δ 56.0 ppm (s). The solution in the NMR tube was then transferred to a 50 mL 2-necked flask. The flask was flushed with nitrogen and the solvent of the solution was removed by vacuo. The residue was washed with hexanes (2 mL x 2). ^1H and $^{31}P\{H\}$ NMR spectra of a $CDCl_3$ solution of the residue were recorded.

4.2.2.7 Synthesis of $TpRu(PPh_3)(C(NHC(O)CH_3)=CHPh)$ (13)

A sample of $TpRuPPh_3(H_2O)(NHCOCH_3)$ (**2**) (0.5 g) was dissolved in THF (8 mL) in a two-necked round-bottom flask which was then evacuated and flushed with nitrogen for three cycles. Phenylacetylene (0.8 mL) was then added to the solution and the resulting solution was refluxed with stirring for 3 h to yield a deep yellow solution. After cooling the solution to room temperature, it was brought to dryness under vacuum. The yellow paste was washed with hexane (2 x 6 mL) and 5/1 hexane/diethyl ether (2 x 6 mL); it was collected and dried under vacuum at room temperature for several hours.

Yield: 0.25 g (45%)

Elemental analysis calcd (%) for $C_{37}H_{35}BN_7OPRu$: C 60.33, H 4.79, N 13.31; found: C 60.26, H 4.77, N 13.25.

IR (KBr, cm^{-1}): υ(C=O) = 1582 (sh,s), υ(C=C) = 1611(s), υ(N-H) = 3259 (med), υ(B-H) = 2487 (med).

^1H NMR (400.13 MHz, C_6D_6, 25 ˚C): δ = 1.51 (s, 3H; NHC(O)C*H*$_3$), 5.89 (t, 1H of Tp), 5.98 (s, 1H; N*H*C(O)CH3), 6.02 (t, 1H of Tp), 6.15 (s, 1H$_\beta$; Ru-C=C*H*Ph), 6.17 (t, 1H of Tp), 6.18 (t, 1H of Tp), 7.17 – 7.60 (m, 20H of PPh_3 and Phenyl ring of Ru=C=CHPh), 7.55 (d, 1H of Tp), 7.72 (d, 1H of Tp), 7.88 (d, 1H of Tp), 7.94 (d, 1H of Tp), 7.96 (d, 1H of Tp), 8.00 (d, 1H of Tp). (all coupling constants for Tp proton resonances are about 2 Hz)

$^{31}P\{^1H\}$ NMR (161.7 MHz, C_6D_6, 25 ˚C): δ = 64.2 (s)

$^{13}C\{^1H\}$ NMR (100.61 MHz, C_6D_6, 25 ˚C):$_3$ δ = 155.9 (s, NH*C*(O)CH_3), 209.3 (d, J_{PC} = 16, Ru-*C*=CHPh)

ESI-MS (CH_2Cl_2): *m/z* :737.10

4.2.2.8 Synthesis of [TpRu(PPh_3)(=C(CH_2Ph)NHC(O)CH_3)][BF_4] (14)

A sample of TpRuPPh_3(PPh_3)(NHC(O)CH_3)(=C=CHPh) (**13**) (40 mg) was dissolved in THF (4 mL) in a two-necked round-bottom flask flushed with nitrogen. HBF_4 (10 μL) was added with stirring for 15 min to yield a red solution. The solution was brought to dryness under vacuum. Diethyl ether (5mL) was added to the residual paste with vigorous stirring to produce a red complex.

Yield: 32 mg (72%)

Elemental analysis calcd (%) for $C_{37}H_{36}B_2F_4N_7OPRu$: C 53.91, H 4.40, N 11.89; found: C 53.76, H 4.38, N 11.81.

IR (KBr, cm^{-1}): υ(C=O) = 1661 (med), υ(N-H) = 3267 (med), υ(B-H) = 2519 (br,med).

^1H NMR (400.13 MHz, $CDCl_3$, 25 ˚C): δ = 2.45 (s, 3H; NHC(O)CH_3), 4.09 (d, J_{HH} = 12.1, 1H; CH_2Ph), 4.87(d, J_{HH} = 12.1, 1H; CH_2Ph), 5.38 (t, 1H of Tp), 5.48 (t, 1H of Tp), 5.93 (t, 1H of Tp), 6.18 (t, 1H of Tp), 6.39 (d, 2H of *o*-H of CH_2Ph), 6.63 (d, 1H of Tp), 6.81 (m, 6H of PPh_3), 6.86 (t, 2H of *m*-H of CH_2Ph), 6.92 (t, H of *p*-H of CH_2Ph), 7.34 (d, 1H of Tp), 7.40 (m, 9H of PPh_3), 7.55 (d, 1H of Tp), 7.63(d, 1H of Tp), 7.94 (d, 1H of Tp), 10.03 (s, 1H; N*H*C(O)CH_3) (all coupling constants for Tp proton resonances are about 2 Hz)

$^{31}P\{^1H\}$ NMR (161.7 MHz, C_6D_6, 25 ˚C): δ = 47.2 (s)

$^{13}C\{^1H\}$ NMR (100.61 MHz, C_6D_6, 25 ˚C): δ 313.3 (d, J_{PC} = 15, Ru=*C*), 173.3 (s, NH*C*(O)CH_3)

ESI-MS (CH_2Cl_2): *m/z*: 738.21

4.2.2.9 Crystallographic structure analysis of [TpRu(PPh_3)(=C(CH_2Ph)NHC(O)CH_3)][BF_4] (14)

Reddish orange crystals of **14** suitable for X-ray diffraction study were obtained by layering diethyl ether on a CH_2Cl_2 solution of the complex. A suitable crystal with dimensions of 0.40 x 0.40 x 0.40 mm was mounted on a Bruker CCD area detector diffractomer and subject to MoK_α radiation (λ = 0.71073 Å) from a

generator operating at 50 kV and 30 mA. The intensity data of **14** were collected in the range of 2θ = 1.77─27.5˚ with oscillation frames of ϕ and ω in the range of 0─180˚. 1321 Frames were taken in four shells. An empirical absorption correction of the SADABS (Sheldrick, 1996) program based on Fourier coefficient fitting was applied. The crystal structure was solved by Patterson function methods, and expanded by difference Fourier syntheses, refined by full-matrix least squares on F^2 using the Bruker Smart and Bruker SHELXTL program packages. All non-hydrogen atoms were refined anisothropically. Hydrogen atoms were placed in ideal positions and refined as riding atoms, except the ones on the boron atom of the Tp ligand, which were located by difference electron density map. The final cycle of the full-matrix least-squares refinement based on 18454 observed reflections (I>2 sigma(I)) and 948 parameters converged to the R and R_w values of 0.072 and 0.1783 for $[TpRu(PPh_3)(=C(CH_2Ph)NHC(O)CH_3)][BF_4]$.

4.3 Results and Discussion

4.3.1 H/D Exchange between Ketones and D_2O

The H/D exchange reactions between ketones and D_2O were carried out in 11 mm tubes with Teflon screw caps at 110^{o}C for 44 h. Results of the **2**-catalyzed H/D exchange between ketones and D_2O are shown in Table 4.1. Complex **2** is an effective catalyst for the selective H/D exchange of the α hydrogen of ketones at moderate temperature. The methyl hydrogen of acetophenone (802) and the α-

hydrogens of cyclohexanone and cyclopentanone (1142 and 678) show high TONs in the **2**-catalyzed H/D exchange reaction. The catalytic activity of **2** is comparable with that of other catalysts. Cyclooctadieneiridium (I) acetylacetonate [189] catalyzes the H/D exchange between α hydrogen of 2-hydroxy-4-methoxyacetophenone and D_2O (TON = 75). Sajiki et al. [206] reported that a Pd/C system catalyzes the H/D exchange between the α hydrogen of cyclooctanone and D_2O at high temperature (160°C) (TON = 248).

Table 4.1 Catalyztic H/D exchange between D2O and ketones with 2[a]

Entry	Substrate	% deuteration at				Turnover number[b,c] (Turnover frequency[d])
		^1H	^2H	^3H	^4H	
1	Acetophenone 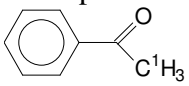	54				^1H: 802(18.2)
2	Benzylacetone 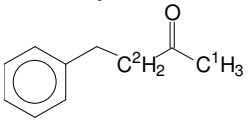	21	18			^1H: 312(7.1) ^2H: 175(4.0)
3	Benylidenacetone 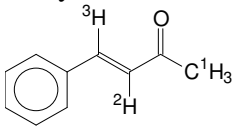	30	18	28		^1H: 450(10.2) ^2H: 92(2.1) ^3H: 141(3.2)
4	2-Butanone 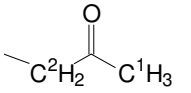	54	45			^1H: 805(18.3) ^2H: 450(10.2)
5	Cyclohexanone 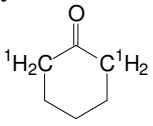	57				^1H: 1142(26.0)
6	Cyclopentanone 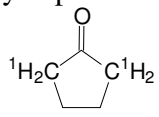	34				^1H: 678(15.4)

7	4-methyl-2-pentanone 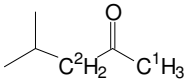	52	9			^{1}H: 777(17.7) ^{2}H: 88(2.0)
8	3-Pentanone 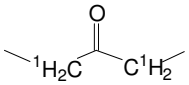	43				^{1}H: 850(19.3)
9	3-Penten-2-one 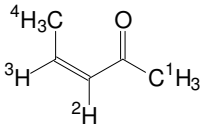	25	14	32	14	^{1}H: 369(8.4) ^{2}H: 68(1.5) ^{3}H: 161(3.7) ^{4}H: 212(4.8)
10	Propanone 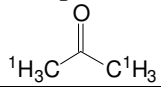	83				^{1}H: 2475(56.3)

[a] Reaction condition: Catalyst, 3.1 μmol; catalyst:ketone:D_2O = 1:500:600; temperature (oil bath) 110°C; time 44 h. [b] Determined by ^{1}H NMR spectroscopy. [c] TON = Mole of C-H bond deuterated per mole of catalyst. [d] TOF = Mole of C-H bond deuterated per mole of catalyst per hour.

The results in Table 4.1 suggest that the active hydrogen atoms can undergo H/D exchange reaction with D_2O. Therefore, the deuterium incorporation is observed only at the α position of the saturated ketones; and in the cases of α,β-unsaturated ketones, methyl hydrogens on α and γ positions as well as the olefinic hydrogens at α and β positions undergo H/D exchange. Three points of note can be observed from Table 4.1. The first is that the α-hydrogen atoms exhibit the largest extent of H/D exchange in α,β-unsaturated ketones. Secondly, hydrogen atoms on the terminal α position (methyl group) showed higher percentage of deuteration than those of the internal α-methylene group in saturated ketones. Lastly, degree of deutration at the α-methylene position is sensitive to the steric hinderence of saturated ketones.

4.3.2 H/D Exchange between Acetylacetone (Hacac) and D_2O under Argon

From the experimental results shown in Table 4.1, we interpret that the enol form of ketone is the active species for the H/D exchange (**Chart 4.1**). Direct observation of the enol-keto tautomerization of the ketone by ^1H NMR spectroscopy was unsuccessful in the course of the H/D exchange process. To show the importance of the enol tautomer, we carried out an H/D exchange reaction between acetylacetone (Hacac) and D_2O.

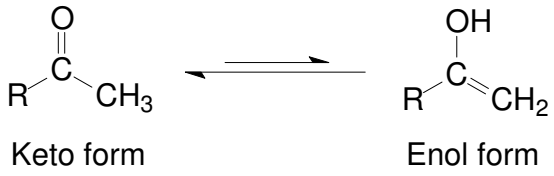

Chart 4.1 Tautomerization of ketone

It is well known that the enol tautomer of Hacac is dominant owing to the formation of a highly stable resonance structure in which the acidic enolic hydrogen bridges the two oxygen atoms (**Chart 4.2**). A 1,4-dioxane-d_8 solution containing 2 mg of **2**, acetylacetone (100 equiv), and D_2O (480 equiv) was heated at 110°C for 12 h in an NMR tube. ^1H NMR spectrum of the resulting solution showed that the methylene group of Hacac (83%) gives a much higher percentage of deuteration than the terminal methyl groups (6%). The turnover number (mole of C-H bond activated/mole of catalyst) of methylene hydrogen is 166, but that of methyl hydrogen is 36. This substantially larger degree (~5-fold) in the deuteration of the methylene group suggests that the enol tautomer might be the active form in the H/D

exchange reaction between ketones and D_2O. Apparently, the methylene hydrogen preferientally tautomerizes to form an enol isomer over the terminal methyl groups. The acidic enolic hydrogen can be deprotonated readily to form a stable acetylacetate, enabling such a higher deuterium incorporation level into the methylene hydrogen atoms. The results of the H/D exchange between some carbonyl compounds and D_2O catalyzed by cyclooctadieneiridium (I) acetylacetonate also indicated that tautomerization between the keto and enol forms is important for H/D exchange on the α hydrogen. Fels et al. [189] showed that 2-hydroxy-4-methoxyacetophenone, which can tautomerize between the keto and enol forms, undergoes H/D exchange at the α hydrogen instead of the *ortha* hydrogen on the phenyl ring. On the contrary, acetophenone oxime, which cannot tautomerize, shows no H/D exchange on the α hydrogen, but exclusively on the two *ortha* positions (**eq 4.1**).

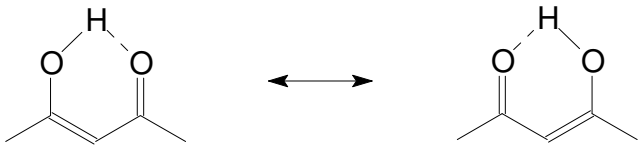

Chart 4.2 Resonance structures of acetylacetone

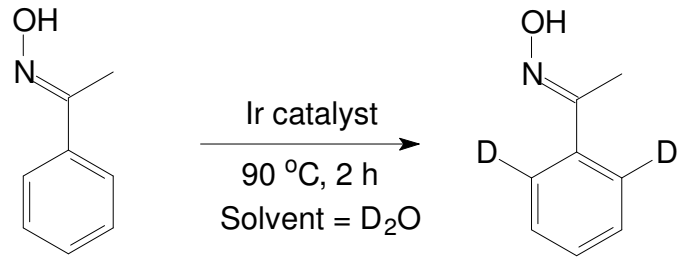

4.1

4.3.3 H/D Exchange of amido hydrogen of $TpRu(PPh_3)(H_2O)(NHCOCH_3)$ (2) with D_2O at Room Temperature

It is noted that the amido hydrogen of **2** is readily deuterated in the presence of D_2O. In a benzene-d_6 solution, the amido hydrogen signal of **2** (δ 4.67 ppm) was easily discernable by ^1H NMR spectroscopy, and its intensity remained unchanged over an extended period of time at room temperature, indicating that the amido hydrogen did not undergo H/D exchange with benzene-d_6 at this temperature. However, the ^1H NMR spectrum of **2** taken overnight after the addition of excess D_2O to the solution showed that the amido hydrogen signal had dropped significantly while the intensities of the other proton signals of the complex remained unchanged, thus indicative of deuteration of only the amido hydrogen of **2** by D_2O at room temperature.

Scheme 4.1 shows a probable mechanism for the H/D exchange between Ru─$NHCOCH_3$ of **2** and D_2O. The reaction may be initiated by an interaction between the Ru─N and D─OD forming a Ru─N···D─OD hydrogen-bonded species. The H/D exchange reaction then proceeds via the reversible formation of amide-hydroxo and aquo-amido species (**Scheme 4.1**). Deprotonation of water by an adjacent amido moiety has been mentioned in Chapter 1, Section 1.8. Complex **2** has also been shown to deprotonate a dihydrogen molecule to form ruthenium hydride (See **Scheme 2.7**).

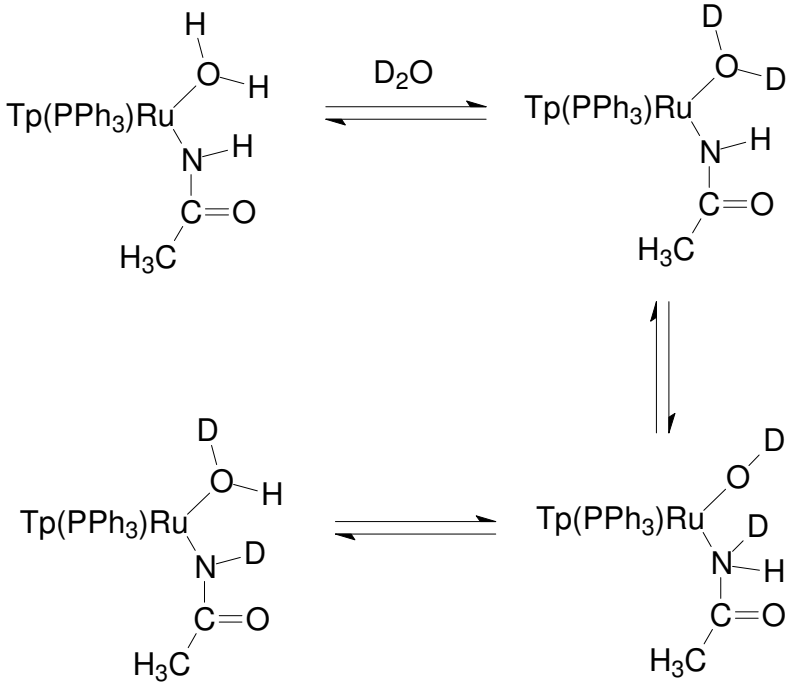

Scheme 4.1 Proposed mechanism 1 of H/D exchange between the amido hydrogen and D_2O

An alternative mechanism for the H/D exchange reaction involves an interaction between amido oxygen and D─OD. The H/D exchange process proceeds via the reversible formation of the iminol-hydroxo, amide-hydroxo, and amido-aquo species (**Scheme 4.2**). Yi et al. [146] reported a similar observation of a facile deuteration of the amido hydrogen when $[(PCy_3)_2(CO)(CH_3CONH)(^iPrOH)RuH]BF_4$ was treated with excess $(CD_3)_2CDOD$ at room temperature. They proposed that the H/D exchange is facilitated by a hydrogen-bonding interaction between the acetamido group and the coordinated alcohol (See Chapter 3, Section 3.3.4), via the iminol-to-amide tautomerization of the acetamido ligand. Crabtree and co-workers also mentioned that similar iminol-

amide tautomerization is initiated by a strong Ir-H···H-X (X = O, N) intramolecular dihydrogen-bonding interaction. [56, 138]

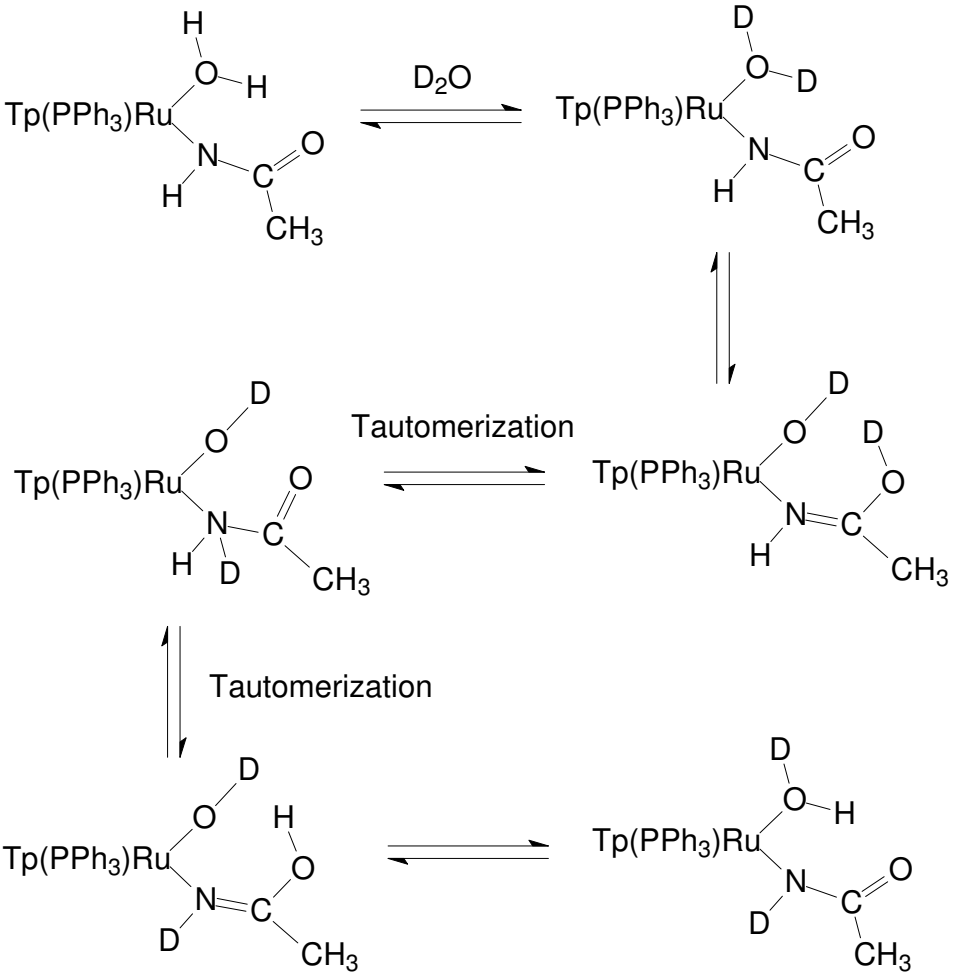

Scheme 4.2 Proposed mechanism 2 of H/D exchange between the amido hydrogen and D_2O

It should be mentioned that coordination of D_2O to the metal center seems to be a necessity for the H/D exchange reaction between amido hydrogen and D_2O. Competitive amido hydrogen/D_2O H/D exchange reactions with **2** and $TpRu(PPh_3)(PMe_3)(NHCOCH_3)$ was performed. The complex

$TpRu(PPh_3)(PMe_3)(NHCOCH_3)$ was formed by mixing a THF solution of **2** with excess PMe_3 at room temperature overnight. The ^1H NMR spectrum of $TpRu(PPh_3)(PMe_3)(NHCOCH_3)$ shows a peak at δ 3.43 ppm which is assignable to the amido hydrogen. A benzene-d_6 solution containing equal amounts of **2** and $TpRu(PPh_3)(PMe_3)(NHCOCH_3)$, and excess D_2O in an NMR tube was kept at room temperature overnight. ^1H NMR spectrum of the resulting solution showed that the amido hydrogen signal of **2** (δ 4.67 ppm) had completely disappeared, but that of $TpRu(PPh_3)(PMe_3)(NHCOCH_3)$ had only undergone around 30% deuteration. This result demonstrated that the coordination of D_2O is important to the H/D exchange process of the amido hydrogen with D_2O.

4.3.4 H/D Exchange between amido deuterium of $TpRu(PPh_3)(D_2O)(NDCOCH_3)$ (2d) and cyclopentanone

The deuterated complex $TpRu(PPh_3)(D_2O)(NDCOCH_3)$ (**2d**) is readily synthesized by refluxing a THF solution of **2** with excess D_2O. The H/D exchange reaction between **2d** and cyclopentanone was carried out in pre-dried benzene-d_6 in a 5mm NMR tube under nitrogen gas. The intensity of the residual amido hydrogen signal of **2d** remained unchanged over 24 h at room temperature, indicating that H/D exchange did not occur between amido hydrogen and cyclopentanone at this temperature. However, the ^1H NMR spectrum taken after heating in the NMR tube for 24 h at 90°C showed that the amido hydrogen signal increased significantly. It also showed 15% deuteration at the α position of the cyclopentanone, thus indicative

of the involvement of the amido deuterium of **2d** in the H/D exchange reaction with the ketone. In addition, the Tp signals remained invariant in the ^{1}H NMR spectrum, indicating that the catalyst was not altered after the H/D exchange reaction.

4.3.5 Mechanism of 2-catalyzed H/D exchange between enolic hydrogens of ketones and D_2O

In light of our work, we suggest two mechanisms; one for the **2**-catalyzed H/D exchange of enolic hydrogens of ketones; another for the **2**-catalyzed H/D exchange of olefinic hydrogens of α,β-unsaturated ketones. The catalytic cycle of **2**-catalyzed H/D exchange between enolic hydrogens and D_2O is depicted in Scheme 4.3. The amido group of **2** acts as a relay to enable the exchange of the deuterium of D_2O with the amido hydrogen, and the amido deuterium with enolic hydrogen of the ketone. The amido hydrogen is first deuterided by D_2O. The enol tautomer of ketone then displaces the HOD. The H/D exchange between the amido deuterium and enolic hydrogen also occurs through two possible pathways similar to the H/D exchange between the amido hydrogen and D_2O shown in Schemes 4.1 and 4.2. The incoming D_2O eventually displaces the deuterated enol tautomer to regenerate **2**.

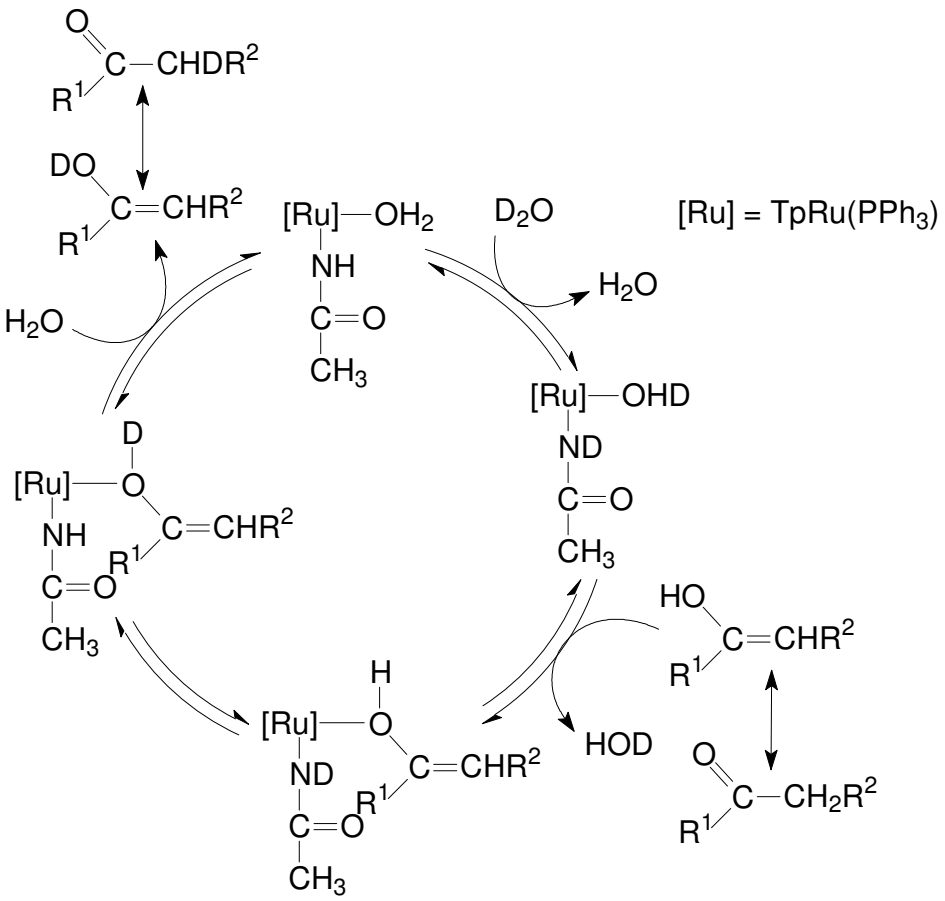

Scheme 4.3 Proposed mechanism of catalytic H/D exchange between enolic hydrogen and D_2O

It has been mentioned in Section 4.3.2 that the deuterium incorporation levels of α position of saturated ketones as well as α,β-unsaturated ketones are high. This is because the α hydrogens of ketones can be activated by keto-enol tautomerization. Methyl ketones can tautomerize to two enol isomers with different stabilities. (**Chart 4.3**) The monosubstitiuted enol, which is thermodynamically less stable, is formed by the tautomerization of terminal methyl group. The disubstitiuted enol, which is a relatively sterically bulky enol, is formed by the tautomerization of internal methylene group.[207] Our results of higher percentage of deuteration on

the terminal α position (methyl group) than that on the internal α position (methylene group) in saturated ketones showed that the catalysis is governed by both stability and steric hindrance of the formed enol. For the less bulky substrates (Entry 4), the difference in deuteration between these two groups is not significant. It is believed that the steric effect of enol becomes less important, thus the comparatively more stable disubstituted enol is capable of undergoing H/D exchange with D_2O. On the contrary, for some bulky substrates (Entry 7), the α hydrogen on the terminal methyl group is exchanged preferentially, because the tautomerization of the terminal methyl group gives the relatively less bulky monosubstituted enol.

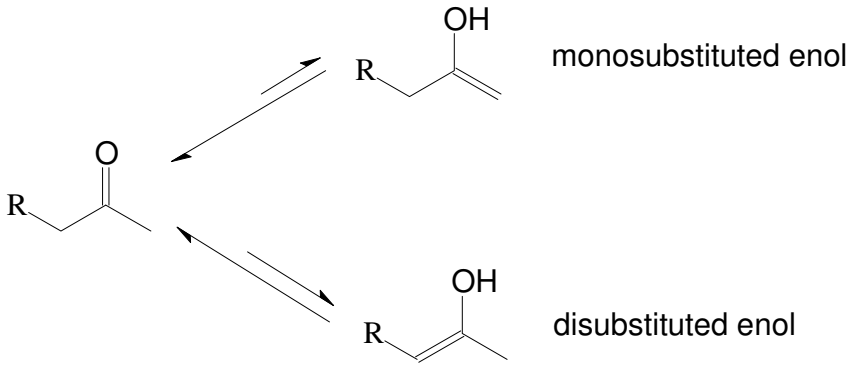

Chart 4.3 Two tautomers of methyl ketone

We have noticed that the deuteration of the internal methylene group is controlled by the steric bulkiness of the disubstituted enol. The bulkier the substitutant attached on the enol, the lower is the deuteration. Bulky substrates like entries 2 and 7 showed lower levels of deuterium incorporation. On the other hand, cyclohexanone showed the highest deuteration because rotations of the two

substitutants are restricted by a cyclic linkage. Ketones with short aliphatic chains also showed higher deuteration (Entries 4 and 8).

Hydrogen atoms on the γ positions on the α,β-unsaturated ketones can rearrange to form an active dienol via a mechanism similar to 1,5-sigmatropic rearrangement in conjugated unsaturated hyrocarbons. Through this rearrangement, the hydrogen shifts from position 5 to 1 (**Chart 4.4**). Owing to the odd number chain, the symmetries of the frontier orbitals on positions 1 and 5 are equal. It is, therefore, a symmetry-allowed rearrangement. The hydrogen is capable of migrating to the terminal position with the same face of the conjugated π system (suprafacial shift). The hydrogen on γ position as well as the double bond between α and β positions shifts to form dienol.

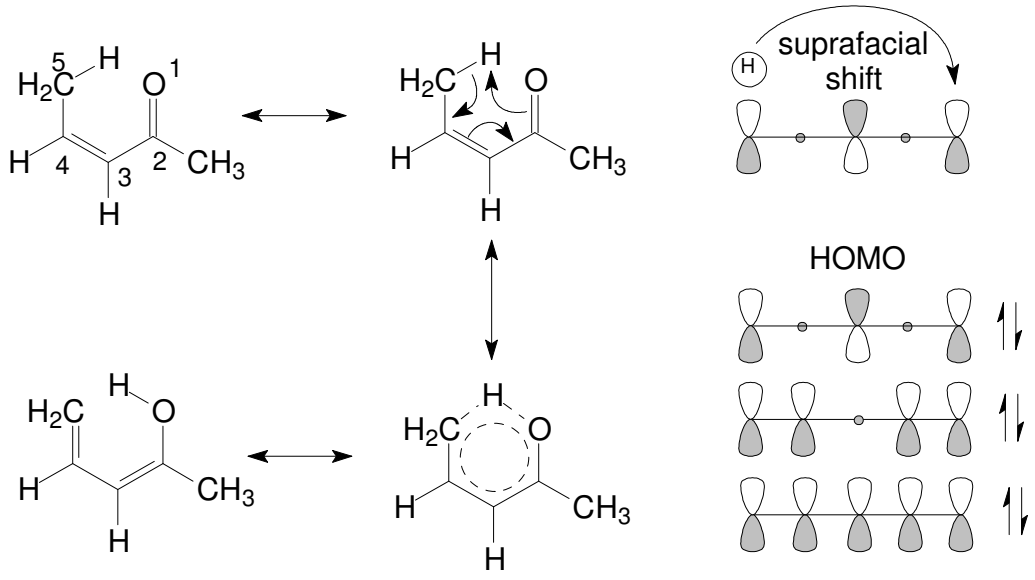

Chart 4.4 Sigmatroptic rearrangement of 3-penten-2-one

4.3.6 Mechanism of 2-catalyzed H/D exchange between olefinic hydrogens of α,β-unsaturated ketones and D_2O

As mentioned in the Chapter 2, **2** is unable to catalyze H/D exchange between benzene and D_2O. Several attempts to incorporate deuterium from D_2O into ethylene with **2** under different conditions also failed. Our results showed that only the olefinic hydrogens next to the carbonyl group can be exchanged. The conjugated system shown in Chart 4.5 can activate the olefinic hydrogens on α and β positions of the α,β-unsaturated ketones. Evans et al. [183] showed that deuteration of *ortho* hydrogens of acetanilide catalyzed by $[Ir(COD)(PCy_3)(Py)]PF_6$ was prompted by the presence of an amido functional group. Heys [182] reported similar observation using $[IrH_2(Me_2CO)_2(PPh_3)_2]BF_4$ to catalyze deuterium incorporation into the *ortho* position of the phenyl ring with different functional groups.

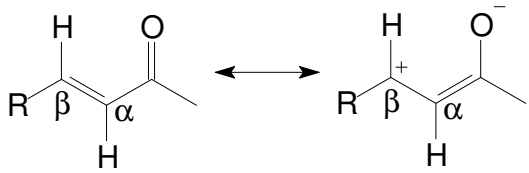

Chart 4.5 Conjugation of α,β-unsaturated ketone

A detailed mechanism of the H/D exchange reaction between this olefinic hydrogen in the α,β-unsaturated ketones and D_2O, however, is not clear. Work is in progress for figuring out the possible mechanism. We believe tentatively that the carbonyl group enhances the acidity of olefinic hydrogens, enabling the

deprotonation by the adjacent acetamido moiety. Milstein et al. reported that the agostic hydrogen of aromatic η^2-C,H σ-bonding is more acidic than that of the aliphatic one. Thus, the *ortho* hydrogen of phenyl group in the rhodium catalyst shown in Chart 1.2 is capable of exchanging with D_2O via an aromatic η^2-C,H σ-complex. (See Section 1.5)

4.3.7 Reactivity studies of 2

We have learned from the previous sections that the aquo ligand of **2** is labile and is easily displaced by others substrates (e.g. nitrile) even in the presence of intramolecular hydrogen bonding between the aquo ligand and the adjacent amido ligand. To study the reactivity of **2**, experiments using **2** as catalyst or as reagent were carried out.

It is noted that methanol and triethylamine can also readily displace the aquo ligand of **2** to *in-situ* generate $TpRu(PPh_3)(HOMe)(NHCOCH_3)$ and $TpRu(PPh_3)(NEt_3)(NHCOCH_3)$, respectively. These complexes are not isolable in pure form and are always contaminated by a small amount of **2**. The reason is that these complexes were synthesized by stirring a THF solution of **2** with methanol and triethylamine, respectively at room temperature; however, during the work up, when vauum was applied for removal of the solution, a small amount of **2** was reformed, probably due to the fact that water present in the solution was not as readily removed as the methanol and triethylamine, therefore water concentration in the solution

increaed. The reaction of **2** with acetaldehyde gives a carbonyl complex $TpRu(PPh_3)(CO)(CH_3)$ and an acetamide molecule. The possible reaction pathway is depicted in Scheme 4.4.

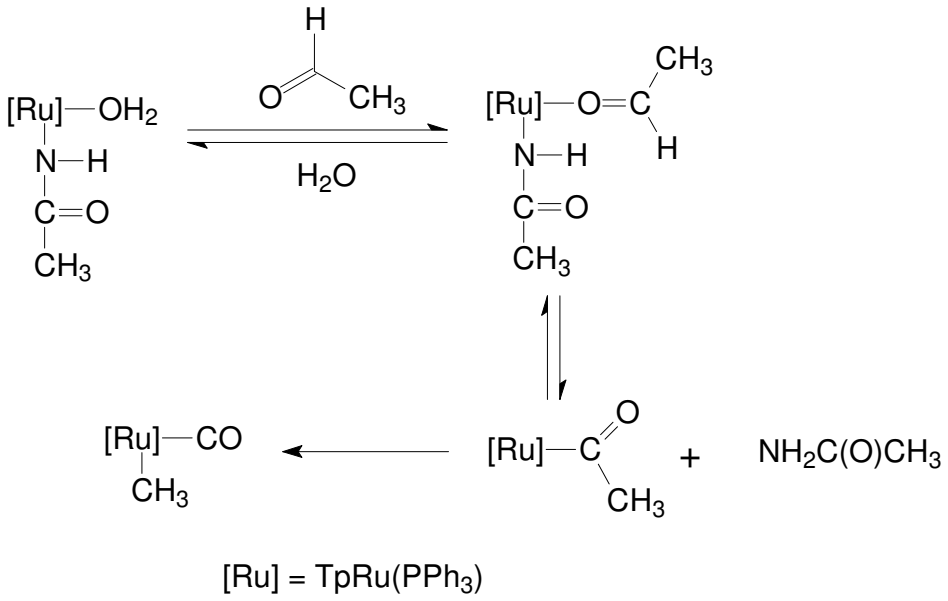

Scheme 4.4 Reaction sequence between 2 and acetaldehyde

Complex **2** was used to catalyze transamidation of primary amide with secondary amine and hydroamidation of alkene and alkyne. However, there were no catalytic activities shown in these reactions. In the **2**-catalyzed hydroamidation of alkyne (such as phenylacetylene), we found that **2** reacted with phenylacetylene to generate $TpRu(PPh_3)(C(NHC(O)CH_3)=CHPh)$ (**13**). Complex **13** could be further converted to $[TpRu(PPh_3)(=C(CH_2Ph)NHC(O)CH_3)][BF_4]$ (**14**) by the addition of HBF_4. (*vide infra*)

4.3.8 Synthesis of $TpRu(PPh_3)(C(NHC(O)CH_3)=CHPh)$ (13) and $[TpRu(PPh_3)(=C(CH_2Ph)NHC(O)CH_3)][BF_4]$ (14)

The amido vinyl complex (**13**) was readily prepared by reacting a THF solution of **2** with phenylacetylene. The amido hydrogen (N-H) and the β hydrogen of the vinyl group appear as slightly broadened singlets at δ 5.98 and δ 6.15 ppm in the ^{1}H NMR spectrum, respectively. It was reported that vinyl ruthenium complexes $[Ru(CH=CHPh)(NCCH_3)_3(P^iPr_3)_2]Cl$ [208] and $[RuCl(CH=CHPh)(CO)(PCy_3)_2]$ [209] exhibit similar signals of the β hydrogen of the vinyl group at δ 6.34 and 5.92 ppm, respectively. The olefinic hydrogen (*italic*) of N-styrylacetamide molecule ($Ph\mathit{H}C=C(H)NHC(O)CH_3$) [210] shows a doublet at 6.09 ppm, similar to the β hydrogen signal in **13**. The ^{13}C NMR spectrum of **13** shows a singlet δ 155.9 ppm and a doublet δ 209.3 ppm (J_{PC} = 16 Hz) corresponding to the carbonyl carbon of the acetamido ligand and α carbon of the amido vinyl moiety, respectively. The vinyl carbon (C_α), generally showing signals from δ 159.7 –138.4 ppm [208, 211], exhibits a downfield-shift to δ 209.3 ppm in **13**. It may be due to the presence of electron-withdrawing group (acetamido) attached on this carbon. The phosphine ligand of **13** appears as a singlet at δ 64.2 ppm in the $^{31}P\{^1H\}$ NMR spectrum.

The cyclic amido carbene complex (**14**) was readily prepared by reacting a THF solution of **13** with HBF_4 at room temperature for 15 min. The amido hydrogen (N-H) appears as a slightly broadened singlet at δ 10.03 ppm in the ^{1}H NMR spectrum. Kirchner et al. [212] reported that the amido hydrogen of TpRu(Haapy)Cl

shows a singlet at δ 11.18 ppm in the ^{1}H NMR spectrum (**Chart 4.6**). It is noteworthy that the two methylene hydrogen atoms of the amido carbene ligand are chemical inequivalent, showing two doublets at δ 4.88 and δ 4.10 ppm (d, J_{HH} = 12.1Hz) in the ^{1}H NMR spectrum. The ^{13}C NMR spectrum of **14** shows a singlet and a doublet at δ 173.3 ppm and δ 313.3 ppm (J_{PC} = 15 Hz), corresponding to the carbonyl carbon and carbene carbon of the cyclic amido carbene ligand, respectively. The phosphine ligand of **14** appears as a singlet at δ 47.2 ppm in the ^{31}P{^{1}H} NMR spectrum.

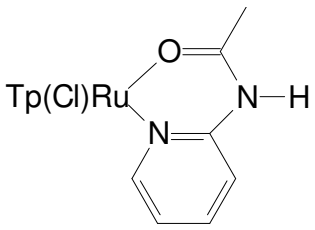

Chart 4.6 Molecular structure of TpRu(Haapy)Cl

4.3.9 X-ray crystallographic study of [TpRu(PPh$_3$)(=C(CH$_2$Ph)NHC(O)CH$_3$)][BF4] (14)

Crystals of **14** suitable for X-ray diffraction study were obtained by layering hexane on a CH_2Cl_2 solution of the complex. Figure 4.1 shows the molecular structure of **14**. The crystal data and refinement details are given in Table 4.2. Selected bond distances and angles are listed in Table 4.3.

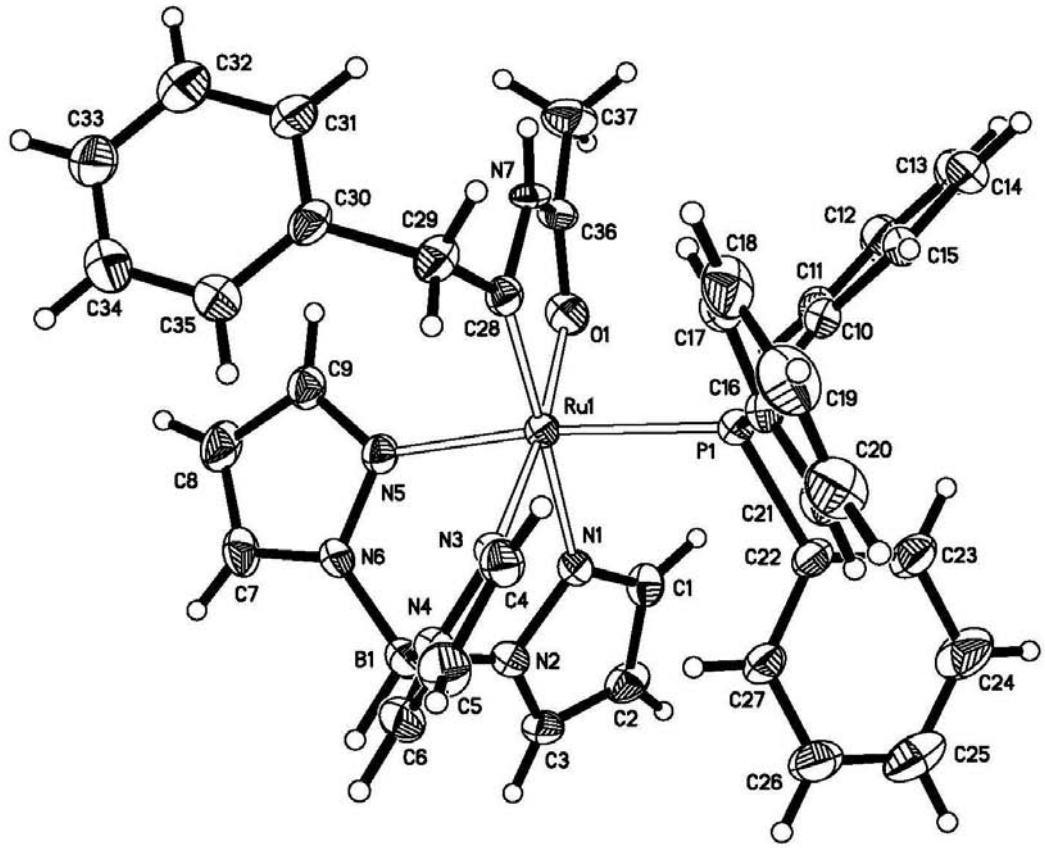

Figure 4.1 Molecular structure of [TpRu(PPh$_3$)(=C(CH$_2$Ph)NHC(O)CH$_3$)][BF$_4$] (14)

Table 4.2 Crystal data and structure refinement for [TpRu(PPh$_3$)(=C(CH$_2$Ph)NHC(O)CH$_3$)][BF$_4$] (14)

	[TpRu(PPh$_3$)(=C(CH$_2$Ph)NHC(O)CH$_3$)][BF$_4$] (14)
Empirical formula	[Ru($C_{10}H_{11}NO$)(P(C_6H_5)$_3$)($C_9H_9N_6BH$)].BF_4
Formula weight	824.39
Temperature	296(2) K
Wavelength	0.71073 Å
Crystal system	Monoclinic
Space group	C2/c
Unit cell dimensions	a = 47.8459(6) Å α = 90^o b = 17.1831(3) Å β = 115.6880(10)^o c = 21.7245(3) Å γ = 90^o
Volume	16095.4(4) Å^3
Z	16
Density (calculated)	1.361 Mg/m^3
Absorption coefficient	0.486 mm^{-1}
F(000)	6720
Crystal size	0.40 x 0.40 x 0.40 mm^3
θ range for data collection	1.77 to 27.50^o
Index ranges	$-62 \le h \le 62$, $-22 \le h \le 22$, $-28 \le l \le 28$
No. of Reflections collected	153044
No. of Independent reflections	18454 [R(int) = 0.1703]
Completeness to θ = 27.50^o	99.7%
Absorption correction	Semi-empirical from equivalents
Max. and Min. transmission	1.000 and 0.834
Refinement method	Full-matrix least-squares on F^2
No. of data / restraints / params	18454 / 113 / 948
Goodness-of-fit on F^2	1.005
Final R indices [I > 2σ(I)]	R1 = 0.0720, wR2 = 0.1783
R indices (all data)	R1 = 0.1618, wR2 = 0.2270
Largest diff peak and hole	0.917 and -0.601 e. Å^{-3}

Table 4.3 Selected bond distances (Å) and bond angles (^{o}) for [TpRu(PPh$_3$)(=C(CH$_2$Ph)NHC(O)CH$_3$)][BF$_4$] (14):

Bond Distances (Å)			
Ru(1) – N(1)	2.198(3)	Ru(1) – N(3)	2.103(2)
Ru(1) – N(5)	2.115(3)	Ru(1) – C(28)	1.885(4)
Ru(1) – O(1)	2.053(2)	O(1) – C(36)	1.285(5)
N(7) – C(36)	1.357(4)	N(7) –C(28)	1.401(4)
C(28) – C(29)	1.494(5)		

Bond Angles (^{o})			
C(28)-Ru(1)-O(1)	79.01(12)	C(28) -Ru(1)- N(3)	97.51(12)
C(28)-Ru(1)-N(5)	94.44(13)	C(28)-Ru(1)-P(1)	93.03(11)
O(1)-Ru(1)-P(1)	93.25(8)	O(1) -Ru(1)- N(5)	89.22(10)
O(1)-Ru(1)- N(1)	94.82(10)	N(3)-Ru(1)-N(5)	85.42(10)
N(3)-Ru(1)-N(1)	88.24(10)	N(3)-Ru(1)-P(1)	92.55(8)
N(1)-Ru(1)-P(1)	91.17(8)	N(5)-Ru(1)-N(1)	81.51(11)
N(7)-C(28)- Ru(1)	115.5(2)	C(29)-C(28)-Ru(1)	137.6(3)
O(1)-C(36)-C(37)	127.2(3)		

The cyclic amido carbene chelate ring in **14** is basically planar. The bond distances of N(7)-C(36), 1.357(4) Å, and O(1)-C(36), 1.285(5) Å are comparable to those in the amido carbene ligand in the ruthenium complex, $RuHCl(P^iPr_3)_2(C_6H_9NO)$ (N-C = 1.350(6) Å and O-C = 1.245(6) Å) (**Chart 4.7**). [213] The bond distance of Ru(1)-C(28), 1.885(4) Å is only slightly different from that Ru-C bond (1.897(2) Å) in TpRu amido carbene complex, $TpRu(=C(CH_2Ph)aapy)Cl$ (Haapy = 2-acetamidopyridine) (**Chart 4.8**). [212] The environment about ruthenium corresponds to a slightly distorted octahedron, as shown in Figure 4.1. The two Ru-N(Tp) bond distances cis to the carbene moiety (Ru(1)-N(3), 2.103(2) Å and Ru(1)-N(5), 2.115(3) Å) are obviously shorter than the one trans to the carbene unit (Ru(1)-N(1), 2.198(3) Å). This is because of the strong trans influence of the strong π-accepting carbene. Similar observation in $TpRu(=C(CH_2R)aapy)Cl$ (R = Ph and ^{n}Bu) has been reported by Kirchner and co-workers. [212] The bond length of Ru-N(Tp) trans to the carbene ligand (2.216(2) Å; R = Ph and 2.220(2) Å; R = ^{n}Bu) is longer than those cis to the carbene moiety (2.061(2) Å and 2.081(2) Å; R = Ph and 2.066 Å and 2.090(2) Å; R = ^{n}Bu).

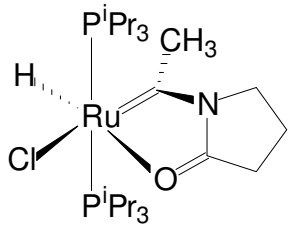

Chart 4.7 Molecular structure of $RuHCl(P^iPr_3)_2(C_6H_9NO)$

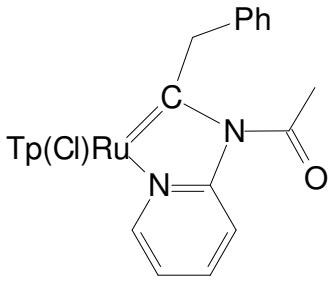

Chart 4.8 Molecular structure of TpRu(=C(CH_2Ph)aapy)Cl

4.3.10 Possible Mechanism of Formation of TpRu(PPh_3)(C(NHC(O)CH_3)=CHPh) (13) and [TpRu(PPh_3)(=C(CH_2Ph)NHC(O)CH_3)][BF_4] (14)

The complex TpRu(PPh_3)(C(NHC(O)CH_3)=CHPh) (**13**) is synthesized by reacting a THF solution of **2** with phenylacetylene at room temperature. Formation of the amido vinyl ligand in **13** requires coordination of phenylacetylene to form a vinylidene complex and subsequent intramolecular nucleophilic attack of the amido group to the α carbon of the vinylidene ligand (**Scheme 4.5**). Although, formation of amido vinyl complexes is rarely reported, insertion of alkynes to the metal-hydride or metal-methyl bond to form vinyl complexes can be regarded as analogous examples[208, 209, 214-216]. Otto et al. [215] reported that the carbonyl hydride ruthenium complex RuHCl(CO)(P^iPr_3)$_2$ reacts with alkynes HC≡CR (R = H, Ph) by insertion to give a five-coordinate vinyl metal complexes Ru(CH=CHR)Cl(CO)(P^iPr_3)$_2$ (R = H, Ph). Werner and co-worker [208] domonstrated that the reaction of the vinylidene(hydrido)ruthenium complexes

[RuHCl(=C=CHR)(PCy_3)$_2$] (R = H, Ph) with excess KPF_6 in DCM/acetonitrile afford the five-coordinate vinyl complexes [Ru(CH=CHR)($NCCH_3$)$_2$(PCy_3)$_2$]PF_6.

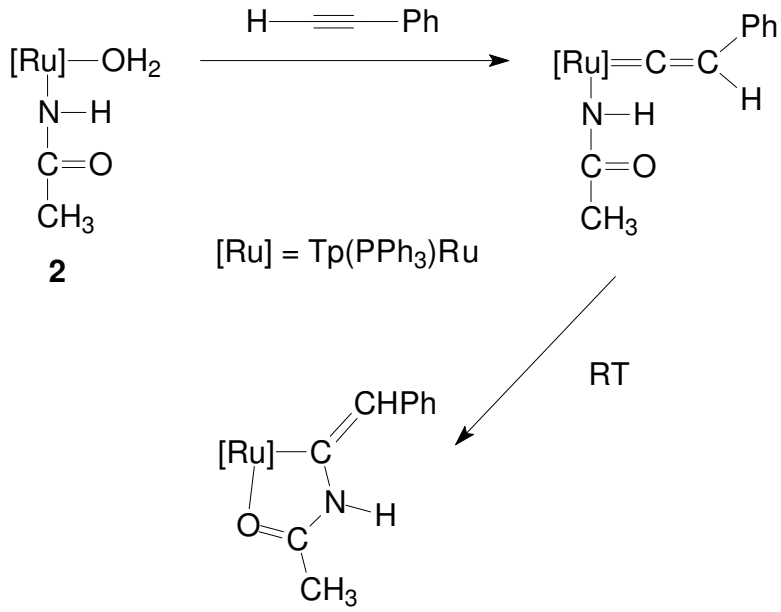

Scheme 4.5 Proposed mechamism of formation of 13

The formation of vinylidene intermediate, which could not be isolated or detected spectroscopically in our case, is vital for this C-N bond formation. The α carbon of the vinylidene ligand is electron-deficient, facilitating the attack of the weak nucleophile, the amido ligand. Vegas et al. [217] showed that vinylidene complexes are capable of undergoing nucleophilic attack by alcohol. Indenyl ruthenium complexes (η^5-C_9H_7)Ru(Cl)LL' react with 5-hexyn-1-ol to yield hydroxyalkylvinylidene ruthenium complexes [Ru(=C=C(H)C_4H_8OH)(η^5-C_9H_7)LL']PF_6 which can undergo intramolecular nucleophilic attack of OH group to

the α carbon of hydroxyalkylvinylidene to form 2-oxacycloheptylidene complexes. (**Chart 4.9**)

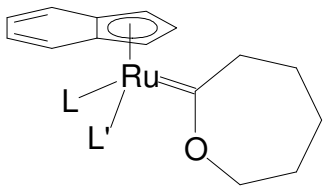

L = L' = PPh_3;
L = L' = PMe_2Ph;
L = PPh_3, L' = PMe_3

Chart 4.9 Molecular structures of 2-oxacycloheptylidene complexes

The complex $[TpRu(PPh_3)(=C(CH_2Ph)NHC(O)CH_3)][BF_4]$ (**14**) is synthesized by reacting a THF solution of $TpRu(PPh_3)(C(NHC(O)CH_3)=CHPh)$ (**13**) with HBF_4 at room temperature. Formation of the amido carbene ligand in **14** requires protonation of amido vinyl group. (**Scheme 4.6**) Mechanistic study of the formation of $[RuCl(=C(H)CH_2R)(CO)(L)_2]BF_4$ (R = H, Ph, ^tBu) indicated that the amido vinyl precursor $[RuCl(CH=CHR)(CO)(L)_2]$ reacts with HBF_4 whose proton preferientally attacks at the C_β carbon atom of the amido vinyl ligand to afford an amido carbene complex. [209] Werner and co-workers [208] demonstrated that the vinyl ligands of $[Ru(CH=CH_2)(NCCH_3)_2(PCy_3)_2]X$ (X = BF_4, BAr_f) can be protonated by HX to yield carbene complexes $[Ru(=C(H)CH_3)(NCCH_3)_2(PCy_3)_2]X_2$.

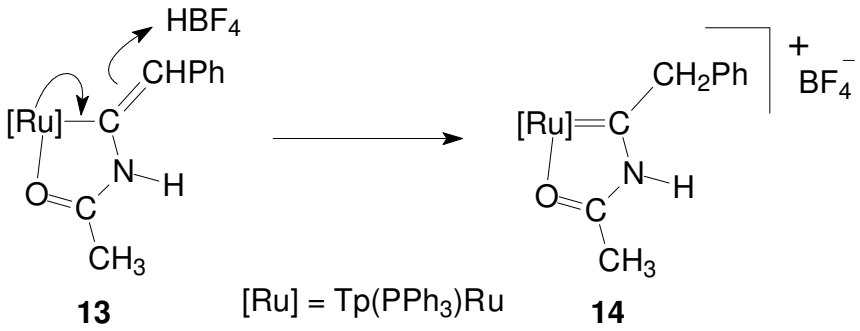

Scheme 4.6 Proposed mechamism of formation of 14

Chapter Five Conclusion

The first part of our study is to continue our previous work on C–H activation and catalytic H/D exchange between deuterated organic molecules and CH_4 with the solvento hydride complex $TpRu(PPh_3)(CH_3CN)H$ (**1**). We found that the catalytic systems based on **1** are capable of affecting the H/D exchange into organic compounds with D_2O. This part of our work represents a new entry into the study of metal-catalyzed H/D exchange between organic molecules and D_2O; reports on incorporation of deuterium into C–H bonds of organic molecules using D_2O as deuterium source are relatively rare. Our ruthenium systems are, at this stage, still far from being practically useful. However, our work indicates that transition-metal solvento hydride complexes, by virtue of facile deuteration of the M–H bond with D_2O to form M–D and subsequent H/D exchange of the deuteride ligand with R–H, have high potentials to act as active catalysts for the deuteration of organic compounds using D_2O as deuterium source. Furthermore, the formation of the acetamido complex $TpRu(PPh_3)(H_2O)(NHCOCH_3)$ (**2**) might provide more insight into the mechanisms of the catalytic hydration reactions of nitriles with transition-metal hydride complexes.

Previous research on kinetic and mechanistic studies on transition-metal-catalyzed hydration of nitriles in the literature illustrates that intramolecular or external nucleophilic hydroxo attack at the carbon atom of the η^1-coordinated nitrile molecule gives the metal amide intermediate, subsequent protonation of the amido

ligand by an adjacent aquo ligand generates the product. We have, however, in the second part of my work, shown that the aquo–amido complexes **2** and **8** ($TpRu(PPh_3)(H_2O)(NHCOPh)$ phenyl analogue of **2**) that we employ for study of nitrile hydration are stable toward intramolecular protonation of the amido ligand by the aquo ligand; instead, displacement of the aquo ligand in **2** or **8** by a nitrile molecule and N-amido/O-imido linkage isomerization starts the catalytic cycle of nitrile hydration. Our work demonstrates that catalytic hydration of nitriles with **2** or **8** proceeds via a unique mechanism involving the intermediacy of a relatively stable complex containing a chelating *N*-imidoylimidato ligand, ring-opening nucleophilic attack of this ligand by water generates the product. Moreover, our work also represents one of the examples of detailed theoretical investigation of the mechanism of nitrile hydration with homogeneous organometallic systems.

Last part in our work involves an effective and selective H/D exchange reaction between ketones and D_2O. Our results show that H/D exchange occurs selectively in the α position of the ketones and α, β, and γ positions of the α,β-unsaturated ketones. We suggest that the deuterium first exchanges from the D_2O into the amido hydrogen of **2**. The amido deuterium then exchanges with the enolic hydrogen of enol form of ketone. The cycle is completed by displacement of the deuterated enol with D_2O. The product, deuterated ketone, is formed after the tautomerization. This mechanism shows clearly that the amido moiety is acting as a rally enabling the exchange of the deuterium of D_2O with the active hydrogen of ketone.

Reactivity of the amido complex such as **2** has also been studied. Although **2** was not capable of catalyzing transamidation of primary amide with secondary amine and hydroamidation of alkenes and alkynes, we have demonstrated nucleophilic addition of alkyne by the amido ligand. This stoichiometric reaction starts with addition of phenylacetylene to **2**. The mechanism involves the coordination of alkyne to form a vinylidene ligand, and subsequent intramolecular nucleophilic attack of the adjacent amido moiety to form an amido vinyl complex (**13**), which can be protonated to form an amido carbene complex (**14**). It shows that the amido group can be used as a reagent toward C-N bond formation.

It has been shown that the amido moiety can be used as an auxiliary ligand enabling H/D exchange reactions and as an intramolecular nucleophile to attack the adjacent unsaturated organic functions. The versatility of the amido complex, thus, is demonstrated in this work.

Appendix

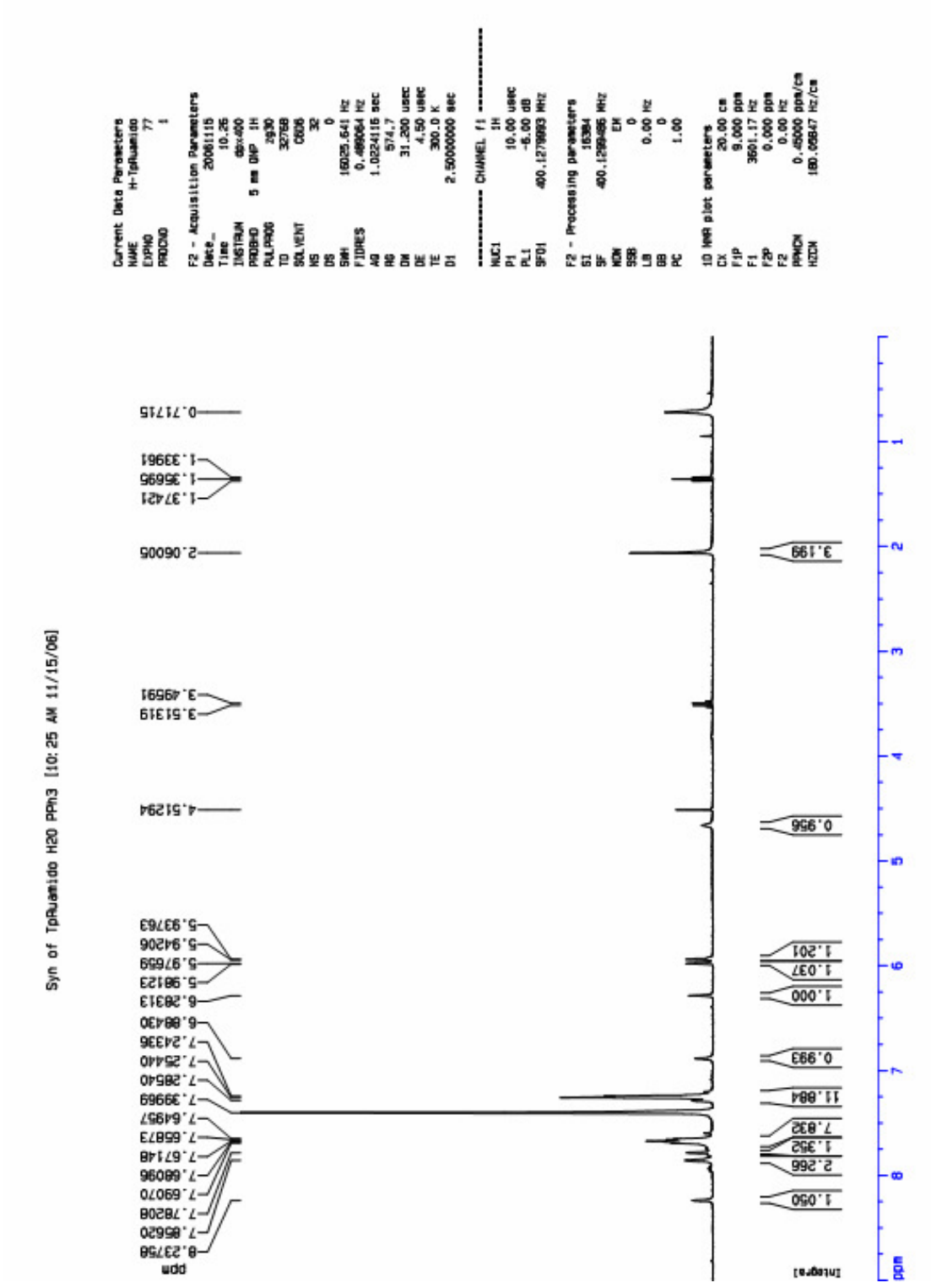

Figure 2.4 400.13 MHz ^{1}H NMR spectrum of TpRu(PPh$_3$)(H$_2$O)(NHC(O)CH$_3$) (2)

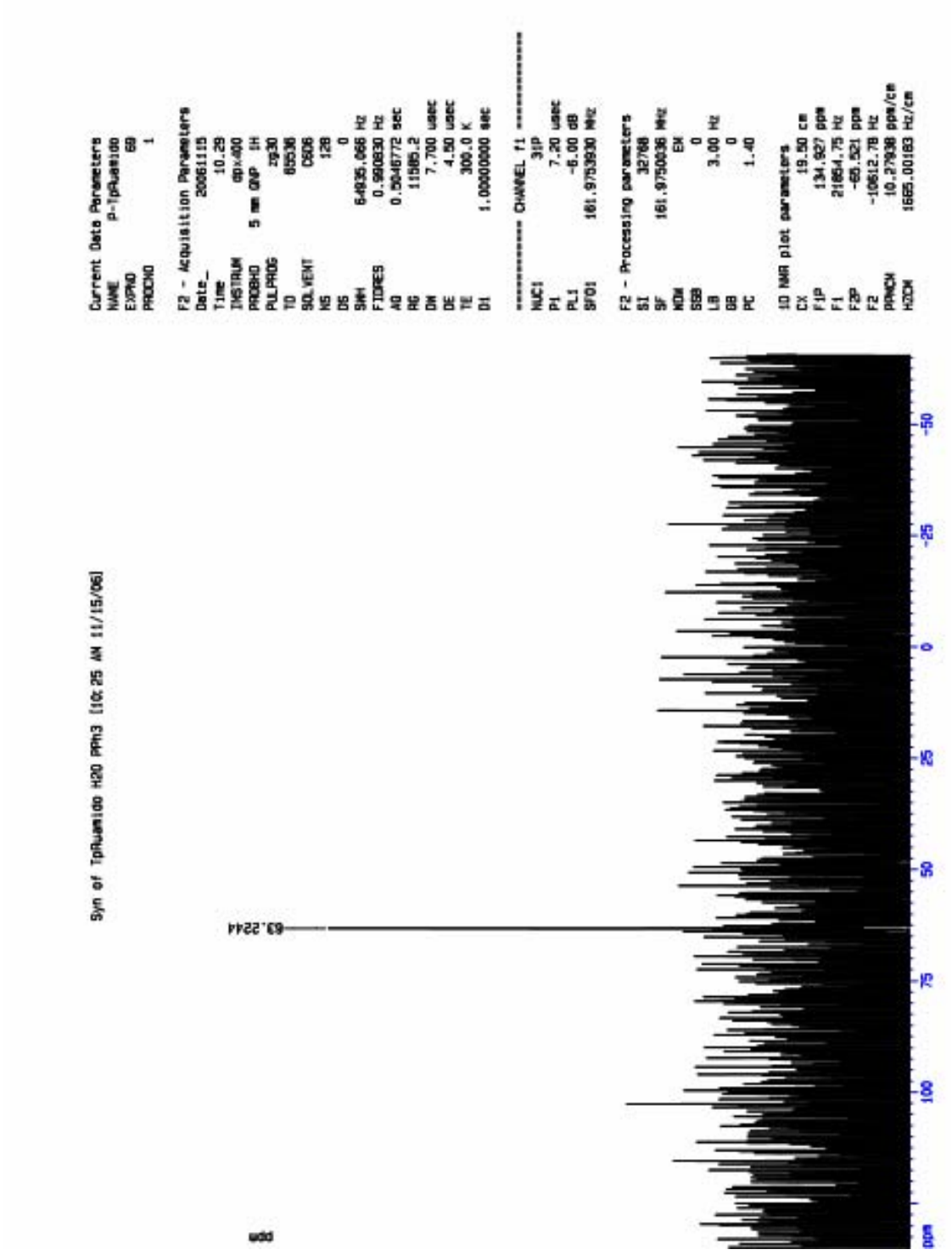

Figure 2.5 161.98 MHz $^{31}P\{^{1}H\}$ NMR spectrum of $TpRu(PPh_3)(H_2O)(NHC(O)CH_3)$ (2)

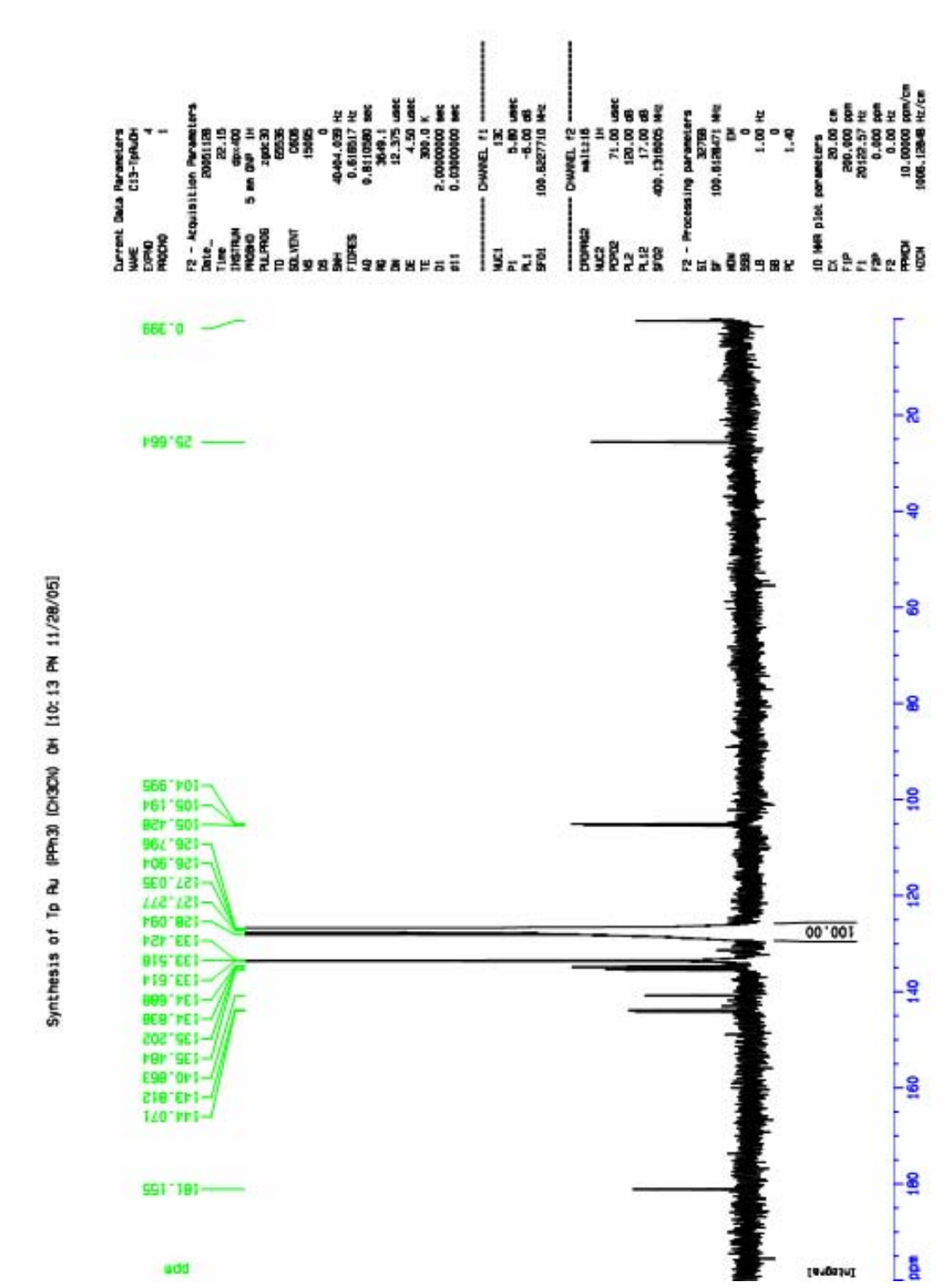

Figure 2.6 100.63 MHz $^{13}C\{^1H\}$ NMR spectrum of $TpRu(PPh_3)(H_2O)(NHC(O)CH_3)$ (2)

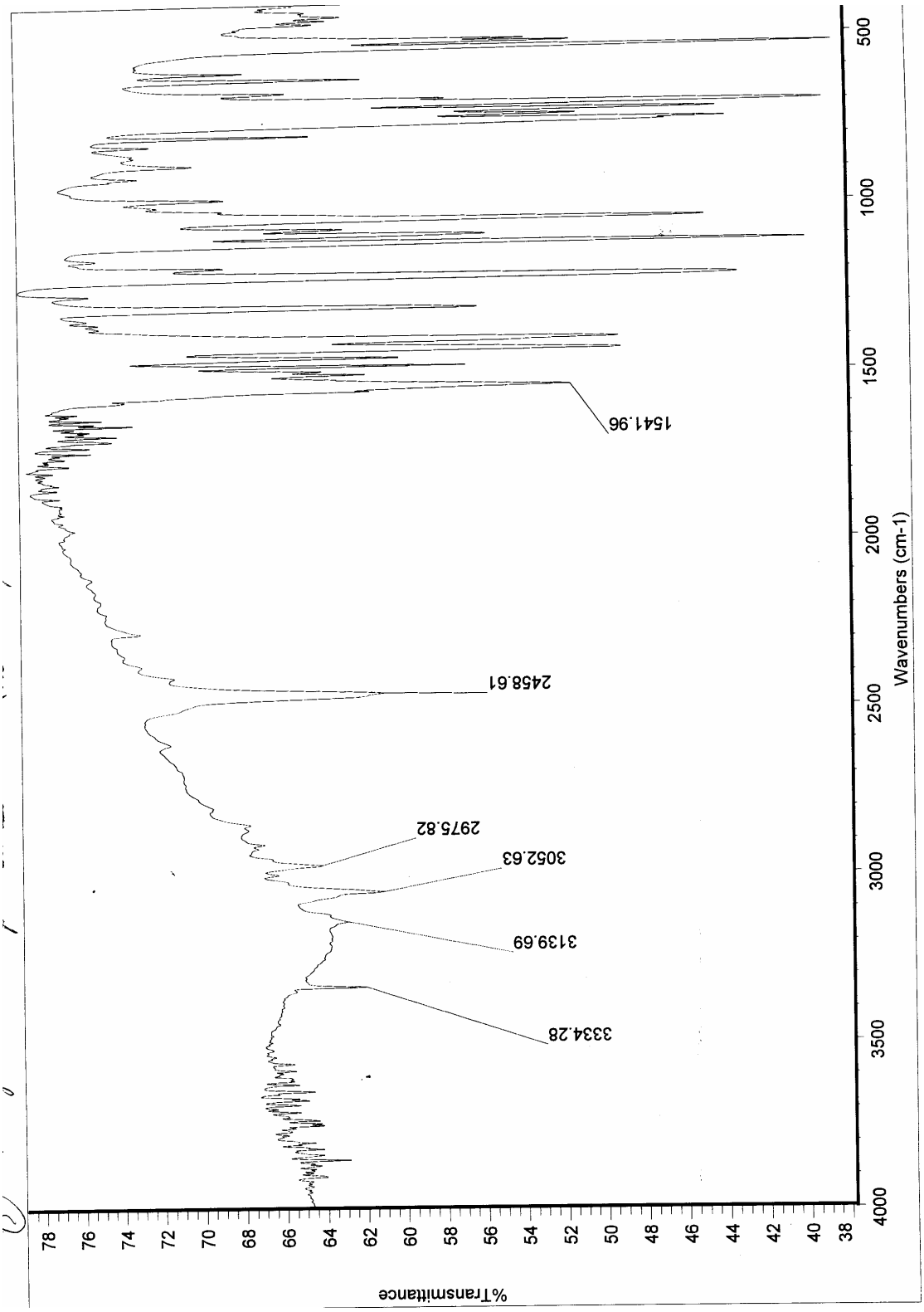

Figure 2.7 Infra-red spectrum of $TpRu(PPh_3)(H_2O)(NHC(O)CH_3)$ (2)

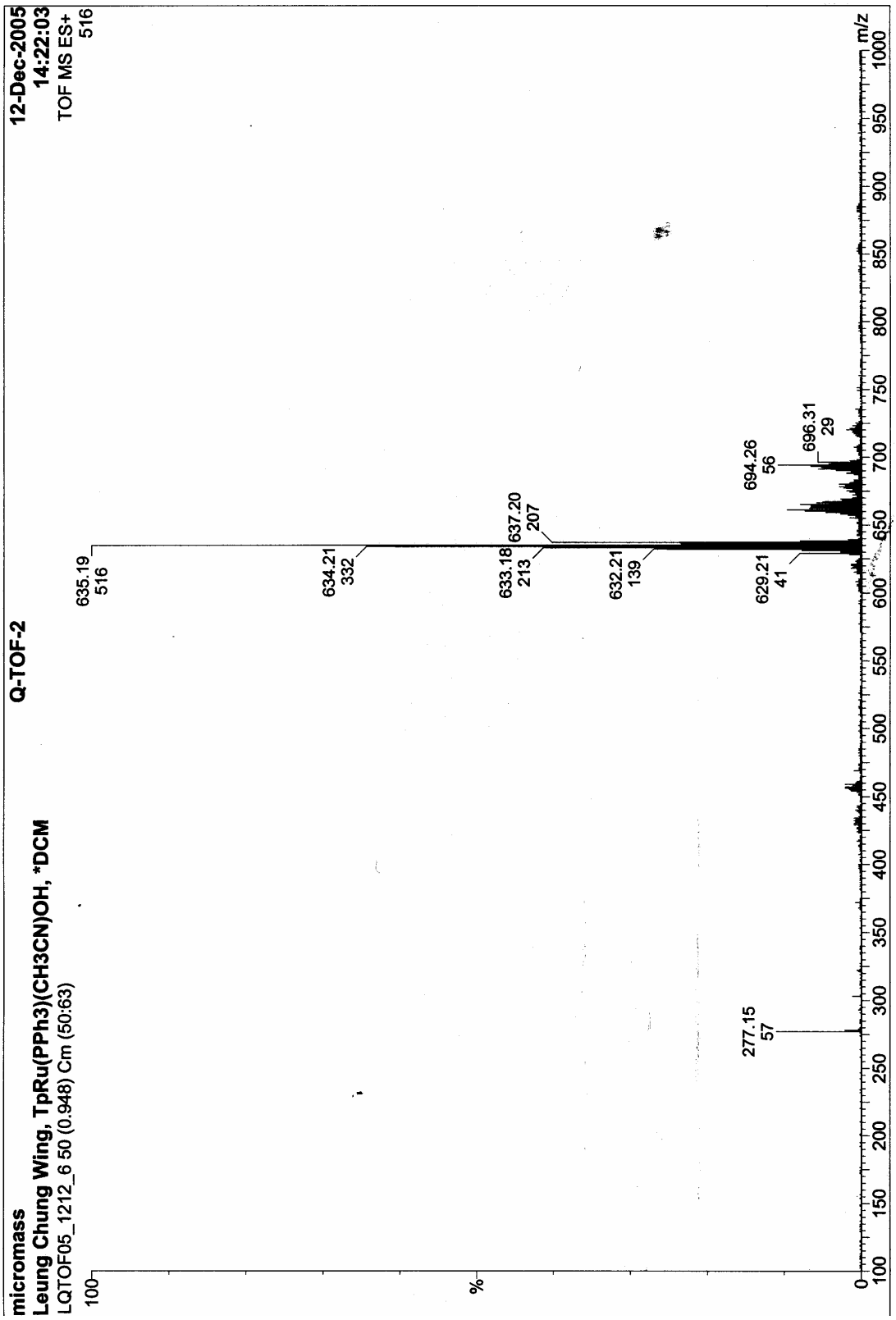

Figure 2.8 Mass spectrum of $TpRu(PPh_3)(H_2O)(NHC(O)CH_3)$ (2)

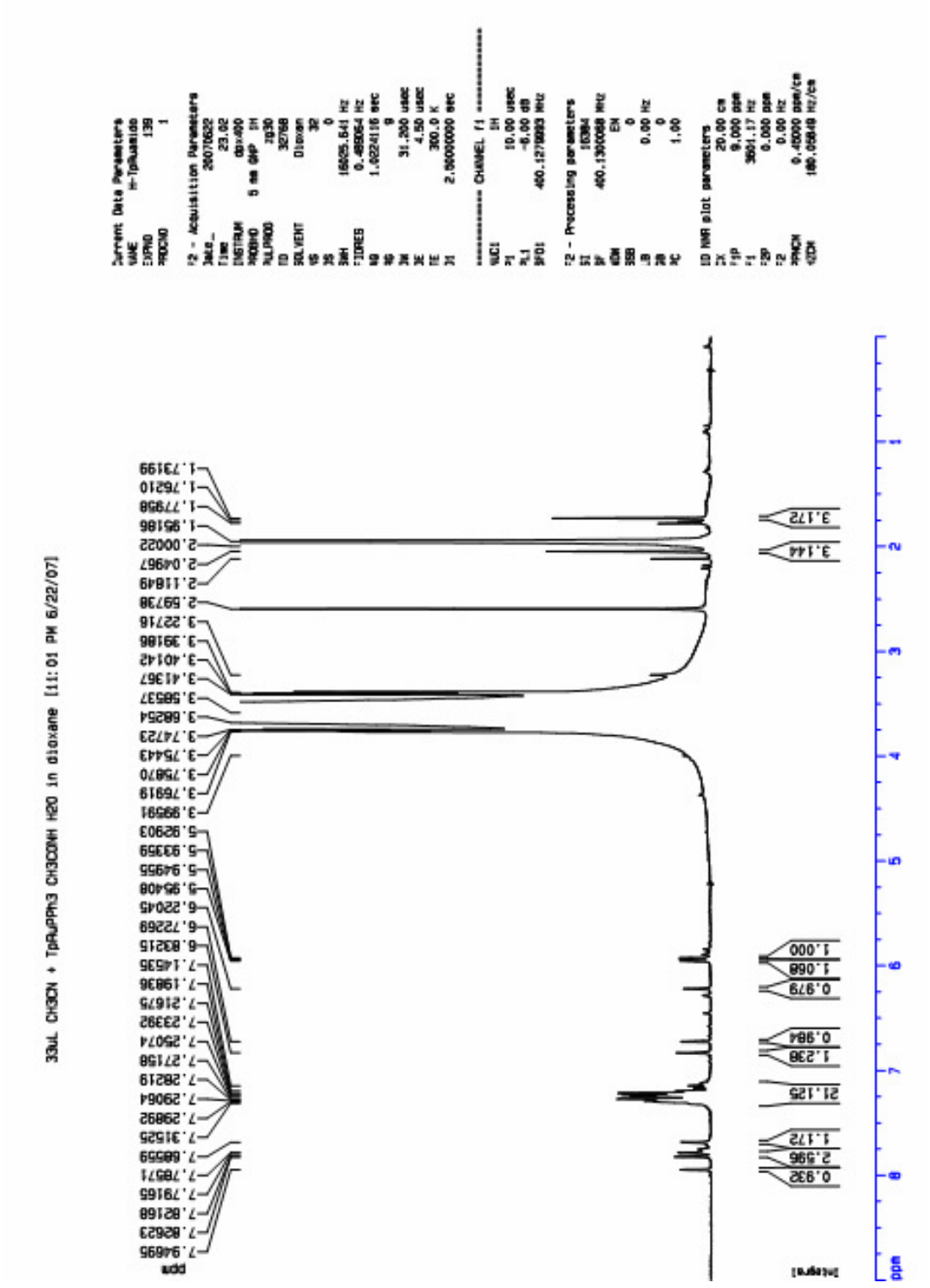

Figure 3.7 400.13 MHz ^{1}H NMR spectrum of TpRu(PPh$_3$)(NCCH$_3$)(NHC(O)CH$_3$) (6)

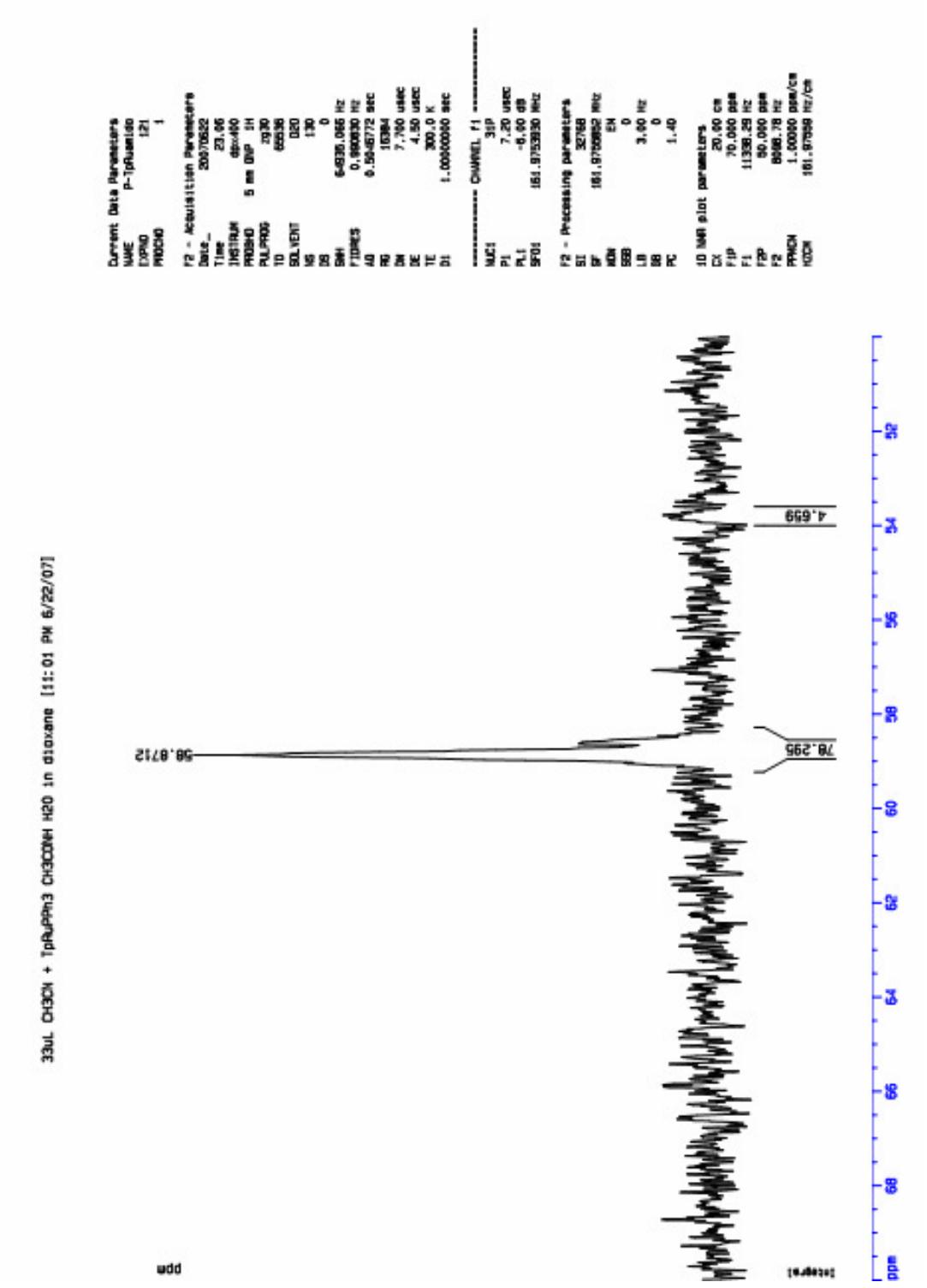

Figure 3.8 161.98 MHz $^{31}P\{^{1}H\}$ NMR spectrum of $TpRu(PPh_3)(NCCH_3)(NHC(O)CH_3)$ (6)

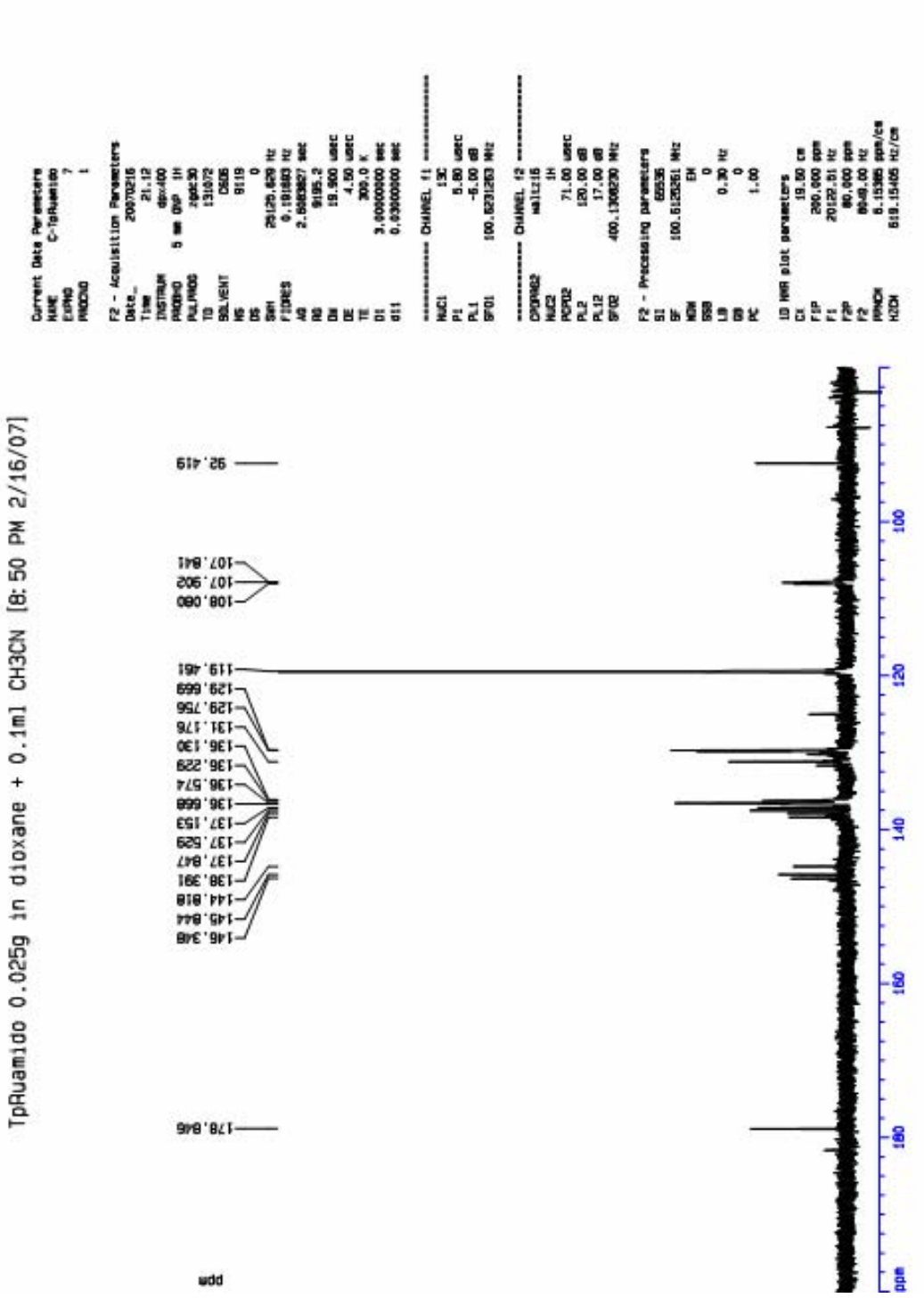

Figure 3.9 100.63 MHz $^{13}C\{^{1}H\}$ NMR spectrum of TpRu(PPh$_3$)(NCCH$_3$)(NHC(O)CH$_3$) (6)

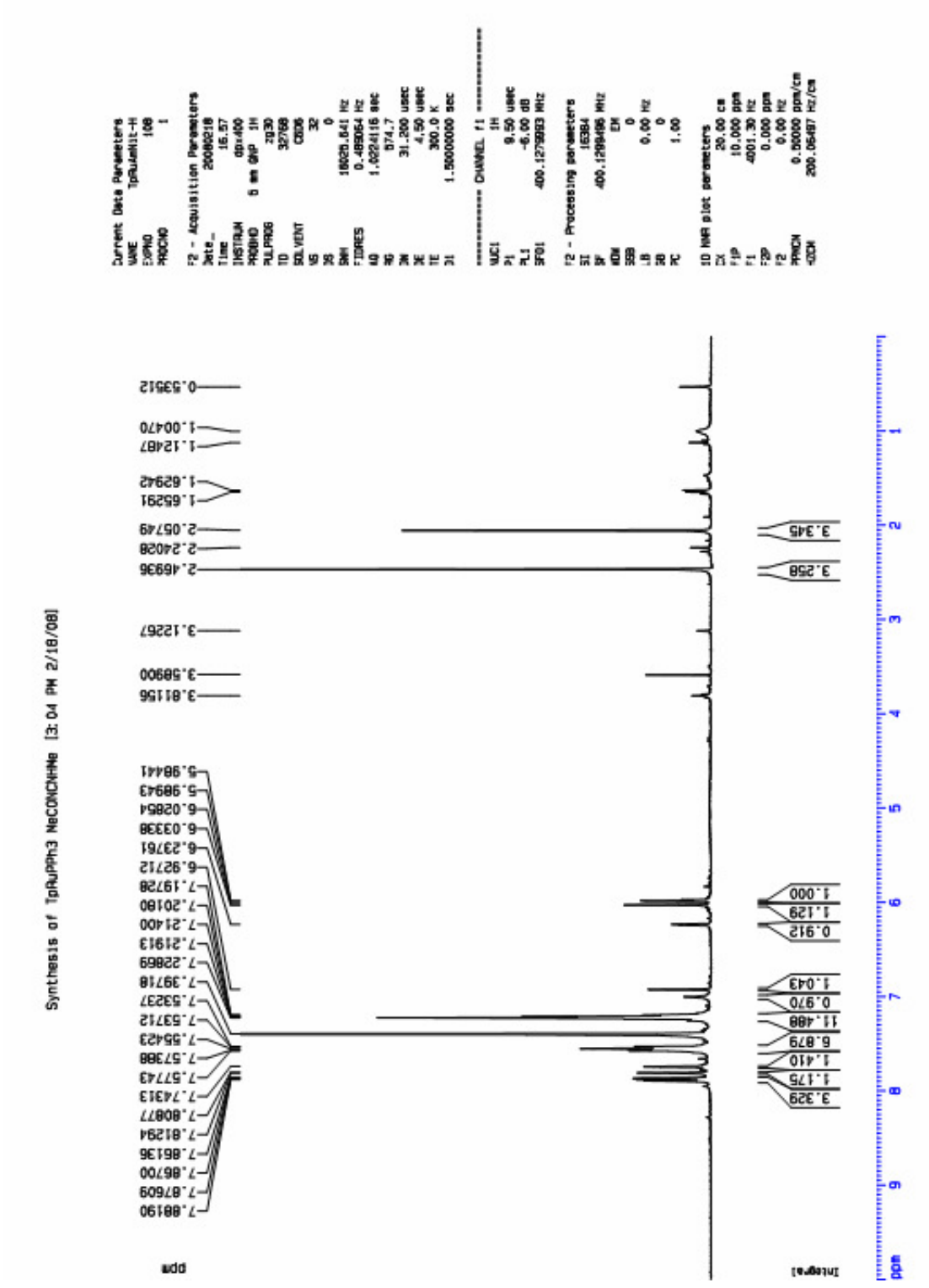

Figure 3.10 400.13 MHz ^{1}H NMR spectrum of TpRu(PPh$_3$)(κ^2-*N,O*-NH=CMeN=CMeO) (7)

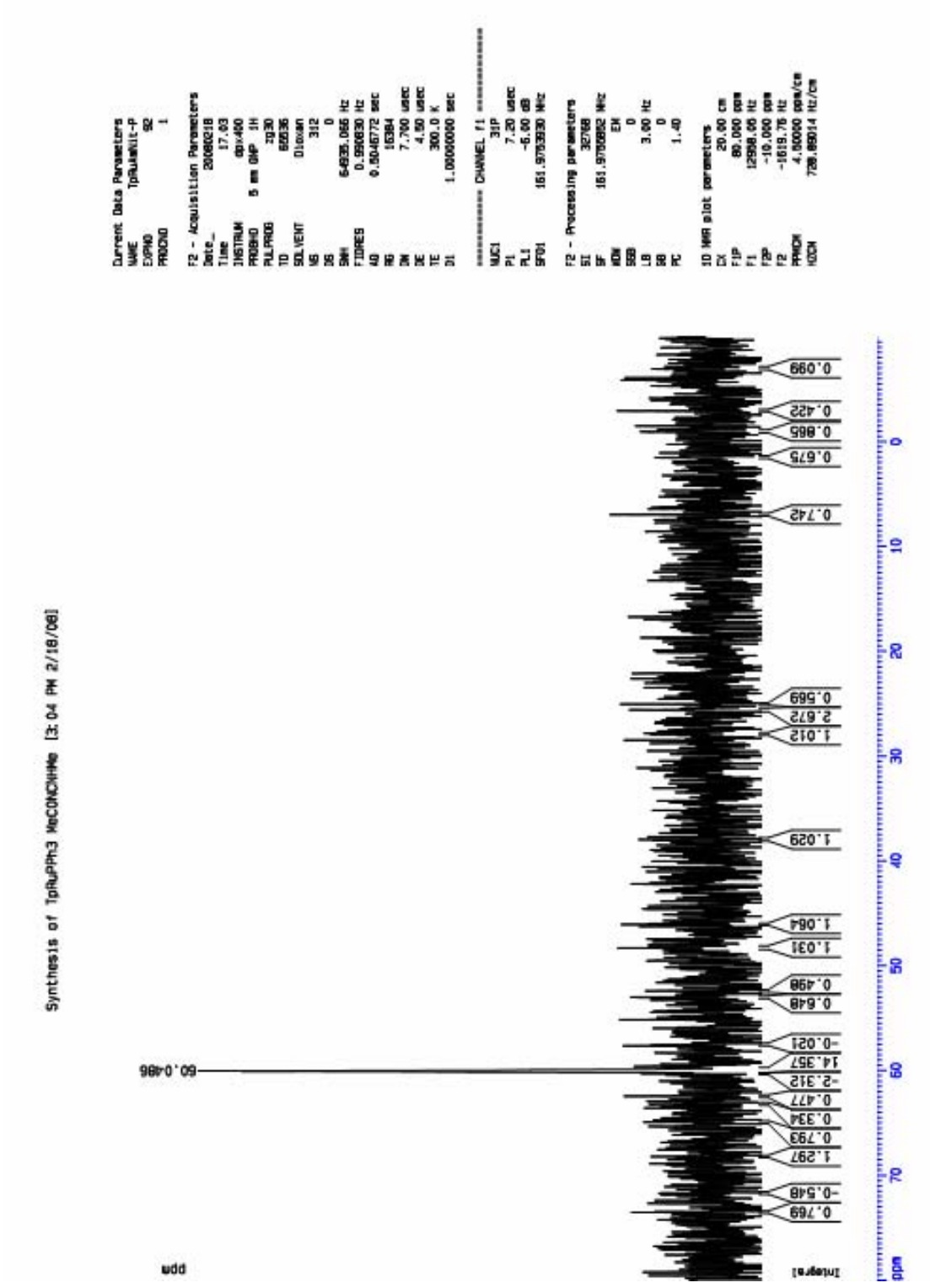

Figure 3.11 161.98 MHz $^{31}P\{^{1}H\}$ NMR spectrum of TpRu(PPh$_3$)(κ^2-*N,O*-NH=CMeN=CMeO) (7)

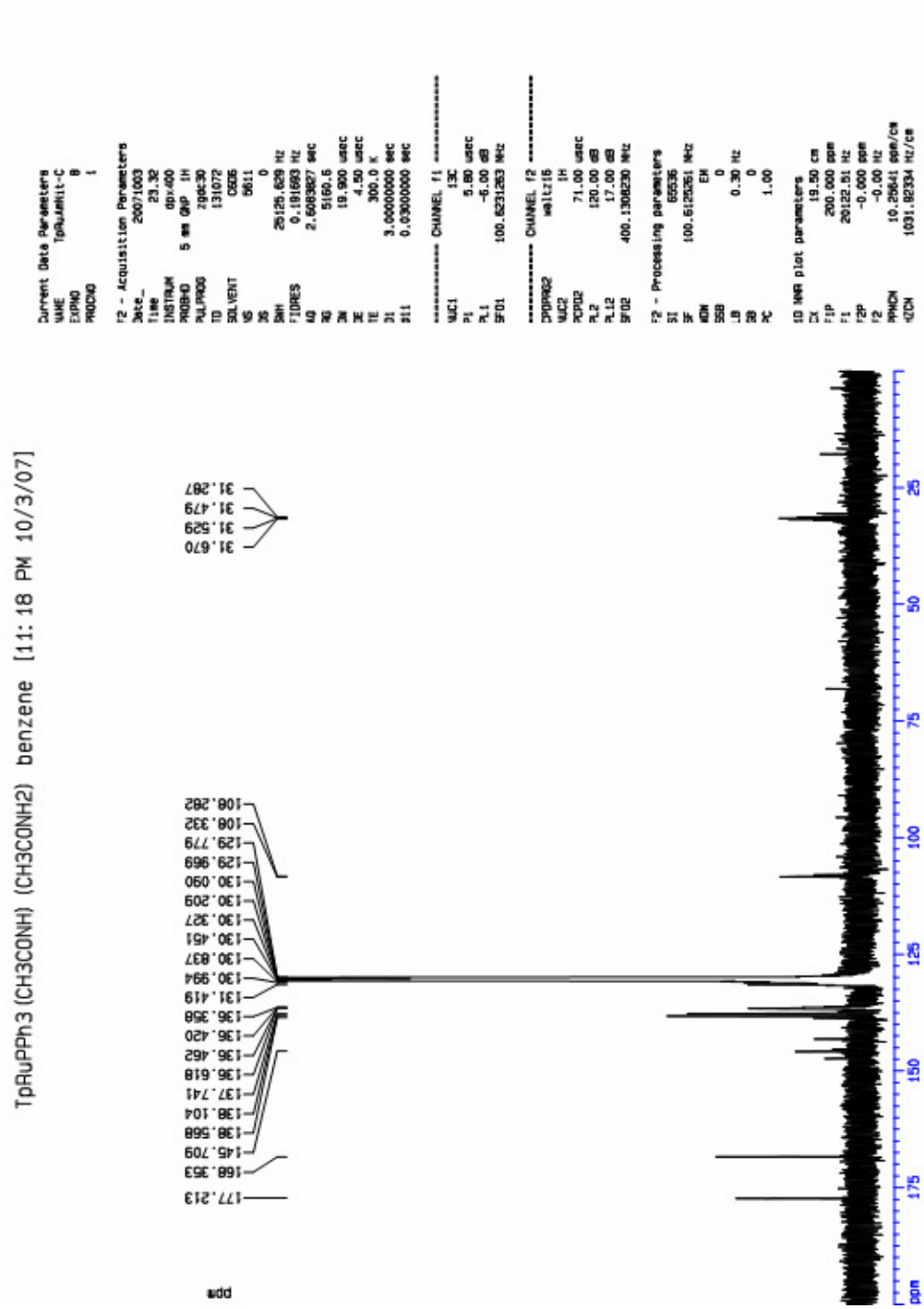

Figure 3.12 100.63 MHz $^{13}C\{^1H\}$ NMR spectrum of TpRu(PPh$_3$)(κ^2-*N,O*-NH=CMeN=CMeO) (7)

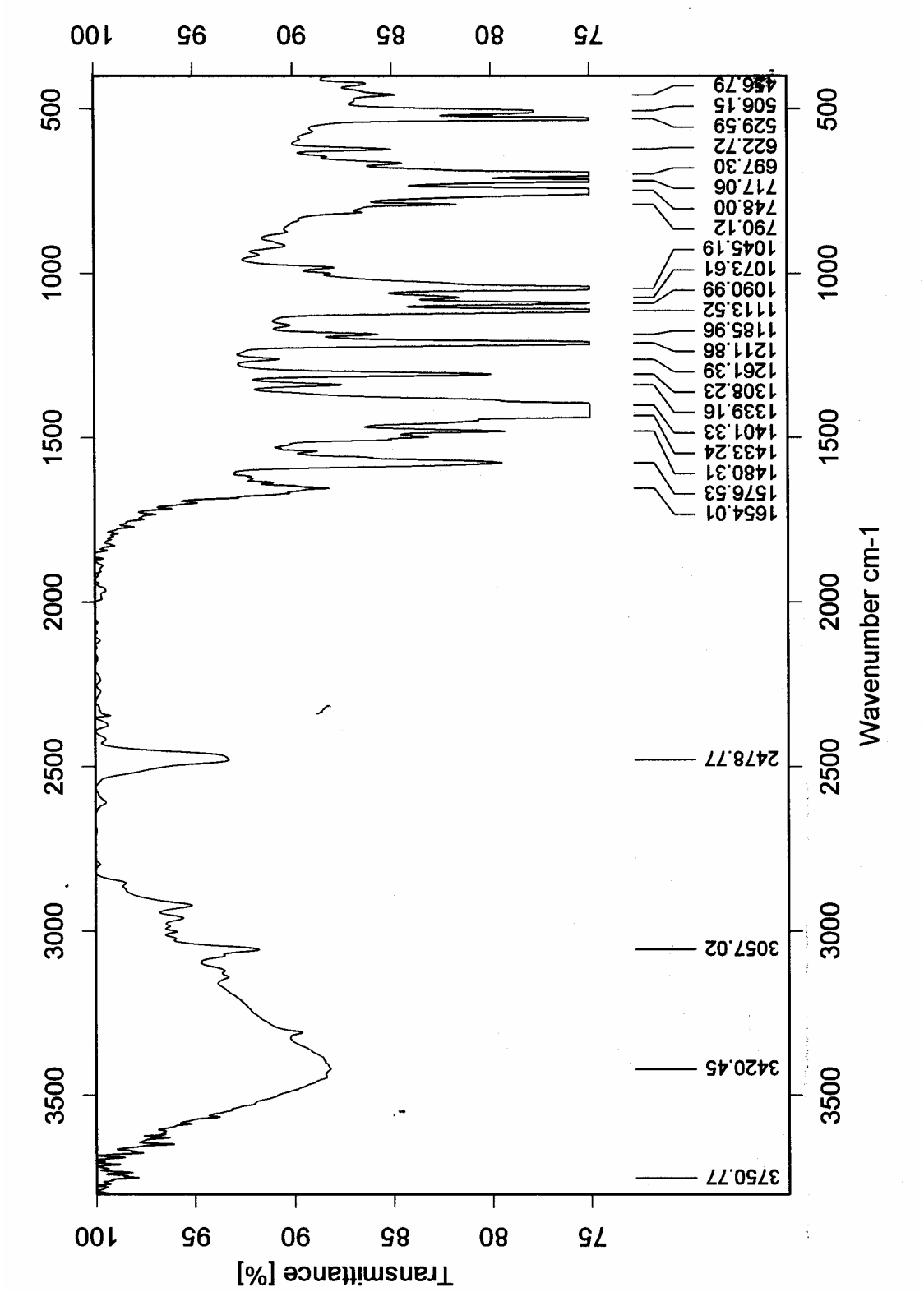

Figure 3.13 Infra-red spectrum of TpRu(PPh$_3$)(κ^2-*N,O*-NH=CMeN=CMeO) (7)

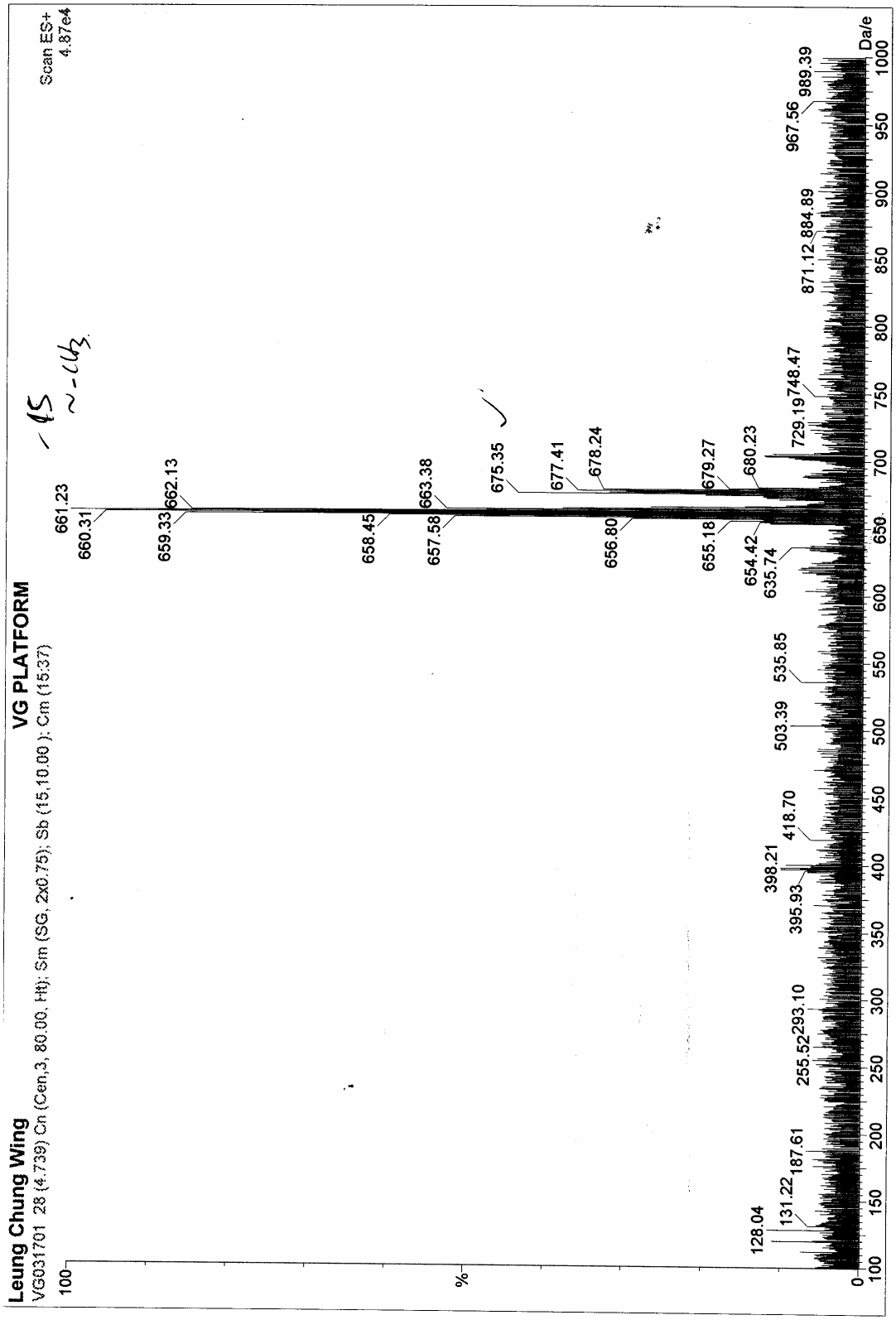

Figure 3.14 Mass spectrum of TpRu(PPh$_3$)(κ^2-*N,O*-NH=CMeN=CMeO) (7)

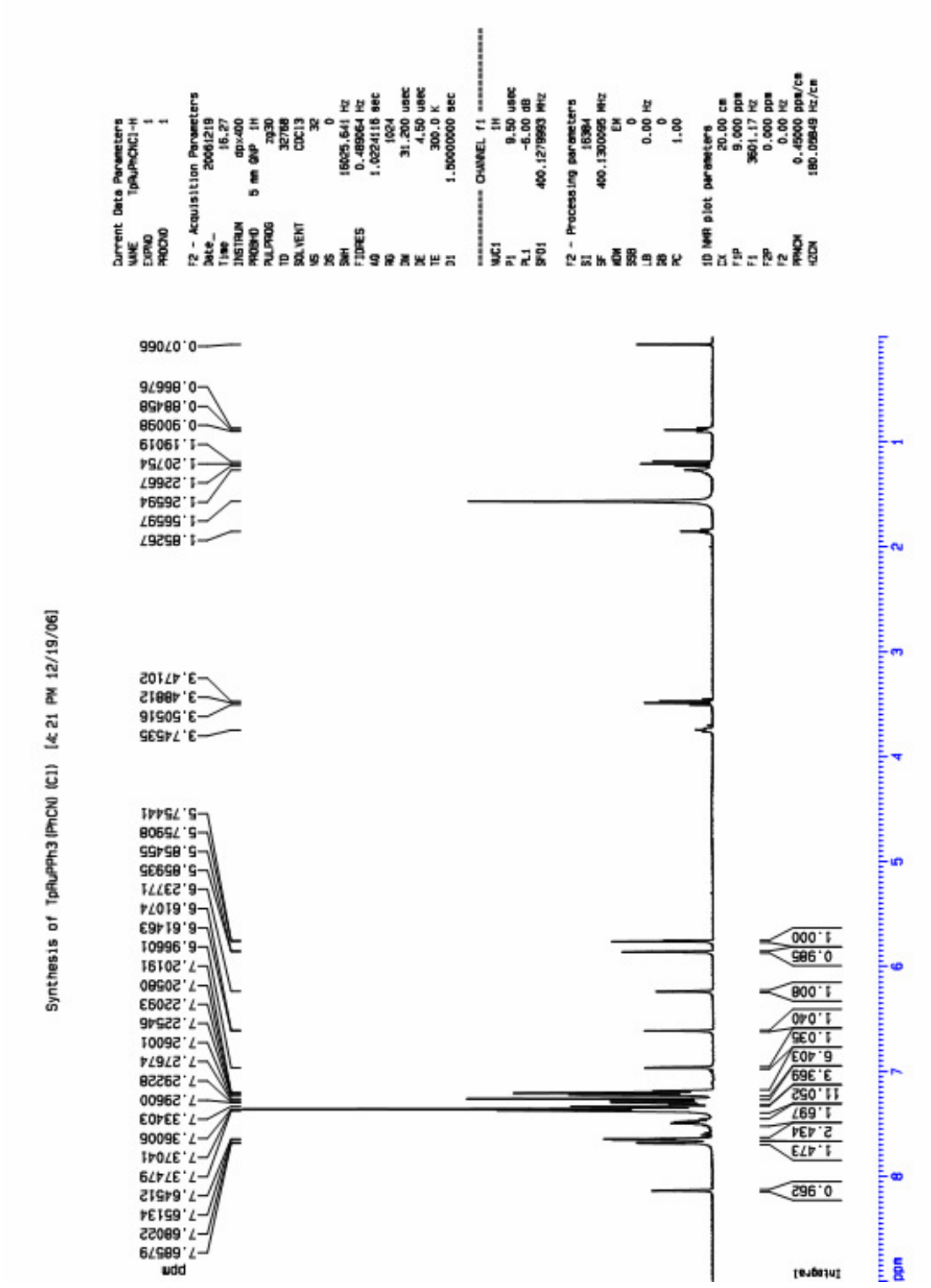

Figure 3.15 400.13 MHz ^{1}H NMR spectrum of TpRu(PPh$_3$)(PhCN)(Cl)

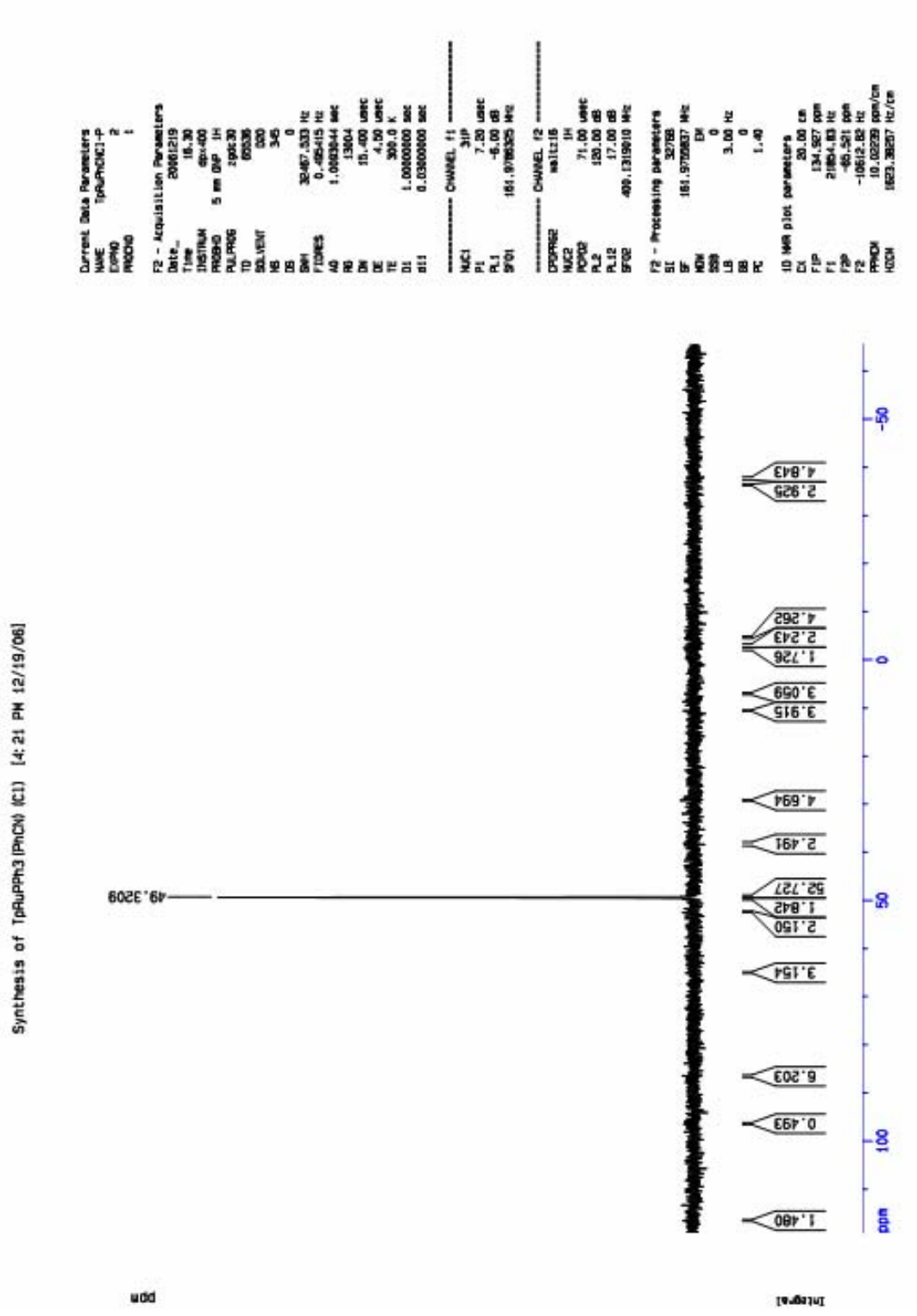

Figure 3.16 161.98 MHz $^{31}P\{^{1}H\}$ NMR spectrum of TpRu(PPh_3)(PhCN)(Cl)

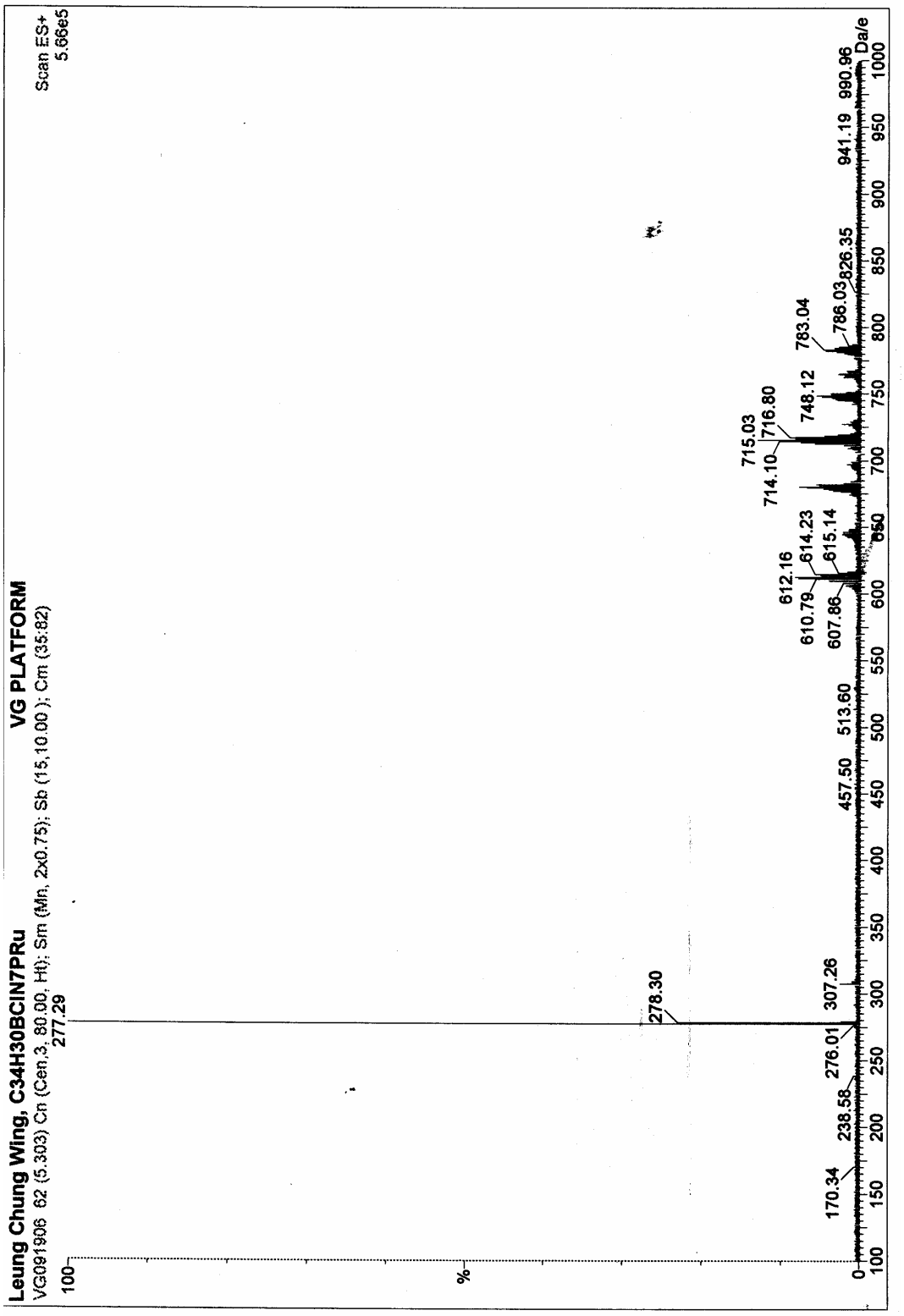

Figure 3.17 Mass spectrum of TpRu(PPh_3)(PhCN)(Cl)

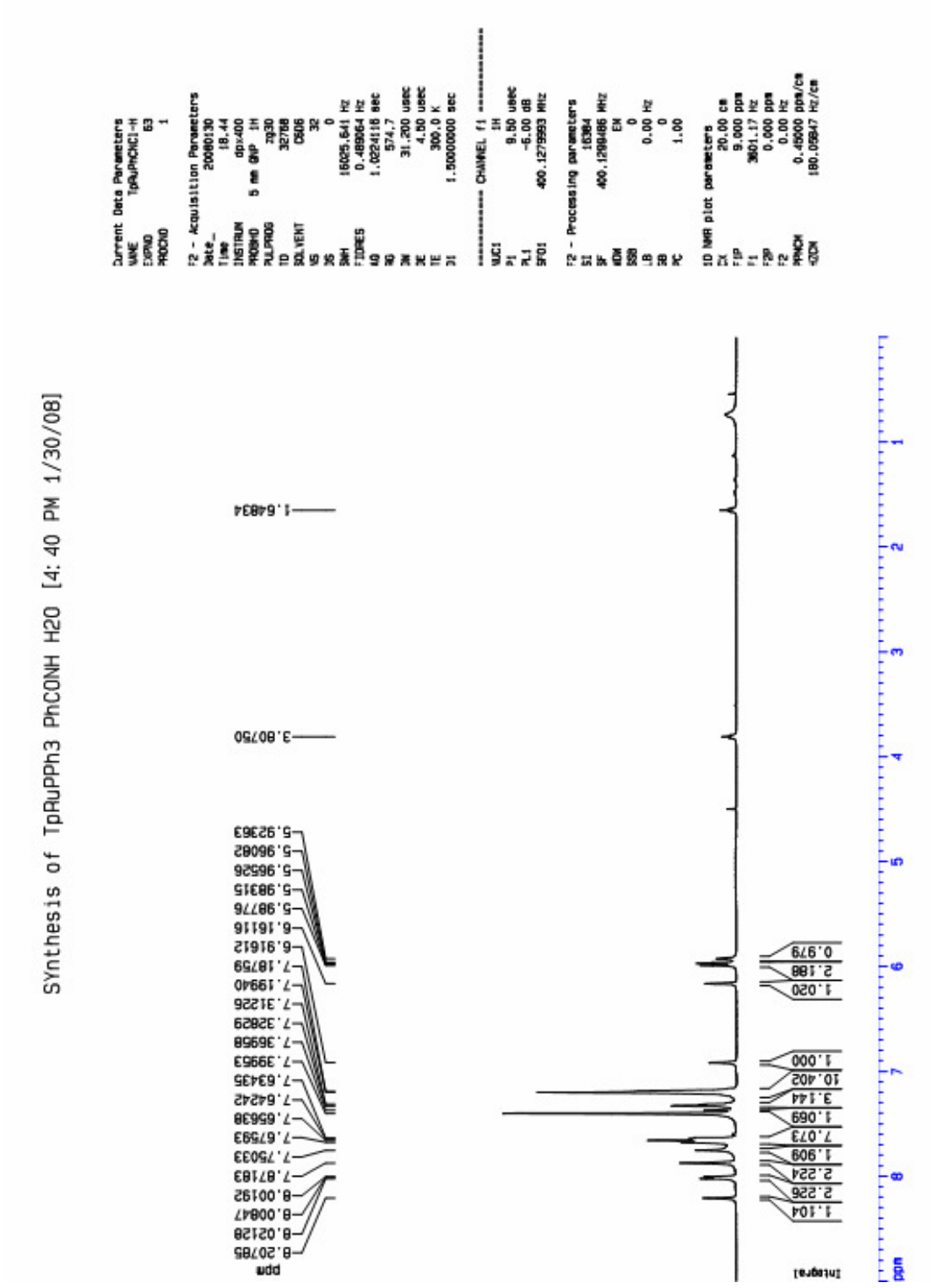

Figure 3.18 400.13 MHz ^{1}H NMR spectrum of TpRu(PPh$_3$)(H$_2$O)(NHC(O)Ph) (8)

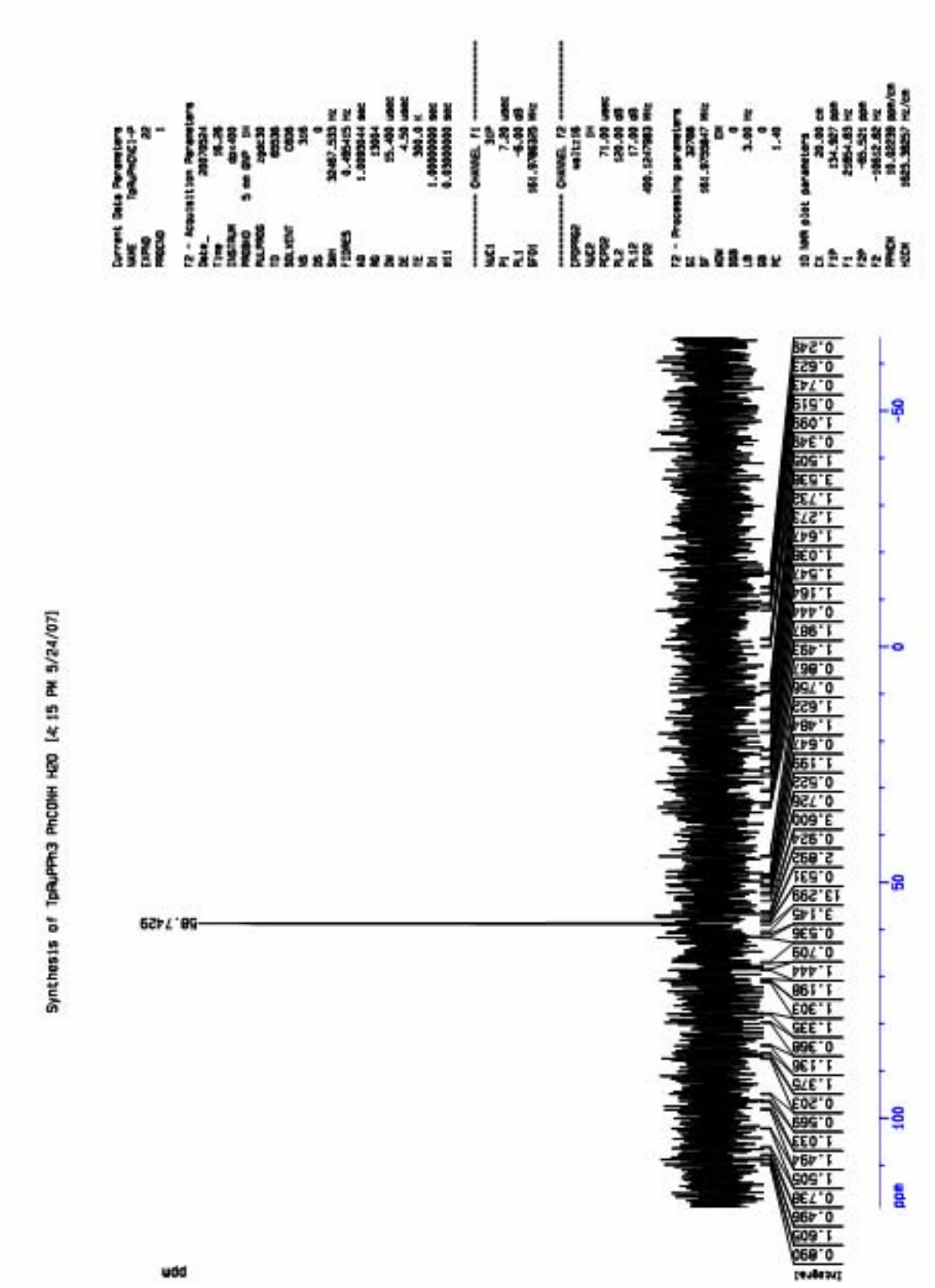

Figure 3.19 161.98 MHz $^{31}P\{^{1}H\}$ NMR spectrum of $TpRu(PPh_3)(H_2O)(NHC(O)Ph)$ (8)

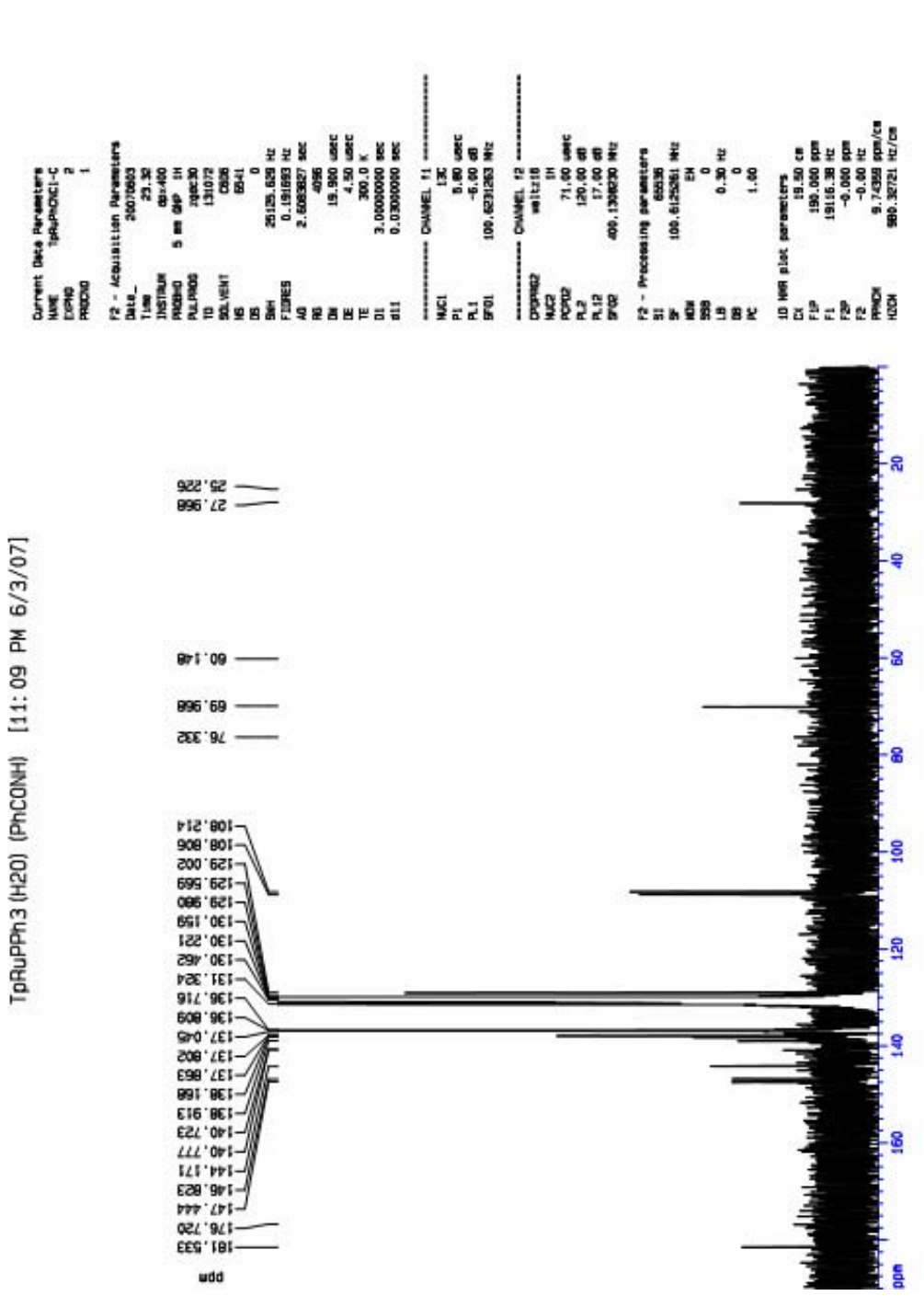

Figure 3.20 100.63 MHz $^{13}C\{^{1}H\}$ NMR spectrum of $TpRu(PPh_3)(H_2O)(NHC(O)Ph)$ (8)

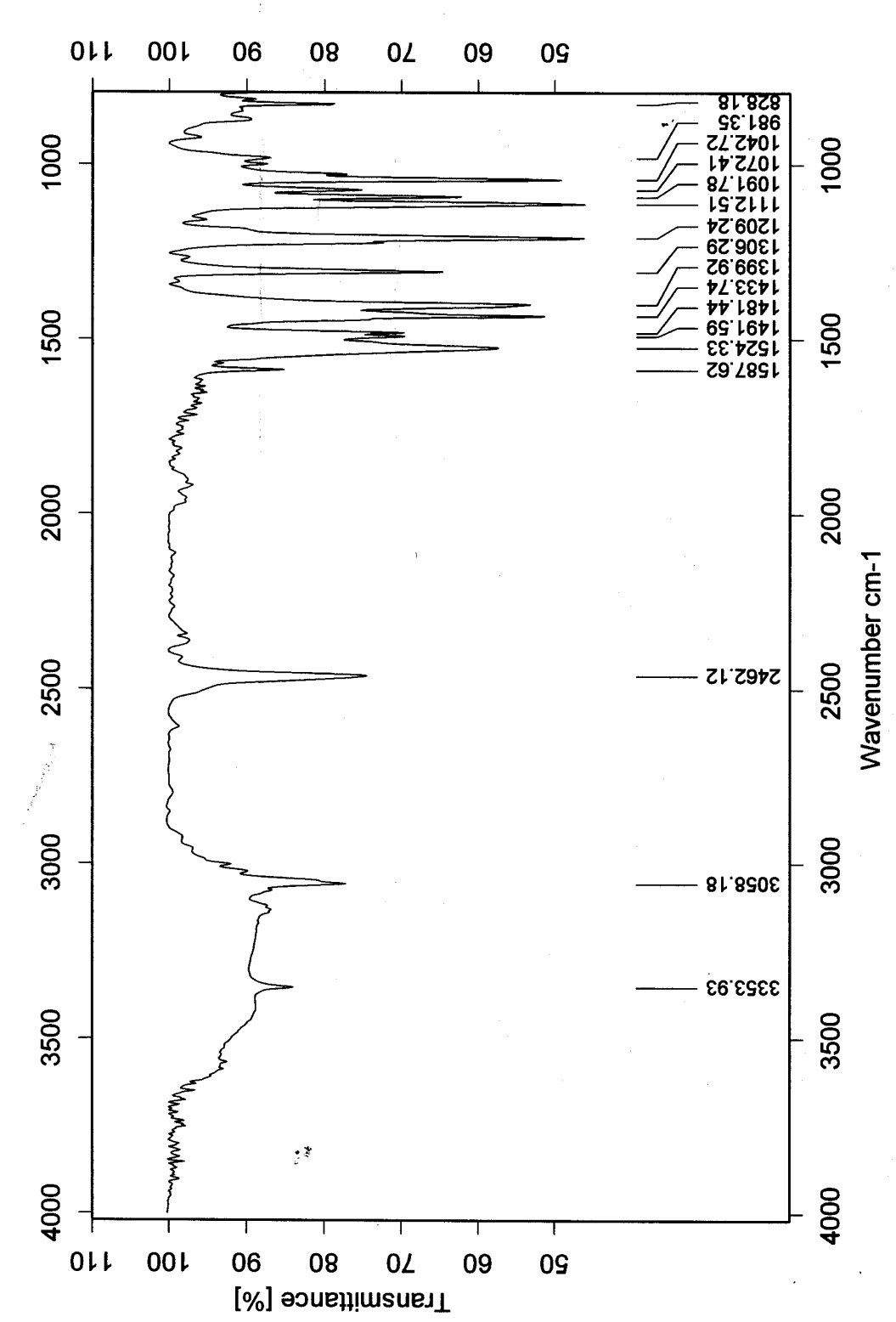

Figure 3.21 Infra-red spectrum of $TpRu(PPh_3)(H_2O)(NHC(O)Ph)$ (8)

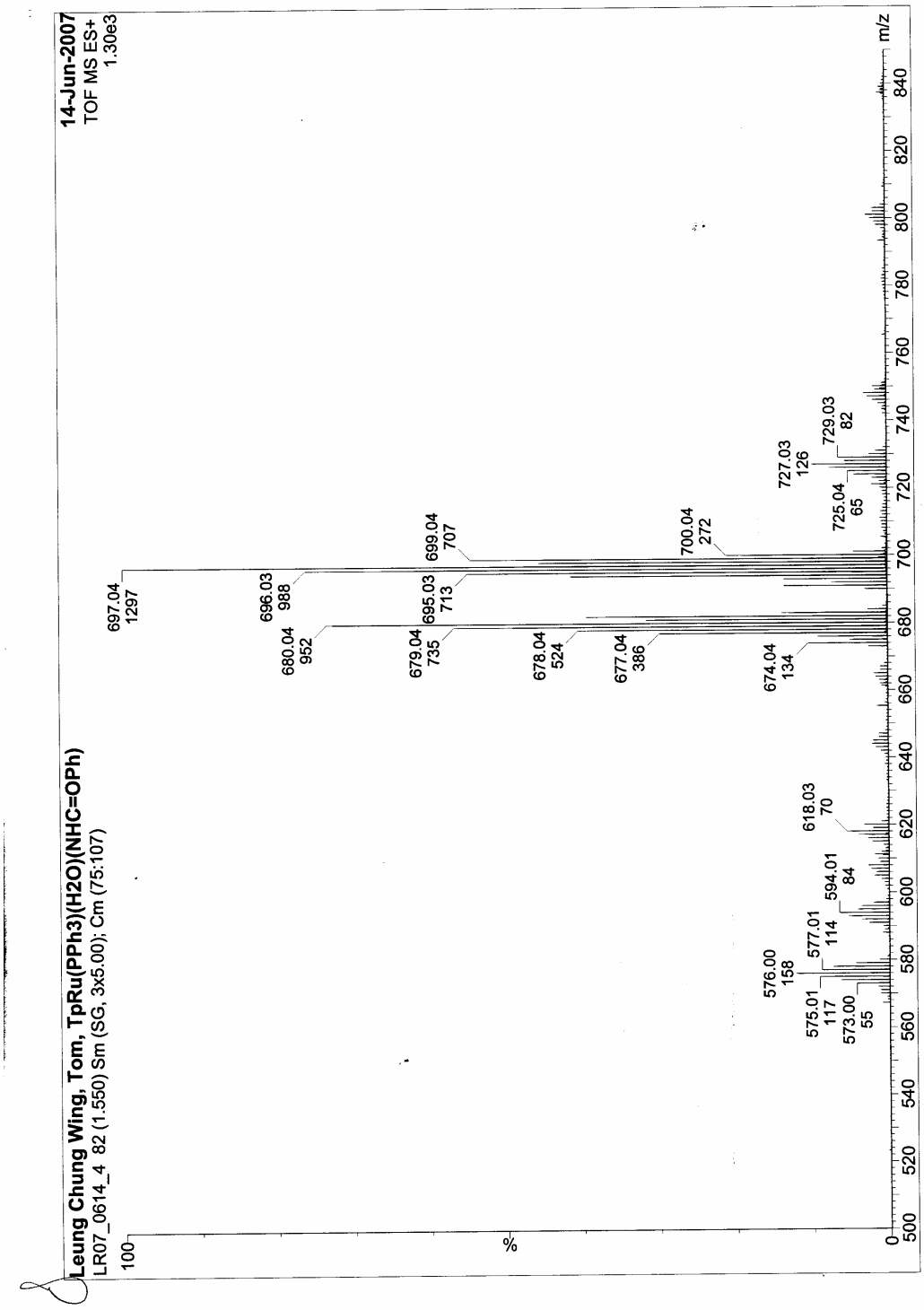

Figure 3.22 Mass spectrum of TpRu(PPh$_3$)(H$_2$O)(NHC(O)Ph) (8)

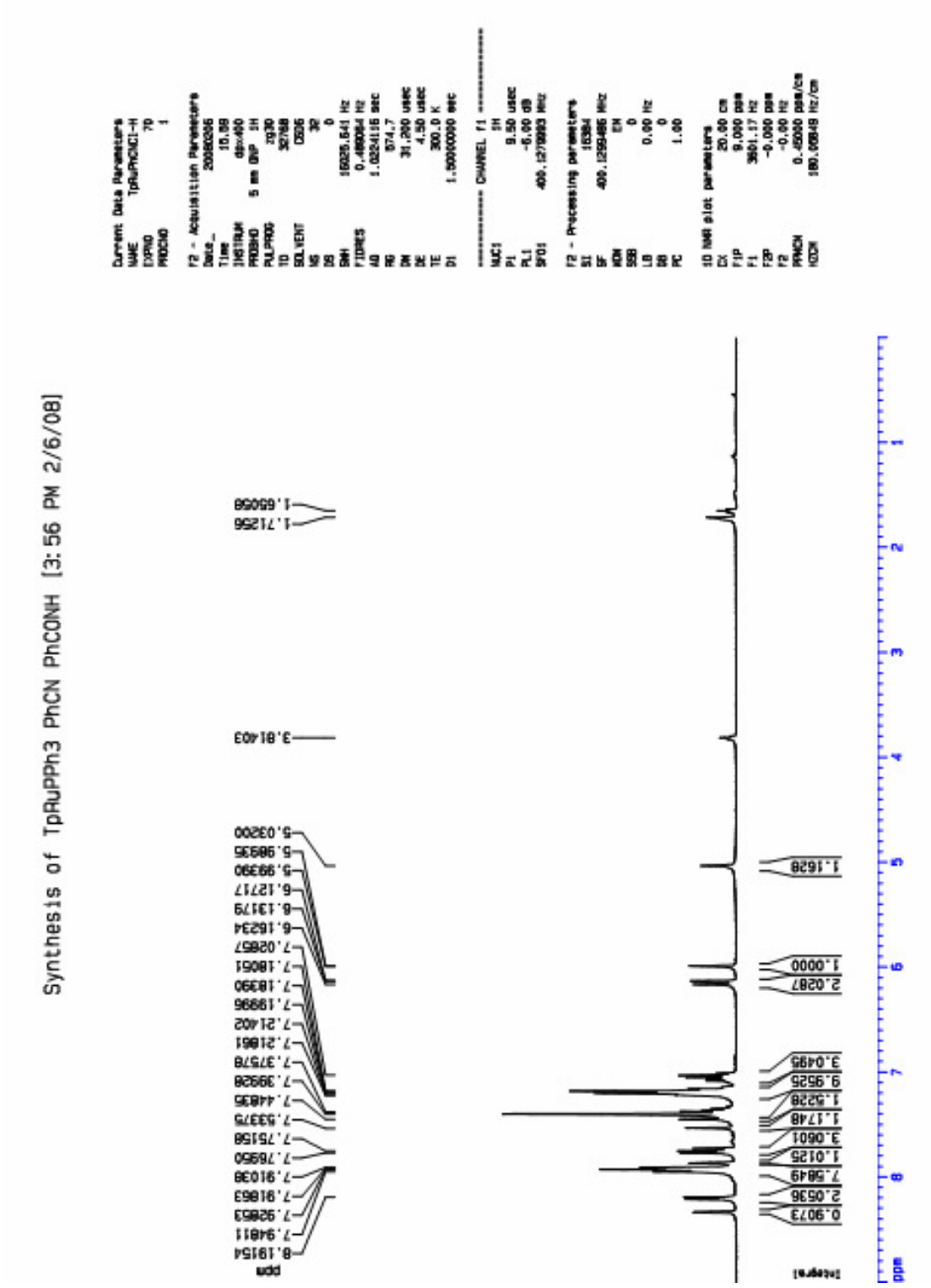

Figure 3.23 400.13 MHz ^{1}H NMR spectrum of TpRu(PPh$_3$)(NCPh)(NHC(O)Ph) (9)

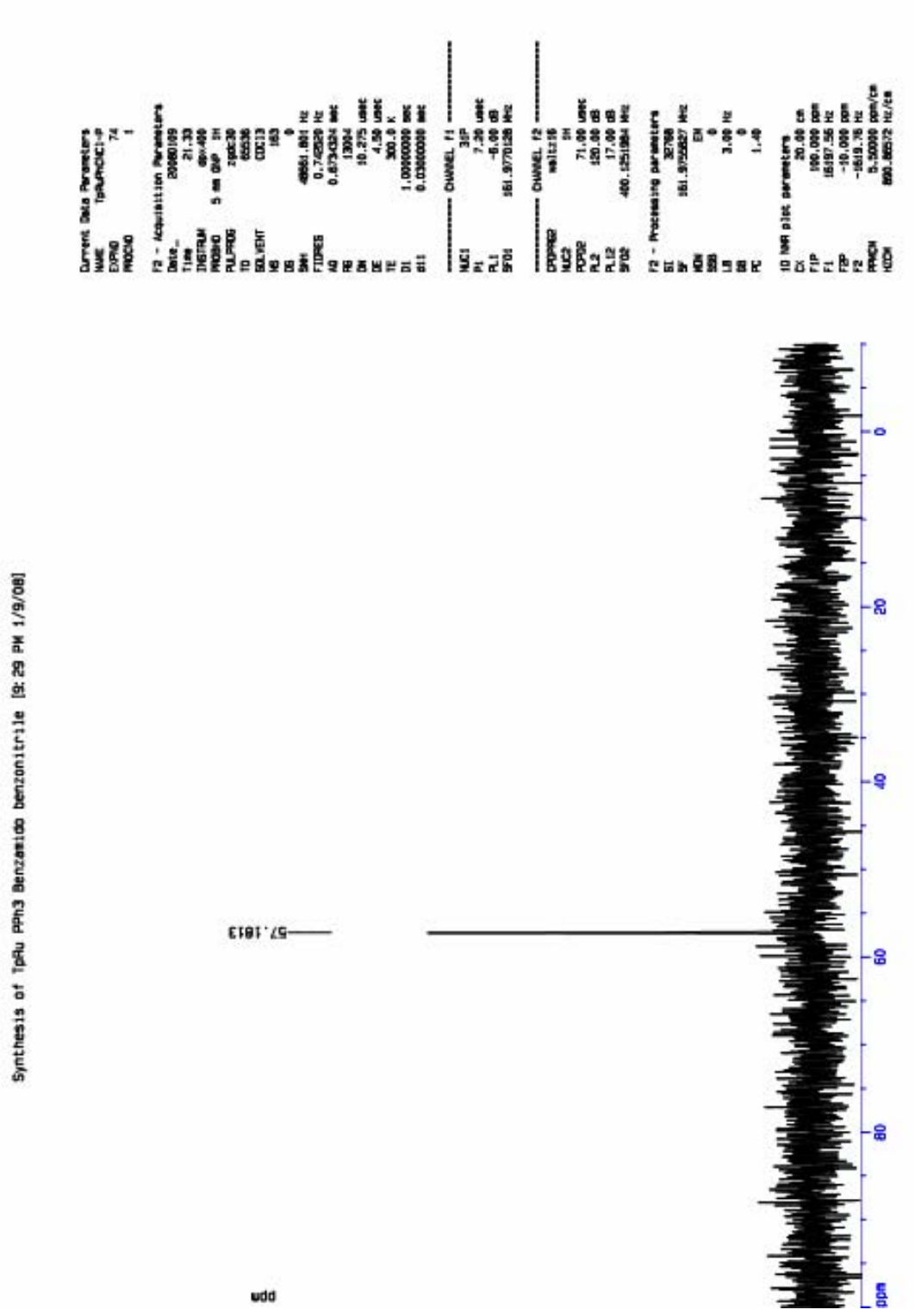

Figure 3.24 161.98 MHz $^{31}P\{^{1}H\}$ NMR spectrum of TpRu(PPh$_3$)(NCPh)(NHC(O)Ph) (9)

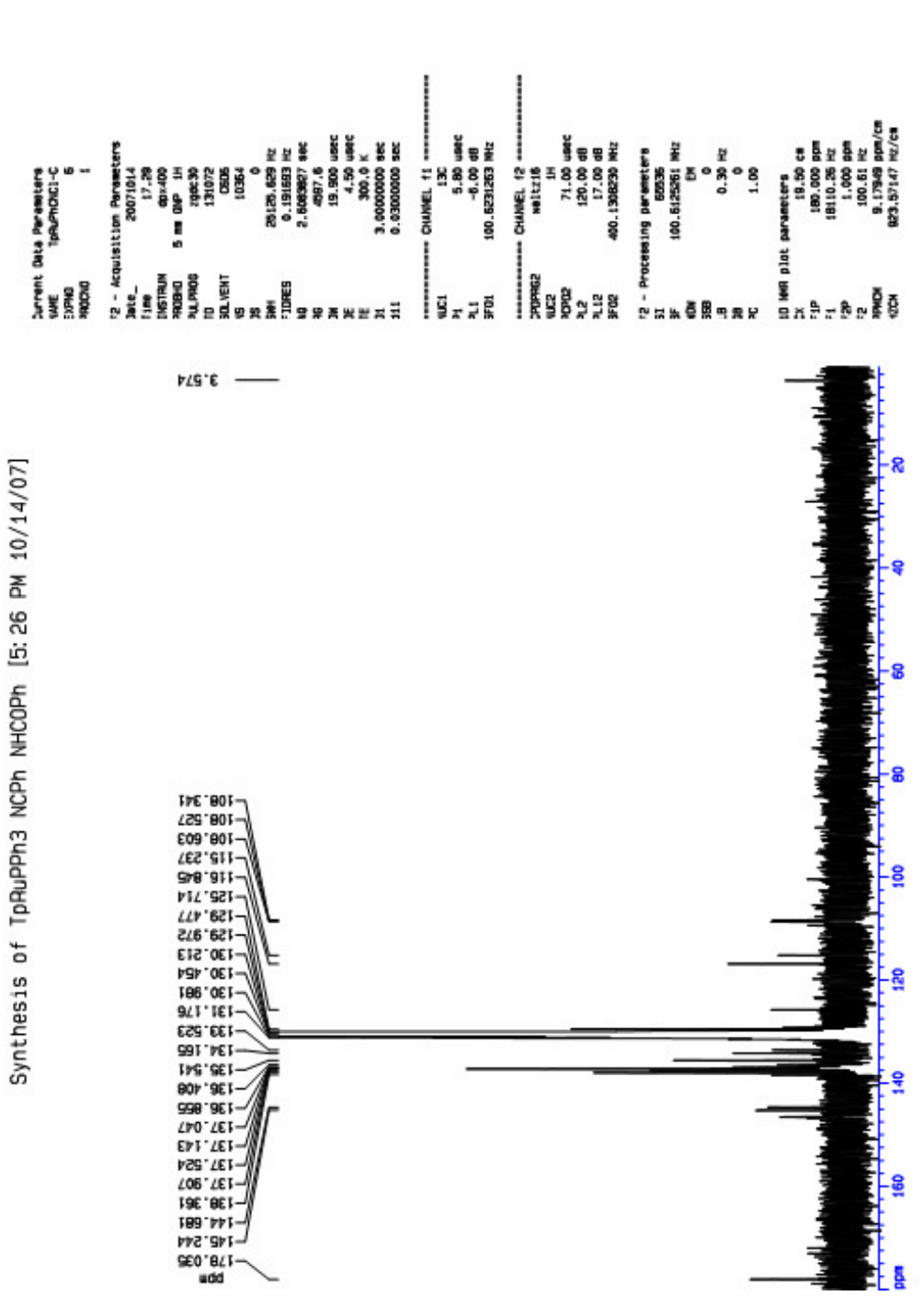

Figure 3.25 100.63 MHz $^{13}C\{^{1}H\}$ NMR spectrum of TpRu(PPh_3)(NCPh)(NHC(O)Ph) (9)

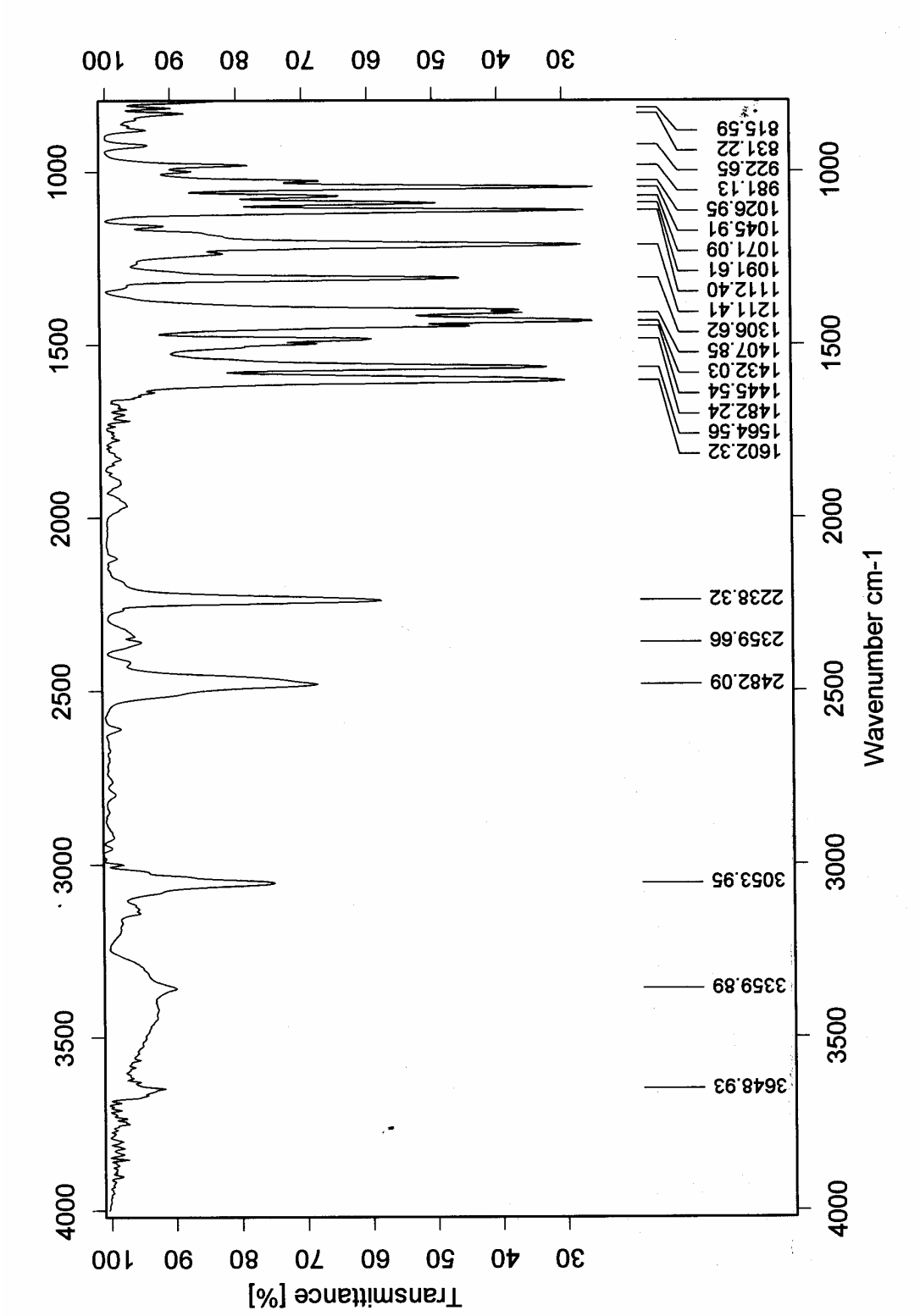

Figure 3.26 Infra-red spectrum of $TpRu(PPh_3)(NCPh)(NHC(O)Ph)$ (9)

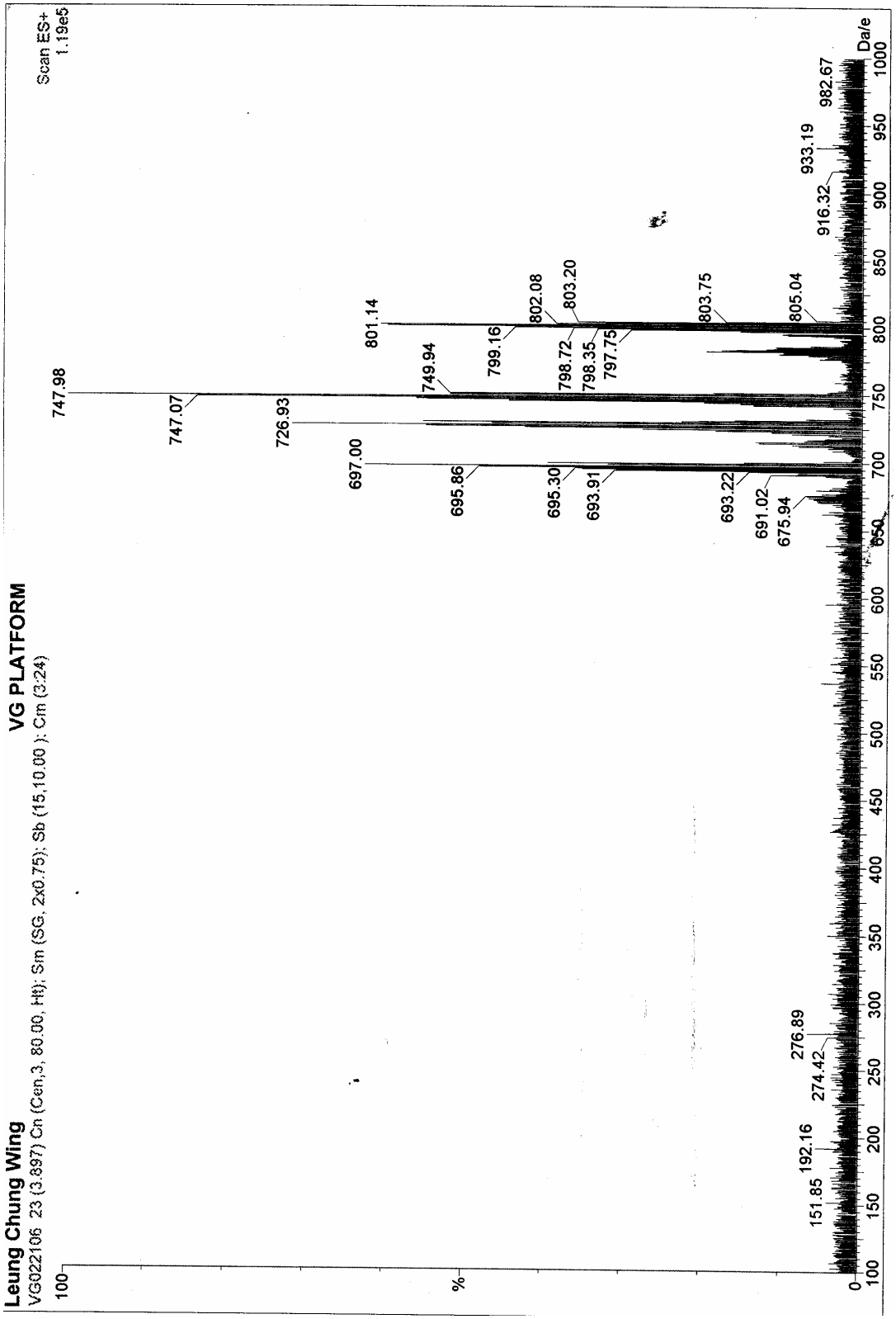

Figure 3.27 Mass spectrum of $TpRu(PPh_3)(NCPh)(NHC(O)Ph)$ (9)

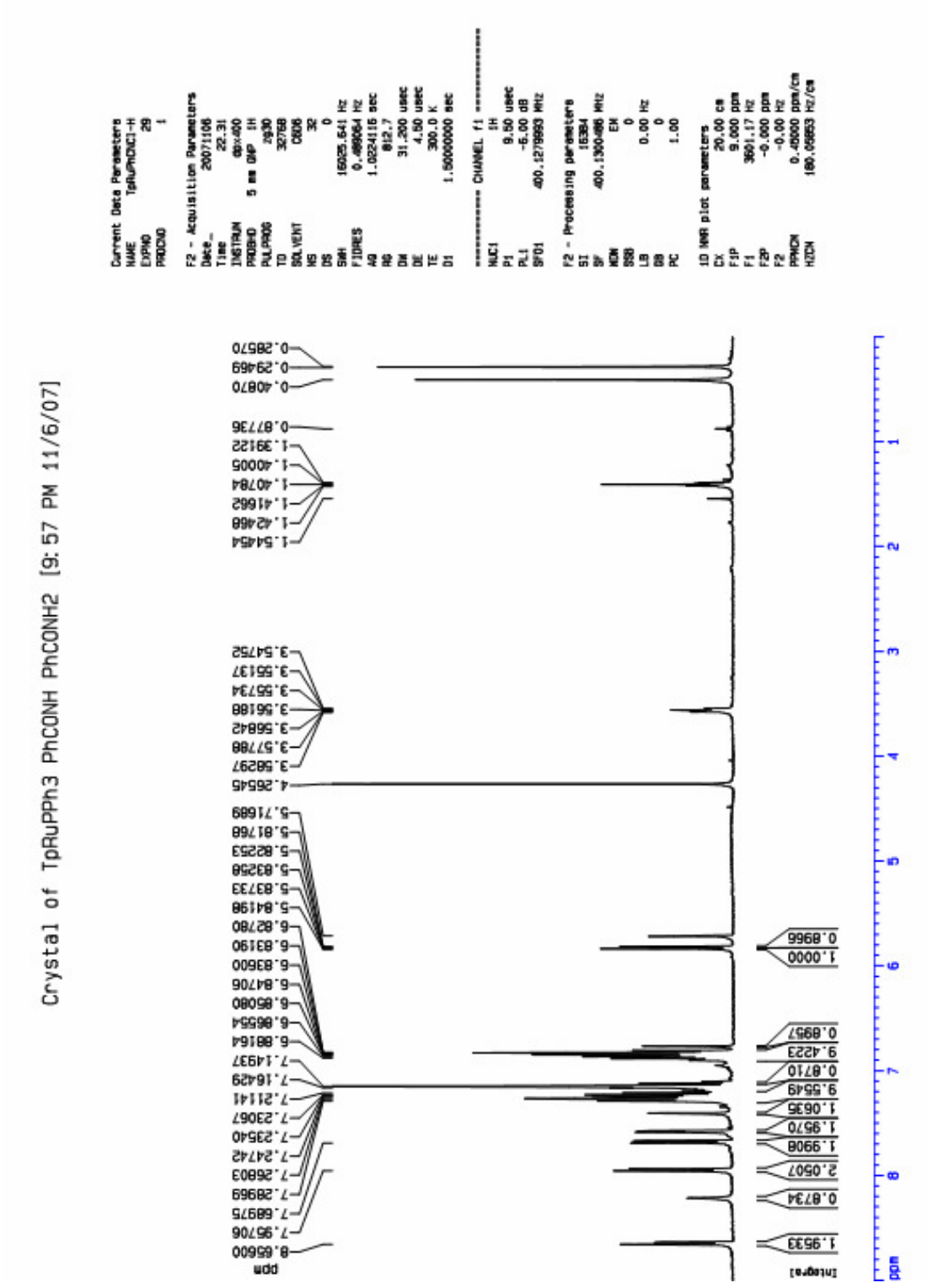

Figure 3.28 400.13 MHz ^{1}H NMR spectrum of TpRu(PPh$_3$)(κ^2-*N,O*-NH=CPhN=CPhO) (10)

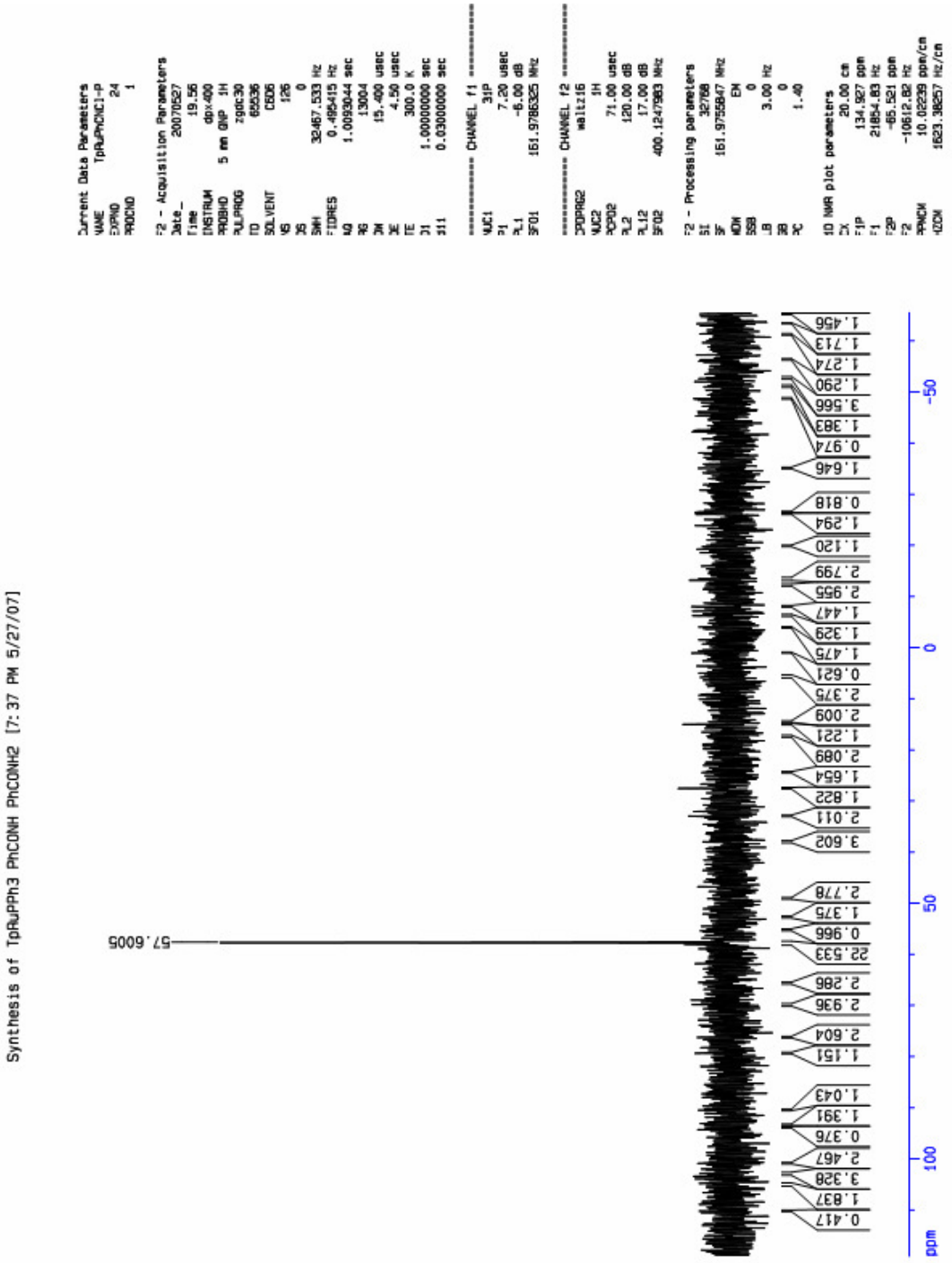

Figure 3.29 161.98 MHz $^{31}P\{^{1}H\}$ NMR spectrum of TpRu(PPh$_3$)(κ^2-*N,O*-NH=CPhN=CPhO) (10)

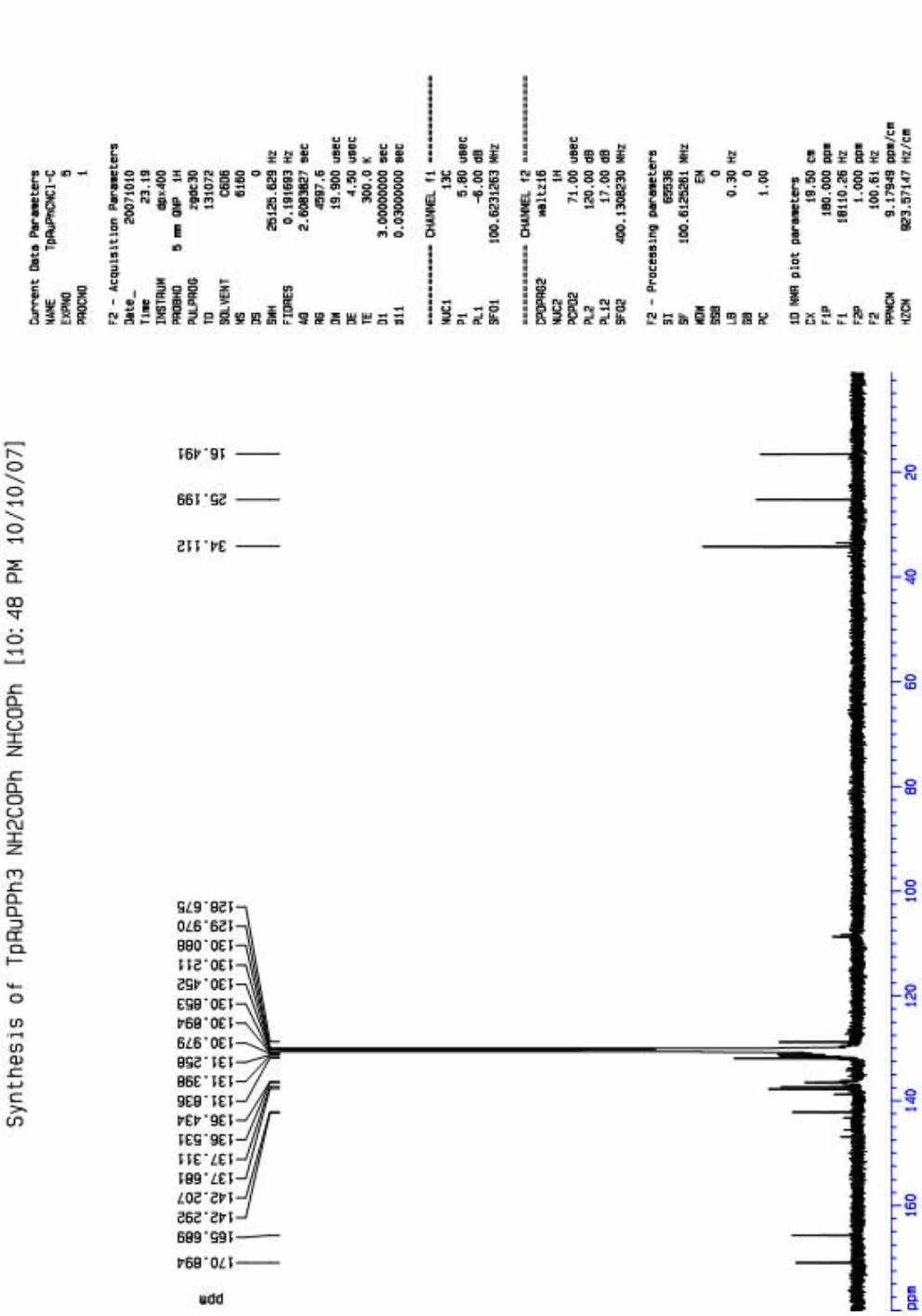

Figure 3.30 100.63 MHz $^{13}C\{^1H\}$ NMR spectrum of TpRu(PPh$_3$)(κ^2-*N,O*-NH=CPhN=CPhO) (10)

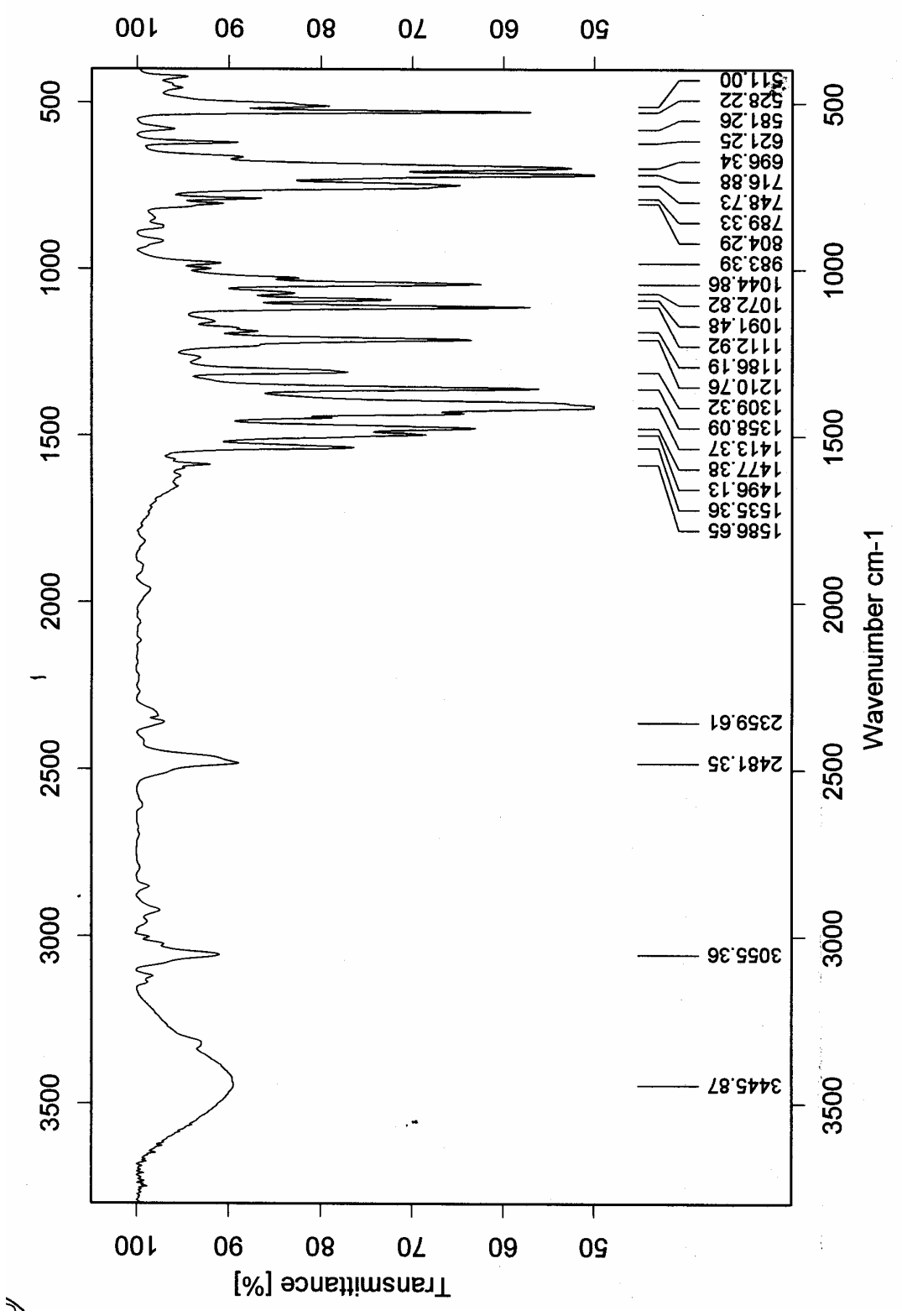

Figure 3.31 Infra-red spectrum of TpRu(PPh$_3$)(κ^2-*N,O*-NH=CPhN=CPhO) (10)

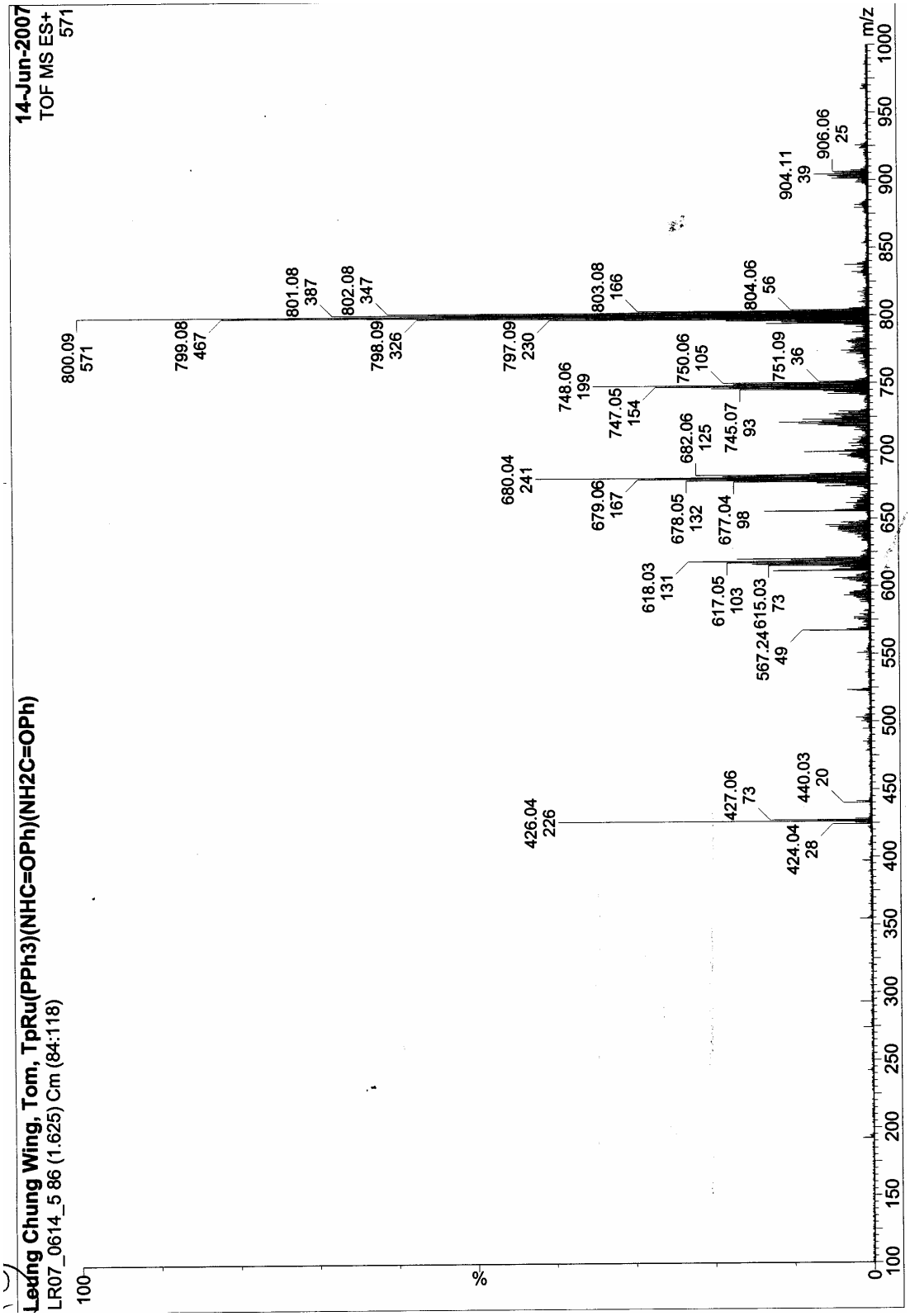

Figure 3.32 Mass spectrum of TpRu(PPh$_3$)(κ^2-*N,O*-NH=CPhN=CPhO) (10)

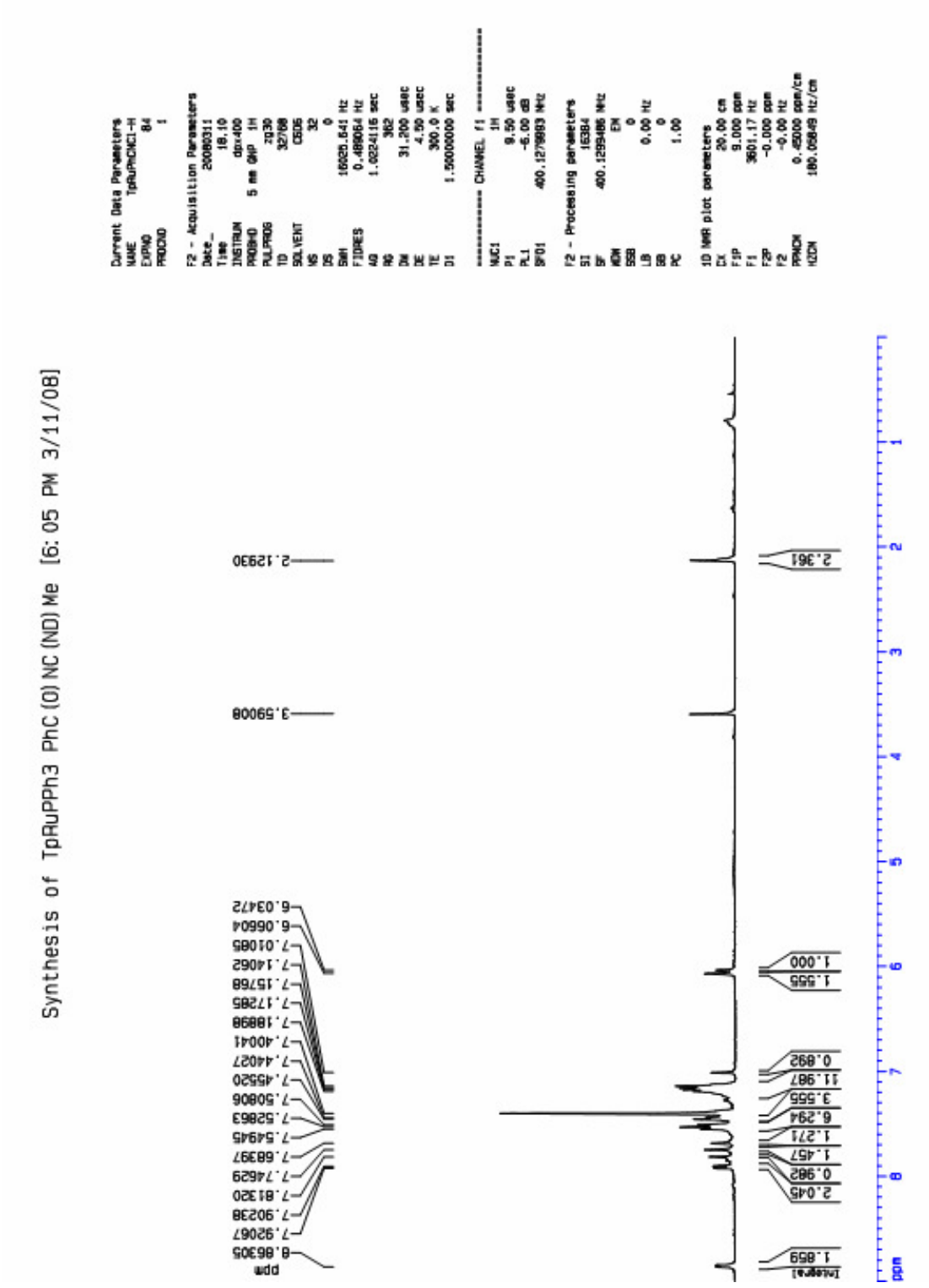

Figure 3.33 400.13 MHz ^{1}H NMR spectrum of TpRu(PPh$_3$)(κ^2-*N,O*-NH=CMeN=CPhO) (11)

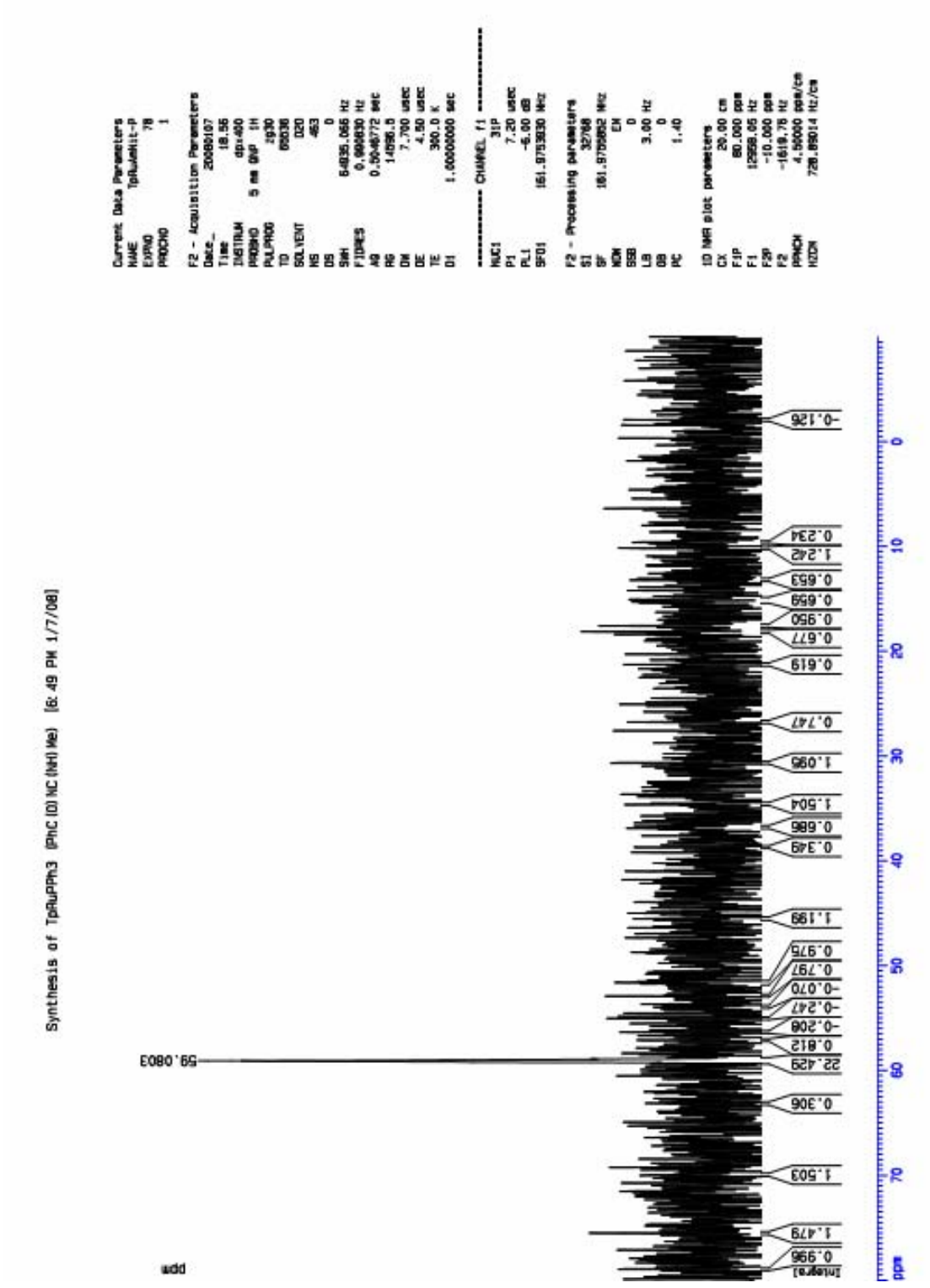

Figure 3.34 161.98 MHz $^{31}P\{^{1}H\}$ NMR spectrum of TpRu(PPh$_3$)(κ^2-*N,O*-NH=CMeN=CPhO) (11)

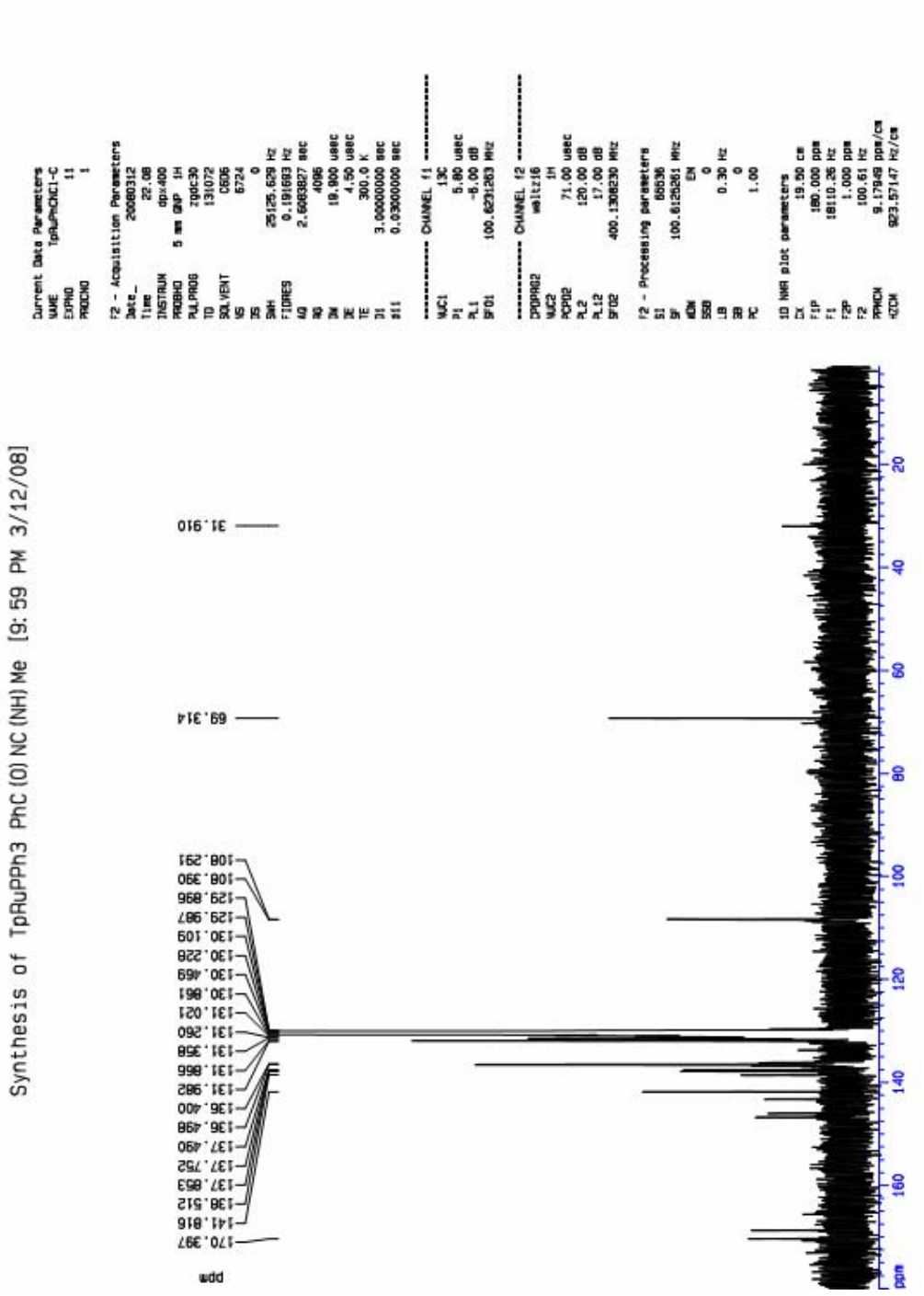

Figure 3.35 100.63 MHz $^{13}C\{^{1}H\}$ NMR spectrum of TpRu(PPh$_3$)(κ^2-*N,O*-NH=CMeN=CPhO) (11)

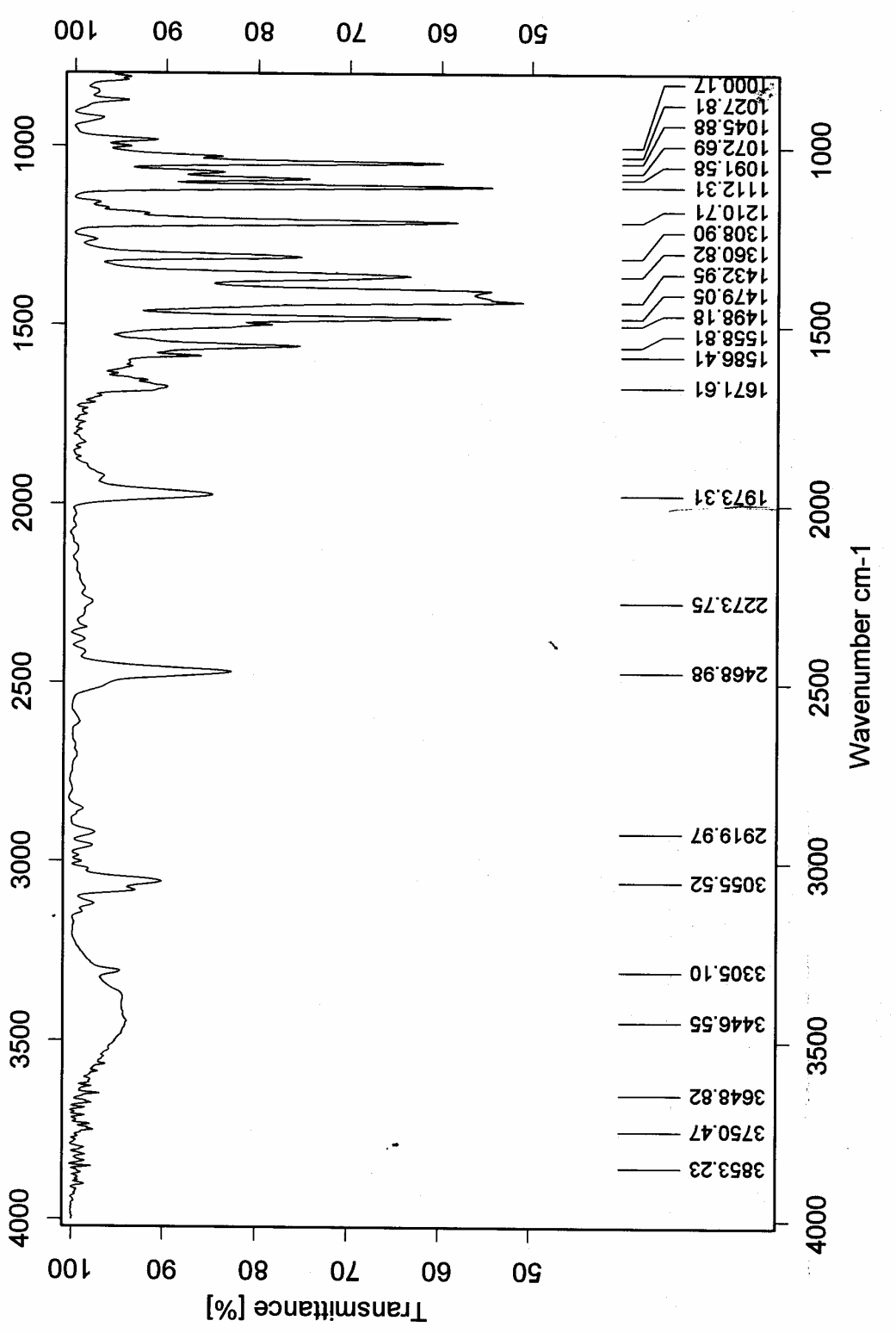

Figure 3.36 Infra-red spectrum of TpRu(PPh$_3$)(κ^2-*N,O*-NH=CMeN=CPhO) (11)

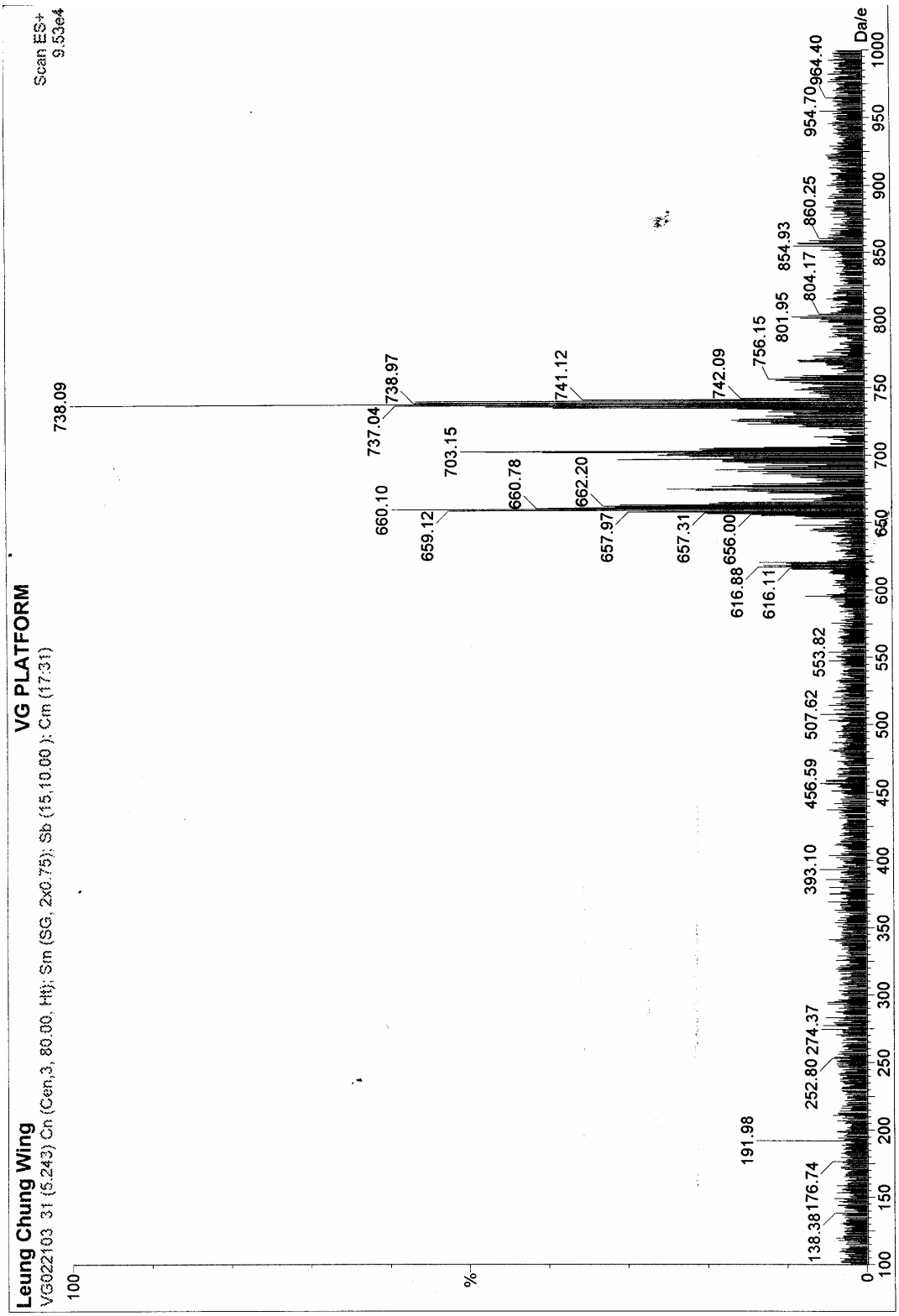

Figure 3.37 Mass spectrum of TpRu(PPh$_3$)(κ^2-*N,O*-NH=CMeN=CPhO) (11)

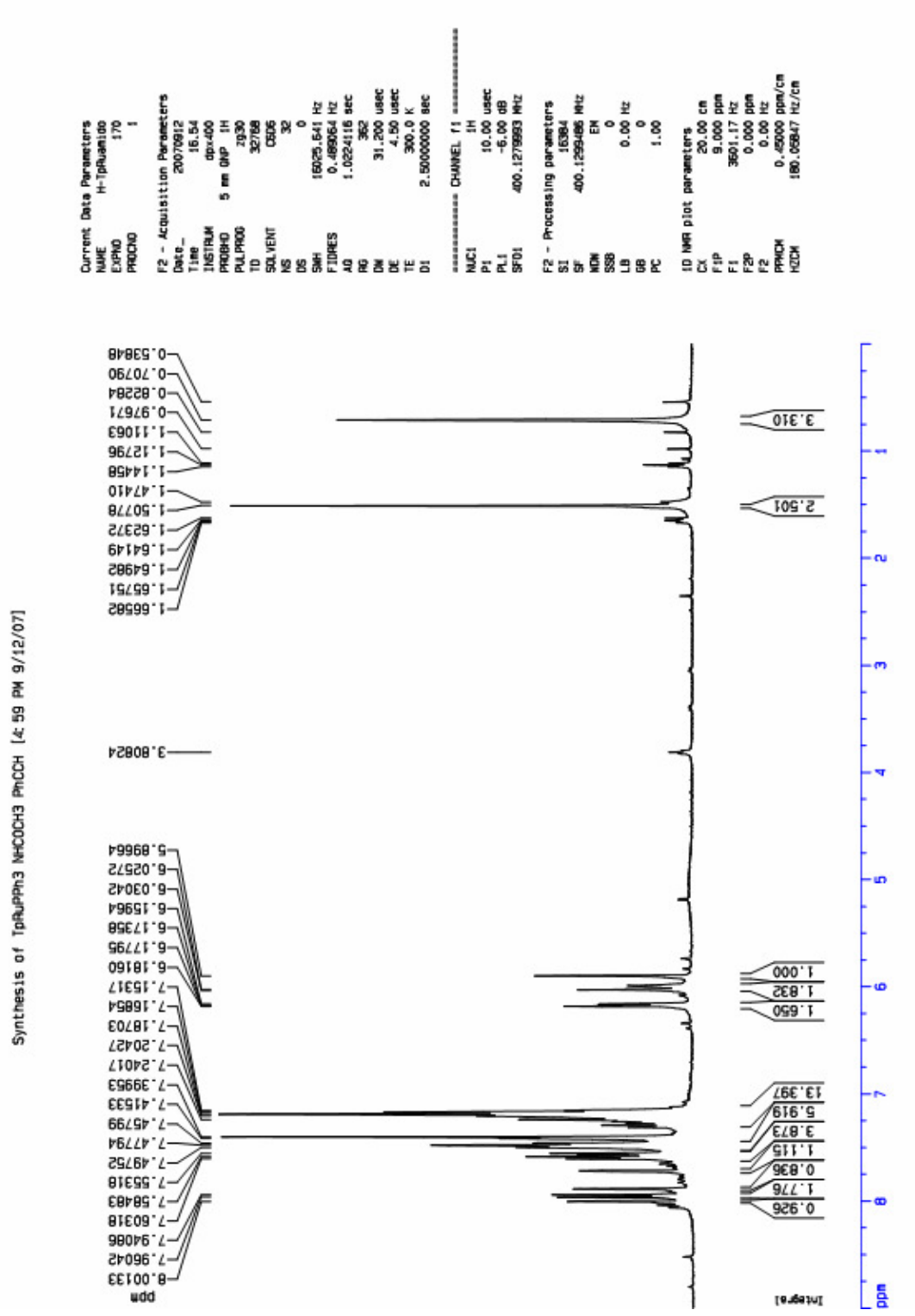

Figure 4.2 400.13 MHz ^{1}H NMR spectrum of TpRu(PPh$_3$)(C(NHC(O)CH$_3$)=CHPh) (13)

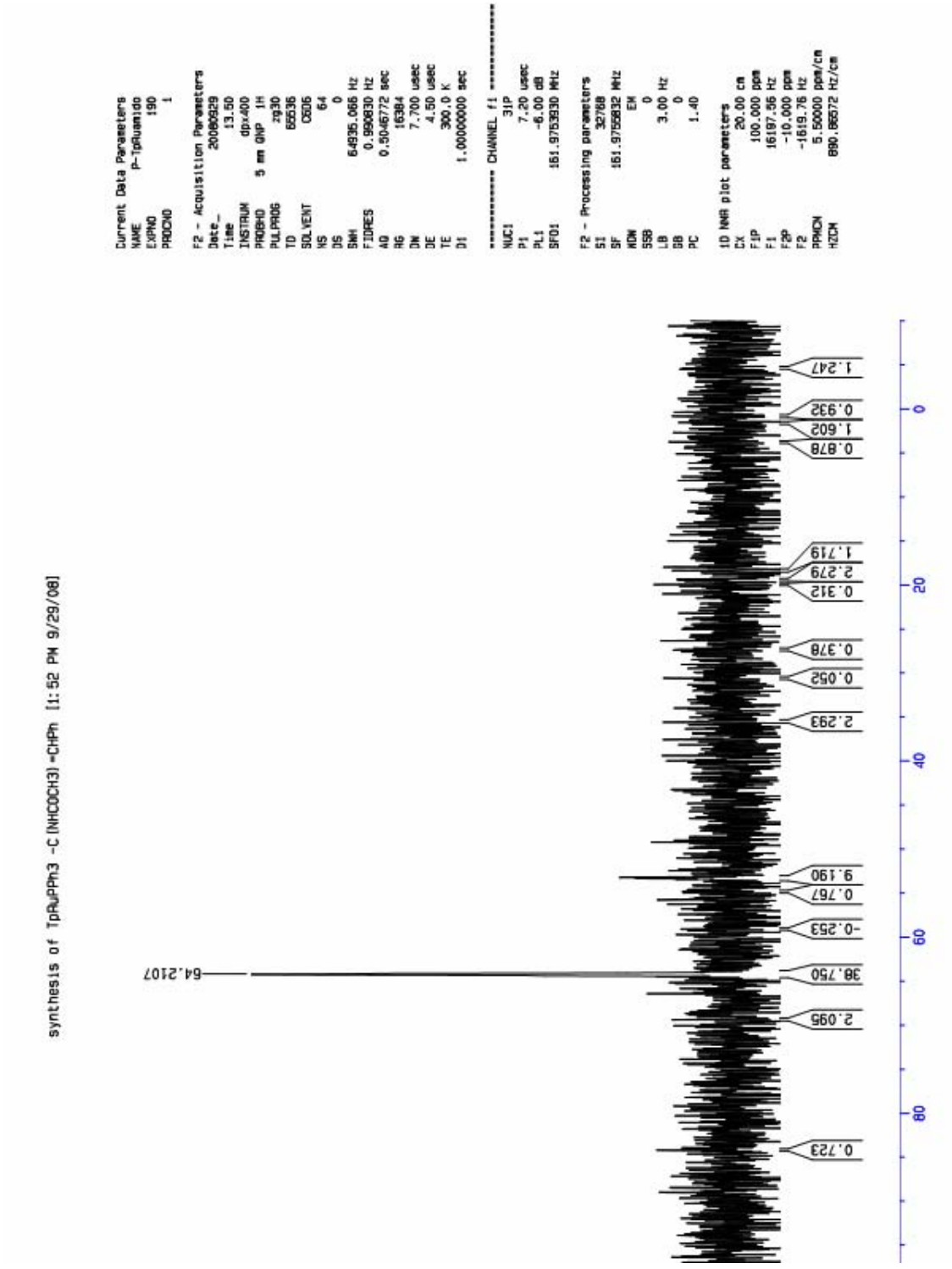

Figure 4.3 161.98 MHz $^{31}P\{^{1}H\}$ NMR spectrum of TpRu(PPh$_3$)(C(NHC(O)CH$_3$)=CHPh) (13)

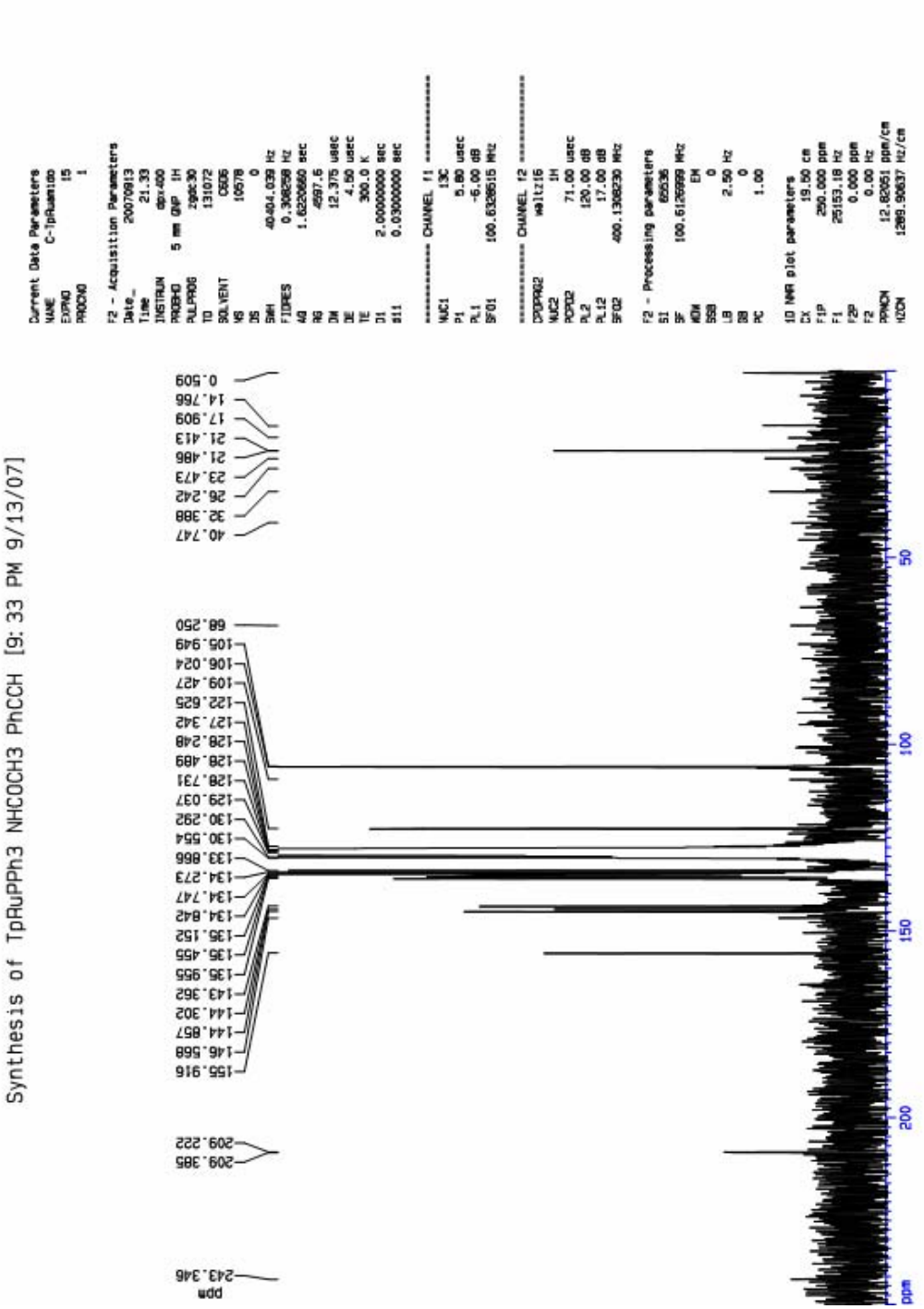

Figure 4.4 100.63 MHz $^{13}C\{^1H\}$ NMR spectrum of TpRu(PPh$_3$)(C(NHC(O)CH$_3$)=CHPh) (13)

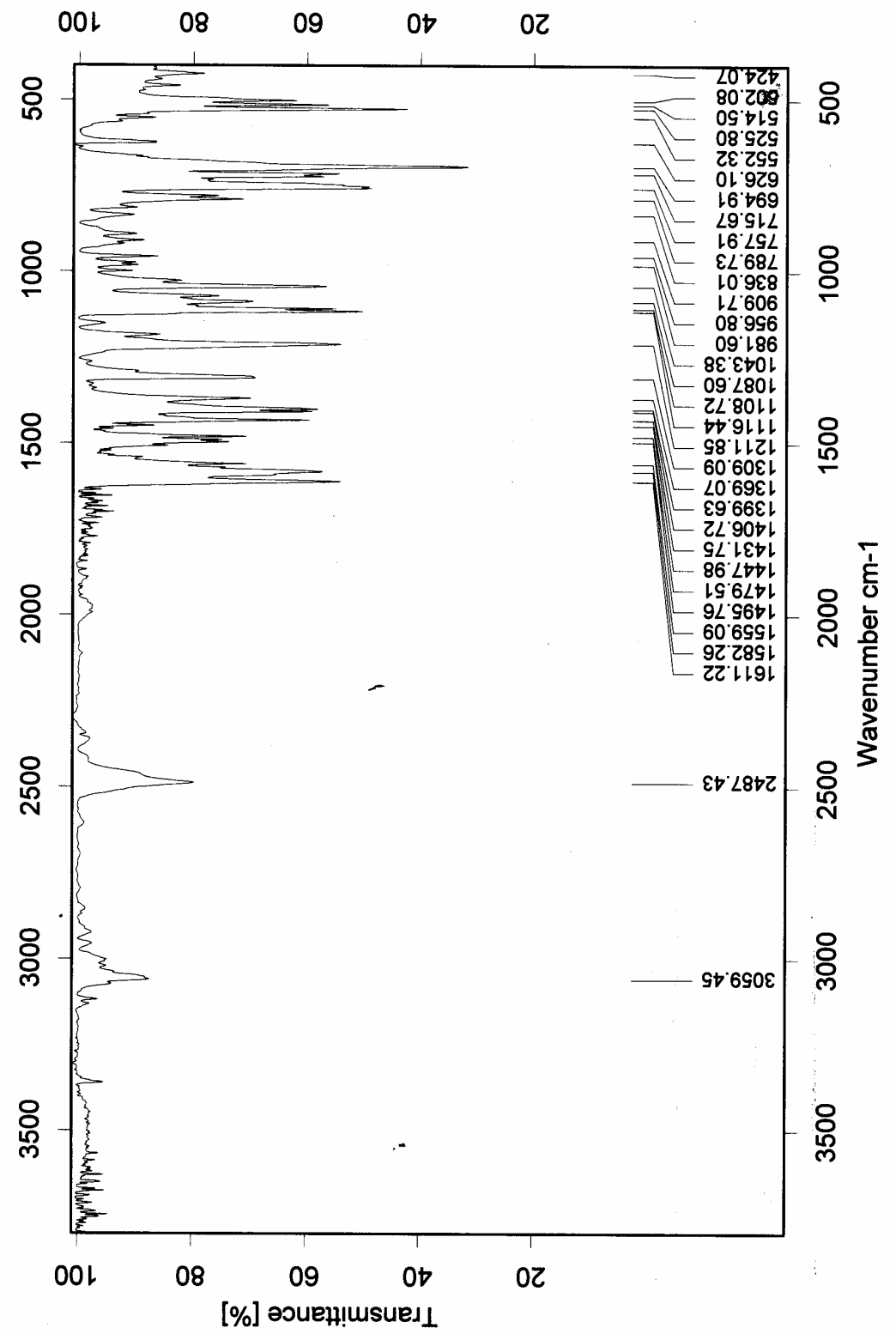

Figure 4.5 Infra-red spectrum of $TpRu(PPh_3)(C(NHC(O)CH_3)=CHPh)$ (13)

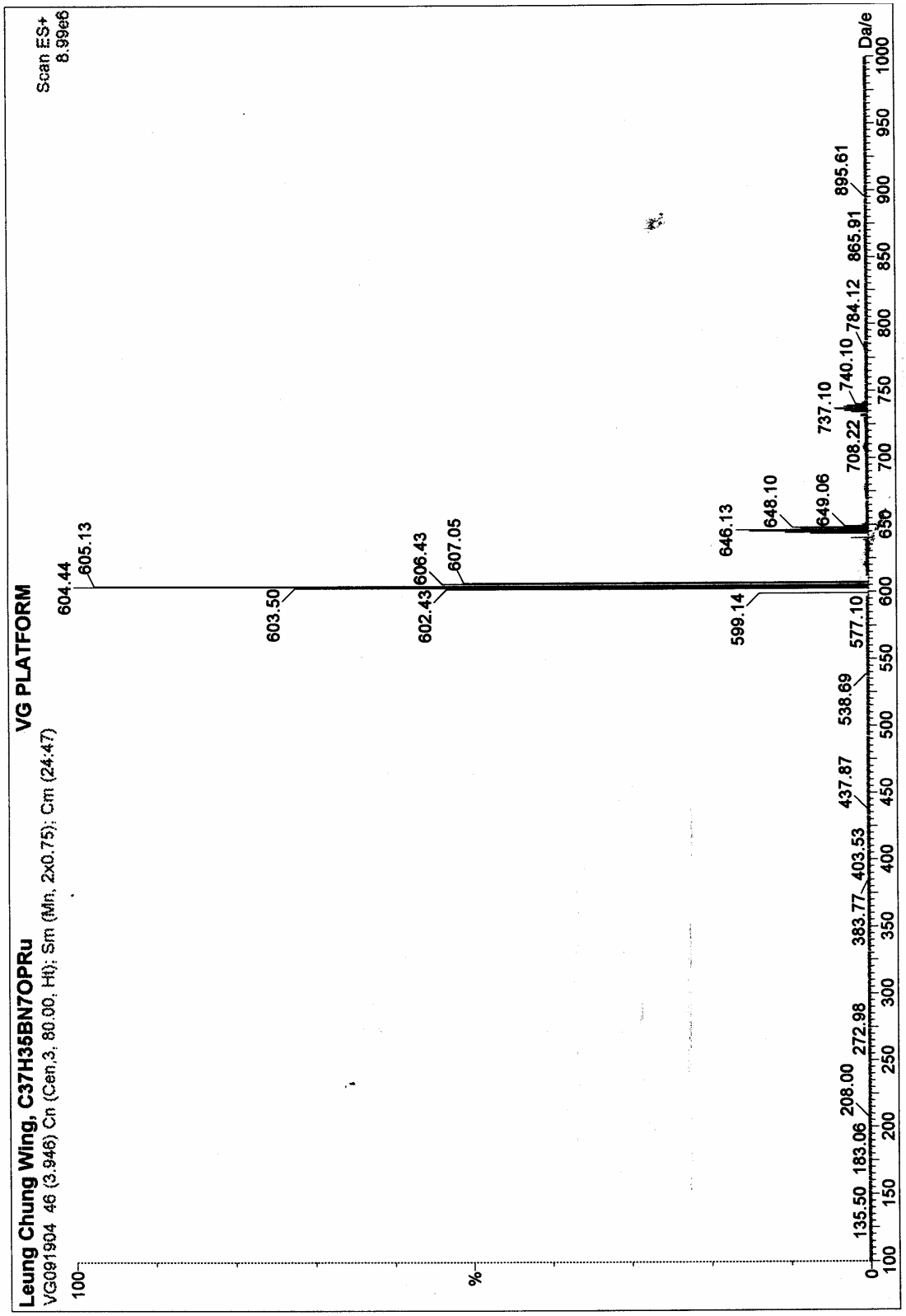

Figure 4.6 Mass spectrum of $TpRu(PPh_3)(C(NHC(O)CH_3)=CHPh)$ (13)

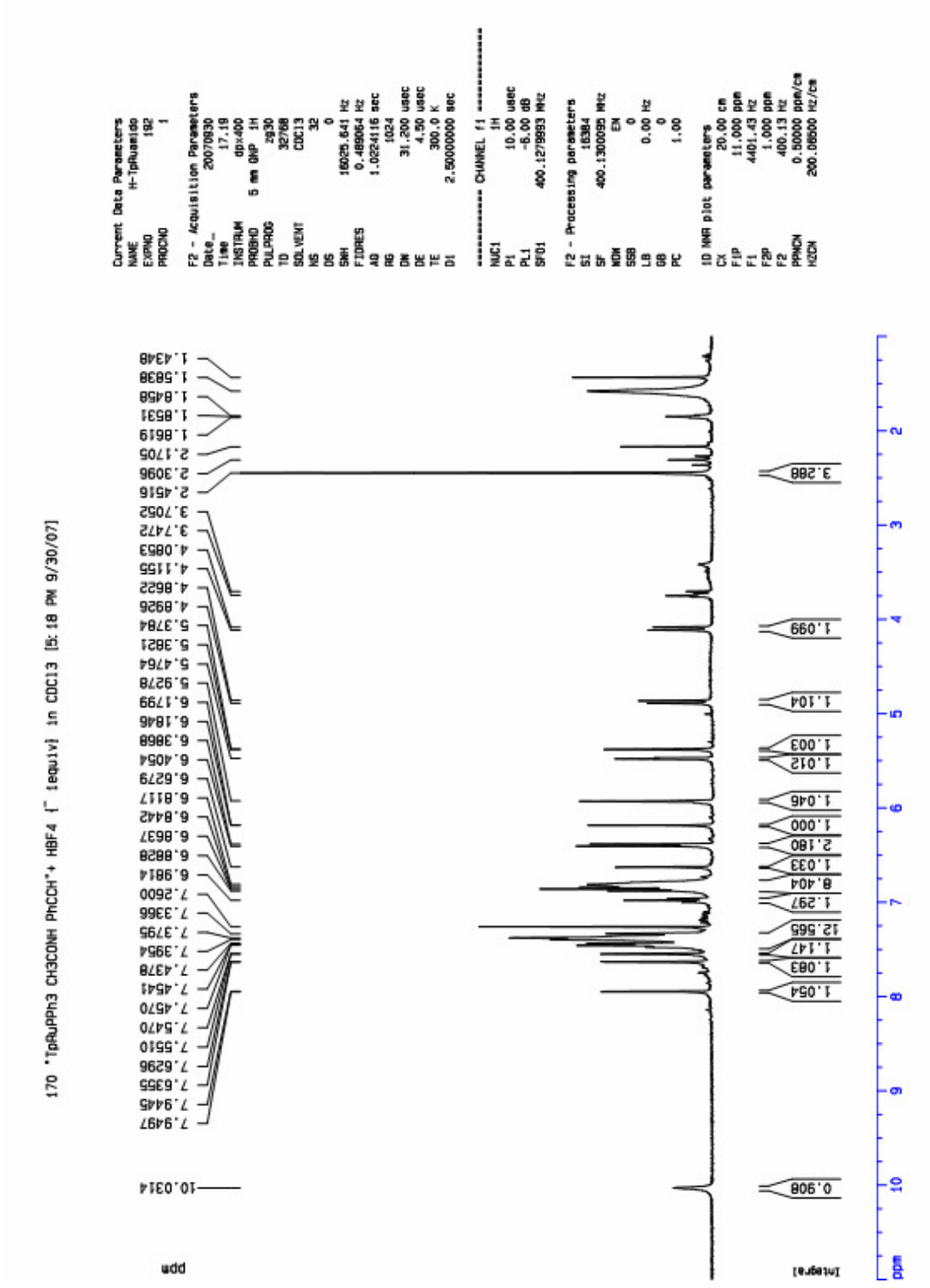

Figure 4.7 400.13 MHz ^{1}H NMR spectrum of [TpRu(PPh$_3$)(=C(CH$_2$Ph)NHC(O)CH$_3$)][BF$_4$] (14)

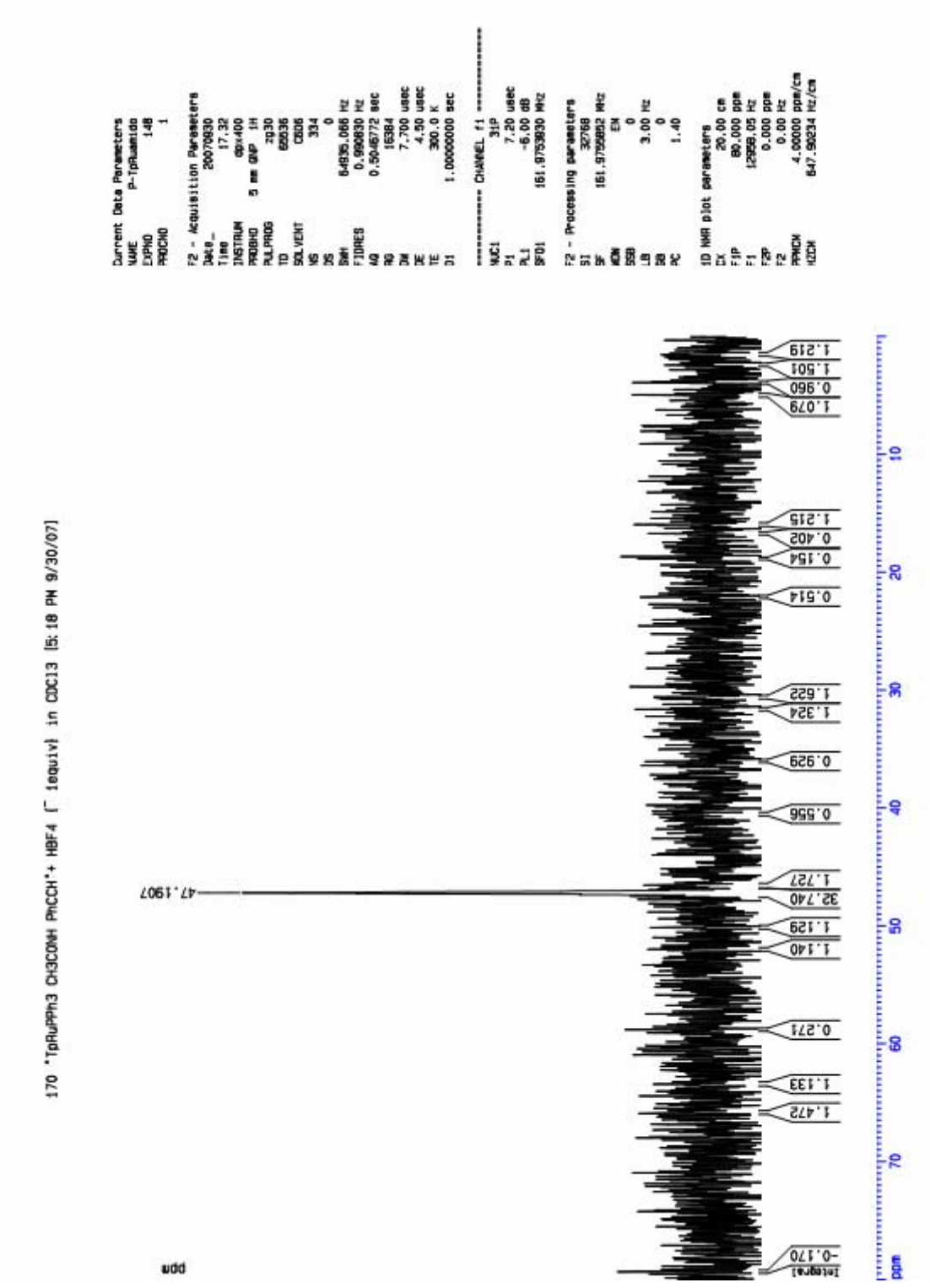

Figure 4.8 161.98 MHz $^{31}P\{^{1}H\}$ NMR spectrum of [TpRu(PPh$_3$)(=C(CH$_2$Ph)NHC(O)CH$_3$)][BF$_4$] (14)

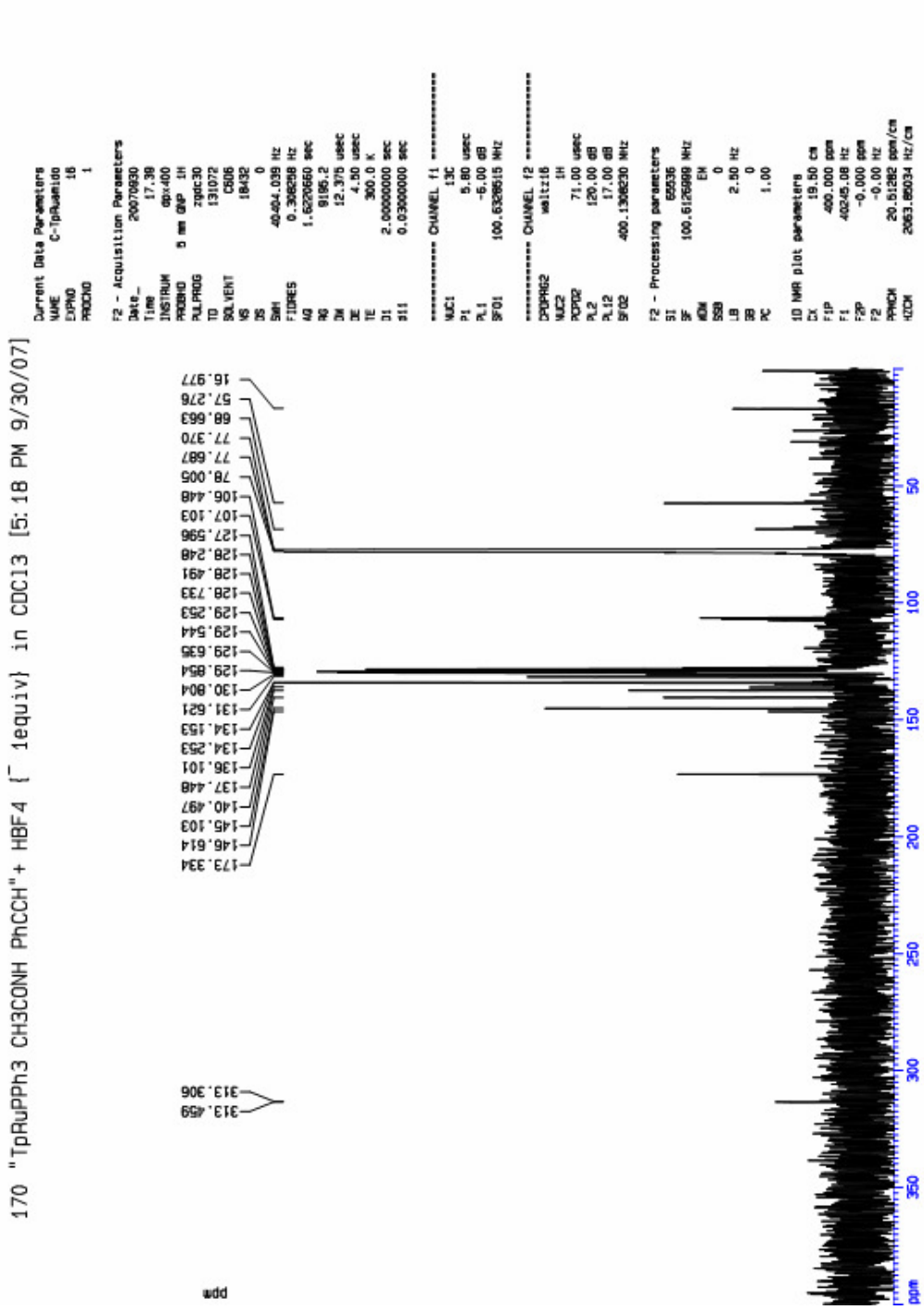

Figure 4.9 100.63 MHz $^{13}C\{^{1}H\}$ NMR spectrum of [TpRu(PPh$_3$)(=C(CH$_2$Ph)NHC(O)CH$_3$)][BF$_4$] (14)

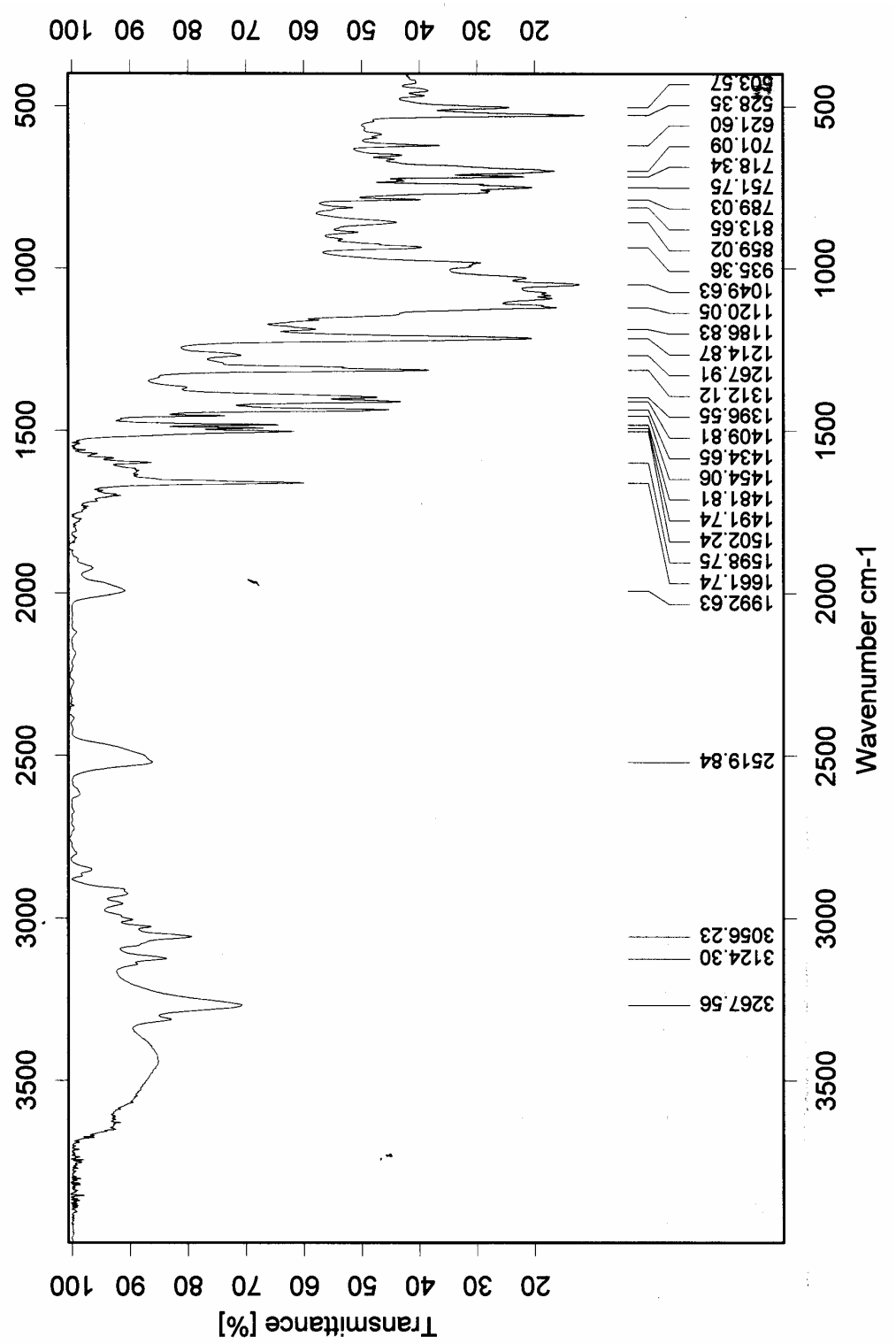

Figure 4.10 Infra-red spectrum of [TpRu(PPh$_3$)(=C(CH$_2$Ph)NHC(O)CH$_3$)][BF$_4$] (14)

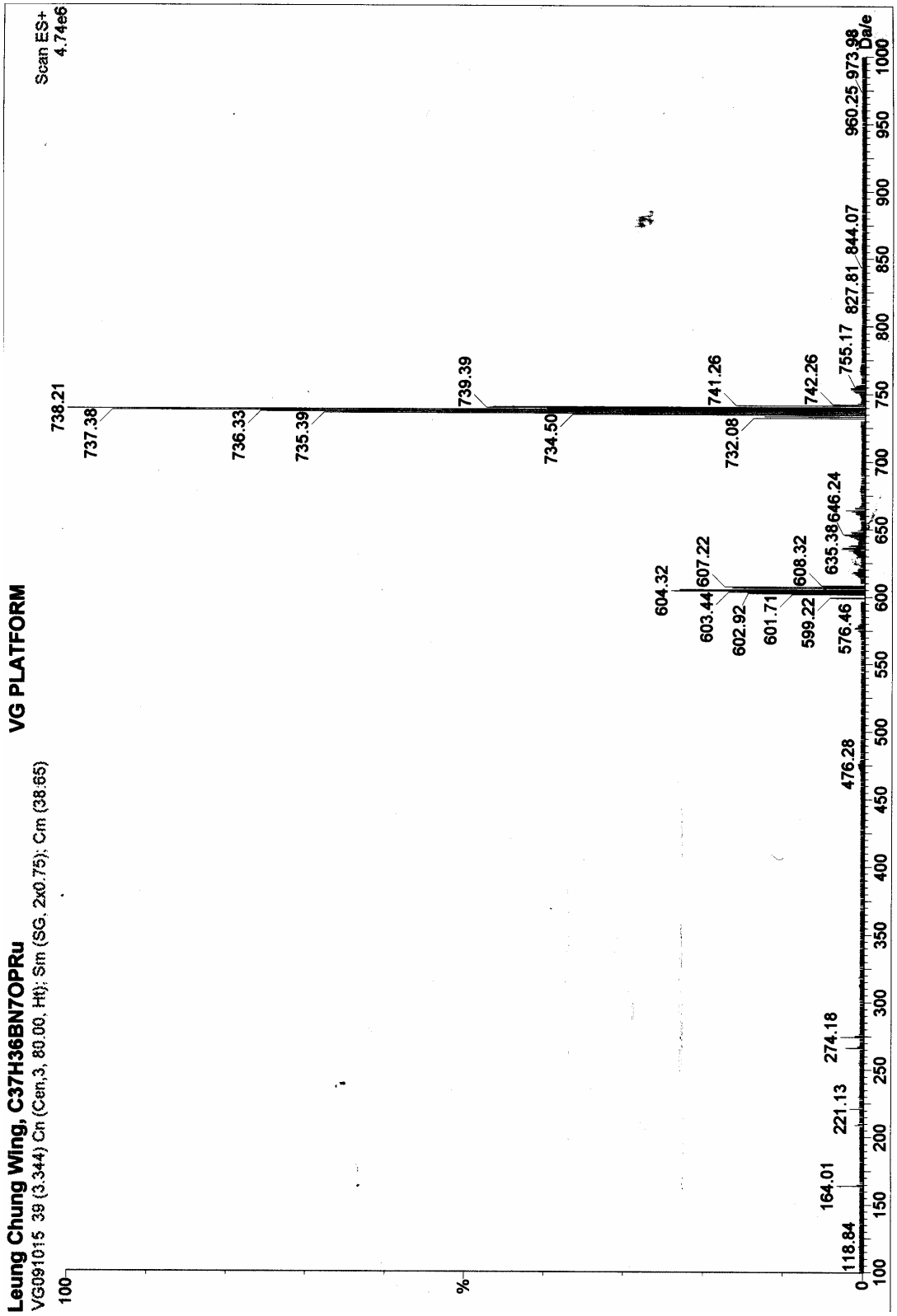

Figure 4.11 Mass spectrum of [TpRu(PPh$_3$)(=C(CH$_2$Ph)NHC(O)CH$_3$)][BF$_4$] (14)

Reference:

1. Beletskaya, I. P. and Cheprakov, A. V., The heck reaction as a sharpening stone of palladium catalysis, *Chemical Reviews*, 2000, 100(8), 3009-3066.
2. Littke, A. F., Dai, C. Y., and Fu, G. C., Versatile catalysts for the Suzuki cross-coupling of arylboronic acids with aryl and vinyl halides and triflates under mild conditions, *Journal of the American Chemical Society*, 2000, 122(17), 4020-4028.
3. Jia, C. G., Kitamura, T., and Fujiwara, Y., Catalytic functionalization of arenes and alkanes via C-H bond activation, *Accounts of Chemical Research*, 2001, 34(8), 633-639.
4. Ritleng, V., Sirlin, C., and Pfeffer, M., Ru-, Rh-, and Pd-catalyzed C-C bond formation involving C-H activation and addition on unsaturated substrates: Reactions and mechanistic aspects, *Chemical Reviews*, 2002, 102(5), 1731-1769.
5. Shilov, A. E. and Shul'pin, G. B., Activation of C-H bonds by metal complexes, *Chemical Reviews*, 1997, 97(8), 2879-2932.
6. Brookhart, M., Green, M. L. H., and Wong, L. L., Carbon Hydrogen Transition-Metal Bonds, *Progress in Inorganic Chemistry*, 1988, 36, 1-124.
7. Brookhart, M. and Green, M. L. H., Carbon-Hydrogen-Transition Metal Bonds, *Journal of Organometallic Chemistry*, 1983, 250(1), 395-408.
8. Dawoodi, Z., Green, M. L. H., Mtetwa, V. S. B., Prout, K., Schultz, A. J., Williams, J. M., and Koetzle, T. F., Evidence for Carbon Hydrogen Titanium Interactions - Synthesis and Crystal-Structures of the Agostic Alkyls

[$TiCl_3(Me_2PCH_2CH2PMe_2)R$] (R = Et or Me), *Journal of the Chemical Society-Dalton Transactions*, 1986(8), 1629-1637.

9. Rasku, S. and Wähälä, K., Synthesis of deuterium labeled polyhydroxy flavones and 3-flavonols, *Tetrahedron*, 2000, 56(6), 913-916.

10. Rasku, S., Wähälä, K., Koskimies, J., and Hase, T., Synthesis of isoflavonoid deuterium labeled polyphenolic phytoestrogens, *Tetrahedron*, 1999, 55(11), 3445-3454.

11. Scheigetz, J., Berthelette, C., Li, C., and Zamboni, R. J., Base-catalyzed deuterium and tritium labeling of aryl methyl sulfones, *Journal of Labelled Compounds & Radiopharmaceuticals*, 2004, 47(12), 881-889.

12. Atzrodt, J., Derdau, V., Fey, T., and Zimmermann, J., The renaissance of H/D exchange, *Angewandte Chemie-International Edition*, 2007, 46(41), 7744-7765.

13. Stahl, S. S., Labinger, J. A., and Bercaw, J. E., Exploring the mechanism of aqueous C-H activation by Pt(II) through model chemistry: Evidence for the intermediacy of alkylhydridoplatinum(IV) and alkane sigma-adducts, *Journal of the American Chemical Society*, 1996, 118(25), 5961-5976.

14. Johansson, L., Ryan, O. B., and Tilset, M., Hydrocarbon activation at a cationic platinum(II) diimine aqua complex under mild conditions in a hydroxylic solvent, *Journal of the American Chemical Society*, 1999, 121(9), 1974-1975.

15. Holtcamp, M. W., Henling, L. M., Day, M. W., Labinger, J. A., and Bercaw, J. E., Intramolecular and intermolecular C-H activation at a cationic Pt^{II} center, *Inorganica Chimica Acta*, 1998, 270(1-2), 467-478.

16. Klei, S. R., Tilley, T. D., and Bergman, R. G., The mechanism of silicon-hydrogen and carbon-hydrogen bond activation by iridium(III): Production of a silylene complex and the first direct observation of Ir(III)/Ir(V) C-H bond oxidative addition and reductive elimination, *Journal of the American Chemical Society*, 2000, 122(8), 1816-1817.

17. Wick, D. D. and Goldberg, K. I., C-H activation of Pt(II) to form stable Pt(IV) alkyl hydrides, *Journal of the American Chemical Society*, 1997, 119(42), 10235-10236.

18. Heiberg, H., Johansson, L., Gropen, O., Ryan, O. B., Swang, O., and Tilset, M., A combined experimental and density functional theory investigation of hydrocarbon activation at a cationic platinum(II) diimine aqua complex under mild conditions in a hydroxylic solvent, *Journal of the American Chemical Society*, 2000, 122(44), 10831-10845.

19. Mylvaganam, K., Bacskay, G. B., and Hush, N. S., Homogeneous conversion of methane to methanol. 2. Catalytic activation of methane by cis- and trans-platin: A density functional study of the Shilov type reaction, *Journal of the American Chemical Society*, 2000, 122(9), 2041-2052.

20. Luecke, H. F. and Bergman, R. G., Synthesis and C-H activation reactions of cyclometalated complexes of Ir(III): $Cp^*(PMe_3)Ir(CH_3)^+$ does not undergo

intermolecular C-H activation in solution via a cyclometalated intermediate, *Journal of the American Chemical Society*, 1997, 119(47), 11538-11539.

21. Strout, D. L., Zaric, S., Niu, S. Q., and Hall, M. B., Methane metathesis at a Cationic Iridium Center, *Journal of the American Chemical Society*, 1996, 118(25), 6068-6069.

22. Alaimo, P. J. and Bergman, R. G., Modeling the proposed intermediate in alkane carbon-hydrogen bond activation by Cp*(PMe_3)Ir(Me)OTf: Synthesis and stability of novel organometallic iridium(V) complexes, *Organometallics*, 1999, 18(14), 2707-2717.

23. Burger, P. and Bergman, R. G., Facile Intermolecular Activation of C-H Bonds in Methane and Other Hydrocarbons and Si-H Bonds in Silanes with the Ir(III) Complex Cp*(PMe_3)Ir(CH_3)(OTf), *Journal of the American Chemical Society*, 1993, 115(22), 10462-10463.

24. Arndtsen, B. A. and Bergman, R. G., Unusually Mild and Selective Hydrocarbon C-H Bond Activation with Positively Charged Iridium(III) Complexes, *Science*, 1995, 270(5244), 1970-1973.

25. Goldshleger, N. F., Tyabin, M. B., Shilov, A. E., and Shteinma, A. A., Activation of Saturated Hydrocarbons - Deuterium-Hydrogen Exchange in Solutions of Transition Metal Complexes, *Zhurnal Fizicheskoi Khimii*, 1969, 43(8), 2174.

26. Goldshleger, N. F., Shteinma, A. A., Shilov, A. E., and Eskova, V. V., Alkane Reactions in Solutions of Chloride Complexes of Platinum, *Zhurnal Fizicheskoi Khimii*, 1972, 46(5), 1353.

27. Thompson, M. E., Baxter, S. M., Bulls, A. R., Burger, B. J., Nolan, M. C., Santarsiero, B. D., Schaefer, W. P., and Bercaw, J. E., "σ-bond metathesis" for C-H bonds of hydrocarbons and Sc-R (R = H, alkyl, aryl) bonds of permethylscandocene derivatives. Evidence for noninvolvement of the π system in electrophilic activation of aromatic and vinylic C-H bonds, *Journal of the American Chemical Society*, 1987, 109(1), 203-219.

28. Bruno, J. W., Smith, G. M., Marks, T. J., Fair, C. K., Schultz, A. J., and Williams, J. M., C-H Activation Mechanisms and Regioselectivity in the Cyclometalation Reactions of Bis(Pentamethylcyclopentadienyl)Thorium Dialkyl Complexes, *Journal of the American Chemical Society*, 1986, 108(1), 40-56.

29. Watson, P. L. and Parshall, G. W., Organolanthanides in Catalysis, *Accounts of Chemical Research*, 1985, 18(2), 51-56.

30. Watson, P. L., Methane Exchange-Reactions of Lanthanide and Early-Transition-Metal Methyl Complexes, *Journal of the American Chemical Society*, 1983, 105(21), 6491-6493.

31. Fendrick, C. M. and Marks, T. J., Thermochemically Based Strategies for C-H Activation on Saturated-Hydrocarbon Molecules - Ring-Opening Reactions of a Thoracyclobutane with Tetramethylsilane and Methane, *Journal of the American Chemical Society*, 1984, 106(7), 2214-2216.

32. Eisen, M. S. and Marks, T. J., Organometallic Molecule Inorganic Surface Coordination and Catalytic Chemistry - Facile and Selective Alkane

Activation by Supported Tetraalylthorium, *Organometallics*, 1992, 11(12), 3939-3941.

33. Rabaâ, H., Saillard, J. Y., and Hoffmann, R., H-H and C-H Activation Reactions at d^0 Metal Centers, *Journal of the American Chemical Society*, 1986, 108(15), 4327-4333.

34. Folga, E., Ziegler, T., and Fan, L. Y., A Theoretical-Study on the Hydrogen-Exchange Reaction between CL_2Lu-H and H_2, *New Journal of Chemistry*, 1991, 15(10-11), 741-748.

35. Steigerwald, M. L. and Goddard, W. A., 2s + 2s Reactions at Transition-Metals .1. The Reactions of D_2 with Cl_2TiH^+, Cl_2TiH, and Cl_2ScH, *Journal of the American Chemical Society*, 1984, 106(2), 308-311.

36. Siegbahn, P. E. M. and Crabtree, R. H., Modeling the solvent sphere: Mechanism of the Shilov reaction, *Journal of the American Chemical Society*, 1996, 118(18), 4442-4450.

37. Wilkinson, G. and Birmingham, J. M., Biscyclopentadienylrhenium Hydride - a New Type of Hydride, *Journal of the American Chemical Society*, 1955, 77(12), 3421-3422.

38. Crabtree, R. H., *The organometallic chemistry of the transition metals*. 4th ed., Hoboken, New Jersey: Wiley-Interscience, 2005.

39. McGrady, G. S. and Guilera, G., The multifarious world of transition metal hydrides, *Chemical Society Reviews*, 2003, 32(6), 383-392.

40. Peruzzini, M. and Poli, R., *Recent advances in hydride chemistry*. 1st ed., Amsterdam ; New York: Elsevier Science Ltd., 2001.

41. Lau, C. P., Ng, S. M., Jia, G. C., and Lin, Z. Y., Some ruthenium hydride, dihydrogen, and dihydrogen-bonded complexes in catalytic reactions, *Coordination Chemistry Reviews*, 2007, 251(17-20), 2223-2237.

42. Cotton, F. A., *Advanced inorganic chemistry*. 6th ed., New York, NY: Wiley, 1999.

43. Albéniz, A. C., Schulte, G., and Crabtree, R. H., Facile Reversible Metalation in an Agostic Complex and Hydrogenolysis of a Metal Aryl Complex Via a Dihydrogen Complex, *Organometallics*, 1992, 11(1), 242-249.

44. Luo, X. L. and Crabtree, R. H., Solution Equilibrium between Classical and Nonclassical Polyhydride Tautomers $[ReH_4(CO)L_3]^+$ and $[ReH_2(\eta^2\text{-}H_2)(CO)L_3]^+$ (L = PMe_2Ph). - Equilibrium Isotope Effects and an Intermediate Trihydrogen Complex in Intramolecular Site Exchange of Dihydrogen and Hydride Ligands, *Journal of the American Chemical Society*, 1990, 112(19), 6912-6918.

45. Toner, A. J., Grundemann, S., Clot, E., Limbach, H. H., Donnadieu, B., Sabo-Etienne, S., and Chaudret, B., Ruthenium assisted reversible proton transfer from an aromatic carbon to a hydride, *Journal of the American Chemical Society*, 2000, 122(28), 6777-6778.

46. Ng, S. M., Lam, W. H., Mak, C. C., Tsang, C. W., Jia, G. C., Lin, Z. Y., and Lau, C. P., C-H bond activation by a hydrotris(pyrazolyl)borato ruthenium hydride complex, *Organometallics*, 2003, 22(4), 641-651.

47. Golden, J. T., Andersen, R. A., and Bergman, R. G., Exceptionally low-temperature carbon-hydrogen/carbon-deuterium exchange reactions of organic and organometallic compounds catalyzed by the $Cp^*(PMe_3)IrH(ClCH_2Cl)^+$ cation, *Journal of the American Chemical Society*, 2001, 123(24), 5837-5838.

48. Niu, S. Q., Zaric, S., Bayse, C. A., Strout, D. L., and Hall, M. B., Theoretical studies of inorganic and organometallic reaction mechanisms. 14. β-hydrogen transfer and alkene/alkyne insertion at a cationic iridium center, *Organometallics*, 1998, 17(23), 5139-5147.

49. Klei, S. R., Golden, J. T., Tilley, T. D., and Bergman, R. G., Iridium-catalyzed H/D exchange into organic compounds in water, *Journal of the American Chemical Society*, 2002, 124(10), 2092-2093.

50. Garnett, J. L. and Hodges, R. J., Homogeneous Metal-Catalyzed Exchange of Aromatic Compounds . A New General Isotopic Hydrogen Labeling Procedure, *Journal of the American Chemical Society*, 1967, 89(17), 4546-4547.

51. Garnett, J. L. and Hodges, R. J., Homogeneous Metal-Catalyzed Isotopic Hydrogen Exchange in Aromatic Compounds . Labelling of Nitrobenzene Bromobenzene Naphthalene and Acetophenone, *Chemical Communications (London)*, 1967(19), 1001b-1003.

52. Shilov, A. E. and Shteinman, A. A., Activation of Saturated-Hydrocarbons by Metal-Complexes in Solution, *Coordination Chemistry Reviews*, 1977, 24(2-3), 97-143.

53. Tenn, W. J., Young, K. J. H., Bhalla, G., Oxgaard, J., Goddard, W. A., and Periana, R. A., CH activation with an O-donor iridium-methoxo complex, *Journal of the American Chemical Society*, 2005, 127(41), 14172-14173.

54. Rybtchinski, B., Cohen, R., Ben-David, Y., Martin, J. M. L., and Milstein, D., Aromatic vs aliphatic C-H bond activation by rhodium(I) as a function of agostic interactions: Catalytic H/D exchange between olefins and methanol or water, *Journal of the American Chemical Society*, 2003, 125(36), 11041-11050.

55. Stevens, R. C., Bau, R., Milstein, D., Blum, O., and Koetzle, T. F., Concept of the H(δ+)···H(δ-) interaction. A low-temperature neutron diffraction study of cis-$[(PMe_3)_4IrH(OH)]PF_6$, *Journal of the Chemical Society-Dalton Transactions*, 1990(4), 1429-1432.

56. Lee, J. C., Peris, E., Rheingold, A. L., and Crabtree, R. H., An Unusual Type of H...H Interaction - Ir-H...H-O and Ir-H...H-N Hydrogen-Bonding and Its Involvement in Sigma-Bond Metathesis, *Journal of the American Chemical Society*, 1994, 116(24), 11014-11019.

57. Lough, A. J., Park, S., Ramachandran, R., and Morris, R. H., Switching on and Off a New Intramolecular Hydrogen-Hydrogen Interaction and the Heterolytic Splitting of Dihydrogen - Crystal and Molecular-Structure of$[Ir\{H(\eta^1\text{-}SC_5H_4NH)\}_2(PCy_3)_2]BF_4\cdot 2.7CH_2Cl_2$, *Journal of the American Chemical Society*, 1994, 116(18), 8356-8357.

58. Yao, W. B. and Crabtree, R. H., An η^1-aldehyde complex and the role of hydrogen bonding in its conversion to an η^1-imine complex, *Inorganic Chemistry*, 1996, 35(10), 3007-3011.

59. Rerek, M. E., Ji, L. N., and Basolo, F., The Indenyl Ligand Effect on the Rate of Substitution-Reactions of $Rh(\eta\text{-}C_9H_7)(CO)_2$ and $Mn(\eta\text{-}C_9H_7)(CO)_3$, *Journal of the Chemical Society-Chemical Communications*, 1983(21), 1208-1209.

60. Calhorda, M. J., Romao, C. C., and Veiros, L. F., The nature of the indenyl effect, *Chemistry-a European Journal*, 2002, 8(4), 868-875.

61. Fung, W. K., Huang, X., Man, M. L., Ng, S. M., Hung, M. Y., Lin, Z. Y., and Lau, C. P., Dihydrogen-bond-promoted catalysis: Catalytic hydration of nitriles with the indenylruthenium hydride complex $(\eta^5\text{-}C_9H_7)Ru(dppm)H$ (dppm = bis(diphenylphosphino)methane), *Journal of the American Chemical Society*, 2003, 125(38), 11539-11544.

62. Kukushkin, V. Y. and Pombeiro, A. J. L., Additions to metal-activated organonitriles, *Chemical Reviews*, 2002, 102(5), 1771-1802.

63. Murahashi, S. and Takaya, H., Low-valent ruthenium and iridium hydride complexes as alternatives to Lewis acid and base catalysts, *Accounts of Chemical Research*, 2000, 33(4), 225-233.

64. Kukushkin, V. Y. and Pombeiro, A. J. L., Metal-mediated and metal-catalyzed hydrolysis of nitriles, *Inorganica Chimica Acta*, 2005, 358(1), 1-21.

65. Michelin, R. A., Mozzon, M., and Bertani, R., Reactions of transition metal-coordinated nitriles, *Coordination Chemistry Reviews*, 1996, 147, 299-338.

66. Storhoff, B. N. and Lewis, H. C., Organonitrile Complexes of Transition-Metals, *Coordination Chemistry Reviews*, 1977, 23(1), 1-29.

67. Ghaffar, T. and Parkins, A. W., The catalytic hydration of nitriles to amides using a homogeneous platinum phosphinito catalyst, *Journal of Molecular Catalysis A - Chemical*, 2000, 160(2), 249-261.

68. Ghaffar, T. and Parkins, A. W., A New Homogeneous Platinum-Containing Catalyst for the Hydrolysis of Nitriles, *Tetrahedron Letters*, 1995, 36(47), 8657-8660.

69. Hazell, A., Jensen, K. B., Mckenzie, C. J., and Toftlund, H., Synthesis and reactivity of (μ-oxo)diiron(III) complexes of tris(2-pyridylmethyl)amine. X-ray crystal structures of [Tpa(OH)FeOFe(H_2O)Tpa](ClO_4)$_3$ and [Tpa(Cl)FeOFe(Cl)tpa](ClO_4)$_2$, *Inorganic Chemistry*, 1994, 33(14), 3127-3134.

70. Wilkinson, E. C., Dong, Y. H., and Que, L., Modeling Hydrolysis at Dinuclear Iron Centers, *Journal of the American Chemical Society*, 1994, 116(18), 8394-8395.

71. Meyer, F., Heinze, K., Nuber, B., and Zsolnai, L., Tuning the metal-metal separation in pyrazolate-based dinuclear complexes by the length of chelating side arms, *Journal of the Chemical Society-Dalton Transactions*, 1998(2), 207-213.

72. Frey, S. T., Murthy, N. N., Weintraub, S. T., Thompson, L. K., and Karlin, K. D., Hydrolysis of unactivated esters and acetonitrile hydration by a hydroxo-dicopper(II) complex, *Inorganic Chemistry*, 1997, 36(6), 956-957.

73. Mckenzie, C. J. and Robson, R., High Turnover Catalysis at Bimetallic Sites of the Hydration of Nitriles to Carboxamides Co-Catalyzed by Acid - Highly Specific Hydration of Acrylonitrile to Acrylamide, *Journal of the Chemical Society-Chemical Communications*, 1988(2), 112-114.

74. Bauer, C. B., Concolino, T. E., Eglin, J. L., Rogers, R. D., and Staples, R. J., Synthesis of dirhenium species with benzamidate ligands via hydrolysis of benzonitrile, *Journal of the Chemical Society-Dalton Transactions*, 1998(17), 2813-2817.

75. Meyer, F., Kaifer, E., Kircher, P., Heinze, K., and Pritzkow, H., Cooperative transformations of small molecules at a dinuclear nickel(II) site, *Chemistry-a European Journal*, 1999, 5(5), 1617-1630.

76. Meyer, F., Hyla-Kryspin, I., Kaifer, E., and Kircher, P., Cooperative binding of nitrile moieties within a bimetallic pocket: Enforcing side-on π-interaction with a high-spin nickel(II) site, *European Journal of Inorganic Chemistry*, 2000(4), 771-781.

77. Breno, K. L., Pluth, M. D., and Tyler, D. R., Organometallic chemistry in aqueous solution. Hydration of nitriles to amides catalyzed by a water-soluble molybdocene, $[Cp^*_2Mo(OH)(H_2O)]^+$, *Organometallics*, 2003, 22(6), 1203-1211.

78. Yoshida, T., Matsuda, T., Okano, T., Kitani, T., and Otsuka, S., Activation of Water Molecule .2. Generation of Strong Hydroxo Bases by the Reaction of Water with Platinum(0) Phosphine Complexes and the Applications as

Catalysts for H-D Exchange and Hydration Reactions, *Journal of the American Chemical Society*, 1979, 101(8), 2027-2038.

79. Yoon, M. and Tyler, D. R., Activation of water by permethyltungstenocene; Evidence for the oxidative addition of water, *Chemical Communications*, 1997(6), 639-640.

80. Villain, G., Constant, G., Gaset, A., and Kalck, P., Selective Catalysis of the Hydration of Nitriles to Amides - Evidence for an Efficient Homogeneous Precursor Containing a Pd-OH Bond, *Journal of Molecular Catalysis*, 1980, 7(3), 355-364.

81. Kim, J. H., Britten, J., and Chin, J., Kinetics and Mechanism of a Co(III) Complex Catalyzed Hydration of Nitriles, *Journal of the American Chemical Society*, 1993, 115(9), 3618-3622.

82. Kaminskaia, N. V. and Kostić, N. M., Nitrile hydration catalysed by palladium(II) complexes, *Journal of the Chemical Society-Dalton Transactions*, 1996(18), 3677-3686.

83. Oshiki, T., Yamashita, H., Sawada, K., Utsunomiya, M., Takahashi, K., and Takai, K., Dramatic rate acceleration by a diphenyl-2-pyridylphosphine ligand in the hydration of nitriles catalyzed by $Ru(acac)_2$ complexes, *Organometallics*, 2005, 24(26), 6287-6290.

84. Curtis, N. J., Hagen, K. S., and Sargeson, A. M., Intramolecular Hydrolysis of Coordinated Acetonitrile in a Binuclear μ-Amido-Octaamminedicobalt(III) Complex, *Journal of the Chemical Society-Chemical Communications*, 1984(23), 1571-1573.

85. Curtis, N. J. and Sargeson, A. M., Synthesis and Base Hydrolysis of Pentaammine N,N-Dimethylformamide and Acetonitrile Complexes of Rh(III) and Ir(III), *Journal of the American Chemical Society*, 1984, 106(3), 625-630.

86. Zanella, A. W. and Ford, P. C., Base Hydrolyses of Penta-Ammineruthenium(III) Complexes of Organonitriles, *Journal of the Chemical Society-Chemical Communications*, 1974(19), 795-796.

87. Hiraki, K., Kinoshita, Y., KinoshitaKawashima, J., and Kawano, H., Formation of N-imidoylimidatoruthenium(II) complexes via ruthenium-promoted hydration of nitriles, *Journal of the Chemical Society-Dalton Transactions*, 1996(3), 291-298.

88. Rochon, F. D., Kong, P. C., and Melanson, R., Hydrolysis and Dimerization of Nitrile to Diacetamide and Crystal-Structures of Chloro(2,2,2,2',2',2'-Hexachlorodiacetamido)(Dimethyl Sulfoxide)Platinum(II) and Cis-Aquadichloro(Dimethyl Sulfoxide)Platinum(II), *Inorganic Chemistry*, 1990, 29(15), 2708-2712.

89. Bokach, N. A., Pakhomova, T. B., Kukushkin, V. Y., Haukka, M., and Pombeiro, A. J. L., Hydrolytic metal-mediated coupling of dialkylcyanamides at a Pt(IV) center giving a new family of diimino ligands, *Inorganic Chemistry*, 2003, 42(23), 7560-7568.

90. Thomson, R. K., Patrick, B. O., and Schafer, L. L., Synthesis, characterization, and reactivity of the first hafnium alkyl complex stabilized

by amidate ligands, *Canadian Journal of Chemistry-Revue Canadienne De Chimie*, 2005, 83(6), 1037-1042.

91. Giesbrecht, G. R., Shafir, A., and Arnold, J., Synthesis and structure of a linked-bis(amidate) ligand and some complexes with titanium, *Inorganic Chemistry*, 2001, 40(23), 6069-6072.

92. Li, C. Y., Thomson, R. K., Gillon, B., Patrick, B. O., and Schafer, L. L., Amidate complexes of titanium and zirconium: a new class of tunable precatalysts for the hydroamination of alkynes, *Chemical Communications*, 2003(19), 2462-2463.

93. Lee, A. V. and Schafer, L. L., Modular *N*,*O*-chelating ligands: Group-4 amidate complexes for catalytic hydroamination, *European Journal of Inorganic Chemistry*, 2007(16), 2243-2255.

94. Broomhead, J. A., Evans, J., Grumley, W. D., and Sterns, M., Crystal-Structure of Mer-Trichloro(Dimethylformamide)(1,10-Phenanthroline)Chromium(III), *Journal of the Chemical Society-Dalton Transactions*, 1977(2), 173-176.

95. Chen, W. Z. and Matsumoto, K., Pivalamidate-bridged dinuclear platinum and platinum-palladium complexes: synthesis, NMR and X-ray structural characterization of cis-$[Pt(NH_3)_2(NHCO^tBu)_2]\cdot 2H_2O$, and cis-$[Pt(NH_3)_2(NHCO^tBu)_2MLL]$ X_n (M=Pt, LL'=cod; L=L'=dmso; L-Cl, L'=dmso; M=Pd, L=L'=NH_3; X=ClO_4^-, NO_3^-), *Inorganica Chimica Acta*, 2003, 342, 88-96.

96. Fairlie, D. P., Ilan, Y., and Taube, H., Oxygen versus nitrogen bonding of carboxamides to pentaammineruthenium(II/III), *Inorganic Chemistry*, 1997, 36(6), 1029-1037.

97. Fairlie, D. P., Angus, P. M., Fenn, M. D., and Jackson, W. G., Factors Influencing the Nitrogen Vs Oxygen Bonding Mode of Amides Bound to Pentaamminecobalt(III) and the Kinetics and Mechanism of Rearrangement, *Inorganic Chemistry*, 1991, 30(7), 1564-1569.

98. Chin, C. S., Chong, D. S., Lee, S., and Park, Y. J., Addition of OH^- and alcohols or amines to $-C\equiv N$ and $-CH=CH_2$ groups of CH_2=CHCN coordinated to Cp* Ir(η^3-$CH_2CHCHPh$), *Organometallics*, 2000, 19(20), 4043-4050.

99. Chin, C. S., Chong, D., Lee, B., Jeong, H., Won, G., Do, Y., and Park, Y. J., Activation of acetonitrile in $[Cp^*Ir(\eta^3\text{-}CH_2CHCHPh)(NCMe)]^+$: Crystal structures of iridium-amidine, imino-ether, amido, and amide complexes, *Organometallics*, 2000, 19(4), 638-648.

100. Chen, W. Z., Liu, F. H., Nishioka, T., and Matsumoto, K., Heterotrimetallic complexes $[\{Pt(RNH_2)_2(\mu\text{-}NHCOtBu)_2\}_2M](ClO_4)_n$ (M = Mn, Co, Cu, Ni, Cd, and Zn, n = 2; M = In, n = 3), $[\{Pt(NH_3)(\mu\text{-}DACHCOtBu)(\mu\text{-}NHCOtBu)\}_2Ni](ClO_4)_2$, and $[\{Pt(RNH_2)_2(NHCOtBu)2\}_3Ag_3](ClO_4)_3$ bridged by amidate ligands: A novel amidate-amine interligand reaction during the Pt-Ni bond formation, *European Journal of Inorganic Chemistry*, 2003(23), 4234-4243.

101. Erxleben, A., Mutikainen, I., and Lippert, B., Conversion of Acetonitrile into Acetamide in the Coordination Spheres of cis- and trans-$M^{II}(amine)_2$ (M=Pt or Pd) - Solution and Crystal Structural Studies, *Journal of the Chemical Society-Dalton Transactions*, 1994(24), 3667-3675.

102. Ruiz, J., Cutillas, N., Rodriguez, V., Sampedro, J., Lopez, G., Chaloner, P. A., and Hitchcock, P. B., Reactivity of hydroxo complexes of palladium(II) towards nitriles: formation of carboxamide and imino ether derivatives of palladium(II), *Journal of the Chemical Society-Dalton Transactions*, 1999(17), 2939-2946.

103. Rochon, F. D., Boutin, S., Kong, P. C., and Melanson, R., Study of the aqueous reactions of $K[Pt(Ph_2SO)Cl_3]$ with nitrile ligands and crystal structures of $N(C_4H_9)_4[Pt(Ph_2SO)Cl_3]$, $N(C_2H_5)_4[Pt(Ph_2SO)Br_3]$ and cis-$Pt(Ph_2SO)(C_3H_5CN)Cl_2$, *Inorganica Chimica Acta*, 1997, 264(1-2), 89-100.

104. Kim, J. H., Britten, J., and Chin, J., Catalytic Hydration of Acrylonitrile to Acrylamide under Mild Conditions, *Angewandte Chemie-International Edition in English*, 1990, 29(5), 523-525.

105. Sanchez, G., Ruiz, F., Garcia, J., de Arellano, M. C. R., and Lopez, G., Organonickel(II) complexes with anionic N-donor ligands, hydration of coordinated nitriles at a nickel(II) site, *Helvetica Chimica Acta*, 1997, 80(8), 2477-2485.

106. Zhang, Z., Leitch, D. C., Lu, M., Patrick, B. O., and Schafer, L. L., An easy-to-use, regioselective, and robust bis(amidate) titanium hydroamination precatalyst: Mechanistic and synthetic investigations toward the preparation

of tetrahydroisoquinolines and benzoquinolizine alkaloids, *Chemistry-a European Journal*, 2007, 13(7), 2012-2022.

107. Thomson, R. K., Bexrud, J. A., and Schafer, L. L., A pentagonal pyramidal zirconium imido complex for catalytic hydroamination of unactivated alkenes, *Organometallics*, 2006, 25(17), 4069-4071.

108. Thomson, R. K., Zahariev, F. E., Zhang, Z., Patrick, B. O., Wang, Y. A., and Schafer, L. L., Structure, bonding, and reactivity of Ti and Zr amidate complexes: DFT and X-ray crystallographic studies, *Inorganic Chemistry*, 2005, 44(24), 8680-8689.

109. Braunstein, P. and Nobel, D., Transition-Metal-Mediated Reactions of Organic Isocyanates, *Chemical Reviews*, 1989, 89(8), 1927-1945.

110. Gambarotta, S., Strologo, S., Floriani, C., Chiesivilla, A., and Guastini, C., Insertion of carbon dioxide-like molecules into zirconium-carbon bonds: reactivity of dialkylbis(cyclopentadienyl)zirconium(IV) with diphenylketene, aryl isocyanates, and p-tolylcarbodiimide, *Inorganic Chemistry*, 1985, 24(5), 654-660.

111. Watson, D. A., Chiu, M., and Bergman, R. G., Zirconium bis(amido) catalysts for asymmetric intramolecular alkene hydroamination, *Organometallics*, 2006, 25(20), 4731-4733.

112. Kim, H., Lee, P. H., and Livinghouse, T., Intramolecular alkene hydroaminations catalyzed by a bis(thiophosphinic amidate) Zr(IV) complex, *Chemical Communications*, 2005(41), 5205-5207.

113. Gott, A. L., Clarke, A. J., Clarkson, G. J., and Scott, P., Structure-activity relationships for group 4 biaryl amidate complexes in catalytic hydroamination/cyclization of aminoalkenes, *Organometallics*, 2007, 26(7), 1729-1737.

114. Wood, M. C., Leitch, D. C., Yeung, C. S., Kozak, J. A., and Schafer, L. L., Chiral neutral zirconium amidate complexes for the asymmetric hydroamination of alkenes, *Angewandte Chemie-International Edition*, 2007, 46(3), 354-358.

115. Zhang, Z. and Schafer, L. L., Anti-Markovnikov intermolecular hydroamination: A bis(amidate) titanium precatalyst for the preparation of reactive aldimines, *Organic Letters*, 2003, 5(24), 4733-4736.

116. Gooβen, L. J., Rauhaus, J. E., and Deng, G. J., Ru-catalyzed anti-markovnikov addition of amides to alkynes: A regio- and stereoselective synthesis of enamides, *Angewandte Chemie-International Edition*, 2005, 44(26), 4042-4045.

117. Lee, J. M., Ahn, D. S., Jung, D. Y., Lee, J., Do, Y., Kim, S. K., and Chang, S. K., Hydrogen-bond-directed highly stereoselective synthesis of Z-enamides via Pd-catalyzed oxidative amidation of conjugated olefins, *Journal of the American Chemical Society*, 2006, 128(39), 12954-12962.

118. Kondo, T., Tanaka, A., Kotachi, S., and Watanabe, Y., Ruthenium Complex-Catalyzed Addition of N-Aryl Substituted Amides to Alkynes - Novel Synthesis of Enamides, *Journal of the Chemical Society-Chemical Communications*, 1995(4), 413-414.

119. Eldred, S. E., Stone, D. A., Gellman, S. H., and Stahl, S. S., Catalytic transamidation under moderate conditions, *Journal of the American Chemical Society*, 2003, 125(12), 3422-3423.

120. Hoerter, J. M., Otte, K. M., Gellman, S. H., and Stahl, S. S., Mechanism of Al(III)-catalyzed transamidation of unactivated secondary carboxamides, *Journal of the American Chemical Society*, 2006, 128(15), 5177-5183.

121. Garnett, J. L., Long, M. A., Mclaren, A. B., and Peterson, K. B., Iridium(III) Salts as Homogeneous Metal-Catalysts for Hydrogen Isotope-Exchange in Organic Compounds - Comparison with Heterogeneous Iridium for Deuteriation of Alkylbenzenes, *Journal of the Chemical Society-Chemical Communications*, 1973(19), 749-750.

122. Garnett, J. L. and West, J. C., Homogeneous Metal-Catalyzed Isotope-Exchange and Oxidation of Aromatic and Aliphatic-Compounds in Aqueous Acetic-Acid Containing Platinum(IV) Halide, *Australian Journal of Chemistry*, 1974, 27(1), 129-142.

123. Maegawa, T., Fujiwara, Y., Inagaki, Y., Esaki, H., Monguchi, Y., and Sajiki, H., Mild and efficient H/D exchange of alkanes based on C-H activation catalyzed by rhodium on charcoal, *Angewandte Chemie-International Edition*, 2008, 47(29), 5394-5397.

124. Prechtl, M. H. G., Holscher, M., Ben-David, Y., Theyssen, N., Loschen, R., Milstein, D., and Leitner, W., H/D exchange at aromatic and heteroaromatic hydrocarbons using D_2O as the deuterium source and ruthenium dihydrogen

complexes as the catalyst, *Angewandte Chemie-International Edition*, 2007, 46(13), 2269-2272.

125. Feng, Y., Lail, M., Barakat, K. A., Cundari, T. R., Gunnoe, T. B., and Petersen, J. L., Evidence for the net addition of arene C-H bonds across a Ru(II)-hydroxide bond, *Journal of the American Chemical Society*, 2005, 127(41), 14174-14175.

126. Feng, Y., Lail, M., Foley, N. A., Gunnoe, T. B., Barakat, K. A., Cundari, T. R., and Petersen, J. L., Hydrogen-Deuterium Exchange between $TpRu(PMe_3)(L)X$ (L = PMe_3 and X = OH, OPh, Me, Ph, or NHPh; L = NCMe and X = Ph) and Deuterated Arene Solvents: Evidence for Metal-Mediated Processes, *Journal of the American Chemical Society*, 2006, 128(24), 7982-7994.

127. Chan, W. C., Lau, C. P., Chen, Y. Z., Fang, Y. Q., Ng, S. M., and Jia, G. C., Syntheses and characterization of hydrotris(1-pyrazolyl)borate dihydrogen complexes of ruthenium and their roles in catalytic hydrogenation reactions, *Organometallics*, 1997, 16(1), 34-44.

128. Gaus, P. L., Kao, S. C., Darensbourg, M. Y., and Arndt, L. W., Hydrogen-Deuterium Exchange of the Anionic Group-6b Transition-Metal Hydrides - Convenient, Insitu Deuterium Transfer Reagents, *Journal of the American Chemical Society*, 1984, 106(17), 4752-4755.

129. Feracin, S., Bürgi, T., Bakhmutov, V. I., Eremenko, I., Vorontsov, E. V., Vimenits, A. B., and Berke, H., Hydrogen/Hydrogen Exchange and

Formation of Dihydrogen Derivatives of Rhenium Hydride Complexes in Acidic Solutions, *Organometallics*, 1994, 13(11), 4194-4202.

130. Paterniti, D. P., Roman, P. J., and Atwood, J. D., Activation of hydrogen on iridium(I) centers in water: Solvent effects, pH effects, and iridium-hydride exchange with D2O, *Organometallics*, 1997, 16(15), 3371-3376.

131. Kuo, L. Y., Weakley, T. J. R., Awana, K., and Hsia, C., Aqueous "green" organometallic chemistry: Structure of the molybdocene monohydride used for carbonyl reduction in water, *Organometallics*, 2001, 20(23), 4969-4972.

132. Frost, B. J. and Mebi, C. A., Aqueous organometallic chemistry: Synthesis, structure, and reactivity of the water-soluble metal hydride $CpRu(PTA)_2H$, *Organometallics*, 2004, 23(22), 5317-5323.

133. Halcrow, M. A., Chaudret, B., and Trofimenko, S., Tris-Pyrazolyl-Borate Dihydrogen Complexes of Ruthenium, *Journal of the Chemical Society-Chemical Communications*, 1993(5), 465-467.

134. Moreno, B., Saboetienne, S., Chaudret, B., Rodriguez, A., Jalon, F., and Trofimenko, S., Synthesis and Reactivity of Hydridotris(Pyrazolyl) Borate Dihydrogen Ruthenium Complexes, *Journal of the American Chemical Society*, 1995, 117(28), 7441-7451.

135. Chen, Y. Z., Chan, W. C., Lau, C. P., Chu, H. S., Lee, H. L., and Jia, G. C., Synthesis of alkyl- and aryl[hydrotris(pyrazolyl)borato]carbonylruthenium complexes by decarbonylation of alcohols. Synthesis of $TpRuH(H_2)(PPh_3)$ [Tp = hydrotris(pyrazolyl)borate], an observable intermediate in the decarbonylation reaction, *Organometallics*, 1997, 16(6), 1241-1246.

136. Ng, S. M., Fang, Y. Q., Lau, C. P., Wong, W. T., and Jia, G. C., Synthesis, characterization, and acidity of ruthenium dihydrogen complexes with 1,4,7-triazacyclononane, 1,4,7-trimethyl-1,4,7-triazacyclononane, and hydrotris(pyrazolyl)borato ligands, *Organometallics*, 1998, 17(10), 2052-2059.

137. Crabtree, R. H., Chemistry - A new type of hydrogen bond, *Science*, 1998, 282(5396), 2000-2001.

138. Crabtree, R. H., Siegbahn, P. E. M., Eisenstein, O., and Rheingold, A. L., A new intermolecular interaction: Unconventional hydrogen bonds with element-hydride bonds as proton acceptor, *Accounts of Chemical Research*, 1996, 29(7), 348-354.

139. Custelcean, R. and Jackson, J. E., Dihydrogen bonding: Structures, energetics, and dynamics, *Chemical Reviews*, 2001, 101(7), 1963-1980.

140. Belkova, N. V., Shubina, E. S., and Epstein, L. M., Diverse world of unconventional hydrogen bonds, *Accounts of Chemical Research*, 2005, 38(8), 624-631.

141. Belkova, N. V., Collange, E., Dub, P., Epstein, L. M., Lemenovskii, D. A., Lledos, A., Maresca, O., Maseras, F., Poli, R., Revin, P. O., Shubina, E. S., and Vorontsov, E. V., Experimental and computational studies of hydrogen bonding and proton transfer to [Cp*Fe(dppe)H], *Chemistry-a European Journal*, 2005, 11(3), 873-888.

142. Ilan, Y. and Kapon, M., Crystal-Structures of (Glycinamido)Tetraaminеruthenium(III) and

(Glycinato)Tetraammineruthenium(III) Chelates - Effects of the Metal Center Electronic Configuration on Coordinated Amido and Carboxylato Groups, *Inorganic Chemistry*, 1986, 25(14), 2350-2354.

143. Chou, M. H., Szalda, D. J., Creutz, C., and Sutin, N., Reactivity and Coordination Chemistry of Aromatic Carboxamide $RC(O)NH_2$ and Carboxylate Ligands - Properties of Pentaammineruthenium(II) and Pentaammineruthenium(III) Complexes, *Inorganic Chemistry*, 1994, 33(8), 1674-1684.

144. Kobayashi, A., Konno, H., Sakamoto, K., Sekine, A., Ohashi, Y., Iida, M., and Ishitani, O., Transition metal complexes coordinated by an NAD(P)H model compound and their enhanced hydride-donating abilities in the presence of a base, *Chemistry-a European Journal*, 2005, 11(14), 4219-4226.

145. Nagao, H., Hirano, T., Tsuboya, N., Shiota, S., Mukaida, M., Oi, T., and Yamasaki, M., Reactions of acetonitrile coordinated to a nitrosylruthenium complex with H_2O or CH_3OH under mild conditions: Structural characterization of imido-type complexes, *Inorganic Chemistry*, 2002, 41(24), 6267-6273.

146. Yi, C. S., He, Z. J., and Guzei, I. A., Transfer hydrogenation of carbonyl compounds catalyzed by a ruthenium-acetamido complex: Evidence for a stepwise hydrogen transfer mechanism, *Organometallics*, 2001, 20(17), 3641-3643.

147. Scheiner, S., Bent Hydrogen-Bonds and Proton Transfers, *Accounts of Chemical Research*, 1994, 27(12), 402-408.

148. Gilli, P., Bertolasi, V., Ferretti, V., and Gilli, G., Covalent Nature of the Strong Homonuclear Hydrogen-Bond - Study of the O-H---O System by Crystal-Structure Correlation Methods, *Journal of the American Chemical Society*, 1994, 116(3), 909-915.

149. Carey, F. A. and Sundberg, R. J., *Advanced Organic Chemistry Part A. Structure and Mechanisms*. 3rd ed., New York: Plenum Press, 1990.

150. Guthrie, J. P., *In The Chemistry of Enols*, ed. Z. Rappoport, New York: Wiley, 1990.

151. Toullec, J., *In The Chemistry of Enols*, ed. Z. Rappoport, New York: Wiley, 1990.

152. Keeffe, J. R. and Kresge, A. J., *In The Chemistry of Enols*, ed. Z. Rappoport, New York: Wiley, 1990.

153. Lin, Z. Y. and Hall, M. B., Transition-Metal Polyhydride Complexes - a Theoretical View, *Coordination Chemistry Reviews*, 1994, 135, 845-879.

154. Kubas, G. J., *Metal Dihydrogen and Sigma-Bond Complexes*, New York: Kluwer Academic/Plenum Publishers, 2001.

155. Sandoval, C. A., Ohkuma, T., Muniz, K., and Noyori, R., Mechanism of asymmetric hydrogenation of ketones catalyzed by BINAP/1,2-diamine-ruthenium(II) complexes, *Journal of the American Chemical Society*, 2003, 125(44), 13490-13503.

156. Conner, D., Jayaprakash, K. N., Cundari, T. R., and Gunnoe, T. B., Synthesis and reactivity of a coordinatively unsaturated ruthenium(II) parent amido

complex: Studies of X-H activation (X = H or C), *Organometallics*, 2004, 23(11), 2724-2733.

157. Abdur-Rashid, K., Faatz, M., Lough, A. J., and Morris, R. H., Catalytic cycle for the asymmetric hydrogenation of prochiral ketones to chiral alcohols: Direct hydride and proton transfer from chiral catalysts trans-$Ru(H)_2$diphosphine)(diamine) to ketones and direct addition of dihydrogen to the resulting hydridoamido complexes, *Journal of the American Chemical Society*, 2001, 123(30), 7473-7474.

158. Fryzuk, M. D., Montgomery, C. D., and Rettig, S. J., Synthesis and Reactivity of Ruthenium Amide Phosphine Complexes - Facile Conversion of a Ruthenium Amide to a Ruthenium Amine Via Dihydrogen Activation and Ortho Metalation - X-Ray Structure of $RuCl(C_6H_4PPh_2)[NH(SiMe_2CH_2PPh_2)_2]$, *Organometallics*, 1991, 10(2), 467-473.

159. Bianchini, C., Perez, P. J., Peruzzini, M., Zanobini, F., and Vacca, A., Classical and Nonclassical Polyhydride Ruthenium(II) Complexes Stabilized by the Tetraphosphine $P(CH_2CH_2PPh_2)_3$, *Inorganic Chemistry*, 1991, 30(2), 279-287.

160. Bianchini, C., Linn, K., Masi, D., Peruzzini, M., Polo, A., Vacca, A., and Zanobini, F., Classical, Nonclassical, and Mixed-Metal Osmium(Ii) Polyhydrides Stabilized by the Tetraphosphine $P(CH_2CH_2PPh_2)_3$ - H/D Isotope-Exchange Reactions Promoted by a Strongly Bound Dihydrogen Ligand, *Inorganic Chemistry*, 1993, 32(11), 2366-2376.

161. Heinekey, D. M. and Oldham, W. J., Preparation and Properties of $[TpIr(PMe_3)(H_2)H]BF_4$ - Observation of Novel Isotopic Perturbation, *Journal of the American Chemical Society*, 1994, 116(7), 3137-3138.

162. Oldham, W. J., Hinkle, A. S., and Heinekey, D. M., Synthesis and characterization of hydrotris(pyrazolyl)borate dihydrogen/hydride complexes of rhodium and iridium, *Journal of the American Chemical Society*, 1997, 119(45), 11028-11036.

163. Chinn, M. S. and Heinekey, D. M., Dihydrogen Complexes of Ruthenium .2. Kinetic and Thermodynamic Considerations Affecting Product Distribution, *Journal of the American Chemical Society*, 1990, 112(13), 5166-5175.

164. Albeniz, A. C., Heinekey, D. M., and Crabtree, R. H., Dihydrogen Complexes in Catalysis - Isotope Exchange-Reactions, *Inorganic Chemistry*, 1991, 30(19), 3632-3635.

165. Kubas, G. J., Burns, C. J., Khalsa, G. R. K., Vandersluys, L. S., Kiss, G., and Hoff, C. D., Dihydrogen - a Better Ligand Than Water - Ir and X-Ray Evidence for Aquo Coordination in $W(CO)_3(PR_3)_2(H_2O)$, Thermodynamics of H_2O Versus η^2-H_2 Binding, and H_2O/D_2 Isotopic Exchange - Implications on the Biological Activation of Hydrogen, *Organometallics*, 1992, 11(10), 3390-3404.

166. Kovács, G., Nádasdi, L., Laurenczy, G., and Joó, F., Aqueous organometallic catalysis. Isotope exchange reactions in H_2-D_2O and D_2-H_2O systems catalyzed by water-soluble Rh- and Ru-phosphine complexes, *Green Chemistry*, 2003, 5(2), 213-217.

167. Georgakaki, I. P., Miller, M. L., and Darensbourg, M. Y., Requirements for functional models of the iron hydrogenase active site: D_2/H_2O exchange activity in $\{(\mu\text{-SMe})(\mu\text{-pdt})[Fe(CO)_2(PMe_3)]_2^+\}[BF_4^-]$, *Inorganic Chemistry*, 2003, 42(8), 2489-2494.

168. Kovács, G., Schubert, G., Joó, F., and Pápai, I., Theoretical mechanistic study of rhodium(I) phosphine-catalyzed H/D exchange processes in aqueous solutions, *Organometallics*, 2005, 24(13), 3059-3065.

169. Jensen, C. M. and Trogler, W. C., Kinetics and Mechanism of Nitrile Hydration Catalyzed by Unhindered Hydridobis(Phosphine)Platinum(II) Complexes - Regioselective Hydration of Acrylonitrile, *Journal of the American Chemical Society*, 1986, 108(4), 723-729.

170. Breno, K. L., Pluth, M. D., and Tyler, D. R., Organometallic chemistry in aqueous solution. Hydration of nitriles to amides catalyzed by a water-soluble molybdocene, $(MeCp)_2Mo(OH)(H_2O)^+$, *Organometallics*, 2003, 22(6), 1203-1211.

171. Ghaffar, T. and Parkins, A. W., The catalytic hydration of nitriles to amides using a homogeneous platinum phosphinito catalyst, *Journal of Molecular Catalysis a-Chemical*, 2000, 160(2), 249-261.

172. Hazell, A., Jensen, K. B., Mckenzie, C. J., and Toftlund, H., Synthesis and Reactivity of (μ-Oxo)Diiron(III) Complexes of Tris(2-Pyridylmethyl)Amine - X-Ray Crystal-Structures of $[Tpa(OH)FeOFe(H_2O)Tpa](ClO_4)_3$ and $[Tpa(Cl)FeOFe(Cl)Tpa](ClO_4)_2$, *Inorganic Chemistry*, 1994, 33(14), 3127-3134.

173. Thallaj, N. K., Przybilla, J., Welter, R., and Mandon, D., A ferrous center as reaction site for hydration of a nitrile group into a carboxamide in mild conditions, *Journal of the American Chemical Society*, 2008, 130(8), 2414-2415.

174. Leung, C. W., Zheng, W. X., Wang, D. X., Ng, S. M., Yeung, C. H., Zhou, Z. Y., Lin, Z. Y., and Lau, C. P., Catalytic H/D exchange between organic compounds and D_2O with $TpRu(PPh_3)(CH_3CN)H$ (Tp = hydro(trispyrazolyl)borate). Reaction of $TpRu(PPh_3)(CH_3CN)H$ with water to form acetamido complex $TpRu(PPh_3)(H_2O)(NHC(O)CH_3)$, *Organometallics*, 2007, 26(8), 1924-1933.

175. Alcock, N. W., Burns, I. D., Claire, K. S., and Hill, A. F., Ruthenatetraboranes - Synthesis of $[Ru(B_3H_8)(PPh_3)(HB(Pz)_3)]$ and Crystal-Structure of $[RuCl(PPh_3)_2(HB(Pz)_3)]$ (Pz = Pyrazol-1-yl), *Inorganic Chemistry*, 1992, 31(13), 2906-2908.

176. Arroyo, M., Miguel, D., Villafane, F., Nieto, S., Pérez, J., and Riera, L., Rhenium-mediated coupling of acetonitrile and pyrazoles. New molecular clefts for anion binding, *Inorganic Chemistry*, 2006, 45(17), 7018-7026.

177. Hursthouse, M. B., Mazid, M. A., Robinson, S. D., and Sahajpal, A., Complexes of the Platinum Metals .46. 1,1,1,5,5,5-Hexafluoro-3-Azapentane-2,4-Diiminato Derivatives of Ruthenium, Osmium and Iridium - Crystal-Structure of $[Ru(NHC(CF_3)NC(CF_3)NH)H(CO)(PPh_3)_2]$, *Journal of the Chemical Society-Dalton Transactions*, 1994(24), 3615-3620.

178. Robinson, V., Taylor, G. E., Woodward, P., Bruce, M. I., and Wallis, R. C., Cyclopentadienyl-Ruthenium and Cyclopentadienyl-Osmium Chemistry .14. The Reaction between Chloro(Cyclopentadienyl)Bis(Triphenylphosphine)-Ruthenium and Trifluoroacetonitrile - Crystal-Structure of [RuNH=C(CF_3)N=C(CF_3)NH(P($OMe)_3$)(C_5H_5)], *Journal of the Chemical Society-Dalton Transactions*, 1981(5), 1169-1173.

179. Green, M., Taylor, S. H., Daly, J. J., and Sanz, F., Reaction of Trifluoroacetonitrile with π-Allylic-Iridium Complexes - Crystal-Structure of an Iridium(I) 6-Membered Ring Chelate Complex, *Journal of the Chemical Society-Chemical Communications*, 1974(10), 361-362.

180. Allen, F. H., Kennard, O., Watson, D. G., Brammer, L., Orpen, A. G., and Taylor, R., Tables of Bond Lengths Determined by X-Ray and Neutron-Diffraction .1. Bond Lengths in Organic-Compounds, *Journal of the Chemical Society-Perkin Transactions 2*, 1987(12), S1-S19.

181. Courmier, D., Gardebien, F., Minot, C., and St-Amant, A., A computational study of the water-catalyzed formation of NH_2CH_2OH, *Chemical Physics Letters*, 2005, 405(4-6), 357-363.

182. Heys, R., Investigation of [$IrH_2(Me_2CO)_2(PPh_3)_2$]BF_4 as a Catalyst of Hydrogen Isotope Exchange of Substrates in Solution, *Journal of the Chemical Society-Chemical Communications*, 1992(9), 680-681.

183. Hesk, D., Das, P. R., and Evans, B., Deuteration of Acetanilides and Other Substituted Aromatics Using [Ir(COD)(Cy_3P)(Py)]PF_6 as Catalyst, *Journal of Labelled Compounds & Radiopharmaceuticals*, 1995, 36(5), 497-502.

184. Shu, A. Y. L., Saunders, D., Levinson, S. H., Landvatter, S. W., Mahoney, A., Senderoff, S. G., Mack, J. F., and Heys, J. R., Direct tritium labeling of multifunctional compounds using organoiridium catalysis. 2., *Journal of Labelled Compounds & Radiopharmaceuticals*, 1999, 42(8), 797-807.

185. Shu, A. Y. L., Chen, W., and Heys, J. R., Organoiridium catalyzed hydrogen isotope exchange: Ligand effects on catalyst activity and regioselectivity, *Journal of Organometallic Chemistry*, 1996, 524(1-2), 87-93.

186. Junk, T. and Catallo, W. J., Hydrogen isotope exchange reactions involving C-H (D,T) bonds, *Chemical Society Reviews*, 1997, 26(5), 401-406.

187. Lowry, T. H. and Richardson, K. S., *Mechanism and theory in organic chemistry*. 3rd ed., New York: Harper & Row, 1987.

188. Pleiss, U. and Voges, R., *Synthesis and applications of isotopically labelled compounds. Volume 7 : proceedings of the seventh international symposium, Dresden, Germany, 18-22 June 2000*, Chichester ; New York: John Wiley & Sons, 2001.

189. Kruger, J., Manmontri, B., and Fels, G., Iridium-catalyzed H/D exchange, *European Journal of Organic Chemistry*, 2005(7), 1402-1408.

190. Yet, L., Chemistry and biology of salicylihalamide A and related compounds, *Chemical Reviews*, 2003, 103(11), 4283-4306.

191. Mohrle, H. and Kilian, R., Cis-N-Styryl-Aminoacyl-Verbindungen, *Tetrahedron*, 1969, 25(23), 5745-5753.

192. Couture, A., Deniau, E., and Grandclaudon, P., A Convenient Synthesis of Enamides and Dienamides by Horner-Wittig and Wadsworth-Emmons Reactions, *Tetrahedron Letters*, 1993, 34(9), 1479-1482.

193. Dupau, P., Le Gendre, P., Bruneau, C., and Dixneuf, P. H., Optically active amine derivatives: Ruthenium-catalyzed enantioselective hydrogenation of enamides, *Synlett*, 1999(11), 1832-1834.

194. Shono, T., Matsumura, Y., Tsubata, K., Sugihara, Y., Yamane, S., Kanazawa, T., and Aoki, T., Electroorganic Chemistry .60. Electroorganic Synthesis of Enamides and Enecarbamates and Their Utilization in Organic-Synthesis, *Journal of the American Chemical Society*, 1982, 104(24), 6697-6703.

195. Torii, S., Inokuchi, T., and Kubota, M., A Practical Access to Methyl 3,3-Dimethoxypropionates, N-Protected Beta-Aminoacrylates, and Beta-Aminoacrylonitrile Using an Electrochemical Procedure, *Journal of Organic Chemistry*, 1985, 50(21), 4157-4160.

196. Wang, X. and Porco, J. A., Modification of C-terminal peptides to form peptide enamides: Synthesis of chondriamides A and C, *Journal of Organic Chemistry*, 2001, 66(24), 8215-8221.

197. Bayer, A. and Maier, M. E., Synthesis of enamides from aldehydes and amides, *Tetrahedron*, 2004, 60(31), 6665-6677.

198. Boeckman, R. K., Goldstein, S. W., and Walters, M. A., Synthetic Studies of the Cyclopropyl Iminium Ion Rearrangement .3. Application of the Cyclopropyl Acyliminium Ion Rearrangement to a Concise and Highly

Convergent Synthesis of (+/-)-Lycorine, *Journal of the American Chemical Society*, 1988, 110(24), 8250-8252.

199. Kinderman, S. S., van Maarseveen, J. H., Schoemaker, H. E., Hiemstra, H., and Rutjes, F. P. J. T., Enamide-olefin ring-closing metathesis, *Organic Letters*, 2001, 3(13), 2045-2048.

200. Brettle, R. and Mosedale, A. J., Synthesis of Enamides, *Journal of the Chemical Society-Perkin Transactions 1*, 1988(8), 2185-2195.

201. Stefanuti, I., Smith, S. A., and Taylor, R. J. K., Unsaturated enamides via organometallic addition to isocyanates: the synthesis of Lansamide-I, Lansiumamides A-C and SB-204900, *Tetrahedron Letters*, 2000, 41(19), 3735-3738.

202. Ager, D. J., The Peterson Reaction, *Synthesis-Stuttgart*, 1984(5), 384-398.

203. Furstner, A., Brehm, C., and Cancho-Grande, Y., Stereoselective synthesis of enamides by a Peterson reaction manifold, *Organic Letters*, 2001, 3(24), 3955-3957.

204. Zhou, Y. G., Yang, P. Y., and Han, X. W., Synthesis and highly enantioselective hydrogenation of exocyclic enamides: (Z)-3-arylidene-4-acetyl-3,4-dihydro-2H-1,4-benzoxazines, *Journal of Organic Chemistry*, 2005, 70(5), 1679-1683.

205. Goossen, L. J., Rauhaus, J. E., and Deng, G. J., Ru-catalyzed anti-markovnikov addition of amides to alkynes: A regio- and stereoselective synthesis of enamides, *Angewandte Chemie-International Edition*, 2005, 44(26), 4042-4045.

206. Esaki, H., Ohtaki, R., Maegawa, T., Monguchi, Y., and Sajiki, H., Novel Pd/C-catalyzed redox reactions between aliphatic secondary alcohols and ketones under hydrogenation conditions: Application to H-D exchange reaction and the mechanistic study, *Journal of Organic Chemistry*, 2007, 72(6), 2143-2150.

207. Carey, F. A. and Sundberg, R. J., *Advanced organic chemistry*. 4th ed., New York: Kluwer Academic/Plenum Pub., 2000.

208. Jung, S., Ilg, K., Wolf, J., and Werner, H., Cationic vinyl and dicationic carbene ruthenium(II) complexes from a vinylidene(hydrido) precursor, *Organometallics*, 2001, 20(11), 2121-2123.

209. Jung, S., Brandt, C. D., Wolf, J., and Werner, H., Vinyl and carbene ruthenium(II) complexes from hydridoruthenium(II) precursors, *Dalton Transactions*, 2004(3), 375-383.

210. Cheng, P., Jiang, Z. Y., Wang, R. R., Zhang, X. M., Wang, Q., Zheng, Y. T., Zhou, J., and Chen, J. J., Synthesis and biological evaluation of N-acetyl-β-aryl-1,2-didehydroethylamines as new HIV-1 RT inhibitors in vitro, *Bioorganic & Medicinal Chemistry Letters*, 2007, 17(16), 4476-4480.

211. Maurer, J., Linseis, M., Sarkar, B., Schwederski, B., Niemeyer, M., Kaim, W., Zalis, S., Anson, C., Zabel, M., and Winter, R. F., Ruthenium complexes with vinyl, styryl, and vinylpyrenyl ligands: A case of non-innocence in organometallic chemistry, *Journal of the American Chemical Society*, 2008, 130(1), 259-268.

212. Slugovc, C., Mereiter, K., Schmid, R., and Kirchner, K., Ruthenium tripyrazolylborate complexes. 9. Formation and characterization of amidocarbene complexes, *Organometallics*, 1998, 17(5), 827-831.

213. Coalter, J. N., Bollinger, J. C., Huffman, J. C., Werner-Zwanziger, U., Caulton, K. G., Davidson, E. R., Gerard, H., Clot, E., and Eisenstein, O., Coordinated carbenes from electron-rich olefins on $RuHCl(P^iPr_3)_2$, *New Journal of Chemistry*, 2000, 24(1), 9-26.

214. Hua, R. M., Akita, M., and MoroOka, Y., Reduction of a diruthenium bridging vinylidene species $Cp_2Ru_2(=C=CH_2)(CO)(\mu\text{-}CO)(MeCN)$ by hydrosilane leading to a vinyl complex $Cp_2Ru_2(\mu\text{-}CH=CH_2)(CO)_2(SiR_3)$ and vinylsilane: A model system for production of an olefinic product from a vinylidene intermediate, *Inorganica Chimica Acta*, 1996, 250(1-2), 177-183.

215. Werner, H., Esteruelas, M. A., and Otto, H., Insertion Reactions of the 16-Electron Complexes $RuHCl(CO)P^iPr_3)_2$, $OsHCl(CO)P^iPr_3)_2$ with Alkynes - the X-Ray Crystal-Structure of $Os((E)\text{-}CH=CHPh)Cl(CO)(P^iPr_3)_2$, *Organometallics*, 1986, 5(11), 2295-2299.

216. Wang, L. S. and Cowie, M., Bridging Vinylidene Complexes of RhMn and Evidence for Migratory Insertions to Give Terminal Vinyl Groups, *Organometallics*, 1995, 14(5), 2374-2386.

217. Gamasa, M. P., Gimeno, J., Martin-Vaca, B. M., Isea, R., and Vegas, A., Synthesis and characterization of 2-oxacycloalkylideneruthenium(II) complexes: X-ray crystal structure of the 2-oxacycloheptylidene complex

[Ru{=COCH$_2$(CH$_2$)$_3$CH$_2$}(η^5-C$_9$H$_7$)(PPh$_3$)$_2$][PF$_6$] CH$_2$Cl$_2$, *Journal of Organometallic Chemistry*, 2002, 651(1-2), 22-33.